# Wind Turbine Control: Robust Model Based Approach

**Mirzaei, Mahmood**

*Publication date:*
2012

*Document Version*
Publisher's PDF, also known as Version of record

# Wind Turbine Control: A Robust Model Based Approach

Mahmood Mirzaei

Kongens Lyngby 2012
IMM-PhD-2012-281

Technical University of Denmark
Department of Applied Mathematics and Computer Science
Matematiktorvet, Building 303B, DK-2800 Kongens Lyngby, Denmark
Phone +45 4525 3031, Fax +45 4588 2673
compute@compute.dtu.dk
www.compute.dtu.dk IMM-PhD-2012-281

# Preface

This thesis was prepared at the Department of Applied Mathematics and Computer Science, the Technical University of Denmark (DTU) in partial fulfillment of the requirements for acquiring the PhD degree in engineering. The work has been supervised by Associate Professor Niels Kjølstad Poulsen from the Department of Applied Mathematics and Computer Science, the Technical University of Denmark and Associate Professor Hans Henrik Niemann from the Department of Electrical Engineering, the Technical University of Denmark. The project was funded by the Danish Agency for Science, Technology and Innovation through the "Concurrent Aero-Servo-Elastic Analysis and Design of Wind Turbines" project.

The thesis deals with model based and robust model based control of wind turbines.

The thesis consists of a summary report and nine research papers, written during the period August 2009 to August 2012. Six of the research papers are published in international peer-reviewed scientific conferences and two are submitted to international peer-reviewed scientific journals.

Lyngby, 24-September-2012

M. Mirzaei

Mahmood Mirzaei

تقدیم به روح پاک پدرم ...

# Acknowledgements

This thesis would not have been possible without the guidance and the help of several individuals who in one way or another contributed and extended their valuable assistance in the preparation and completion of this study.

First and foremost I offer my sincerest gratitude to my supervisors, Assoc. Prof. Niels Kjølstad Poulsen from Department of Applied Mathematics and Computer Science and Assoc. Prof. Hans Henrik Niemann from Department of Electrical Engineering, who have supported me throughout my thesis with their advice, patience and knowledge whilst giving me enough freedom to work in my own way, make my own mistakes and learn from them.

In my daily work I have been blessed with a friendly and cheerful group of fellow PhD students and colleagues, who helped me feeling at home and have a smooth start when I arrived and never felt lonely during the PhD period. It was a great experience to be working with them, thank you guys very much for everything!

I am also very grateful to my family who, in spite of the long distance, always supported me. I thank my mother, my brother and my sisters. I am sure without their support I could not have followed my dreams.

Last but not least I am very grateful to my wife, Mehrnoosh, who has always been there and supported me when I was tired of daily work or desperate of daily problems. She has been the one who would listen to my thoughts and put up with me when I was stressed.

# Summary (English)


In the 1970s the oil price crisis encouraged investigation of non-petroleum energy sources of which wind energy was the most promising one. Lately global warming concerns have even intensified the demand for green and sustainable energy resources and opened up several lines of research in this area. Wind turbines are the most common wind energy conversion systems and are hoped to be able to compete economically with fossil fuel power plants in near future. However this demands better technology to reduce the price of electricity production. Control can play an essential part in this context. This is because, on the one hand, control methods can decrease the cost of energy by keeping the turbine close to its maximum efficiency. On the other hand, they can reduce structural fatigue and therefore increase the lifetime of the wind turbine.

The power produced by a wind turbine is proportional to the square of its rotor radius, therefore it seems reasonable to increase the size of the wind turbine in order to capture more power. However as the size increases, the mass of the blades increases by cube of the rotor size. This means in order to keep structural feasibility and mass of the whole structure reasonable, the ratio of mass to size should be reduced. This trend results in more flexible structures.

Control of the flexible structure of a wind turbine in a wind field with stochastic nature is very challenging. In this thesis we are examining a number of robust model based methods for wind turbine control. Firstly we examine potentials of $\mu$-synthesis methods and use $\mu$-tools to analyze robustness of the resulting controllers both in terms of robust stability and robust performance. Afterwards we employ model predictive control (MPC) and show that the way MPC solves control problems suits wind turbine control problems very well, especially when

we have preview measurements of wind speed using LIDARs. For the control problem with LIDAR measurements we have proposed a new MPC approach which gives better results than linear MPC while it has almost the same computational complexity. We have also tackled wind turbine control using robust MPC. In general, robust MPC problems are very computationally demanding, however we have shown that with some approximations the resulting robust MPC problem can be specialized with reduced computational complexity.

After a short introduction on wind energy and wind turbines in chapter 1, we briefly explain wind turbine modeling in chapter 2. Introductions to different control design methods are given in chapter 3. The goal of this chapter is to show how different control methods are chosen. The next eight chapters comprise the body of the thesis and are scientific papers that are published or going to be published. Control methods which were briefly introduced in chapter 3 are explained in these chapters in details.

# Summary (Danish)

Siden energikrisen i 1972 har der været en stigende interesse i at udnytte energiresourser, der ikke er baseret på olie. Vindenergi er en af de mest lovende. Senere har bekymringen for global opvarmning øget interessen for grøn og vedvarende energi. Dette har intensiveret forskningen indenfor dette område. Vindmøller er klart de mest dominerende energisystemer indenfor vedvarende energi og håbet er at de indenfor den nærmeste fremtid kan konkurrere økonomisk med kraftværker baseret på fossile brandstof. Dette kræver imidlertid en forbedret teknologi for at reducere omkostningerne ved produktionen af elektrisk energi. Regulering kan spille en central rolle i den forbindelse. Dette skyldes først og fremmest at reguleringen kan reducere produktions omkostningerne ved at vindmøllerne køres mere effektivt. Dernæst kan reguleringen reducere udmattelses af strukturen såsom tårn og blade og derved forøge vindmøllers levetid.

En vindmølles effektproduktion er groft sagt proportional med kvadratet af rotorens radius. Det virker derfor fornuftigt at øge størrelsen af vindmøllerne for at øge effektproduktionen. Desværre bliver bladenes vægt også forøget og med kubus af rotorradius. For at modvirke dette forhold må strukturen gøres lettere og med det resultat at strukturen bliver mere fleksibel.

Regulering af vindmøllers fleksible struktur i et stokastisk vind felt er meget udfordrende. I denne afhandling er der fokuseret på en række forskellige robuste og modelbaseret metoder til regulering af vindmøller. Først er mu-syntese metoder egenskaber undersøgt i forbindelse med robust stabilitet og robust performance. Derefter er MPC regulatorer undersøgt i forbindelse med regulering af vindmøller. Disse giver gode resultater, specielt når der indgår målinger af vindhastigheden med LIDAR. En LIDAR baseret MPC regulering er bedre end

en linear MPC, mens den ikke kræver væsentlig mere regnekraft. En tredje type regulering er baseret på robust MPC regulering. Generelt er disse meget krævende mht. regnekraft. I afhandlingen er der undersøgt approksimationer, der resulterer i robuste MPC regulatorer, som ikke er så krævende mht. regnekraft.

Efter en kort introduktion om vind energi og vindmøller i kapitel 1 er der i kapitel 2 givet en kort beskrivelse af modeller for vindmøller. Kapitel 3 vedrører forskellige metoder til design af regulatorer. Målsætningen med dette kapitel er at give en kort indføring, hvordan forskellige reguleringsformer kan vælges. De efterfølgende 9 kapitler udgør afhandlingens hoveddel og består af artikler, der er publiceret eller vil blive publiceret. Metoder, der er introduceret i kapitel 3, er gennemgået i detaljer her.

# List of publiations

**Paper A** Mahmood Mirzaei, Hans H. Niemann, and Niels K. Poulsen, "DK-Iteration robust control design of a wind turbine," IEEE Multi-Conference on Systems and Control, 2011, Denver, CO, United States

**Paper B** Mahmood Mirzaei, Hans H. Niemann, and Niels K. Poulsen, "A $\mu$-synthesis approach to robust control of a wind turbine," the 50th IEEE Conference on Decision and Control and European Control Conference, 2011, Orlando, FL, United States

**Paper C** Mahmood Mirzaei, Niels K. Poulsen and Hans H. Niemann, "Model Predictive Control of a Nonlinear System with Known Scheduling Variable," In: Proceedings of the 17th Nordic Process Control Workshop, Kogens Lyngby, Technical University of Denmark, Lyngby, Denmark

**Paper D** Mahmood Mirzaei, Niels K. Poulsen and Hans H. Niemann, "Robust Model Predictive Control of a Nonlinear System with Known Scheduling Variable and Uncertain Gain," 7th IFAC Symposium on Robust Control Design, June 20-22, 2012, Aalborg, Denmark

**Paper E** Mahmood Mirzaei, Niels K. Poulsen and Hans H. Niemann, "Robust Model Predictive Control of a Wind Turbine," American Control Conference, June 27-29, 2012, Montréal, Canada

**Paper F** Mahmood Mirzaei, Lars C. Henriksen, Niels K. Poulsen and Hans H. Niemann, Morten H. Hansen, "Individual Pitch Control Using LIDAR Measurements," IEEE Multi-Conference on Systems and Control, October 3-5, 2012, Dubrovnik, Croatia

# Contents

# Part I

# Summary report

Chapter 1

# Introduction

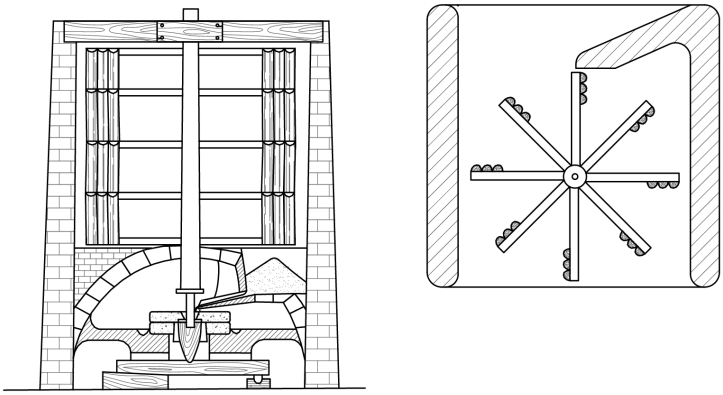

**Figure 1.1:** Early Persian wind mill

## 1.1 Wind Energy

Wind energy or kinetic energy in the wind is due to mass movement of the air which itself is a result of temperature difference between two neighboring regions. This temperature difference is caused by differential heating of the sun. Wind energy has been used for hundreds of years in sailboats and sail ships. It has also been used for milling grains and pumping water around the world. The earliest proved historical records show that Persians were among the first people who employed wind energy to mill grains. Figure 1.1 shows an illustration of an early vertical axis Persian mill. This type of wind mill employs drag force to extract power from wind. Later on in Europe more efficient wind mills were invented which employed lift force instead. The concepts of lift and drag forces will be explained shortly.

Using wind energy to produce electricity goes back to 1888 when Charles F. Brush from Ohio, the United States, invented the first automatically operated wind turbine. In the 1890s, the Danish scientist and inventor Poul la Cour constructed wind turbines to generate electricity. He used the generated power for electrolysis and stored the produced hydrogen and oxygen mixture to use as a fuel. La Cour was the first to discover that fast rotating wind turbines with fewer rotor blades are more efficient than other designs. However it was in the 1970s when the oil price crisis encouraged investigation of non-petroleum energy sources of which wind energy was the most promising one. Lately global warming concerns have even intensified the demand for green and sustainable energy resources and opened up several lines of research in this area. In the next section we will give a short introduction to wind energy conversion systems.

### 1.1.1 The Wind

In order to harvest the wind energy efficiently we need to understand its nature. According to van der Hoven [vdH57], the concentration of energy around two separated frequencies in wind power spectrum allows splitting the wind speed signal into two main components:

$$v = v_m + v_t \tag{1.1}$$

$v_m$ is quasi-steady and it is called *mean wind speed* and $v_t$ is the *turbulent* term in the wind speed. $v_m$ could be found by averaging wind speed over a sufficiently long period of time:

$$v_m(t) = \frac{1}{T} \int_{t-T/2}^{t+T/2} v(\tau) d\tau \tag{1.2}$$

The probability distribution of the mean wind speed follows a Weibull distribution and knowledge about this distribution determines economical viability of wind energy projects at a specific site [Bur11]. The Weibull distribution of mean wind speed is:

$$p(v_m) = \frac{k}{C} \left(\frac{v_m}{C}\right)^{k-1} e^{(-v_m/C)^k} \tag{1.3}$$

In which $k$ and $C$ are the shape and scale coefficients, respectively. They are adjusted such that the distribution matches data at a particular site [WJ97]. In this work we assume the mean wind speed to be constant since the simulation periods are at the scale of hundreds of seconds.

The turbulent term of the wind speed $v_t$ can be modeled as a complicated nonlinear stochastic process. However for practical control purposes it could be approximated by a linear model [JLSM06]. More details will be given in the section for modeling the wind in 2.2.1.

The wind equation presented in 1.1 gives the model of a point wind speed, however wind speed has different values over the rotor disc of a wind turbine. The whole wind profile over the rotor disc could be considered as a set of point wind speeds. The point wind speed has both spatial stochastic and deterministic components. The deterministic changes of wind speed over the rotor disc is due to wind shear and tower shadow. Skin friction of the Earth causes a decrease in mean wind speed as the height decreases. This phenomena is known as wind shear. Towers are obstacles in the wind inflow, therefore they reduce the inflow normal to the rotor plane. This wind speed reduction is felt by blades when passing the tower. This phenomena is called tower shadow.

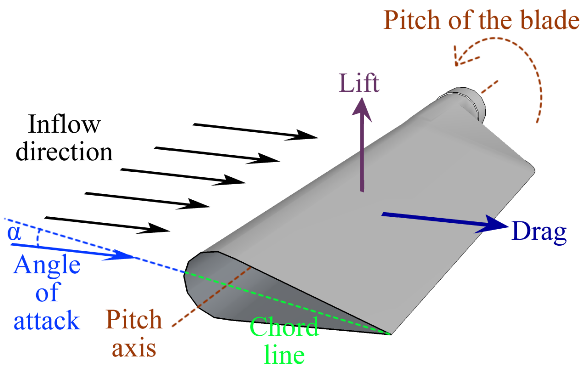


**Figure 1.2:** Illustration of lift and drag forces on an airfoil

Considering a full field wind speed makes controller design complicated. If pitch of the blades are not adjusted individually, which is called individual pitch control (IPC), there is no need for this level of complexity in wind modeling and we can approximate the effect of the whole full field wind speed on the rotor with a single wind speed called *effective wind speed* ($v_e$). Hereafter we use effective wind speed in our designs and simulations unless otherwise stated.

## 1.2 Wind Energy Conversion Systems

A system that transforms kinetic energy of the wind to useful work is a wind energy conversion system (WECS). Different types of WECS have been invented such as wind turbines, laddermills [Ock01] and power kites [CFM10] of which only the technology of the wind turbines is mature enough to produce large scale power.

When air is blowing past the surface of a body, it exerts a surface force on the body. Lift is the component of this force that is perpendicular to the oncoming flow direction and drag is the component which is parallel to it. Lift and drag forces on an airfoil are shown in figure 1.2. Lift and drag forces are used in WECS to convert kinetic energy in the wind to mechanical energy. Different WECS employ these forces differently. For example in wind turbines these forces are applied on blades which cause them to rotate around an axis and to produce mechanical energy. Next section gives more details.

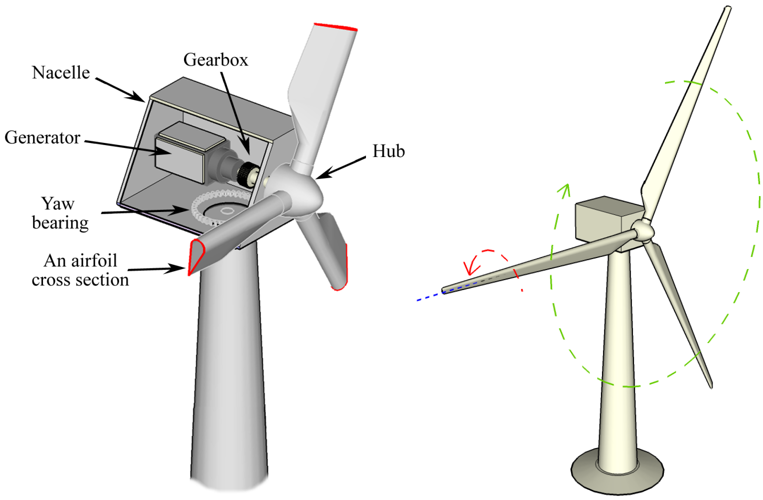


**Figure 1.3:** A horizontal axis wind turbine (HAWT)

## 1.3 Introduction to Wind Turbines

As mentioned earlier nowadays wind turbine technology is the only mature technology which is being used to produce economical electricity from wind energy. Based on the orientation of the rotation axis, wind turbines can be categorized into vertical axis and horizontal axis machines. As the names suggest, the blades of vertical axis and horizontal axis turbines rotate around the axes which are place vertically and horizontally, respectively. Horizontal axis wind turbines (HAWTs) have several advantages over vertical axis ones which make them more common in practice [Bur11]. Among all types of HAWTs, Danish concept is the most popular wind turbine. The Danish concept is a horizontal axis fixed speed wind turbine with three blades. The turbine is connected directly to the utility grid. The Danish concept was dominating the wind turbine industry until new advances in power electronics made it possible to have variable rotor rotational speeds. Different parts of a three bladed HAWT could be seen in figure 1.3. Nacelle is a cubicle which holds the hub and houses the gearbox and the generator. It is placed on top of a tall and normally cylindrical tower where there is more wind with less turbulence. In this type, blades are connected to the low speed shaft through hub. In order to always stay facing the coming wind, there is a mechanism called yawing system that rotates the nacelle on top of the tower. Wind turbine blades have a specific aerodynamic design to produce maximum power. In the next section we will give an overview of wind turbine aerodynamics.

### 1.3.1 Wind turbine aerodynamics

Wind turbines interact with wind and capture part of its kinetic energy and convert it to mechanical work. The mechanical work is subsequently converted to electrical power. Wind turbines are aerodynamically designed such that the conversion from kinetic energy of wind to mechanical work is maximized. Aerodynamics of wind turbines explain how airflow develops forces on wind turbine rotor. There are several methods to explain this phenomena [Bur11], however we use two methods here which are the simplest ones and can explain aerodynamics at an acceptable yet simple level for controller design. These methods are the actuator disc model [Bur11] and the blade element momentum theory [Han08].

#### 1.3.1.1 Actuator disc model

In the actuator disc model, the turbine rotor is considered as an actuator disc, which is a generic device that extracts energy from the wind. Here we skip the mathematics which could be found in [Bur11] and [BBM06] and just mention that using the actuator disc model we can get an upper bound on the wind power conversion efficiency known as *the Betz limit*.

#### 1.3.1.2 Blade element momentum theory

In order to find mathematical model of a wind turbine we need to calculate aerodynamic torque ($Q_a$) and thrust ($Q_t$) as functions of the wind speed ($v_e$), the rotational speed of the rotor ($\omega_r$) and the pitch angle of the blades ($\beta$). The aerodynamic torque is the result of the in-plane aerodynamic forces applied to the rotor elements. The aerodynamic torque rotates the rotor and produces power. The aerodynamic thrust is the normal force that is exerted on the rotor plane and subsequently on the whole turbine structure. To calculate these forces we divide a whole blade into infinitesimal length elements (see figure 1.4). Each element is an airfoil and having its characteristics (namely lift and drag coefficients which for a specific airfoil are given as functions of angle of attack), we are able to calculate lift and drag forces on the airfoil. Blade element momentum (BEM) theory is used to calculate lift and drag forces as quasi-steady functions of wind speed, pitch of the blades and rotational speed of the rotor. The lift and drag forces subsequently could be used to calculate aerodynamic torque and thrust on the rotor. After calculating torque and thrust of one element, we integrate over all the blade elements from hub to the tip of the

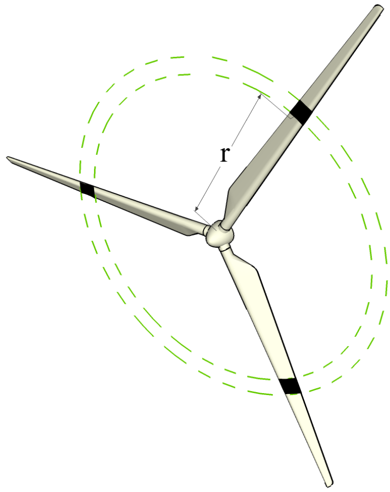


**Figure 1.4:** A blade element in BEM calculations

blades.

$$Q_t = \int_{r_h}^{R} q_t(r)dr \qquad \text{Aerodynamic thrust} \tag{1.4}$$

$$Q_a = \int_{r_h}^{R} q_a(r)dr \qquad \text{Aerodynamic torque} \tag{1.5}$$

In which $q_a(r)$ and $q_t(r)$ are torque and normal force to the blade elements, respectively. $r_h$ and $R$ are the hub and rotor radius. We skip the mathematics here and refer the interested reader to [Han08]. Calculating these quantities using BEM results in the following equations for aerodynamic torque and thrust:

$$Q_t = \frac{1}{2}\rho\pi R^2 C_t(\lambda,\beta)v_e^2 \tag{1.6}$$

$$Q_a = \frac{1}{2}\rho\pi R^3 C_q(\lambda,\beta)v_e^2 \tag{1.7}$$

Thereafter power is calculated as:

$$P_r = C_p(\lambda,\beta)P_v = \frac{1}{2}\rho\pi R^2 C_q(\lambda,\beta)v_e^3 \tag{1.8}$$

In which:

$$C_p(\lambda,\beta) = C_q(\lambda,\beta)\lambda = \frac{\text{Converted power}}{\text{Available power in the wind (in } \pi R^2)} \tag{1.9}$$

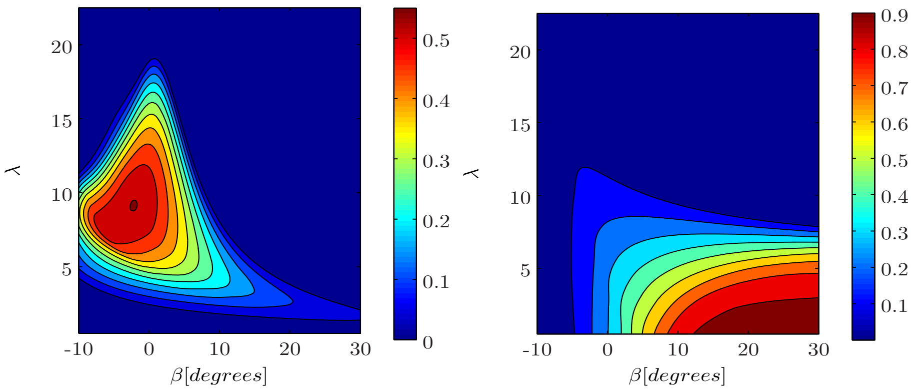


**Figure 1.5:** $C_p$ curve (left) and $C_t$ curve (right)

Therefore aerodynamic torque in terms of $C_p(\lambda, \beta)$ could be written as:

$$Q_a = \frac{1}{2\omega}\rho\pi R^2 C_p(\lambda, \beta) v_e^3 \tag{1.10}$$

where $\rho$ is the air density, $R$ is the rotor radius, $C_q$, $C_p$ and $C_t$ are torque, power and thrust coefficients, respectively. These coefficients are calculated using BEM and the results are stored in look-up tables which are functions of $\theta$ (collective pitch of the blades) and $\lambda$ (tip speed ratio). Tip speed ratio (TSR) is defined as $\lambda = R\omega/v_e$ in order to simplify mathematical formulations. A sample $C_p$ and $C_t$ are shown in figure 1.5.

## 1.4 Wind Turbine Control

In this section we will review control of wind turbines. First we will give a short description of what wind turbine control means and what our manipulating variables are for controlling such system. Afterward, control objectives will be discussed and we will explain how these objectives are mathematically formulated in different control methods. Later on, we will explain wind turbine control challenges (from a control engineer's point of view) and discuss limitations of performance in control systems and show how performance of wind turbine control could be limited. Then, different modes of operation for a turbine will be explained. Control variables and objectives are different for these modes of operation. Finally, different wind turbine types (with respect to control variables) are described in 1.4.4 and 1.4.5.

### 1.4.1 What does wind turbine control mean?

Wind turbines are essentially flexible structures in stochastic wind and we expect them to produce maximum power as long as the wind speed is below the rated value, and regulate their outputs, namely the rotational speed of the rotor and the generated power, when the wind speed goes beyond rated value. Finally they should shut down when wind speed passes a certain value called cut-out wind speed. All these goals should be achieved while keeping dynamic loads on the whole structure minimized. For variable speed-variable pitch wind turbines we have the possibility of manipulating pitch of the blades (see figure 1.3) and reaction torque of the generator in order to control the aforementioned outputs.

### 1.4.2 Objectives

Before we start to define control strategies and methods for wind turbines, firstly we need to have a clear understanding of wind turbine control objectives. Thereafter these objectives could be formulated differently for different control methods. For example in $\mathcal{H}_\infty$ and $\mu$-synthesis methods they are defined as frequency based weighting functions while in model predictive control and LQG they are normally achieved by appropriate tuning of weighting matrices in the objective functions.

The most basic control objective of a wind turbine is to maximize produced power for the entire life time of the machine or minimizing cost per unit of produced power. This means maximizing captured power (up until rated power) and prolonging life time of the turbine. The first objective is obtained by keeping the operating point close to maximum efficiency point and the second objective is achieved by minimizing the dynamic loads on the turbine. The maximum efficiency point is an operating point for a wind turbine where the power coefficient ($C_p$) is as close to the Betz limit as possible. Generally, maximizing power is considered in the partial load region and minimizing fatigue loads is mainly considered in full load region.

In the partial load region (below rated wind speed), the speed of the rotor is regulated by varying the reaction torque from the generator in order to stay close to the maximum aerodynamic efficiency. This is done in response to a measurement of the rotor speed and/or the generated power. In most cases pitch of the blades are kept constant in this region.

In the full load region (above rated wind speed), pitch of the blades is regulated to limit the power. As the wind speed increases, the amount of energy available in the wind increases at roughly the cube of the wind speed. High wind speed is not encountered frequently enough to make it economic to extract the total energy available and increase rated values of wind turbines. Therefore aerodynamic power limiting is used. At the rated wind speed the limit on output power of the wind turbine which is called rated power is reached. If the wind speed increases beyond rated wind speed, in order to keep turbine in its operating range, the excess power in the wind should be discarded. This is achieved by pitching the blades and letting the wind pass through the rotor disc without producing more torque on the rotor. In the full load region the rotational speed and generated power regulations should be achieved while trying to minimize dynamic loads on the wind turbine structure.

Apart from these basic objective, there are other control objectives for example ensuring safe operation as well as acoustic emission and power quality standards. However we are not going to cover them in this work.

### 1.4.3 Challenges

In this section we review the basic limits of performance for control systems which prove to be challenges for the wind turbine control, too.

#### 1.4.3.1 Input-output controllability

First we tackle the basic question of how well the turbine could be controlled. The answer to this question is addressed by input-output controllability [SP01]. Due to economic benefits there is a tendency for big wind turbines. As wind turbines become bigger, the structure becomes more flexible and input-output controllability will be reduced. Reduced input-output controllability of large wind turbines with flexible structures is a big challenge to the development of multi Mega-Watt machines. However this challenge could be resolved by introducing new sensors (e.g. pitot tubes [LMT05]) and new actuators (e.g. trailing edge flaps [And10]).

#### 1.4.3.2 Right-half plane zeros

Another point that should be considered is the presence of right-half plane zeros. Right-half plane zeros impose bounds on the performance of a system. Right-half plane zeros can emerge when in the dynamics of a system there is a subtraction between a fast dynamic and a slow dynamic. For example wind turbines dynamics from the pitch to the rotational speed of the rotor can be modeled with two competing dynamics. When the controller pitches out (increases pitch of the blades), the aerodynamic torque decreases and therefore rotational speed (having kept generator torque constant) decreases. However, pitching out results in reduced thrust force which causes the tower to move temporarily forward. This movement subsequently increases relative wind speed on the rotor and therefore results in a short increase in aerodynamic torque. The counteract effect of these two dynamics from the pitch to the rotational speed becomes prominent close to the rated wind speed, where the aerodynamics gain from the blade pitch to the thrust force is big, and therefore it produces a right-half plane zero in the dynamics of the wind turbine.

#### 1.4.3.3 Limited actuator bandwidth

Perfect control in which we get perfect regulation or tracking might demand big actuator bandwidth. However in reality actuator bandwidth is limited and therefore real and economical actuators could limit achievable performance. For example in wind turbines blade pitch actuators have limited pitch rate and acceleration.

#### 1.4.3.4 Model uncertainty

Uncertainty in the model is another factor that limits achievable performance. Without uncertainty in the system under control we could use feedforward control and avoid instability concerns (for stable systems) which is a result of feedback control. Although feedback control counteracts the effect of uncertainty at frequencies where the loop gain is large, uncertainty in the crossover frequency region can result in poor performance and even instability [SP01]. Therefore, it is important to take into account the effect of uncertainties and trade off performance of the system in favor of robustness of the controlled system.

### 1.4.4 Wind turbine modes of operation

Wind turbines operate in different modes of operation for different wind speeds. These modes are determined by minimum rotational speed, rated power and rated rotational speed, as well as cut-in, cut-out and rated wind speeds. The lowest wind speed at which the turbine starts to generate power is called the

| Regions | Wind speed | Rotational speed | Power |
|---|---|---|---|
| Region I: Low region | $v_{\text{cut in}} \leq v_e \leq v_1$ | $\omega_{\text{min}}$ | $P_{\text{max}}(v_e)$ |
| Region II: Mid region | $v_1 \leq v_e \leq v_2$ | $\omega_{\text{min}} \leq \omega \leq \omega_{\text{rated}}$ | $P_{\text{max}}(v_e)$ |
| Region III: High region | $v_2 \leq v_e \leq v_{\text{rated}}$ | $\omega_{\text{rated}}$ | $P_{\text{max}}(v_e)$ |
| Region IV: Top region | $v_{\text{rated}} \leq v_e \leq v_{\text{cut out}}$ | $\omega_{\text{rated}}$ | $P_{\text{rated}}$ |

**Table 1.1:** Different operating regions

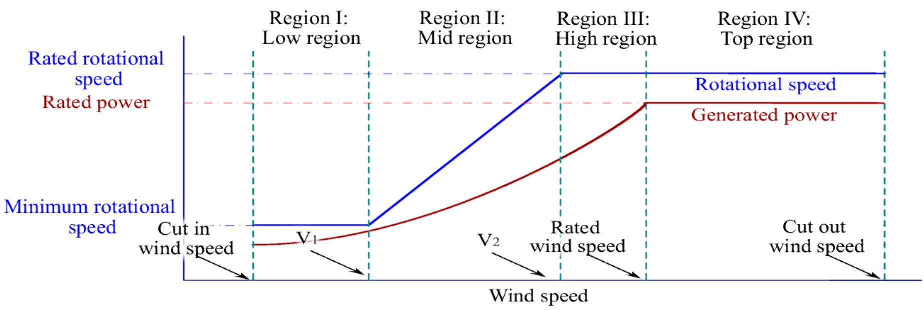


**Figure 1.6:** Rotational speed and generated power as functions of wind speed in different operating regions

cut-in wind speed. Cut-out wind speed is the speed at which the turbine is designed to shut down in order to prevent damage to it and at rated wind speed, wind turbine starts to produce rated power. Figure 1.6 shows rotational speed and generated power of a wind turbine in steady states as functions of wind speed and Table 1.1 shows different operating modes of a wind turbine. The first three regions (regions I,II and III) are called partial load where the machine is not operating at its rated values and the last region (region IV) is called full load where wind speed is above rated value and the turbine is producing its rated power while rotating at rated rotational speed. Control objective are different for the partial load and the full load. In the partial load the objective is to maximize captured power, while in the full load we try to regulate the produced power and the rotational speed at their rated values while minimizing the dynamic loads. The different control objectives need different control strategies. In this work we mainly focus on full load operation of the turbine.

### 1.4.5 Wind turbine types

Based on ability to pitch the blades and to have different rotational speed of the rotor, wind turbines can be categorized as:

- Fixed speed, fixed pitch
- Variable speed, fixed pitch
- Fixed speed, variable pitch
- Variable speed, variable pitch

In this work we consider a variable speed, variable pitch wind turbine in which in partial load the speed is adjusted such that the machine is kept at its maximum aerodynamic efficiency and in full load the blades pitch is adjusted such that the captured power is regulated at its rated value.

## 1.5 Contributions

This thesis deals with robust model based control design of wind turbines. The contributions are listed as follows:

- In Paper A an uncertain model of a wind turbine is obtained. The uncertainties are considered to be in the parameters of the linearized model and in the drivetrain damping and stiffness. A $DK$-iteration method is used to design a robust controller.
- In Paper B the results of Paper A are extended and several controllers are designed for different operating points. An extended Kalman filter is designed to estimate wind speed and finally a procedure based on estimated wind speed is formulated to calculate control inputs to the wind turbine.
- In Paper C a model predictive controller of a linear parameter varying system is formulated. In this work the scheduling variable of the system is considered to be known for the entire prediction horizon. The case study is a wind turbine with LIDAR measurements.
- In Paper D a robust model predictive control approach is used to control a wind turbine. In this paper it is shown that with some approximations the uncertainty could be considered to be in the gain of the system. This greatly reduces the computational complexity of the minimax optimization problem of the robust MPC.
- In Paper E, the ideas in Paper C and Paper D are combined and a robust model predictive control based on a linear parameter varying system with uncertain gain is formulated. The case study is a wind turbine whose pitch gain is considered to be uncertain due to uncertainties in its aerodynamics.

- In Paper F, the method proposed in Paper C is used to design an individual pitch controller.
- In Paper G the results of Paper B are extended, tower fore-aft dynamics are included, a detailed robust stability and performance analysis are presented and finally performance of the system is compared against a standard PI controller.
- In Paper H, the results of Paper F are extended. In this work blade dynamics are included and controller performance in terms of output regulations and damage equivalent loads are compared against a standard PI individual (cyclic) pitch controller.
- In Paper I, uncertainty in the wind propagation time which results in lead-lag error in the LIDAR measurements is addressed. This problem is solved by estimating the lead-lag error. An Extended Kalman filter is employed to estimate the effective wind speed and the results are compared against the LIDAR measurements using some signal processing techniques to find the temporal shift in the signal.

## 1.6 Outline of the thesis

This thesis is divided into two parts. The first part contains Chapters 1 to 4. It provides a summary report in which a short overview of the modeling and control design methods of wind turbines is given. The second part which contains Chapters 5 to 12 is a collection of publications. Chapter 2 is a brief review of wind turbine modeling. Subjects such as modeling wind speed for estimation, aerodynamics of wind turbines, modeling flexible structures and linearization of nonlinear dynamical systems are briefly reviewed. In Chapter 3 we turn our attention to using the obtained model from Chapter 2 to design controllers. In this chapter different model based and robust model based controller design methods are reviewed. The control design methods presented in this chapter are explained in details in Chapters 5 to 12.

In this thesis two different robust control design methods are employed. We have used parametric uncertainties to model wind turbines. Uncertainties are considered to be mainly in the parameters of the linear model. And the controllers are designed to be robust with respect to uncertain variations in those parameters. In Chapter 5 $DK$-iteration technique is used to design a robust controller. The model contains two degrees of freedom, namely rotation of the rotor and the drivetrain torsion. Only one linearized model is used to design the controller, therefore the simulations are performed only around the linearization point. In Chapter 6 the results of the previous chapter are extended. In this chapter different controllers are designed and a suitable switching strategy is formulated to employ different controllers for different operating regions. Using this approach we could cover the whole full load region. In Chapter 7 a special model predictive control for nonlinear systems is presented. In this method the scheduling variable that determines the operating point of the system is assumed to be known for the entire prediction horizon. The method is used on wind turbine control. We argue that LIDAR measurements could be used to find effective wind speed. The effective wind speed determines the operating point of wind turbines, and therefore using LIDARs we can have the scheduling variable of the wind turbine for the entire prediction horizon of the model predictive control. In Chapter 8 robust model predictive control is employed for wind turbine control. In this chapter we show that with approximation the uncertainty in the model could be considered to be in the gain of the system and therefore using special minimax formulations, we can reduce computational complexity of the controller. Chapter 9 basically combines the ideas presented in 7 and 8. In Chapter 10 we use the method presented in 7 to design an individual pitch controller. In Chapter 11, the idea presented in Chapter 6 is revisited, however this time, tower fore-aft is included and a thorough robust stability and performance analysis is presented and the results are compared against a standard PI controller. Chapter 12 employs the method presented in Chapter 7 and extends the results of Chapter 10 by including blade dynamics and giving performance comparisons in stochastic wind field against a standard individual pitch control. And finally Chapter 13 considers uncertainty in the wind propagation time and therefore uncertainty in the LIDAR measurements (lead-lag error) and solves the problem (compensates for the error) by estimating the effective wind speed on the rotor and comparing it with LIDAR measurements.

Chapter 2

# Wind Turbine Modeling

## 2.1 Introduction

Two different sets of models have been used in this work which will be explained in this chapter. Simulation models and controller design models. The simulation model contains most of the nonlinearities and degrees of freedom that we are able to model for a wind turbine. We have used FAST [JJ05] as our simulation model in the thesis. Simulation models are normally too complicated for control design, therefore we need to develop a design model as well. Design model or control oriented model has more trade offs, and the most important one is that the model should only include essential dynamics of the wind turbine and should be as simple as possible. This is because in many control design methods (such as $\mathcal{H}_\infty$ and $\mu$-Synthesis) the order of the resulting controller is at least equal to the order of the model and high order controllers become problematic in the implementation phase. Therefore we try to keep the model as simple as possible. There is always a trade off between simplicity and accuracy of the model. In this work we have used several design models which are slightly different.

## 2.2 Modeling for control and estimation

For modeling purposes, the whole wind turbine can be divided into 4 subsystems: aerodynamics subsystem, mechanical subsystem, electrical subsystem and actuator subsystem. The aerodynamic subsystem converts wind forces into mechanical torque and thrust on the rotor. The mechanical subsystem consists of the drivetrain, tower and blades. The drivetrain transfers rotor torque to the electrical generator. The tower holds the nacelle and withstands the thrust force and the blades transform wind forces into the aerodynamics torque and thrust. The generator subsystem converts mechanical energy to electrical energy and finally the blade-pitch and generator-torque actuator subsystems are part of the control system. To model the whole wind turbine, models of these subsystems are obtained and at the end they are connected together. A wind model is obtained and augmented with the wind turbine model to be used for wind speed estimation. Figure 2.1 shows the basic subsystems and their interactions.

The dominant dynamics of the wind turbine come from its flexible structure. Although there are dynamics in the aerodynamics of wind turbines (e.g. dynamic inflow and dynamic stall), for the sake of simplicity we always consider aerodynamics to be in the steady state. Several degrees of freedom could be considered to model the flexible structure, but for control design purposes, usually just a few important degrees of freedom are considered. Mostly the degrees of freedom whose eigen frequencies lie inside actuator bandwidth are considered

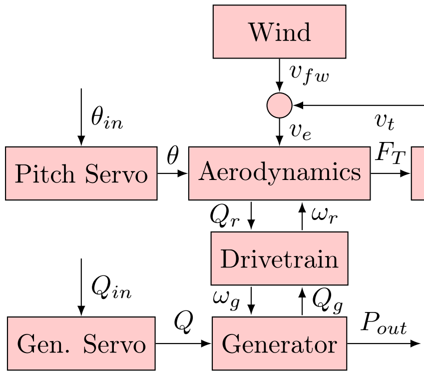


**Figure 2.1:** Wind turbine subsystems

otherwise including them into the design model is useless and makes the design model unnecessarily complicated. In figure 2.2, basic degrees of freedom which are normally considered in the design model are shown. However in this work we only consider three degrees of freedom, namely the rotation of the rotor, the drivetrain torsion and the tower fore-aft. And in one case for individual pitch we include a model of the blades. In individual pitch we have individual values for pitch of the blades opposed to collective pitch which is having one value for all the three blades.

### 2.2.1 Wind model

Wind has a stochastic nature both temporally (changes over time) and spatially (changes in the space). Wind turbines experiences both variations besides some variations which are the result of deterministic components in the wind profile. One of the deterministic components is wind shear which could be both vertical and horizontal. The vertical wind shear is the result of aerodynamic friction on the ground which decreases wind speed close to the surface. This effect is reduced by height. Wind shear could be described using an exponential law:

$$v_m(z) = v_m(z_{ref}) \left( \frac{z}{z_{ref}} \right)^{\alpha} \tag{2.1}$$

Where $\alpha$ is called surface roughness exponent and has different values for different types of terrain. $z_{ref}$ is reference height (e.g. $10m$).

As it was explained in chapter 1, tower shadow is another deterministic component.

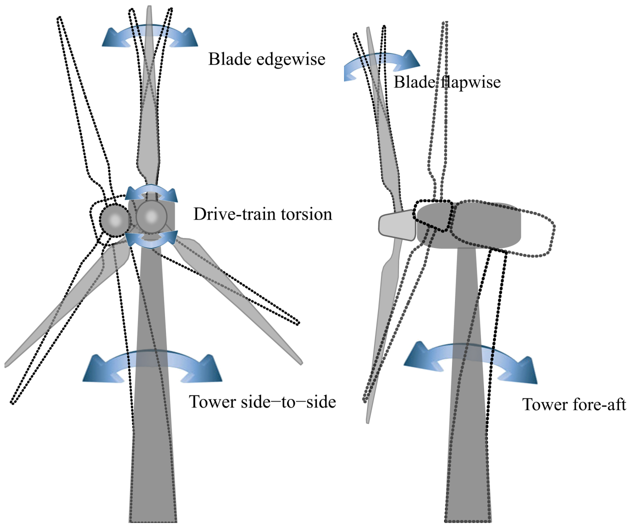


**Figure 2.2:** Basic degrees of freedom

From the above argument we conclude that there is no such a thing as wind speed for the wind turbine because different parts of the rotor swept area has different wind speeds. But for the sake of simplicity (unless otherwise stated) we consider the effect of the wind over the whole rotor swept area as a uniformly distributed wind speed profile with one value representing the wind speed. This value is called effective wind speed. Spatial distribution of wind is mainly considered when designing individual pitch control. This is because spatially turbulent wind smaller than rotor swept area causes unbalanced loadings on the structure and increases fatigue loads, and using individual pitch can reduce these loads.

Effective wind speed can be modeled as a complicated nonlinear stochastic process. However for practical control purposes it could be approximated by a linear model [JLSM06]. In this model the wind has two elements, mean value term ($v_m$) and turbulent term ($v_t$). The mean value term was explained in 1.1.1. The turbulent term could be modeled by the following transfer function:

$$v_e = v_m + v_t \tag{2.2}$$

In which:

$$v_m = \frac{1}{T}\int_{t-T/2}^{t+T/2} v(\tau)d\tau \tag{2.3}$$

$$v_t = \frac{k}{(p_1 s + 1)(p_2 s + 1)}e; \quad e \in N(0,1) \tag{2.4}$$

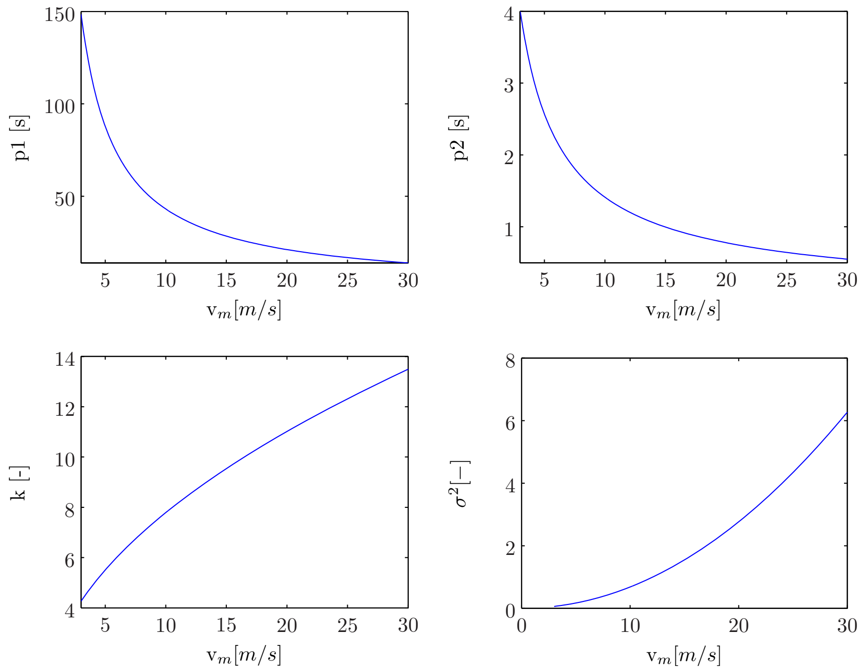


**Figure 2.3:** Parameters of the stochastic term in the wind model

The turbulent term in the state space form could be written as:

$$\begin{pmatrix} \dot{v}_t \\ \ddot{v}_t \end{pmatrix} = \begin{pmatrix} 0 & 1 \\ -\frac{1}{p_1 p_2} & -\frac{p_1+p_2}{p_1 p_2} \end{pmatrix} \begin{pmatrix} v_t \\ \dot{v}_t \end{pmatrix} + \begin{pmatrix} 0 \\ \frac{k}{p_1 p_2} \end{pmatrix} e \tag{2.5}$$

The parameters $p_1, p_2$ and $k$ which depend on the mean wind speed $v_m$ could be found by second order approximation of the wind power spectrum [JLSM06]. For the mean wind speed ($v_m$) we either keep it constant or consider it as a first order model with a big time constant.

### 2.2.2 Aerodynamics

If we consider behavior of the flexible structure of the turbine linear (most of the time this assumption holds) the main source of nonlinearity in the wind turbine modeling is its aerodynamics. Blade element momentum (BEM) theory [Han08] is used to find the nonlinear aerodynamic relations in the model. BEM theory explains the relation between wind speed, rotational speed and pitch angle of a wind turbine to the very important aerodynamic torque and thrust on the rotor. More details on the BEM theory was given in the section 1.3.1.2. Based on this theory torque and thrust on the rotor could be written as functions below:

$$Q_a = \frac{1}{2}\frac{1}{\omega_r}\rho\pi R^2 v_e^3 C_p(\theta,\omega,v_e) \qquad \text{Aerodynamic torque} \tag{2.6}$$

$$Q_t = \frac{1}{2}\rho\pi R^2 v_e^2 C_t(\theta,\omega,v_e) \qquad \text{Aerodynamic thrust} \tag{2.7}$$

### 2.2.3 Flexible structure

If we assume aerodynamics to be in steady state (as explained earlier), the dynamics of the wind turbine come from its flexible structure. In this section we will give a short overview of different methods for modeling flexible structures and afterward we will give models of the flexible components of wind turbines.

Analytical models of a structure can be derived from physical laws, such as Newton's laws of motion, Lagrange's equations of motion, or D'Alembert's principle, which collectively called first principle modeling. Another way is to derive them from finite-element models or apply system identification methods on data from the behavior of structures. The models can be represented either in the time domain in the form of differential equations, or in the frequency domain in the form of transfer functions.

In this work we use linear differential equations to represent structural models in the time domain. The differential equations could be written either in the form of second-order differential equations or in the form of first-order differential equations (as a state-space representation).

Structural engineers normally use the second-order differential equations. The state-space model, on the other hand, is a standard model used by control engineers. This is because most linear control system analysis and design methods are given based on the state-space models. Nevertheless, Transforming a model from second order differential equation to state space representation and vice versa can be easily done. In the following we show how to do the transformation for a simple mass-spring-damper system with an external force $f$ as an input:

Second-order differential equation:

$$m\ddot{x} + c\dot{x} + kx = f$$

State space representation:

$$\dot{x}_1 = x_2$$
$$\dot{x}_2 = -\frac{c}{m}x_2 - \frac{k}{m}x_1 + f$$

We use this transformation several times to represent structural models in the state space form.

Typically, the second-order models are represented either in the nodal coordinates, and are called nodal models, or in the modal coordinates, and are called modal models. The nodal models are derived in nodal coordinates, in terms of nodal displacements, velocities, and accelerations. The model is characterized by the mass, stiffness, and damping matrices, and by the sensors and actuators locations. These models are typically obtained from the finite-element codes or from other Computer-Aided-Design software [Gaw04]. For example HAWC2 [LH], which is a tool to design wind turbine simulation models, uses this approach to model flexible structure of wind turbines.

The second-order models could also be defined in modal coordinates. These coordinates are often used in the dynamics analysis of complex structures modeled by the finite elements to reduce the order of a system. It is also used in the system identification procedures, where modal representation is a natural outcome of the test. For more details on nodal models and modal models see [Gaw04]. The order of a complex flexible structure can be reduced significantly by using modal models while the accuracy of the model does not suffer too much. Some wind turbine simulation codes such as FAST [JJ05] use modal model approach. In modal models approach, behavior of a structure can be represented as a combination of some fixed patterns of deformations. These patterns are called mode shapes. In this work we have used the first (and the most significant) mode shapes of a wind turbine tower, drive train and in one case blades to model behavior of the flexible structure.

#### 2.2.3.1 Model of the Drivetrain

A simple mass-spring-damper is used to model the torsional degree of freedom in the drive train. Figure 2.4 shows the way two inertial objects, namely the rotor and the generator, are connected through a flexible link which has torsion stiffness of $K_d$ and damping of $C_d$. Dynamics of the drivetrain could be written

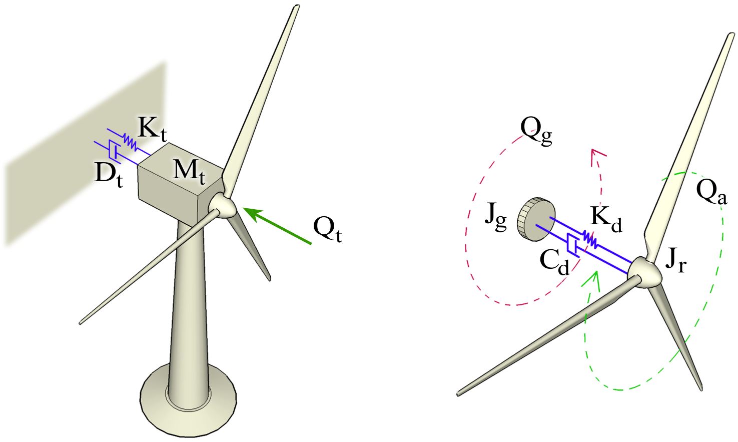


**Figure 2.4:** Modeling flexible tower (left) and drivetrain (right)

as:

$$\dot{\xi}_r = \omega_r \tag{2.8}$$

$$\dot{\xi}_g = \omega_g \tag{2.9}$$

$$J_r \dot{\omega}_r = Q_a - C_d(\omega_r - \omega_g) - K_d(\xi_r - \xi_g) \tag{2.10}$$

$$J_g \dot{\omega}_g = C_d(\omega_r - \omega_g) + K_d(\xi_r - \xi_g) - Q_g \tag{2.11}$$

$Q_a$ and $Q_g$ are aerodynamic and generator reaction torques. $J_r$ and $J_g$ are the rotor and generator inertia translated to the low speed shaft. This means in order to find $J_g$ to be used in the above equation from the given generator inertia, it should be multiplied by $N_g^2$ which $N_g$ is the gearbox ratio. $\omega_r$ and $\omega_g$ are the rotational speed of the rotor and generator and finally $\xi_r$ and $\xi_g$ are their corresponding azimuth angles. We are not interested in the absolute value of the azimuth angles, therefore we use their difference which we call $\phi = \xi_r - \xi_g$. With the new variable being introduced, dynamics of the drivetrain could be written as:

$$\dot{\phi}_r = \omega_r - \omega_g \tag{2.12}$$

$$J_r \dot{\omega}_r = Q_a - C_d(\omega_r - \omega_g) - K_d \phi \tag{2.13}$$

$$J_g \dot{\omega}_g = C_d(\omega_r - \omega_g) + K_d \phi - Q_g \tag{2.14}$$

#### 2.2.3.2 Model of the Tower

In order to model dynamics of the tower, which we have only considered the fore-aft degree of freedom, we have used simple mass-spring-damper model. Figure

2.2 shows movement of the tower in fore-aft direction. Figure 2.4 shows how the tower dynamics are modeled. The dynamics can be written as:

$$\dot{x}_1 = x_2 \tag{2.15}$$

$$\dot{x}_2 = Q_t - \frac{C_t}{M_t}x_2 - \frac{K_t}{M_t}x_1 \tag{2.16}$$

in which $x_1$ and $x_2$ are tower top displacement and velocity respectively. $M_t, C_t$ and $K_t$ are mass, damping and stiffness of the dynamics of the tower and $Q_t$ is the aerodynamic thrust force.

### 2.2.4 Actuator dynamics

A first order and a second order model are used to model the generator reaction torque actuator and the pitch actuators respectively. The transfer function could be written as:

$$\theta(s) = \frac{1}{s^2 + 2\zeta_\theta\omega_\theta s + \omega_\theta^2}\theta_i(s) \qquad \omega_\theta = 1, \zeta_\theta = 0.7$$

$$Q_g(s) = \frac{1}{\tau_g s + 1}Q_i(s) \qquad \tau_g = 0.1$$

In which $\omega_\theta, \zeta_\theta$ and $\tau_g$ determine dynamics of the actuators.

## 2.3 Simulation model

In order to close the loop and test performance of our controller we need a simulation model. The simulation model behavior should be as close to behavior of the real system as possible. We have used different simulation models to verify closed loop behavior in different simulation scenarios. Normally the simulation models include all degrees of freedom and the nonlinearities that could be modeled mathematically. For wind turbines IEC [iec05] gives a list of standard simulation scenarios. These simulation scenarios are to check different load cases which are categorized as extreme and fatigue load cases. There are several simulation models available. For example HAWC2 is a code intended for calculating wind turbine response in the time domain. It has been developed within the years 2003-2006 at the aeroelastic design research program at Risø, National Laboratory, Denmark [LH]. Another publicly available program for simulating wind turbine behaviors is FAST [JJ05]. The FAST (Fatigue, Aerodynamics, Structures, and Turbulence) Code is a comprehensive aeroelastic simulator capable of predicting both the extreme and fatigue loads of two-and three-bladed horizontal-axis wind turbines. In this work FAST is used as the simulation model and the 5MW reference wind turbine is used as the plant [JBMS09]. In the simulation model 10 degrees of freedom are enabled which are: generator, drivetrain torsion, 1st and 2nd tower fore-aft, 1st and 2nd tower side-side, 1st and 2nd blade flapwise, 1st blade edgewise degrees of freedom.

## 2.4 Linearized models

There are different methods to derive linear model of a wind turbine for controller design purposes. We will give a short summary of the methods we have employed in this work.

### 2.4.1 First principle modeling

In the first principle modeling the whole system under study is divided into different parts and sub-models based on basic equations of motions are found for each part. At the end the obtained equations are linked together based on the interaction of the parts in the whole system. Taylor series expansion is used to find linear approximations of the nonlinear functions. To do this firstly we need to determine the steady state operating points of the system, then linearize the nonlinearities around the obtained points. The following equations could be used to find linearized model of the aerodynamic torque and thrust, and electrical power:

$$Q_r = Q_r^* + \begin{bmatrix} \frac{\partial Q_r}{\partial \theta} & \frac{\partial Q_r}{\partial \omega_r} & \frac{\partial Q_r}{\partial v_e} \end{bmatrix}_{(\theta^*, \omega_r^*, v_e^*)} \begin{bmatrix} \Delta\theta \\ \Delta\omega_r \\ \Delta v_e \end{bmatrix} + \text{H.O.T.}$$

$$Q_t = Q_t^* + \begin{bmatrix} \frac{\partial Q_t}{\partial \theta} & \frac{\partial Q_t}{\partial \omega_r} & \frac{\partial Q_t}{\partial v_e} \end{bmatrix}_{(\theta^*, \omega_r^*, v_e^*)} \begin{bmatrix} \Delta\theta \\ \Delta\omega_r \\ \Delta v_e \end{bmatrix} + \text{H.O.T.}$$

$$P_e = P_e^* + \begin{bmatrix} \frac{\partial P_e}{\partial Q_g} & \frac{\partial P_e}{\partial \omega_g} \end{bmatrix}_{(\omega_g^*, Q_g^*)} \begin{bmatrix} \Delta Q_g \\ \Delta\omega_g \end{bmatrix} + \text{H.O.T.}$$

in which the linearized terms for aerodynamic torque are:

$$\left.\frac{\partial Q_r}{\partial \theta}\right|_{(\theta^*,\omega_r^*,v_e^*)} = \frac{1}{2}\frac{1}{\omega_r}\rho\pi R^2 v_e^3 \left.\frac{\partial C_p}{\partial \theta}\right|_{(\theta^*,\omega_r^*,v_e^*)}$$
$$\left.\frac{\partial Q_r}{\partial \omega_r}\right|_{(\theta^*,\omega_r^*,v_e^*)} = \frac{1}{2}\rho\pi R^2 v_e^3 (-\frac{1}{\omega_r^2}C_p + \frac{1}{\omega_r}\frac{\partial C_p}{\partial \omega_r})\Big|_{(\theta^*,\omega_r^*,v_e^*)}$$
$$\left.\frac{\partial Q_r}{\partial v_e}\right|_{(\theta^*,\omega_r^*,v_e^*)} = \frac{1}{2}\frac{1}{\omega_r}\rho\pi R^2 (3v_e^2 C_p + v_e^3\frac{\partial C_p}{\partial v_e})\Big|_{(\theta^*,\omega_r^*,v_e^*)}$$

and for aerodynamic thrust are:

$$\left.\frac{\partial Q_t}{\partial \theta}\right|_{(\theta^*,\omega_r^*,v_e^*)} = \frac{1}{2}\rho\pi R^2 v_e^2 \left.\frac{\partial C_t}{\partial \theta}\right|_{(\theta^*,\omega_r^*,v_e^*)}$$
$$\left.\frac{\partial Q_t}{\partial \omega_r}\right|_{(\theta^*,\omega_r^*,v_e^*)} = \frac{1}{2}\rho\pi R^2 v_e^2 \left.\frac{\partial C_t}{\partial \omega_r}\right|_{(\theta^*,\omega_r^*,v_e^*)}$$
$$\left.\frac{\partial Q_t}{\partial v_e}\right|_{(\theta^*,\omega_r^*,v_e^*)} = \frac{1}{2}\rho\pi R^2 (2v_e C_t + v_e^2\frac{\partial C_t}{\partial v_e})\Big|_{(\theta^*,\omega_r^*,v_e^*)}$$

and for generated power are:

$$\left.\frac{\partial P_e}{\partial Q_g}\right|_{(\omega_g^*,Q_g^*)} = \omega_g^* \qquad \left.\frac{\partial P_e}{\partial \omega_g}\right|_{(\omega_g^*,Q_g^*)} = Q_g^*$$

In the equations above, H.O.T. stands for higher order terms. For the sake of simplicity in notations we use $\theta$, $\omega$ and $v_e$ instead of $\Delta\theta$, $\Delta\omega$ and $\Delta v_e$ respectively from now on.

### 2.4.2 System identification

Basically system identification uses different methods to build mathematical models of dynamical systems from measured data. In this work we have used greybox modeling and output error method to find linear design models. As we did not have access to real measurements we used simulation models to produce time series of wind turbine behavior and used system identification on the obtained data to find appropriate models.

In greybox modeling the basic structure of the dynamical system is known, however the parameters of the model are not known. After formulating the model with unknown parameters, system identification techniques can be used to estimate them. To clarify our method we explain our approach to identify parameters of the tower fore-aft dynamics.

The state space model of the tower fore-aft which is modeled as a mass-spring-damper is:

$$\begin{pmatrix} \dot{x}_1 \\ \dot{x}_2 \end{pmatrix} = \begin{pmatrix} 0 & 1 \\ -c_t/m_t & -k_t/m_t \end{pmatrix} \begin{pmatrix} x_1 \\ x_2 \end{pmatrix} + \begin{pmatrix} 0 \\ 1/m_t \end{pmatrix} Q_t \tag{2.17}$$

In which $\begin{pmatrix} x_1 & x_2 \end{pmatrix}^T$ are the states of the system, $m_t, c_t$ and $k_t$ are tower mass, damping and stiffness respectively and $Q_t$ is the thrust force that acts on the tower in the fore-aft direction. Hypothetically we assume we have the thrust force (we put a sensor in the FAST simulation model to measure the thrust force) and tower fore-aft velocity. Having these measurements we can obtain parameters of the mass-spring-damper model of the tower in the fore-aft direction.

### 2.4.3 Numerical linearization

In the numerical linearization method, the nonlinear model is perturbed at its equilibrium point with small perturbations from the inputs. To do so, firstly the equilibrium points of the nonlinear system is found, for example for a nonlinear system of the form $\dot{x} = f(x, u)$, the equilibrium is the set $\{x^*, u^*\}$ for which $f(x^*, u^*) = 0$. Thereafter we apply small perturbations to the nonlinear system and we get:

$$\dot{x} = f(x^* + \Delta x, u^* + \Delta u) \tag{2.18}$$

$$= \underbrace{f(x^*, u^*)}_{0} + \left.\frac{\partial f}{\partial x}\right|_* \Delta x + \left.\frac{\partial f}{\partial u}\right|_* \Delta u \tag{2.19}$$

And as we are at the equilibrium point we get:

$$\dot{x} = \left.\frac{\partial f}{\partial x}\right|_* \Delta x + \left.\frac{\partial f}{\partial u}\right|_* \Delta u \tag{2.20}$$

Therefore by measureing $\Delta x$ and $\Delta u$ we can calculate the derivatives $\left.\frac{\partial f}{\partial x}\right|_*$ and $\left.\frac{\partial f}{\partial u}\right|_*$ which give us the linear model parameters. This method is used in the linearization procedure of FAST.

Chapter 3

# Wind Turbine Control

## 3.1 Introduction

The power in the wind pass through rotor disc of a turbine is proportional to the square of the rotor radius. Therefore in order to increase produced power by a single turbine which means reduction in the cost of wind power production, it seems reasonable to increase rotor radius as much as possible. This explains the almost exponential growth in the size of wind turbines in the past two decades. However this growth is limited by several factors of which control is a key factor. Big wind turbines are aeroelastic structures in tempo-spatial stochastic wind. Control of such a system introduces a challenging problem in control engineering.

Control can play an essential role in reducing power production costs. Because control methods on one hand can decrease the cost of energy by keeping the turbine close to its maximum efficiency and on the other hand reduce structural fatigue and therefore increase lifetime of the wind turbine. Control methods can also enable production of bigger turbines with more power generation capacity. There are several methods for wind turbine control ranging from classical control methods [LC00] which are the most used methods in real applications, to advanced control methods which have been the focus of research in the past few years [LPW09]; gain scheduling [BBM06], adaptive control [JF08], MIMO methods [GC08], nonlinear control [Tho06], robust control [Øst08], model predictive control [Hen07], $\mu$-Synthesis design [MNP11] are just a few. Advanced control methods are thought to be the future of wind turbine control as they can employ new generations of sensors on wind turbines (e.g. LIDAR [HHW06]), new generation of actuators (e.g. trailing edge flaps [And10]) and also conveniently treat the turbine as a MIMO system. The last feature seems to become more important than before as wind turbines become bigger and more flexible which make decoupling different modes and designing controller for each mode more difficult.

In this chapter a brief introduction to different control methods will be given. We start by introducing gain scheduled PI controller developed at the national renewable energy laboratory (NREL), the United States, which is a standard controller on reference baseline wind turbine [JBMS09]. We have used this controller as a benchmark against some model based controllers we have designed. Afterwards a brief introduction to different model based control methods will be given. In the next chapters we will explain each controller in more details.

## 3.2 Classical gain scheduled PI

The conventional approach for controlling a wind turbine using PI controllers relies on the design of two basic control systems: a generator-torque controller and a full-span rotor-collective blade-pitch controller. The two control systems are designed to work independently. The goal of the generator-torque controller is to maximize captured power below the rated operating point and regulate the produced power above this point. The goal of the blade-pitch controller is to regulate generator speed above the rated operation point [JBMS09]. Generator rotational speed is used as the main measurement to control both power and rotational speed. A low pass filter is designed to remove measurement noise and then the filtered signal is fed to the generator torque and the collective pitch controllers. In the top region (full load region) the generator torque is inversely proportional to the generator speed.

$$Q_g = \frac{P_0}{\omega_g} \tag{3.1}$$

Therefore the generator torque signal can be calculated as:

$$\Delta Q_g = \frac{P_0}{\omega_{g,0}} - \frac{P_0}{\omega_{g,0}^2}\Delta\omega_g \tag{3.2}$$

And using a PI controller, the collective pitch signal is calculated as:

$$\Delta\theta = K_P(\theta)\Delta\omega_g + K_I(\theta)\int_0^t \Delta\omega_g d\tau \tag{3.3}$$

In which $K_P(\theta)$ and $K_I(\theta)$ are proportional and integral gains which are scheduled based on pitch angle of the blades. We will not go into the details of how these gains are calculated. For more details we refer the reader to [JBMS09].

## 3.3 Model Based Control

As it was mentioned earlier advanced model based control are thought to be the future of wind turbine control. First we introduce some model based control methods without considering uncertainty in the system. In this context $\mathcal{H}_\infty$ and model predictive control (MPC) are explained. Afterwards we take some steps further and include uncertainties in the models and design robust controllers. $\mu$-synthesis and robust model predictive control are the two robust controllers which we have employed. The wind turbine in this work is treated as a MIMO system with pitch ($\theta_i$) and generator reaction torque ($Q_i$) as inputs and rotor rotational speed ($\omega_r$), generated power ($P_e$) and sometimes tower fore-aft velocity ($v_t$) as outputs.

### 3.3.1 $\mathcal{H}_\infty$ control design

In the frequency domain we can formulate wind turbine controller design objectives in the form of minimizing some norm of the system from disturbances, which are the wind speed fluctuations and measurement noises, to the system outputs, which are rotational speed, generated power and tower fore-aft velocity. If we do not account for the uncertainties in the model, the problem is called nominal performance problem.

$\mathcal{H}_\infty$ control theory [SP01] is used to solve the nominal performance problem. In this problem the perturbation matrix (uncertainty in the model) is considered to be zero and then in order to find the controller the following optimization problem is solved:

$$K(s) = \arg \min_{K \in \mathcal{K}} \| \mathcal{W}_o F_l(P, K) \mathcal{W}_i(j\omega) \|_{\mathcal{H}_\infty} \tag{3.4}$$

$F_l(P, K)$ is the lower linear fractional transformation (LFT) of the plant $P$ and the controller $K$ (see figure 3.1). $\mathcal{W}_i$ and $\mathcal{W}_o$ are frequency dependent weighting matrices on disturbances and exogenous outputs respectively of the form:

$$\begin{aligned} \mathcal{W}_o &= diag(\mathcal{W}_{o1}, \ldots, \mathcal{W}_{o6}) \\ \mathcal{W}_i &= diag(\mathcal{W}_{i1}, \ldots, \mathcal{W}_{i5}) \end{aligned} \tag{3.5}$$

$\mathcal{W}_i$ and $\mathcal{W}_o$ are our means to enforce our control objectives on the system. For example a low pass filter is considered on the input of wind speed as a source of disturbance with limited bandwidth and high pass filters are considered to show precision of our measurement sensors in low frequencies and effect of noise in high frequencies. For regulating power and rotational speed, $P_e$, $\omega$ are penalized using low pass filters, as high frequency fluctuations on these outputs are out of our actuator bandwidth and the controller should not overreact to them. $\int \omega$ is introduced and penalized to achieve offset free regulation. For minimizing fatigue loads on the tower $\dot{x}_t$ is penalized again using low pass filters.

Figure 3.1 shows nominal performance configuration in which input disturbances

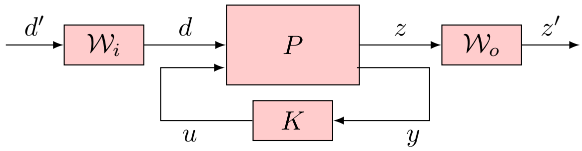


**Figure 3.1:** Nominal performance configuration

($d$) and exogenous outputs ($z$) are:

$$d = v_e \qquad \text{Wind Speed}$$

$$z = \begin{pmatrix} \theta \\ Q_g \\ \omega \\ \dot{x}_t \\ \int \omega \\ P_e \end{pmatrix} \begin{array}{l} \text{Pitch reference} \\ \text{Generator reaction torque reference} \\ \text{Error on the rotational speed} \\ \text{Tower fore-aft velocity} \\ \text{Integral of rotational speed error} \\ \text{Generated power error} \end{array}$$

By solving the optimization problem of 3.4, we are trying to find a controller in the set of all stabilizing controllers that minimizes $\mathcal{H}_\infty$-norm of the weighted sensitivity function. This means we try to minimize the peak frequency of $\mathcal{W}_o S \mathcal{W}_i(j\omega)$. The resulting controller guarantees nominal performance if:

$$\| \mathcal{W}_o F_l(P, K) \mathcal{W}_i(j\omega) \|_{\mathcal{H}_\infty} < 1 \tag{3.6}$$

Which means good attenuation of the effect of the disturbances on the outputs. In chapter 5 we will give more details on this approach.

### 3.3.2 Model Predictive Control (MPC)

Model predictive control (MPC) has been an active area of research and has been successfully applied on different applications in the last decades ([QB96]). The reason for its success is its straightforward ability to handle constraints. Moreover it can employ feedforward measurements in its formulation and can easily be extended to MIMO systems. However the main drawback of MPC was its on-line computational complexity which kept its applications to systems with relatively slow dynamics for a while. Fortunately with the rapid progress of fast computations, better optimization algorithms, off-line computations using multi-parametric programming ([Bao05]) and dedicated algorithms and hardware, its applications have been extended to even very fast dynamical systems such as DC-DC converters ([Gey05]).

Basically MPC uses a *model* of the plant to *predict* its future behavior in order to compute appropriate control signals to *control* the outputs/states of the plant. To do so, at each sample time MPC uses the current measurement of the outputs/states and solves an optimization problem. The result of the optimization problem is a sequence of control inputs of which only the first element is applied to the plant and the procedure is repeated at the next sample time with new measurements ([Mac02]). This approach is called receding horizon control. Therefore basic elements of MPC are: a model of the plant to predict its future, a cost function which reflects control objectives, constraints on inputs and states/outputs, an optimization algorithm and the receding horizon principle.

MPC is an effective tool to deal with multivariable constrained control problems [BM99]. As wind turbines are MIMO systems [GC08] with constraints on inputs and outputs, using MPC seems to be effective. MPC proved to give satisfactory results for offshore wind turbine control [Hen10] and trailing edge flap control of wind turbines [CPBWH11].

### 3.3.3 MPC with known scheduling variable

Depending on the type of the model used for prediction in MPC, the control problem is called linear MPC, hybrid MPC, nonlinear MPC, etc. As it was explained in 1.3.1 because of the nonlinearity in aerodynamics, wind turbines are highly nonlinear systems. Using the obtained nonlinear model directly in MPC formulation results in a formidable nonlinear MPC problem [HPH11]. Nonlinear MPC is normally computationally very expensive and generally there is no guarantee that the solution of the optimization problem is a global optimum.

In this work we extend the idea of linear MPC using linear parameter varying (LPV) systems to formulate a tractable predictive control of nonlinear systems. To do so, we use future values of a disturbance to the system (namely effective wind speed) that acts as the scheduling variable in the model. We assume that the scheduling variable is known for the entire prediction horizon and the operating point of the system mainly depends on the scheduling variable. With the advances in LIDAR technology ([HHW06]) it is possible to measure wind speed ahead of the turbine and this enables us to have the scheduling variable of the wind turbine for the entire prediction horizon. Chapter 7 gives more details on this subject. We start by assuming perfect LIDAR measurements, however LIDAR measurements could be uncertain. We have considered an important uncertainty in the LIDAR measurements namely uncertainty in the the wind propagation, which is the traveling time of wind from the LIDAR measurement point to the rotor. We have used an Extended Kalman filter to estimate the effective wind speed on the rotor and then estimated the propagation time and hence corrected the measurements. More details on this can be found in chapter 13.

## 3.4 Robust Model Based Control

In the previous section we introduced some control methods based on model of the system. However there are always discrepancies between the model and the real plant. A good controller should give satisfactory results (in terms of stability and performance) in the presence of these discrepancies. Such a controller is called to be robust with respect to model mismatches and the procedure to design such a controller is called robust control design. A control system is robust if it is insensitive to differences between the actual system and the model of the system which was used to design the controller. The discrepancies between the model and the real plant are referred to as model/plant mismatch or simply model uncertainty.

Often robust stability is not the main goal of robust control design. In the case of wind turbine design which wind speed fluctuations are considered as disturbances, we try to reduce the effect of these fluctuations on rotational speed and generated power while keeping dynamical loads minimized. The dynamics from the disturbances to the outputs are dependent on the uncertainties in the system and it is the robust controllers' task to reduce these effects on the performance of the system. In our problem before instability occurs, the performance has degraded to an unacceptable level. Therefore our main goal is to pursue robust performance design rather than robust stability design.

Two methods are used to design robust controller, a $\mu$-synthesis controller which will be introduced in section 3.4.1 and explained in details in chapter 6 and a robust model predictive controller which will be introduced in 3.4.2 and explained in details in chapter 8. In both methods we have considered parametric uncertainties in the parameters of the linear model.

### 3.4.1 $\mu$-Synthesis control design

Robust performance analysis examines if the performance objective is satisfied for all possible plants in the uncertainty set. The robust performance condition can be cast into a robust stability problem with an additional perturbation block that defines $\mathcal{H}_\infty$ performance specifications (see figure 3.2). Therefore the perturbation matrix $\Delta'$ of the system could be augmented with an additional

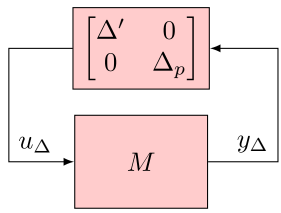


**Figure 3.2:** $M - \Delta$ structure of the robust performance problem

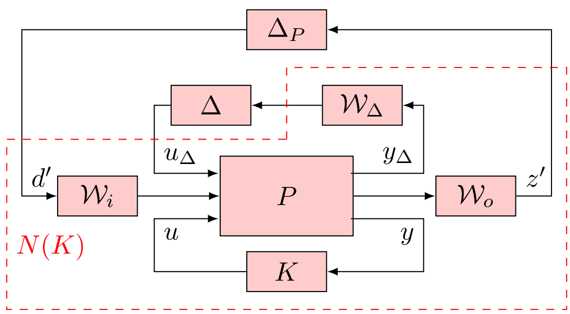


**Figure 3.3:** System setup for robust performance problem

perturbation block $\Delta_p$ which specifies performance of the system:

$$\Delta = \begin{pmatrix} \Delta' & 0 \\ 0 & \Delta_p \end{pmatrix} \tag{3.7}$$

For a closed loop $M - \Delta$ structure robust stability condition is [SP01]:

$$\| M\Delta \|_{\mathcal{H}_\infty} < 1 \tag{3.8}$$

When we have structure in the uncertainty block $\Delta$ we can exploit it and reduce conservativeness of the controller. Structured singular value (also known as $\mu$) is a tool that utilizes structure in the uncertainty block to analysis robust stability of the system. Here we have used structured singular value to solve the robust performance problem as explained above by transforming it into a robust stability problem. The structured singular value of a complex matrix $M$ with respect to a class of perturbations $\Delta$ is given by.

$$\mu_\Delta(M) \triangleq \frac{1}{\inf\{\sigma_{max}(\Delta) | \det(I - M\Delta) = 0\}}, \qquad \Delta \in \boldsymbol{\Delta} \tag{3.9}$$

The structured singular value $\mu$ is a very powerful tool for analysis of robust performance with a given controller. However in order to design a controller, we need a synthesis tool. To that end, a scaled version of the upper bound of $\mu$ is used for controller synthesis. The problem is formulated in the following form:

$$\mu_{\Delta}(N(K)) \leq \min_{D \in \mathcal{D}} \sigma(DN(K)D^{-1}) \tag{3.10}$$

Now, the synthesis problem can be cast into the following optimization problem in which one tries to to find a controller that minimizes the peak value over frequency of this upper bound:

$$\min_{K \in \mathcal{K}} (\min_{D \in \mathcal{D}} \parallel DN(K)D^{-1} \parallel_{\infty}) \tag{3.11}$$

This problem is solved by an iterative approach called $DK$-iteration. For detailed explanations on the method and notations the reader is referred to [SP01] and details of the application of $\mu$-synthesis method on robust control of wind turbines are given in chapters 6 and 11.

### 3.4.2 Robust MPC

Nominal MPC proved to give satisfactory results for offshore wind turbine control [Hen10] and trailing edge flap control of wind turbines [CPBWH11]. However these works have not taken into account uncertainty in the design model and this problem has been bypassed by trial-error and extensive simulations to get the best performance from the controllers. Based on this argument extending nominal MPC of wind turbines to robust MPC and including model uncertainties in the design seems to be natural. The robust MPC method acts as a controller that is aware of system uncertainties and it becomes less demanding where it knows the model is uncertain. Wind turbines are complex nonlinear systems and the nonlinearity mainly comes from the aerodynamics. Quasi stationary calculations of the aerodynamics result in aerodynamic torque and thrust as nonlinear functions of wind speed, blade pitch and rotational speed. Linearization is normally used to solve the control problem and estimated wind speed is used to find the operating point. However there is error in this estimation. We have used a mapping of the confidence interval of the estimated wind speed to the parameters of the linearized model, which has resulted in uncertainties in these parameters. These uncertainties are dealt with using robust MPC. The interesting fact that we have employed here to simplify the optimization problem is that when we do the mapping of the confidence interval in the uncertainties of the linearized model, we observe that uncertainties are significant only in the gain matrix. This will provide us with a special structure of the optimization problem that is much easier to deal with than the normal robust MPC problems.

MPC uses a model of the system (to be controlled) to predict its future behavior. In nominal MPC the prediction of the output is a single value and it is calculated based on one model. However in robust MPC because the model is uncertain, this prediction is no longer a unique value but it is a set instead. An approach to tackle the problem with an uncertain model in MPC is to try to consider the most pessimistic situation with respect to uncertainties. This means maximizing the cost function on the uncertainty set. After maximization, we minimize the obtained cost function over control inputs as we do in nominal MPC. This approach is called minimax MPC and it is a common solution to robust MPC problems [LÖ3]. In chapter 8 we will give more details about this approach.

### 3.4.3 Robust MPC with known scheduling variable

In section 3.3.3 we introduced model predictive control of a system with known scheduling variable. In that formulation we considered a nominal model of the system. As we discussed earlier there are always discrepancies between plant and controller, therefore we have formulated a robust model predictive control problem of wind turbines when wind speed (as the scheduling variable) is known for the entire prediction horizon and there are uncertainties in aerodynamic gains of the pitch actuator. More details on this is given in chapter 9.

### 3.4.4 Kalman filter and extended Kalman filter

Throughout the thesis several times we have employed Kalman filters for state estimation and extended Kalman filters for wind speed estimation. Here we give a brief introduction to Kalman filtering and its nonlinear extension, extended Kalman filtering [GA08].

The Kalman filter is a recursive estimator. This means that in order to estimate the current state, only the current measurement and the estimated state from the previous time step are needed. At each time step, the state of the filter is represented by two variables, $\hat{x}_{k|k}$ the *a posteriori state estimate* at time $k$ given observations up to and including at time k and $P_{k|k}$ the *a posteriori error covariance matrix* (a measure of the estimated accuracy of the state estimate).

For a better understanding, the Kalman filter can be divided into two basic phases, predict phase and update phase. In the predict phase, the state estimate from the previous time step $\hat{x}_{k-1|k-1}$ with the system input $u_{k-1}$ are used to produce an estimate of the state at the current time step $\hat{x}_{k|k-1}$. The predicted state estimate is also known as the *a priori state estimate* because it does not include the observation information $y_k$ from the current time step. In the update phase, the current a priori predictions $\hat{x}_{k|k-1}$ and $P_{k|k-1}$ are combined with the current observation information $y_k$ and the a posteriori state $\hat{x}_{k|k}$ and covariance $P_{k|k}$ are estimated. These improved estimates are called the a posteriori estimates.

**Time update (prediction)**

| | |
|---|---|
| State update | $\hat{x}_{k\|k-1} = A\hat{x}_{k-1\|k-1} + Bu_{k-1}$ |
| Covariance update | $P_{k\|k-1} = AP_{k-1\|k-1}A^T + R_1$ |

**Data update (inference)**

| | |
|---|---|
| Innovation or measurement residual | $\tilde{y} = z_k - C_k\hat{x}_{k\|k-1}$ |
| Innovation (or residual) covariance | $S_k = C_k P_{k\|k-1} C_k^T + R_2$ |
| Optimal Kalman gain | $K_k = P_{k\|k-1} C_k^T S_k^{-1}$ |
| Updated (a posteriori) state estimate | $\hat{x}_{k\|k} = \hat{x}_{k\|k-1} + K_k\tilde{y}_k$ |
| Updated (a posteriori) estimate covariance | $P_{k\|k} = (I - K_k C_k)P_{k\|k-1}$ |

For nonlinear systems whose state transition $f(x_k, u_k, v_k)$ and observation model $g(x_k, u_k, w_k)$ are nonlinear, extended Kalman filter is used for state estimation. In the extended Kalman filtering, essentially we use the same formulas given above for the Kalman filter with $\hat{A}$ and $\hat{C}$ found by linearizing $f$ and $g$ at their operating points and using $f$ and $g$ for state transition and observation model instead of linear models in Kalman filter:

**Time update (prediction)**

| | |
|---|---|
| State update | $\hat{x}_{k\|k-1} = f(\hat{x}_{k-1\|k-1}, u_{k-1})$ |
| Covariance update | $P_{k\|k-1} = \hat{A}P_{k-1\|k-1}\hat{A}^T + R_1$ |

**Data update (inference)**

| | |
|---|---|
| Innovation or measurement residual | $\tilde{y} = z_k - g(\hat{x}_{k\|k-1}, u_{k-1})$ |
| Innovation (or residual) covariance | $S_k = \hat{C}_k P_{k\|k-1} \hat{C}_k^T + R_2$ |
| Optimal Kalman gain | $K_k = P_{k\|k-1} \hat{C}_k^T S_k^{-1}$ |
| Updated (a posteriori) state estimate | $\hat{x}_{k\|k} = \hat{x}_{k\|k-1} + K_k\tilde{y}_k$ |
| Updated (a posteriori) estimate covariance | $P_{k\|k} = (I - K_k \hat{C}_k)P_{k\|k-1}$ |

### 3.4.5 Offset-free control

Persistent disturbances and modeling errors can cause an offset between measured outputs and desired outputs. To avoid this problem, we need to somehow employ an offset free reference tracking approach. The controllers that we have designed in this work solve the regulation problem around operating points. However we regulate around the operating points ($x^*$ and $u^*$) which might be erroneous. Besides, the difference between linearized model and the nonlinear model contributes to an offset from the desired outputs. To avoid these offsets, in our control algorithms we have employed two methods. One natural way of tackling the offset in the output is to use integrators which is the first method we have employed. We have also used disturbance modeling to solve the problem.

#### 3.4.5.1 Error integrator

In order to use integrators for offset free control, we simply include as many integrator states as we have outputs with offsets. In the wind turbine case we have only employed one integrator to regulate the rotational speed to its rated value. After defining the integrator states, we extend the state space matrices to include the new states (integrator states) and new measurement (integrators value as outputs). Therefore for a state space system of the form $(A, B, C, D)$ we get the following augmented system:

$$\begin{pmatrix} x_{k+1} \\ x^i_{k+1} \end{pmatrix} = \begin{pmatrix} A & 0 \\ 0 & I \end{pmatrix} \begin{pmatrix} x_k \\ x^i_k \end{pmatrix} + \begin{pmatrix} B \\ 0 \end{pmatrix} u_k + \begin{pmatrix} 0 \\ I \end{pmatrix} e_k \tag{3.12}$$

$$\begin{pmatrix} y_k \\ y^i_k \end{pmatrix} = \begin{pmatrix} C & 0 \\ 0 & I \end{pmatrix} \begin{pmatrix} x_k \\ x^i_k \end{pmatrix} + \begin{pmatrix} D \\ 0 \end{pmatrix} u_k \tag{3.13}$$

$$e_k = y_k - r_k \tag{3.14}$$

In which $e_k$ is the error between the output $y_k$ and the reference $r_k$.

#### 3.4.5.2 Disturbance modeling

Another method to avoid offset in the outputs is to use disturbance modeling. In this method the plant model is augmented with new states named disturbance states to include constant step disturbance model. The unmeasured disturbances are estimated with an estimator and their undesired influence on the plant is compensated by shifting either the origin of the controller to a new operating point that ensures stable offset-free control of the plant or including them in the feedback control (see [MB02] and [PR03]). State space model of the augmented system is:

$$\tilde{x}_{k+1} = \tilde{A}\tilde{x}_k + \tilde{B}u_k \tag{3.15}$$

$$y_k = \tilde{C}\tilde{x}_k + Du_k \tag{3.16}$$

in which the augmented state and matrices are:

$$\tilde{x}_k = \begin{pmatrix} \hat{x}_{k+1} \\ \hat{d}_{k+1} \\ \hat{p}_{k+1} \end{pmatrix} \qquad \tilde{A} = \begin{pmatrix} A & B_d & 0 \\ 0 & A_d & 0 \\ 0 & 0 & A_p \end{pmatrix} \tag{3.17}$$

$$\tilde{B} = \begin{pmatrix} B & 0 & 0 \end{pmatrix}^T \qquad \tilde{C} = \begin{pmatrix} C & 0 & C_p \end{pmatrix} \tag{3.18}$$

$\hat{x}_k, \hat{d}_k$ and $\hat{p}_k$ are system states, input/state and output disturbances respectively. $(A, B, C, D)$ are matrices of the linearized model, $B_d$ and $C_p$ show the effect of disturbances on states and outputs respectively. $A_d$ and $A_p$ show dynamics of input/state and output disturbances. For more information and how to choose these matrices, we refer to [MB02] and [PR03]. Since the disturbances are not measurable, an extended Kalman filter is designed to estimate them. The estimated disturbances are used to remove any offset between the desired outputs and the measured outputs. Based on this model and estimated disturbances, $u_k^s$ which is the offset free steady state input, can be calculated:

$$\begin{pmatrix} A - I & B \\ C & D \end{pmatrix} \begin{pmatrix} x_k^s \\ u_k^s \end{pmatrix} = \begin{pmatrix} -B_d \hat{d}_k \\ -C_p \hat{p}_k \end{pmatrix} \tag{3.19}$$

Chapter 4

# Conclusions and future developments

Wind turbines are essentially nonlinear systems but most of our model based control methods require linear models. Therefore derivation of linear mathematical models with various complexities from nonlinear models enables an investigation of the potentials of model based control methods in terms of improved power production and life-time of wind turbines. The possibility of varying the model complexity enables an investigation of the relationships between performance, model complexity and robustness of these controllers. Therefore in relation to these goals, various model complexities were chosen and different model based control methods such as $\mathcal{H}_\infty$ and model predictive control and different robust model based control methods such as $\mu$-synthesis and robust model predictive control were employed and compared against a standard PI controller. In all the cases the model based controllers gave better performance in terms of output regulation and dynamic loads reduction.

In all the papers presented in part II, firstly a nonlinear model of wind turbine using blade element momentum theory (BEM) and first principle modeling of the flexible structure is obtained. Different number of degrees of freedom are used in different papers. For example in paper A we have included rotation of the rotor and drivetrain torsion in the design model while in paper G we have included tower fore-aft and in paper H we have included an approximate model of the blades.

Our control methodology is based on linear models, therefore we have used Taylor series expansion to linearize the obtained nonlinear model around system operating points. The operating point is a direct function of the rotor rotational speed, the pitch angle and the wind speed where the rotational speed and the pitch angle are functions of the wind speed themselves. Therefore the wind speed or rather the effective wind speed determines the operating point of the system. In the papers B and D wind speed estimation is used to find the operating point, while in the papers C and H, LIDAR measurements are used to calculate the effective wind speed and find the operating points.

In the papers on robust model based control methods (paper B and paper G) we have shown that uncertainty in the wind speed estimation/measurement will result in an uncertain $A$ and $B$ matrices in our linear models. And in paper D we have concluded that with an acceptable approximation, the uncertainty could be considered to be only in the $B$ matrix. A special minimax model predictive control formulation was derived to take into account the assumed uncertainties.

For all the papers, the final controllers have been applied on a full complexity FAST [JJ05] model and the results are compared against a standard PI controller [JBMS09].

In paper A $DK$-iteration technique is used to design a robust controller. However in this work only one linear model was obtained and consequently one controller was designed. The simulations were performed around one specific linearization point both for the nominal case and the perturbed case. In paper B the method in paper A was extended further and several controllers were designed and applied based on a switching strategy. The resulting controller was performing satisfactorily, however tuning all the controllers in the controller bank and choosing an appropriate switching strategy was cumbersome. Here it is logical to come up with a better solution such as a gain-scheduled controller which can take nonlinearities into account directly. The basic objective in these papers were regulation of the outputs and dynamic load reduction however no comparison was presented. The results were further extended and tower fore-aft degree of freedom was included in paper G. Here the simulation results are compared against a standard PI controller. The resulting controller shows better performance both for the nominal case and the perturbed case.

Paper C and paper E are based on the idea that in certain cases we may have scheduling variable of the nonlinear system in advance. We have employed this idea in the wind turbine control and by formulating a suitable model predictive control we have shown that the method gives superior performance both on output regulation and low actuator activities. However it should be noted that this performance is achieved while considering the LIDAR measurements could be used to calculate effective wind speed precisely which is rather idealistic. In paper I we have tried to make our assumptions about LIDAR measurements more realistic and have considered uncertainties in the propagation time of the wind. In this paper we have used an Extended Kalman filter to estimate the effective wind speed and then compared this estimation with LIDAR measurements and estimate the lead-lag error in the LIDAR measurements and compensated for it. The results of these papers were extended to individual pitch control in paper F. The idea of individual pitch control using LIDAR measurements was further developed in paper H and the superior performance in terms of output regulations, low actuator activity and low fatigue loads were observed. And in the paper I an important problem with LIDAR measurements, namely the uncertainty in the wind propagation time, was considered.

# Bibliography


[And10] Peter Bjørn Andersen. *Advanced Load Alleviation for Wind Turbines using Adaptive Trailing Edge Flaps: Sensoring and Control.* PhD thesis, Technical University of Denmark, Denmark, 2010.

[Bao05] M. Baotic. *Optimal Control of Piecewise Affine Systems – a Multi-parametric Approach.* PhD thesis, March 2005.

[BBM06] Fernando D. Bianchi, Hernan De Battista, and Ricardo J. Mantz. *Wind Turbine Control Systems: Principles, Modelling and Gain Scheduling Design.* Springer, 2006.

[BM99] A Bemporad and M Morari. Robust model predictive control: A survey. *Lecture Notes in Control and Information Sciences*, 245:207–226, 1999.

[Bur11] T. Burton. *Wind energy handbook.* John Wiley & Sons, Chichester, 2011.

[CFM10] M. Canale, L. Fagiano, and M. Milanese. High altitude wind energy generation using controlled power kites. *IEEE Trans. Contr. Syst. Technol.*, 18(2):279–293, 2010.

[CPBWH11] Damien Castaignet, Niels K. Poulsen, Thomas Buhl, and Jens Jakob Wedel-Heinen. Model predictive control of trailing edge flaps on a wind turbine blade. *Proceedings of the American Control Conference*, pages 4398–4403, 2011.

[GA08] Mohinder S. Grewal and Angus P. Andrews. *Kalman filtering : theory and practice using MATLAB.* Wiley, Hoboken, NJ, 2008.

[Gaw04] Wodek Gawronski. *Advanced structural dynamics and active control of structures*. Springer-Verlag, New York, 2004.

[GC08] M. Geyler and P. Caselitz. Robust multivariable pitch control design for load reduction on large wind turbines. *Journal of solar energy engineering*, 130(3):–, 2008.

[Gey05] T. Geyer. *Low Complexity Model Predictive Control in Power Electronics and Power Systems*. PhD thesis, March 2005.

[Han08] Martin O. L. Hansen. *Aerodynamics of Wind Turbines*. Earthscan, 2008.

[Hen07] Lars Christian Henriksen. Model predictive control of a wind turbine. Master's thesis, Technical University of Denmark, Informatics and Mathematical Modelling, 2007.

[Hen10] Lars Christian Henriksen. *Model Predictive Control of Wind Turbines*. PhD thesis, Department of Informatics, Technical University of Denmark (DTU), Kgs. Lyngby, Denmark, 2010.

[HHW06] M. Harris, M. Hand, and A. Wright. LIDAR for turbine control. Technical report, National Renewable Energy Laboratory, 2006.

[HPH11] Lars Christian Henriksen, Niels Kjølstad Poulsen, and Morten Hartvig Hansen. Nonlinear model predictive control of a simplified wind turbine. *Preprints of the 18th IFAC World Congress*, pages 551–556, 2011.

[iec05] IEC 61400-1 wind turbines-part 1: Design requirements., August 2005.

[JBMS09] J. Jonkman, S. Butterfield, W. Musial, and G. Scott. Definition of a 5MW reference wind turbine for offshore system development. Technical report, National Renewable Energy Laboratory,, 1617 Cole Boulevard, Golden, Colorado 80401-3393 303-275-3000, 2009.

[JF08] Johnson and Fingersh. Adaptive pitch control of variable-speed wind turbines. *J. Sol. Energy Eng. (USA)*, 130(3):031012–1–7, 2008.

[JJ05] Jason M. Jonkman and Marshall L. Buhl Jr. Fast user's guide. Technical Report NREL/EL-500-38230, National Renewable Energy Laboratory, Golden, CO, August 2005.

[JLSM06] Allan Juul Larsen and Thomas Stampe Mogensen. Individuel pitchregulering af vindmølle. Master's thesis, Technical University of Denmark, Informatics and Mathematical Modelling, Lyngby, Denmark, 2006.

[Lö03] Johan Löfberg. *Minimax approaches to robust model predictive control.* PhD thesis, Department of Electrical Engineering, Linköping University, 2003.

[LC00] W.E. Leithead and Bill Connor. Control of variable speed wind turbines: Design task. *Int J Control*, 73(13):1189–1212, 2000.

[LH] Torben J. Larsen and Anders Melchior Hansen. How 2 HAWC2, the user's manual. pages –.

[LMT05] Torben Juul Larsen, Helge A. Madsen, and Kenneth Thomsen. Active load reduction using individual pitch, based on local blade flow measurements. *Wind Energy*, 8(1):67–80, 2005.

[LPW09] J.H. Laks, L.Y. Pao, and A.D. Wright. Control of wind turbines: Past, present, and future. *Proceedings of the American Control Conference*, pages 2096–2103, 2009.

[Mac02] J.M. Maciejowski. *Predictive control with constraints.* Pearson Education Lim., Essex, 2002.

[MB02] Kenneth R. Muske and Thomas A. Badgwell. Disturbance modeling for offset-free linear model predictive control. *Journal of Process Control*, 12(5):617–632, 2002.

[MNP11] Mahmood Mirzaei, Hans Henrik Niemann, and Niels Kjølstad Poulsen. A $\mu$-synthesis approach to robust control of a wind turbine. In *the 50th IEEE Conference on Decision and Control and European Control Conference*, pages 645–650, Orlando, Florida, United States, 2011.

[Ock01] Wubbo J. Ockels1. Laddermill, a novel concept to exploit the energy in the airspace. *Aircraft Design*, 4(2-3):81–97, 2001.

[Øst08] Kasper Zinck Østergaard. *Robust, Gain-Scheduled Control of Wind Turbines.* PhD thesis, Automation and Control Department of Electronic Systems, Aalborg University, 2008.

[PR03] Gabriele Pannocchia and James B. Rawlings. Disturbance models for offset-free model-predictive control. *AIChE Journal*, 49(2):426–437, 2003.

[QB96] S. Joe Qin and Thomas A. Badgwell. An overview of industrial model predictive control technology. pages –, 1996.

[SP01] Sigurd Skogestad and Ian Postlethwaite. *Multivariable Feedback Control Analysis and design.* JOHN WILEY & SONS, Second Edition, 2001.

[Tho06] Sven Creutz Thomsen. Nonlinear control of a wind turbine. Master's thesis, Technical University of Denmark, Informatics and Mathematical Modelling, Lyngby, Denmark, 2006.

[vdH57] I. van der Hoven. Power spectrum of horizontal wind speed in the frequency range from 0.0007 to 900 cycles per hour. *Journal of Meteorology*, 14(2):160–164, 1957.

[WJ97] J. Walker and N. Jenkins. *Wind Energy Technology*. John Wiley & Sons, Chichester, UK, 1997.

# Part II

# Papers

# Paper A

# DK-Iteration robust control design of a wind turbine

**Authors:**
M. Mirzaei, H. H. Niemann and N. K. Poulsen

**Presented in:**
IEEE International Conference on Control Applications, 2011

# $DK$-Iteration Robust Control Design of a Wind Turbine[1]

Mahmood Mirzaei[2], Hand Henrik Niemann[3] and Niels Kjølstad Poulsen[2]

**Abstract**

The problem of robust control of a wind turbine is considered in this paper. A controller is designed based on a 2 degrees of freedom linearized model. An extended Kalman filter is used to estimate effective wind speed and the estimated wind speed is used to find the operating point of the wind turbine. Due to imprecise wind speed estimation, uncertainty in the obtained linear model is considered. Uncertainties in the drivetrain stiffness and damping parameters are also considered as these values are lumped parameters of a distributed system and therefore they include inherent uncertainties. We include these uncertainties as parametric uncertainties in the model and design a robust controller using $DK$-iteration method. The controller is applied on a full complexity simulation model and simulations are performed for wind speed step changes.

## 5.1 Introduction

There is an increasing interest in wind energy and wind turbines are the most common wind energy conversion systems (WECS). Control is an essential part of the wind turbine system because control methods can decrease the cost of energy by increasing the power capture by keeping the turbine close to its maximum efficiency and also by reducing structural loadings and therefore increasing lifetime of the wind turbine. Wind turbines essentially have two regions of operation, partial load and full load. In the partial load wind speed is not fast enough to produce rated power. In this region the main control objective is to track the maximum power coefficient($C_{Pmax}$) and extract as much power as possible. Pitch is mostly fixed in this region and generator reaction torque is adjusted to control rotational speed and keep the operating point close to $C_{Pmax}$. In the full load region wind speed is above rated and wind power exceeds rated power of the generator, therefore by decreasing aerodynamics efficiency of the rotor we try to

[1]This work is supported by the CASED Project funded by grant DSF-09- 063197 of the Danish Council for Strategic Research.
[2]DTU Informatics, Technical University of Denmark, Asmussens Alle, building 305, DK-2800 Kgs. Lyngby, Denmark
[3]Department of Electrical Engineering, Technical University of Denmark, Ørsteds Plads, Building 349, DK-2800 Kgs. Lyngby, Denmark

control the captured power and this is done by pitching the blades. There are several methods for wind turbine control ranging from classical control methods [LC00] which are the most used method in real applications to advanced and model based control methods which have been the focus of research in the past few years[LPW09]. Gain scheduling[BBM06], adaptive control[JF08], time invariant MIMO methods[GC08], nonlinear control[Tho06], robust control[Øst08], model predictive control [Hen07] are to mention a few. Advanced control methods are thought to be the future of wind turbine control as they can employ new generations of sensors on wind turbines (e.g. LIDAR[HHW06]), new generation of actuators (e.g. trailing edge flaps[And10]) and also conveniently treat the turbine as a MIMO system. The last feature seems to become more important than before as wind turbines become bigger and more flexible which make decoupling different modes and designing controller for each mode more difficult. The wind turbine in this paper is treated as a MIMO system with pitch reference($\theta_{ref}$) and generator reaction torque($Q_{ref}$) as inputs and rotor rotational speed($\omega_r$), generator rotational speed($\omega_g$) and generated power($P_e$) as outputs. This paper is organized as follows: In the section 5.2 modeling of the wind turbine including modeling for wind speed estimation, linearization and uncertainty modeling is addressed. In the section 5.3.1 controller design is explain and in the section 5.4 robust performance problems is addressed. And finally in the section 5.5 simulation results are presented.

## 5.2 Modeling of the Wind Turbine

For modeling purposes, the whole wind turbine can be divided into 4 subsystems: Aerodynamics subsystem, structural subsystem, electrical subsystem and actuator subsystem. Figure 5.1 shows the basic subsystems and their interactions. The dominant dynamics of the wind turbine come from its flexible structure. Several degrees of freedom could be considered to model the flexible structure, but for control design mostly just a few important degrees of freedom are considered. Mostly the degrees of freedom whose eigen frequencies lie inside actuator bandwidth are considered otherwise including them into the design model is useless and makes the design model unnecessarily complicated. In this work we only consider two degrees of freedom, namely the rotational degree of freedom(DOF) and drivetrain torsion. The aerodynamics subsystem in the model gets effective wind speed($v_e$), pitch angle($\theta$) and rotational speed of the rotor($\omega_r$) and returns aerodynamic torque ($T_r$) and thrust($F_T$). This subsystem is responsible for the nonlinearity in the wind turbine model. More details are presented in the section 5.2.2.

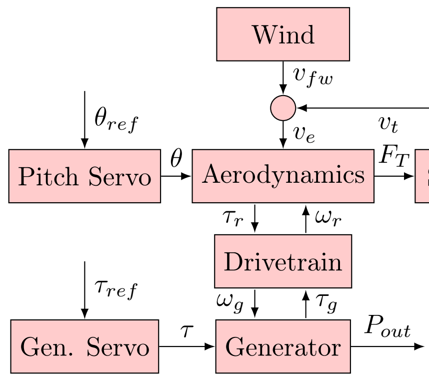


**Figure 5.1:** Wind turbine subsystems

### 5.2.1 Wind Model

Wind model can be modeled as a complicated nonlinear stochastic process, however for practical purposes it could be approximated based on a linear model. In this model the wind has two elements, mean value term($v_m$) and turbulent term($v_t$):

$$v_e = v_m + v_t$$

The turbulent term could be modeled by the following state space model:

$$\begin{pmatrix} \dot{v}_t \\ \ddot{v}_t \end{pmatrix} = \begin{pmatrix} 0 & 1 \\ -\frac{1}{p_1(v_m)p_2(v_m)} & -\frac{p_1(v_m)+p_2(v_m)}{p_1(v_m)p_2(v_m)} \end{pmatrix} \begin{pmatrix} v_t \\ \dot{v}_t \end{pmatrix} + \begin{pmatrix} 0 \\ \frac{k(v_m)}{p_1(v_m)p_2(v_m)} \end{pmatrix} e, \quad e \in N(0,1) \tag{5.1}$$

The parameters $k(v_m)$, $p_1(v_m)$ and $p_2(v_m)$ are estimated by approximating wind power distribution and as it is indicated, they are dependent on the mean wind speed ($v_m$).

### 5.2.2 Nonlinear Model

Blade element momentum(BEM) theory [Han08] is used to calculate aerodynamic torque and thrust on the wind turbine. This theory explains how torque and thrust are related to wind speed, blade pitch angle and rotational speed of the rotor with the following formulas:

$$Q_r = \frac{1}{2}\frac{1}{\omega_r}\rho\pi R^2 v_e^3 C_P(\theta,\omega,v_e)$$
$$Q_t = \frac{1}{2}\rho\pi R^2 v_e^2 C_T(\theta,\omega,v_e)$$

In which $Q_r$ and $Q_t$ are aerodynamic torque and thrust, $\rho$ is air density, $\omega_r$ is rotor rotational speed, $v_e$ is effective wind speed, $C_P$ is the power coefficient and $C_T$ is the thrust force coefficient. For the sake of simplicity, instead of presenting these two coefficients as functions of three variables $\omega$, $v_e$ and $\theta$, they are presented as a function of two variables $\lambda$ and $\theta$ in which $\lambda = \frac{R\omega}{v_e}$ and it is called tip speed ratio. As we have not used individual pitch in this work absolute angular position of the rotor and generator are of no interest to us, therefore we use $\psi = \theta_r - \theta_g$ instead which is the drivetrain torsion. Having aerodynamic torque the whole system equation with 2 degrees of freedom becomes:

$$\begin{aligned} J_r\dot{\omega}_r &= Q_r - c(\omega_r - \frac{\omega_g}{N_g}) - k\psi \\ (N_g J_g)\dot{\omega}_g &= c(\omega_r - \frac{\omega_g}{N_g}) + k\psi - N_g Q_g \end{aligned} \tag{5.2}$$

In which $J_r$ and $J_g$ are rotor and generator moments of inertia, $\psi$ is the drivetrain torsion, $c$ and $k$ are the drivetrain damping and stiffness factors respectively lumped in the low speed side of the shaft. For numerical values of these parameters and other parameters given in this paper, we refer the reader to [JBMS09]. These equations give us a nonlinear model however our control design method is based on linear models, therefore we need to linearize the nonlinear model of the system which could be easily achieve using Taylor expansions around the operating points.

### 5.2.3 Uncertain Model

As it was mentioned, for control design we need to have a linear model of the system and the following model of the wind turbine is used:

$$\begin{pmatrix} \dot{x} \\ y_\Delta \\ y \end{pmatrix} = \left(\begin{array}{c|cc} A & B_1 & B_2 \\ \hline C_1 & D_{11} & D_{12} \\ C_2 & D_{21} & D_{22} \end{array}\right) \begin{pmatrix} x \\ u_\Delta \\ u \end{pmatrix}$$

In which states, inputs and outputs are:

$$\begin{aligned} x &= \begin{pmatrix} \omega_r & \omega_g & \psi & \theta & Q_g & v_e & \dot{v}_e \end{pmatrix}^T \\ u &= \begin{pmatrix} \theta_{ref} & Q_{ref} \end{pmatrix}^T \\ y &= \begin{pmatrix} \omega_r & \omega_g & P_e \end{pmatrix}^T \end{aligned}$$

$\omega_r$ is rotational speed of the rotor, $\omega_g$ is rotational speed of the generator, $\psi$ is drivetrain deflection, $\theta$ pitch of the blade, $Q_g$ is the generator reaction torque, $v_e$ and $\dot{v}_e$ are wind model states, $\theta_{ref}$ is the reference value for pitch angle and $Q_{ref}$ is the reference value for the generator reaction torque and $P_e$ is the electrical power. System equations are:

$$
\begin{aligned}
\dot{\omega}_r &= \frac{a-c}{J_r}\omega_r + \frac{c}{J_r}\omega_g - \frac{k}{J_r}\psi + b_1\theta + b_2 v_e \\
\dot{\omega}_g &= \frac{c}{N_g J_g}\omega_r - \frac{c}{N_g^2 J_g}\omega_g + \frac{k}{N_g J_g}\psi - \frac{Q_g}{J_g} \\
\dot{\psi} &= \omega_r - \frac{\omega_g}{N_g} \\
\dot{\theta} &= -\frac{1}{\tau_\theta}\theta + \frac{1}{\tau_\theta}\theta_{ref} \\
\dot{Q}_g &= -\frac{1}{\tau_g}Q_g + \frac{1}{\tau_g}Q_{ref} \\
P_e &= Q_{g0}\omega_g + \omega_{g0}Q_g \\
\ddot{v}_e &= -\frac{1}{p_1 p_2}v_e - \frac{p_1+p_2}{p_1 p_2}\dot{v}_e + \frac{k}{p_1 p_2}e
\end{aligned}
$$

There are always discrepancies between real system and mathematical models, which lead to uncertain models. In this work, sources of uncertainties are taken to be:

- Uncertainty in the drivetrain stiffness and damping parameters.
- Uncertainty in the linearized model.

Uncertainty in the linearized model could be a result of approximate $C_P$ curve calculations, wrong wind speed estimation which results in picking the wrong operating point or aerodynamic changes due to blade flexibility or ice coatings on the blades. Multiplicative uncertainty is used to represent the uncertain parameters. The uncertainty matrix becomes:

$$
\begin{pmatrix} u_a \\ u_{b_1} \\ u_k \\ u_c \end{pmatrix} = \begin{pmatrix} \delta_a & 0 & 0 & 0 \\ 0 & \delta_{b_1} & 0 & 0 \\ 0 & 0 & \delta_k & 0 \\ 0 & 0 & 0 & \delta_c \end{pmatrix} \begin{pmatrix} y_a \\ y_{b_1} \\ y_k \\ y_c \end{pmatrix}
$$

$y_\Delta = \begin{pmatrix} y_a & y_{b_1} & y_k & y_c \end{pmatrix}^T$ is the uncertainty output, $y$ is the output, $u_\Delta = \begin{pmatrix} u_a & u_{b_1} & u_k & u_c \end{pmatrix}^T$ is the uncertainty input and $u$ is the input. Now having

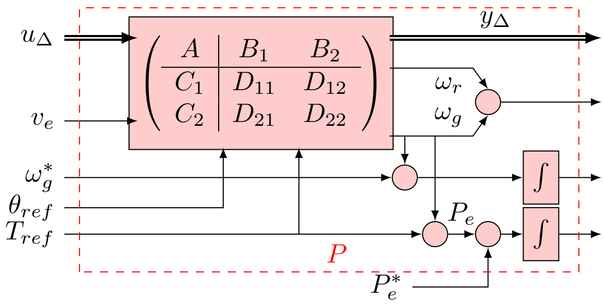


**Figure 5.2:** System interconnections

system equations, we can make the interconnection matrix $P$ (see figure 5.2):

$$\begin{pmatrix} y_\Delta \\ z \\ y \end{pmatrix} = P \begin{pmatrix} u_\Delta \\ d \\ u \end{pmatrix}$$

### 5.2.4 Simulation Model

The FAST (Fatigue, Aerodynamics, Structures, and Turbulence) code [JJ05] is used as the simulation model and the 5MW reference wind turbine is used as the plant [JBMS09]. In the simulation model 10 degrees of freedom are enabled which are: generator, drivetrain torsion, 1st and 2nd tower fore-aft, 1st and 2nd tower side-side, 1st and 2nd blade flapwise, 1st blade edgewise degrees of freedom.

### 5.2.5 Wind Speed Estimation

Based on the nonlinear model given in (5.2) and the wind model given in (5.1) an extended Kalman filter is designed to estimate the effective wind speed. This wind speed is used to find the operating point of the wind turbine ($\theta^*$, $\lambda^*$ and $C_p^*$) and linearize the nonlinear model.

## 5.3 Controller Design

### 5.3.1 Control Objectives

The most basic control objective of a wind turbine is to maximize power capture in the turbine life time, which this in turn means maximizing power captured from the wind and prolonging life time of the wind turbine by minimizing the fatigue loads. Generally maximizing power capture is considered in the partial load and minimizing fatigue loads is mainly considered above rated. As we are operating in the full load region in this work, we have considered the second objective. Control objectives are formulated in the form of weighting functions on input disturbances($d$) and exogenous outputs($z$). In order to avoid high frequency activity of the actuators, we have put high pass filter on control signals to punish high frequency actions. Also we have setup low pass filters to punish low frequency of the system outputs as their high frequency dynamics are outside of our actuator bandwidth and we can not control them anyway. For regulating power and rotational speed, $P_e - P_e^*$ and $\int \omega_g - \omega_g^*$ and for minimizing fatigue loads on the drivetrain $\omega_g - N_g \omega_r$ are punished. The resulting controller is a dynamical system with measurements $y$ as its inputs and control signals $u$ as its outputs:

$$\begin{aligned} \dot{x}_c &= A_c x_c + B_c y \\ u &= C_c x_c \end{aligned}$$

## 5.4 Robust Performance Problem

### 5.4.1 Theory

Robust performance means that the performance objective is satisfied for all possible plants in the uncertainty set. The robust performance condition can be cast into a robust stability problem with an additional perturbation block that defines $H_\infty$ performance specifications [SP01]. The structured singular value $\mu$ is a very powerful tool for the analysis of robust performance with a given controller. However this is an analysis tool, in order to design a controller, we need a synthesis tool. A scaled version of the upper bound of $\mu$ is used for controller synthesis. The problem is formulated in the following form:

$$\mu_\Delta(N(K)) \leq \min_{D \in \mathcal{D}} \sigma(DN(K)D^{-1})$$

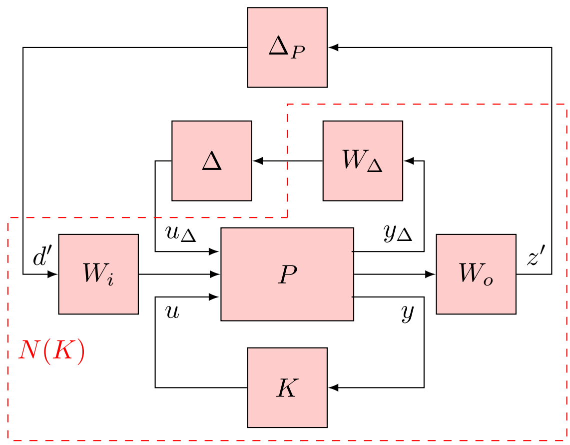


**Figure 5.3:** System setup for robust performance problem

Now, the synthesis problem can be cast into the following optimization problem in which one tries to to find a controller that minimizes the peak value over frequency of this upper bound:

$$\min_{K \in \mathcal{K}} (\min_{D \in \mathcal{D}} \| DN(K)D^{-1} \|_\infty)$$

This problem is solved by an iterative approach which is called $DK$-iteration. For detailed explanations on the method and notations the reader is referred to [SP01].

### 5.4.2 Implementation

We have used $\mu$-Synthesis toolbox [Mat] to implement the $DK$-Iteration algorithm. $W_\Delta$ is used to scale the $\Delta$ matrix. We have taken uncertainty of 10% of the nominal values for drivetrain stiffness and damping coefficients and 20% for the linearization parameters therefore the weighting matrix becomes:

$$W_\Delta = diag(0.2, 0.2, 0.1, 0.1)$$

$\Delta_P$ (scaled by $W_i$ and $W_o$ matrices) defines performance of the system in the form of a complex perturbation matrix. $W_i$ and $W_o$ are frequency dependent weight matrices on disturbances and exogenous outputs respectively of the form:

$$W_o = diag(W_{o1}, \ldots, W_{o5})$$
$$W_i = diag(W_{i1}, W_{i2})$$

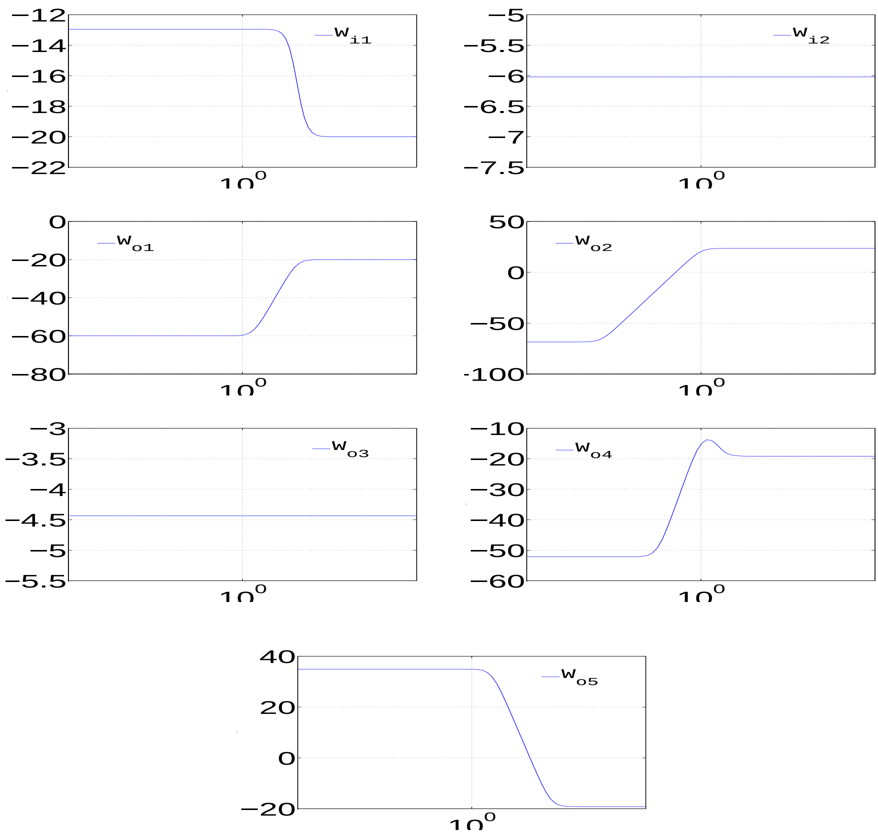


**Figure 5.4:** Bode plots for performance specifications(y-axis is in dB and x-axis is in rad/s)

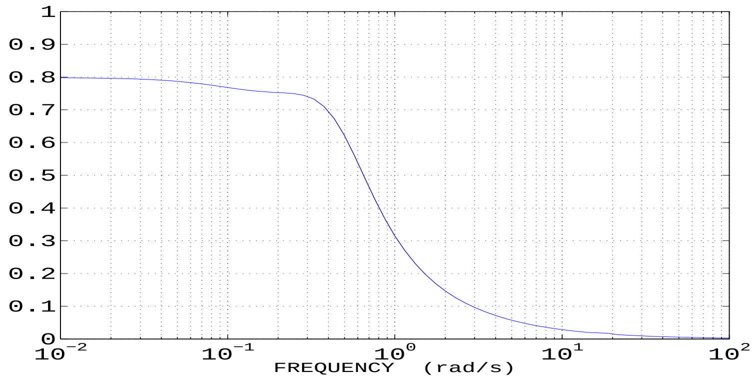


**Figure 5.5:** Closed loop mixed $\mu$

Bode plots of the weighting functions are given in the figure 5.4. Figure 5.4 shows bode plots of weighting functions. Input disturbances ($d$) to the system are:

$$d = \begin{pmatrix} v_e \\ \omega_g^* \end{pmatrix} \begin{matrix} \text{Wind Speed} \\ \text{Rotor rotation reference} \end{matrix}$$

And exogenous outputs ($z$) are:

$$z = \begin{pmatrix} \theta_{ref} \\ Q_{ref} \\ \omega_r^* - \frac{\omega_g}{N_g} \\ \int \omega_g^* - \omega_g \\ \int P_e^* - P_e \end{pmatrix} \begin{matrix} \text{Pitch reference} \\ \text{Generator reaction torque reference} \\ \text{Deflection of the drivetrain} \\ \text{Integral on rotational speed error} \\ \text{Integral on generated power error} \end{matrix}$$

These weightings are used to specify performance of the system. As we have parametric uncertainties in the plant and complex perturbation for performancs, mixed $\mu$ is used to design the controller. The resulting mixed-$\mu$ is given in figure 5.5 and the iteration summery is given in the table 5.1. The obtained controller is of the order 19, and has maximum gain of 15.86dB. As high order controllers are problematic in the real implementations, we have used balanced order reduction [Var91] to reduce its order to 10. Hankel singular values of the controller are shown in figure 5.6 and the jump from order 10 to 11 is found a reasonable place for controller order reduction.

## 5.5 Simulation Results

In this section simulation results for the obtained controller are presented. The controller is implemented in MATLAB and tested on full complexity FAST

| Iteration number | 1 | 2 | 3 |
|---|---|---|---|
| Controller Order | 19 | 19 | 19 |
| $\gamma$ Acheived | 9682006.84 | 45.289 | 7.347 |
| Peak $\mu$-Value | 2482.23 | 0.865 | 0.808 |

**Table 5.1:** $DK$-iteration summery

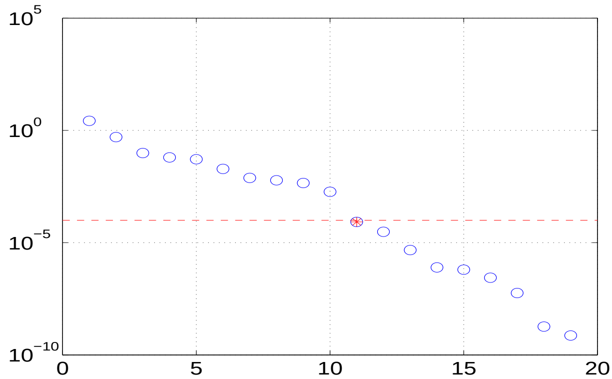


**Figure 5.6:** Hankel singular values of the controller, order of the controller on the x-axis

model of the reference wind turbine [JBMS09]. As it is mentioned in section 5.2.5 we have augmented model of wind turbine with a stochastic wind model, however in order to make evaluation of the controller on nominal and worst case, we have used simulations with step changes in the wind speed.

### 5.5.1 Robust performance simulations

In this section simulation results of a step change in wind speed is presented. Control inputs which are pitch reference $\theta_{ref}$ and generator reaction torque reference $T_{ref}$ along with system outputs which are rotor rotational speed $\omega_r$ and electrical power $P_e$ are plotted in figues 5.7a-5.7e.

### 5.5.2 Simulation for the worst case

In this section worst case scenarios, in which all the uncertainties are taken to be the maximum values, are presented. To do so, wind speed is taken to be $2m/s$ away from the linearization point and nominal values of the drivetrain stiffness and damping are replaced by the following values:

$$k = \bar{k}(1 + P_k\delta_k) \qquad \text{for } \delta_k = \pm 1 \ \& \ P_k = 0.1$$
$$c = \bar{c}(1 + P_c\delta_c) \qquad \text{for } \delta_c = \pm 1 \ \& \ P_c = 0.1$$

As it is seen in figures 5.8 and 5.9, in the worst cases the system becomes oscillatory but it maintains a reasonable performance.

## 5.6 CONCLUSION

In this paper we solved the problem of robust control of a wind turbine using $DK$-iteration technique. The controller is designed for the full load region, and an extension of this work would be to solve the problem for partial load too. Parametric uncertainty is considered in the uncertain model and then we have used $\mu$-synthesis method to design the controller. The full model with augmented wind model is of the order 8 and the resulting controller is of the order 19, however balanced truncation model order reduction is used to reduce order of the controller to 10. The final controller is implemented on a FAST simulation model with 10 degrees of freedom and simulations with wind speed step changes are done for nominal plant and worst case plant. The results suggest that the controller can handle nominal case pretty well and the worst case with a little loss of performance.

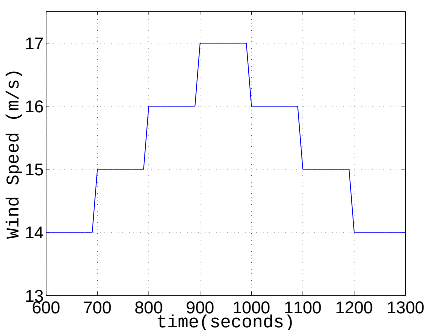


**(a)** Wind speed

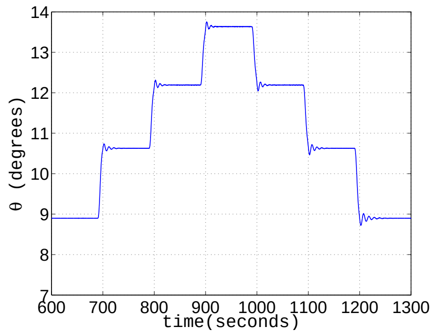


**(b)** Blade-pitch reference

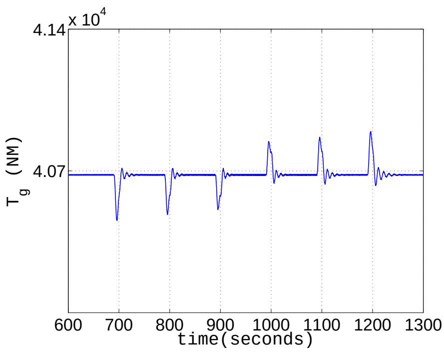


**(c)** Generator-torque reference

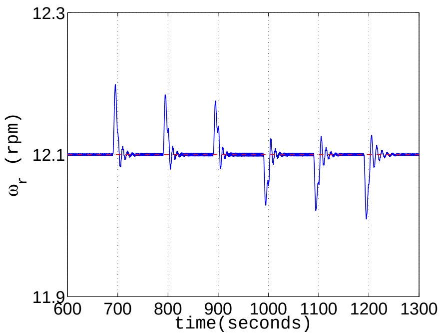


**(d)** Rotor rotational speed($\omega_r$)

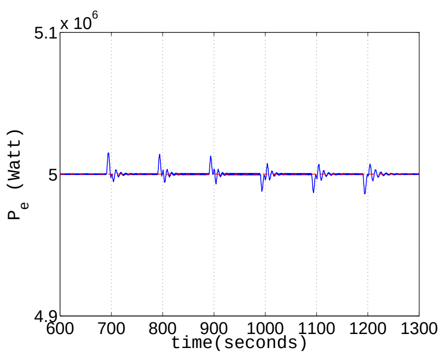


**(e)** Electrical power

**Figure 5.7:** Simulation results

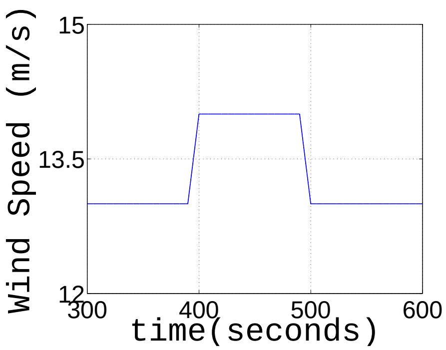


(a) Wind speed

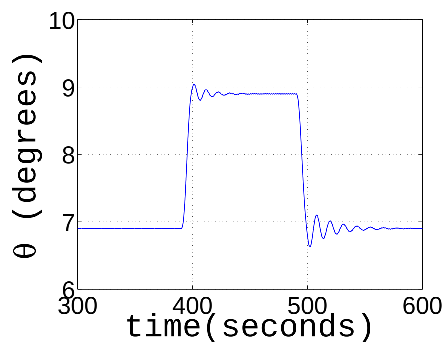


(b) Pitch reference

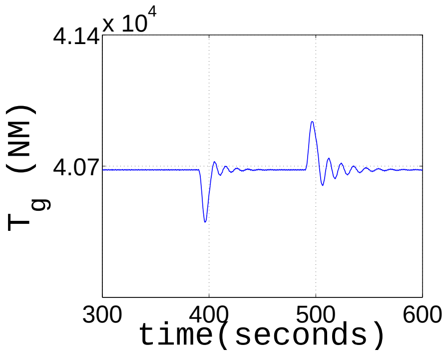


(c) Generator reaction torque reference

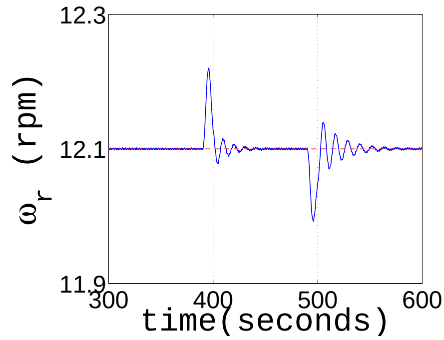


(d) Rotor rotational speed

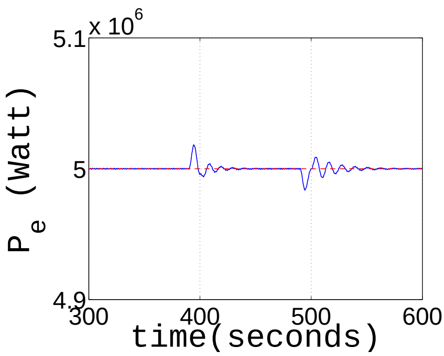


(e) Electrical power

**Figure 5.8:** Worst case scenario with $+2m/s$ wind speed estimation error

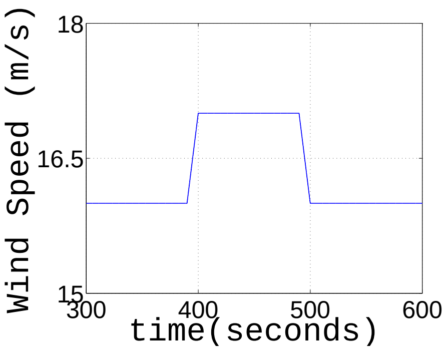


**(a)** Wind speed

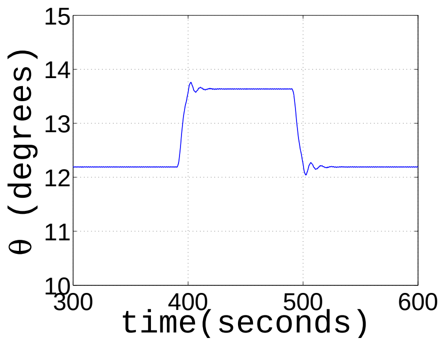


**(b)** Pitch reference

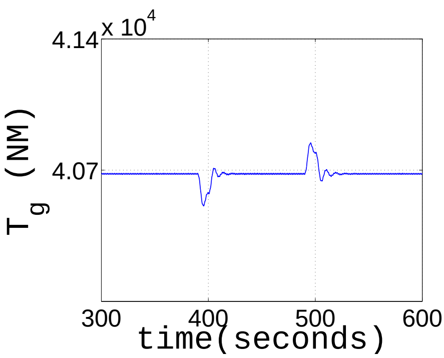


**(c)** Generator reaction torque reference

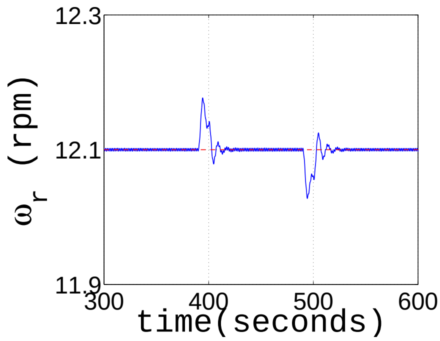


**(d)** Rotor rotational speed

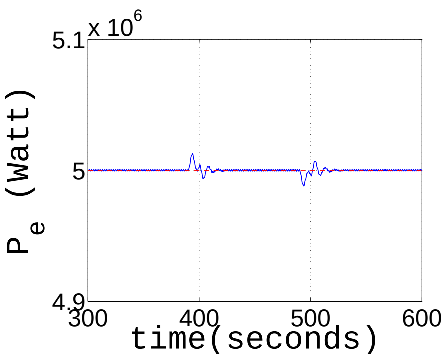


**(e)** Electrical power

**Figure 5.9:** Worst case scenario with $-2m/s$ wind speed estimation error

## Paper A References


[And10] Peter Bjørn Andersen. *Advanced Load Alleviation for Wind Turbines using Adaptive Trailing Edge Flaps: Sensoring and Control.* PhD thesis, Technical University of Denmark, Denmark, 2010.

[BBM06] Fernando D. Bianchi, Hernan De Battista, and Ricardo J. Mantz. *Wind Turbine Control Systems: Principles, Modelling and Gain Scheduling Design.* Springer, 2006.

[GC08] M. Geyler and P. Caselitz. Robust multivariable pitch control design for load reduction on large wind turbines. *Journal of solar energy engineering*, 130(3):–, 2008.

[Han08] Martin O. L. Hansen. *Aerodynamics of Wind Turbines.* Earthscan, 2008.

[Hen07] Lars Christian Henriksen. Model predictive control of a wind turbine. Master's thesis, Technical University of Denmark, Informatics and Mathematical Modelling, 2007.

[HHW06] M. Harris, M. Hand, and A. Wright. LIDAR for turbine control. Technical report, National Renewable Energy Laboratory, 2006.

[JBMS09] J. Jonkman, S. Butterfield, W. Musial, and G. Scott. Definition of a 5MW reference wind turbine for offshore system development. Technical report, National Renewable Energy Laboratory,, 1617 Cole Boulevard, Golden, Colorado 80401-3393 303-275-3000, 2009.

[JF08] Johnson and Fingersh. Adaptive pitch control of variable-speed wind turbines. *J. Sol. Energy Eng. (USA)*, 130(3):031012–1–7, 2008.

[JJ05] Jason M. Jonkman and Marshall L. Buhl Jr. Fast user's guide. Technical Report NREL/EL-500-38230, National Renewable Energy Laboratory, Golden, CO, August 2005.

[LC00] W.E. Leithead and Bill Connor. Control of variable speed wind turbines: Design task. *Int J Control*, 73(13):1189–1212, 2000.

[LPW09] J.H. Laks, L.Y. Pao, and A.D. Wright. Control of wind turbines: Past, present, and future. *Proceedings of the American Control Conference*, pages 2096–2103, 2009.

[Mat] The MathWorks, Inc. *Robust Control Toolbox.*

[Øst08] Kasper Zinck Østergaard. *Robust, Gain-Scheduled Control of Wind Turbines.* PhD thesis, Automation and Control Department of Electronic Systems, Aalborg University, 2008.

[SP01] Sigurd Skogestad and Ian Postlethwaite. *Multivariable Feedback Control Analysis and design.* JOHN WILEY & SONS, Second Edition, 2001.

[Tho06] Sven Creutz Thomsen. Nonlinear control of a wind turbine. Master's thesis, Technical University of Denmark, Informatics and Mathematical Modelling, Lyngby, Denmark, 2006.

[Var91] A. Varga. Balancing free square-root algorithm for computing singular perturbation approximations. *Proc IEEE Conf Decis Control*, 2:1062–1065, 1991.

Paper B

# A $\mu$-synthesis approach to robust control of a wind turbine

**Authors:**
M. Mirzaei, N. K. Poulsen and H. H. Niemann

**Presented in:**
The 50th IEEE Conference on Decision and Control and European Control Conference, 2011.

## A $\mu$-Synthesis Approach to Robust Control of a Wind Turbine[1]

Mahmood Mirzaei[2], Hand Henrik Niemann[3] and Niels Kjølstad Poulsen[2]

**Abstract**

The problem of robust control of a wind turbine is considered in this paper. A set of controllers are designed based on a 2 degrees of freedom linearized model of a wind turbine. An extended Kalman filter is used to estimate effective wind speed and the estimated wind speed is used to find the operating point of the wind turbine. Due to imprecise wind speed estimation, uncertainty in the obtained linear model is considered. Uncertainties in the drivetrain stiffness and damping parameters are also considered as these values are lumped parameters of a distributed system and therefore they include inherent uncertainties. we include these uncertainties as parametric uncertainties in the model and design robust controllers using the $DK$-iteration method. Based on estimated wind speed a pair of controllers are chosen and convex combination of their outputs is applied to the plant. The resulting set of controllers is applied on a full complexity simulation model and simulations are performed for stochastic wind speed according to relevant IEC standard.

# 6.1 Introduction

In the recent decades there has been an increasing interest in green energies of which wind energy is one of the most important ones. Wind turbines are the most common wind energy conversion systems (weCS) and are hoped to be able to compete with fossil fuel power plants on the energy price in near future. However this demands better technology to reduce electricity production price. Control can play an essential part in this context because control methods on one hand can decrease the cost of energy by keeping the turbine close to its maximum efficiency. On the other hand reduce structural fatigue and therefore increase lifetime of the wind turbine. There are several methods for wind turbine control ranging from classical control methods [LC00] which are

[1]This work is supported by the CASED Project funded by grant DSF-09- 063197 of the Danish Council for Strategic Research.

[2]DTU Informatics, Technical University of Denmark, Asmussens Alle, building 305, DK-2800 Kgs. Lyngby, Denmark

[3]Department of Electrical Engineering, Technical University of Denmark, Ørsteds Plads, Building 349, DK-2800 Kgs. Lyngby, Denmark

the most used methods in real applications to advanced control methods which have been the focus of research recently [LPW09]. Gain scheduling [BBM06], adaptive control [JF08], MIMO methods [GC08], nonlinear control [Tho06], robust control [Øst08], model predictive control [Hen07], $DK$-iteration [MNP11] just to mention a few. Advanced control methods are thought to be the future of wind turbine control as they can employ new generations of sensors on wind turbines (e.g. LIDAR [HHW06]), new generation of actuators (e.g. trailing edge flaps [And10]) and also conveniently treat the turbine as a MIMO system. The last feature seems to become more important than before as wind turbines become bigger and more flexible which make decoupling different modes and designing controller for each mode more difficult. The wind turbine in this paper is treated as a MIMO system with pitch ($\theta_{in}$) and generator reaction torque ($Q_{in}$) as inputs and rotor rotational speed ($\omega_r$), generator rotational speed ($\omega_g$) and generated power ($P_e$) as outputs. Parametric uncertainties considered and $DK$-iteration method [SP01] is used to solve the control problem. $DK$-iteration is a method that takes structured uncertainty into account in order to reduce conservativeness of the $H_\infty$ procedure. A set of controllers each of which responsible for a specific region of the operation range are designed. we use wind speed estimation to choose pair of controllers and also to calculate convex combination of controller pair outputs to apply to the plant. This paper is organized as follows: In section 6.2 modeling of the wind turbine including modeling for wind speed estimation, linearization and uncertainty modeling is addressed. In section 6.3 controller design is explained. Finally in section 6.4 simulation results are presented.

## 6.2 Modeling of the Wind Turbine

For modeling purposes, the whole wind turbine can be divided into 4 subsystems: Structural subsystem, aerodynamics subsystem, electrical subsystem and actuator subsystem. The dominant dynamics of the wind turbine come from its structure which includes drivetrain, tower and blades. Several degrees of freedom could be considered to model the structure, but for control design mostly just a few important degrees of freedom are considered. In this work we only consider two degrees of freedom, namely the rotational degree of freedom (DOF) and drivetrain torsion. The aerodynamics subsystem gets effective wind speed ($v_e$), pitch angle ($\theta$) and rotational speed of the rotor ($\omega_r$) and returns aerodynamic torque ($Q_r$) and thrust ($Q_T$). The aerodynamic subsystem is responsible for the nonlinearity in the wind turbine model. More details are presented in section 6.2.2.

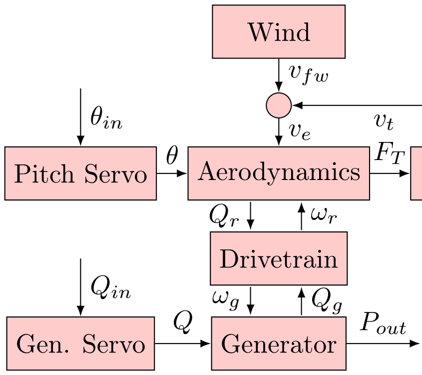


**Figure 6.1:** Wind turbine subsystems

### 6.2.1 Modeling for Estimation

Wind can be modeled as a complicated nonlinear stochastic process, however for practical purposes it could be approximated by a linear model [JLSM06]. In this model the wind has two elements, mean value term ($v_m$) and turbulent term ($v_t$):

$$v_e = v_m + v_t$$

The turbulent term is modeled by the following transfer function:

$$v_t = \frac{k(v_m)}{(p_1(v_m)s + 1)(p_2(v_m)s + 1)} e; \quad e \in N(0, 1)$$

And in the state space form:

$$\begin{aligned} \begin{pmatrix} \dot{v}_t \\ \ddot{v}_t \end{pmatrix} = &\begin{pmatrix} 0 & 1 \\ -\frac{1}{p_1(v_m)p_2(v_m)} & -\frac{p_1(v_m)+p_2(v_m)}{p_1(v_m)p_2(v_m)} \end{pmatrix} \\ &\begin{pmatrix} v_t \\ \dot{v}_t \end{pmatrix} + \begin{pmatrix} 0 \\ \frac{k(v_m)}{p_1(v_m)p_2(v_m)} \end{pmatrix} e \end{aligned} \tag{6.1}$$

This is a second order approximation of the wind power spectrum [JLSM06]. For wind speed estimation, a one DOF nonlinear model of the wind turbine is augmented with the wind model given above. An extended Kalman filter uses this model to estimate the effective wind speed. This wind speed is used to find the operating point of the wind turbine and to calculate appropriate control signals.

### 6.2.2 Nonlinear Model

Blade element momentum (BEM) theory [Han08] is used to calculate aerodynamic torque and thrust on the wind turbine. BEM theory explains how torque and thrust are related to wind speed, blade pitch angle and rotational speed of the rotor with the following formulas:

$$\begin{aligned} Q_r &= \frac{1}{2}\frac{1}{\omega_r}\rho\pi R^2 v_e^3 C_P(\theta,\omega,v_e) \\ Q_t &= \frac{1}{2}\rho\pi R^2 v_e^2 C_T(\theta,\omega,v_e) \end{aligned} \tag{6.2}$$

In which $Q_r$ and $Q_t$ are aerodynamic torque and thrust, $\rho$ is air density, $\omega_r$ is rotor rotational speed, $v_e$ is effective wind speed, $C_P$ is the power coefficient and $C_T$ is the thrust force coefficient. Absolute angular position of the rotor and generator are of no interest to us, therefore we use the drivetrain torsion $\psi = \theta_r - \theta_g$ instead. Having aerodynamic torque the whole system equation with 2 degrees of freedom becomes:

$$\begin{aligned} J_r\dot{\omega}_r &= Q_r - c(\omega_r - \frac{\omega_g}{N_g}) - k\psi \\ (N_g J_g)\dot{\omega}_g &= c(\omega_r - \frac{\omega_g}{N_g}) + k\psi - N_g Q_g \\ P_e &= Q_g\omega_g \end{aligned} \tag{6.3}$$

In which $J_r$ and $J_g$ are rotor and generator moments of inertia, $\psi$ is the drivetrain torsion, $c$ and $k$ are the drivetrain damping and stiffness factors respectively lumped in the low speed side of the shaft and $P_e$ is the generated power. For numerical values of these parameters and other parameters given in this paper, we refer the reader to [JBMS09]. These equations give a nonlinear model. However we need to linearize the nonlinear model of the system. This could be easily achieved using Taylor expansions around the operating points:

$$\begin{aligned} \Delta Q_r &= a\Delta\omega_r + b_1\Delta\theta + b_2\Delta v_e \\ \Delta P_e &= Q_g^*\Delta\omega_g + \omega_g^*\Delta Q_g \end{aligned} \tag{6.4}$$

$Q_g^*$ and $\omega_g^*$ are the nominal values of torque and generator speed. For the sake of simplicity in notations we use variables without $\Delta$ from now on.

### 6.2.3 Uncertain model

As it was mentioned, for control design we need to have a linear model of the system and the following model of the wind turbine is used:

$$\begin{pmatrix} \dot{x} \\ y_\Delta \\ y \end{pmatrix} = \left(\begin{array}{c|cc} A & B_1 & B_2 \\ \hline C_1 & D_{11} & D_{12} \\ C_2 & D_{21} & D_{22} \end{array}\right) \begin{pmatrix} x \\ u_\Delta \\ u \end{pmatrix} \tag{6.5}$$

In which states, inputs and outputs are:

$$\begin{aligned} x &= \begin{pmatrix} \omega_r & \omega_g & \psi & \theta & Q_g & v_e & \dot{v}_e \end{pmatrix}^T \\ u &= \begin{pmatrix} \theta_{in} & Q_{in} \end{pmatrix}^T \\ y &= \begin{pmatrix} \omega_r & \omega_g & P_e \end{pmatrix}^T \end{aligned} \tag{6.6}$$

$\omega_r$ is rotational speed of the rotor, $\omega_g$ is rotational speed of the generator, $\psi$ is drivetrain deflection, $\theta$ pitch of the blade, $Q_g$ is the generator reaction torque, $v_e$ and $\dot{v}_e$ are wind model states, $\theta_{in}$ is the reference value for pitch actuatorm, $Q_{in}$ is the reference value for the generator torque actuator and $P_e$ is the electrical power. Having all the equations, system equations become:

$$\dot{\omega}_r = \frac{a-c}{J_r}\omega_r + \frac{c}{J_r}\omega_g - \frac{k}{J_r}\psi + b_1\theta + b_2 v_e \tag{6.7}$$

$$\dot{\omega}_g = \frac{c}{N_g J_g}\omega_r - \frac{c}{N_g^2 J_g}\omega_g + \frac{k}{N_g J_g}\psi - \frac{Q_g}{J_g} \tag{6.8}$$

$$\dot{\psi} = \omega_r - \frac{\omega_g}{N_g} \tag{6.9}$$

$$\dot{\theta} = -\frac{1}{\tau_\theta}\theta + \frac{1}{\tau_\theta}\theta_{in} \tag{6.10}$$

$$\dot{Q}_g = -\frac{1}{\tau_g}Q_g + \frac{1}{\tau_g}Q_{in} \tag{6.11}$$

$$P_e = Q_{g_0}\omega_g + \omega_{g_0}Q_g \tag{6.12}$$

$$\ddot{v}_e = -\frac{1}{p_1 p_2}v_e - \frac{p_1+p_2}{p_1 p_2}\dot{v}_e + \frac{k}{p_1 p_2}e \tag{6.13}$$

$\tau_\theta$ and $\tau_g$ are time constants of the first order actuator models (see equ. 6.10). Uncertainties for the parameters of the equations 6.7-6.8 are:

$$\begin{array}{lll} a & = \bar{a}(1+p_a\delta_a) & \text{Linearized model} \\ b_1 & = \bar{b}_1(1+p_{b_1}\delta_{b_1}) & \text{Linearized model} \\ k & = \bar{k}(1+p_k\delta_k) & \text{Drivetrain stiffness} \\ c & = \bar{c}(1+p_c\delta_c) & \text{Drivetrain damping} \end{array} \tag{6.14}$$

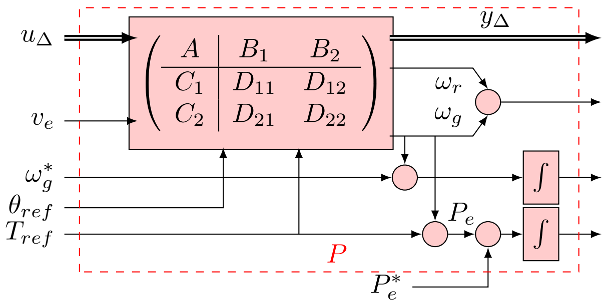


**Figure 6.2:** System interconnections

In which:

$$|\delta_a| \leq 1, \quad |\delta_{b_1}| \leq 1, \quad |\delta_k| \leq 1, \quad |\delta_c| \leq 1 \tag{6.15}$$

And $\bar{a}, \bar{b}_1, \bar{k}$ and $\bar{c}$ are the nominal values and $p_a, p_{b_1}, p_k$ and $p_c$ represent the relative perturbations. Uncertainty in the linearized model could be a result of approximate $C_P$ curve calculations, wrong wind speed estimation which results in picking the wrong operating point or aerodynamic changes due to blade flexibility or ice coatings on the blades. Using the equation 6.14 to represent uncertainties, the uncertainty matrix ($\Delta$) becomes a diagonal matrix which connects $y_\Delta$ and $u_\Delta$:

$$\begin{aligned} u_\Delta &= \mathrm{diag}(\delta_a, \delta_{b_1}, \delta_k, \delta_c) y_\Delta \\ y_\Delta &= \begin{pmatrix} y_a & y_{b_1} & y_k & y_c \end{pmatrix}^T \\ u_\Delta &= \begin{pmatrix} u_a & u_{b_1} & u_k & u_c \end{pmatrix}^T \end{aligned} \tag{6.16}$$

### 6.2.4 Simulation Model

The FAST (Fatigue, Aerodynamics, Structures, and Turbulence) code [JJ05] is used as the simulation model and the 5MW reference wind turbine is used as the plant [JBMS09]. In the simulation model 10 degrees of freedom are enabled which are: generator, drivetrain torsion, 1st and 2nd tower fore-aft, 1st and 2nd tower side-side, 1st and 2nd blade flapwise, 1st blade edgewise degrees of freedom.

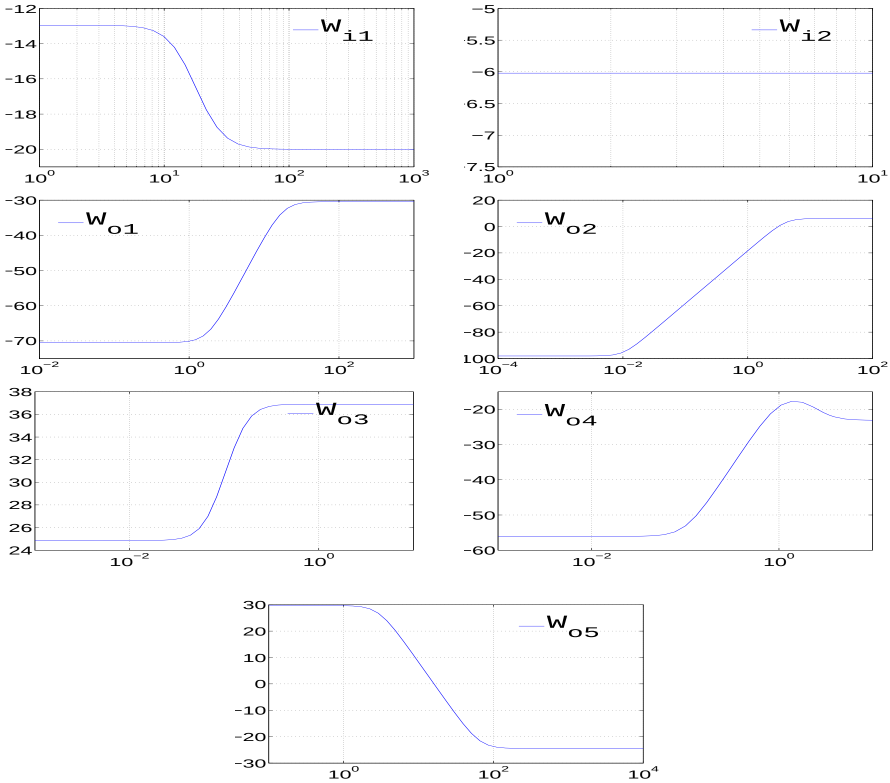


**Figure 6.3:** Bode plots for performance specifications(y-axis is in dB and x-axis is in rad/s)

# 6.3 Controller Design

## 6.3.1 Control Objectives

The most basic control objective of a wind turbine is to maximize captured power and prolong life time of the wind turbine. The second objective is achieved by minimizing the fatigue loads. Generally maximizing power capture is considered in the partial load and minimizing fatigue loads is mainly considered above rated. As we are operating in the full load region in this work, we have considered the second objective. Control objectives are formulated in the form of weighting functions on input disturbances ($d$) and exogenous outputs ($z$). In order to avoid high frequency activity of the actuators, we have put high pass filter on control signals to penalize high frequency actions. Also we have setup low pass filters to penalize only low frequency of some of the system outputs as their high frequency dynamics are outside of our actuator bandwidth and we can not control them. For regulating power and rotational speed, $\int P_e - P_e^*$ and $\int \omega_g - \omega_g^*$ and for minimizing fatigue loads on the drivetrain $\omega_g - N_g\omega_r$ are penalized.

## 6.3.2 Nominal Performance Problem

### 6.3.2.1 Theory

$H_\infty$ control theory [SP01] is used to solve the nominal performance problem. In this problem the $\Delta$ matrix is considered zero (no perturbation) and the following problem is solved:

$$K(s) = \arg \min_{K \in \mathcal{K}} \| W_o F_l(P, K) W_i(j\omega) \|_{\mathcal{H}_\infty} \tag{6.17}$$

In which $F_l(P,K)$ is the lower LFT of plant $P$ (figure 6.2) and controller $K$. $W_i$ and $W_o$ are frequency dependent weighting matrices on disturbances and exogenous outputs respectively of the form:

$$\begin{aligned} W_o &= diag(W_{o1}, \ldots, W_{o5}) \\ W_i &= diag(W_{i1}, W_{i2}) \end{aligned} \tag{6.18}$$

Bode plots of the weighting functions are given in the figure 6.3. Input disturbances ($d$) and exogenous outputs ($z$) are (see figure 6.2)

$$d = \begin{pmatrix} v_e \\ \omega_g^* \end{pmatrix} \begin{array}{l} \text{Wind Speed} \\ \text{Rotor rotation reference} \end{array}$$

$$z = \begin{pmatrix} \theta_{in} \\ Q_{in} \\ \omega_r^* - \frac{\omega_g}{N_g} \\ \int \omega_g^* - \omega_g \\ \int P_e^* - P_e \end{pmatrix} \begin{array}{l} \text{Pitch reference} \\ \text{Generator reaction torque reference} \\ \text{Deflection of the drivetrain} \\ \text{Integral of rotational speed error} \\ \text{Integral of generated power error} \end{array}$$

The optimization problem suggests that we are trying to find a controller in the set of stabilizing controllers that minimizes $H_\infty$-norm of weighted sensitivity function. This means we try to minimize the peak frequency of $W_oSW_i(j\omega)$. The resulting controller guarantees nominal performance if:

$$\| W_o F_l(P, K) W_i(j\omega) \|_{\mathcal{H}_\infty} < 1 \tag{6.19}$$

#### 6.3.2.2 Implementation

The robust control toolbox [BDG$^+$01] is used to solve the above problem. The controller is found trying to minimize transfer function from the disturbances (vector $d$) to the exogenous outputs (vector $z$). The controller that is designed here is used in Simulink on the full complexity FAST model of the 5MW reference wind turbine [JBMS09] (explained in section 6.2.4) .

### 6.3.3 Robust Performance Problem

#### 6.3.3.1 Theory

Robust performance means that the performance objective is satisfied for all possible plants in the uncertainty set. The robust performance condition can be cast into a robust stability problem with an additional perturbation block that defines $H_\infty$ performance specifications[SP01]. The structured singular value $\mu$ is a very powerful tool for the analysis of robust performance with a given controller. However this is an analysis tool, in order to design a controller, we need a synthesis tool. A scaled version of the upper bound of $\mu$ is used for controller synthesis. The problem is formulated in the following form:

$$\mu_\Delta(N(K)) \leq \min_{D\in\mathcal{D}} \sigma(DN(K)D^{-1}) \tag{6.20}$$

Now, the synthesis problem can be cast into the following optimization problem in which one tries to to find a controller that minimizes the peak value over frequency of this upper bound:

$$\min_{K\in\mathcal{K}}(\min_{D\in\mathcal{D}} \parallel DN(K)D^{-1} \parallel_\infty) \tag{6.21}$$

This problem is solved by an iterative approach called $DK$-iteration. For detailed explanations on the method and notations the reader is referred to[SP01].

#### 6.3.3.2 Implementation

we have used the $DK$-Iteration algorithm of the $\mu$-Synthesis toolbox[Mat] to design controllers. Figure 6.4 shows robust performance problem setup. $W_\Delta$ is used to scale the $\Delta$ matrix. we have taken uncertainty of 10% of the nominal

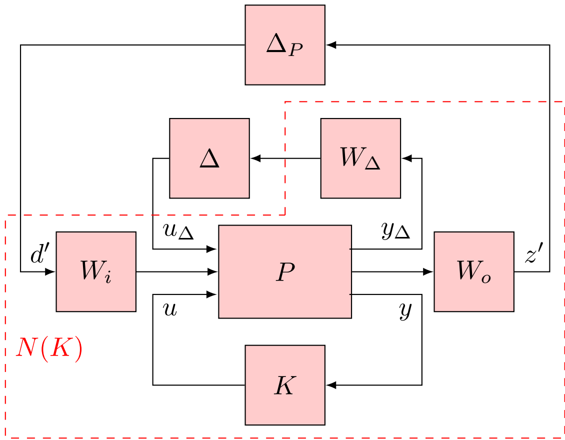


**Figure 6.4:** System setup for robust performance problem

values for the drivetrain stiffness and damping coefficients and 20% for the linearization parameters therefore the weighting matrix becomes:

$$W_\Delta = diag(0.2, 0.2, 0.1, 0.1) \tag{6.22}$$

$\Delta_P$ scaled by $W_i$ and $W_o$ matrices defines performance of the system in the form of a complex perturbation matrix. The resulting mixed-$\mu$ for one of the controllers is given in figure 6.5 and the iteration summery in table 6.1. Order of the resulting controllers (only one is shown in the table 6.1) are between 21 to 27, and since high order controllers are problematic in the implementation phase, we have used balanced order reduction to reduce order of all the controllers to 15.

### 6.3.4 Control Signal Calculation

Wind turbines are highly nonlinear plants and one single controller which is designed based on a linear model of an operating point is not able to handle the

| Iteration number | 1 | 2 | 3 |
|---|---|---|---|
| Controller Order | 21 | 23 | 25 |
| $\gamma$ Acheived | 9682006.84 | 24.327 | 4.726 |
| Peak $\mu$-Value | 1355.81 | 0.527 | 0.475 |

**Table 6.1:** $DK$-iteration summery for one of the controllers

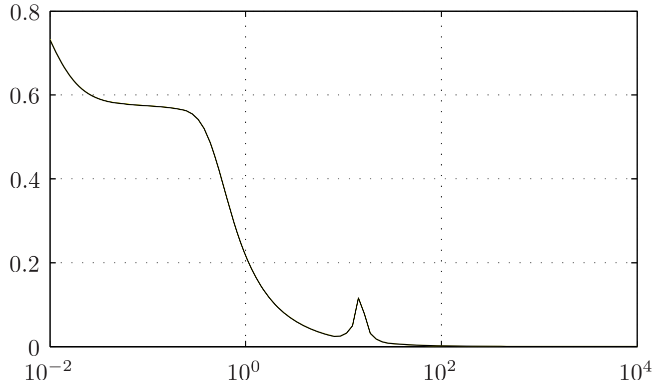


**Figure 6.5:** Mixed $\mu$ for one of the controllers ($v_e = 16m/s$)

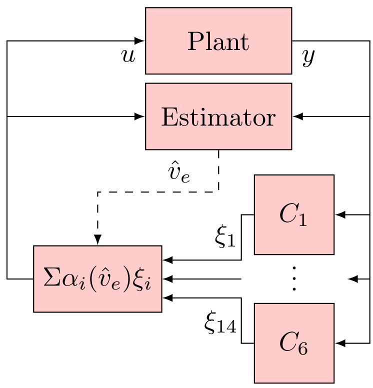


**Figure 6.6:** Control configuration for the whole region

whole operating region unless we give away too much performance in favor of robustness of the controller. One way to avoid this problem is to design a set of controllers each of which is responsible for a specific range of operation. we employ the estimated wind speed to choose a pair of controllers that are closest to the operating point and then use a convex combination of their outputs to calculate control signals to the plant. The following formula is used to calculate the control signal:

$$\begin{aligned} &\alpha(\hat{v}_e) = \hat{v}_e - v_k \quad v_k \leq \hat{v}_e < v_{k+1} \\ &u = (1 - \alpha(\hat{v}_e))\xi_k + \alpha(\hat{v}_e)\xi_{k+1} \end{aligned} \tag{6.23}$$

$\hat{v}_e$ is the estimated wind speed, $v_k \in \mathbb{V}$ which:

$$\mathbb{V} = \{12, 13, \ldots, 25\} \tag{6.24}$$

And $\xi_k$'s are defined as:

$$\begin{aligned} \xi_{1,2} &= C_1 & \xi_{3,4} &= C_2 \\ \xi_{5,6} &= C_3 & \xi_{7,8,9} &= C_4 \\ \xi_{10,11,12} &= C_5 & \xi_{13,14} &= C_6 \end{aligned} \tag{6.25}$$

In which $C_i$'s are controllers outputs. In order to reduce the number of controllers, controllers are designed only for wind speeds of $12, 14, 16, 18, 21, 24(m/s)$. As the aerodynamic gains do not change much in the high wind speeds and one controller can cover a bigger range of operating points, we have made the control grid larger in that area. Figure 6.6 shows the diagram of control signal calculation. In this figure, the block $\Sigma$ gets control signals from all the controllers and based on the estimated wind speed $\hat{v}_e$ calculates control signal $u$. Figure 6.12 shows the controller selection sequence ($u_k$).

## 6.4 Simulation Results

In this section simulation results for the obtained controllers are presented. The controllers are implemented in MATLAB and are tested on the full complexity FAST model of the reference wind turbine[JBMS09]. Kaimal model is used as the turbulence model and in order to stay in the above rated region, a realization of turbulent wind speed from category $C$ of the IEC turbulence categories with $18m/s$ as the mean wind speed is used.

### 6.4.1 Wind Speed Estimation

An extended Kalman filter is used to estimate the wind speed. Figure 6.7 shows the effective and the estimated wind speeds.

### 6.4.2 Stochastic Simulations

In this section simulation results for a stochastic wind speed is presented. Control inputs which are pitch reference $\theta_{in}$ and generator reaction torque reference $Q_{in}$ along with system outputs which are rotor rotational speed $\omega_r$ and electrical power $P_e$ are plotted in figures 6.8-6.11. As it could be seen in figure 6.7 the estimated wind speed is inaccurate and the controller is designed such that it can handle the uncertainties which arise from this inaccuracy. Simulation results show good regulations of generated power and rotational speed, however

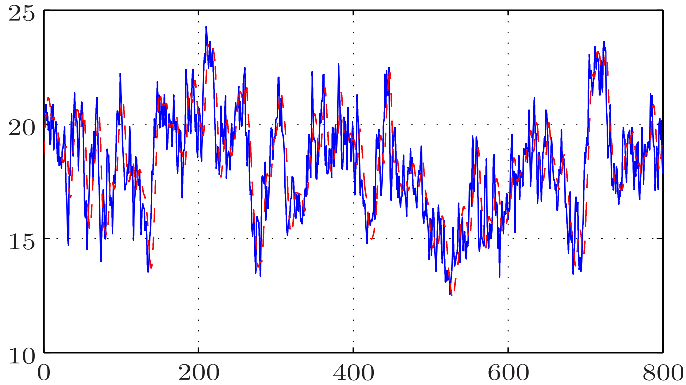


**Figure 6.7:** Wind speed (blue-solid), Estimated wind speed (red-dashed) $(m/s)$

one can get an even better regulation by making the controllers more aggressive which results in higher fatigue loads on the actuators and the drivetrain.

## 6.5 CONCLUSION

In this paper we solved the problem of robust control of a wind turbine using $DK$-iteration technique. Parametric uncertainties are considered in the uncertain model and then we have used $\mu$-synthesis toolbox to design a set of controllers. Estimated wind speed is used to calculate control signal from outputs of controllers. The final controller is implemented on a FAST simulation model with 10 degrees of freedom and simulation with stochastic wind speed based on IEC standard is done. The results show good regulation of generated power and rotational speed for a big range of wind speed changes.

## 6.6 ACKNOWLEDGMENTS

The first author would like to thank Lars Christian Henriksen and Sven Creutz Thomsen for their valuable comments.

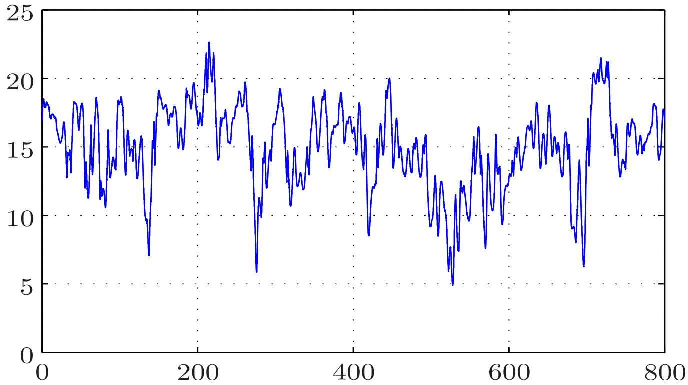


**Figure 6.8:** Blade-pitch reference (degrees)

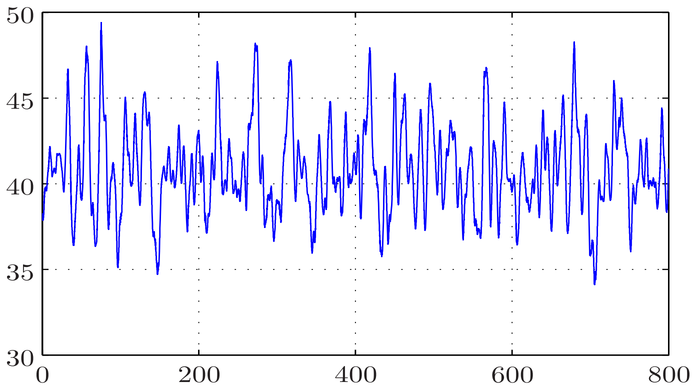


**Figure 6.9:** Generator-torque reference (kilo N.M.)

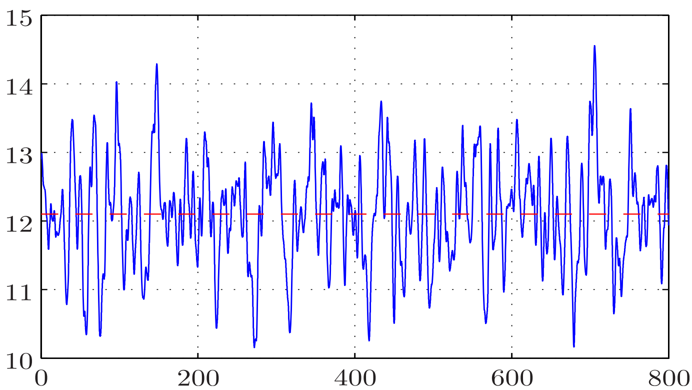


**Figure 6.10:** Rotor rotational speed ($\omega_r$) (rpm)

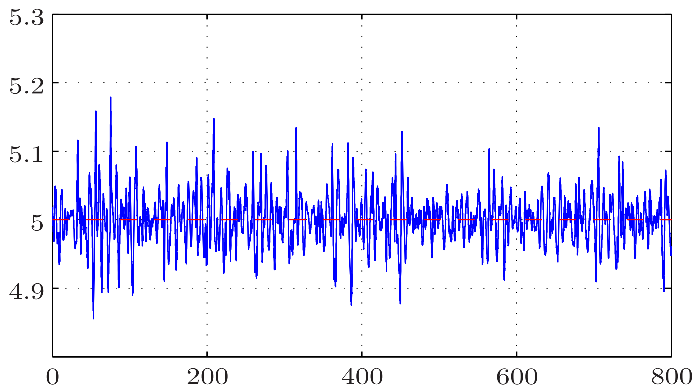


**Figure 6.11:** Electrical power (mega watts)

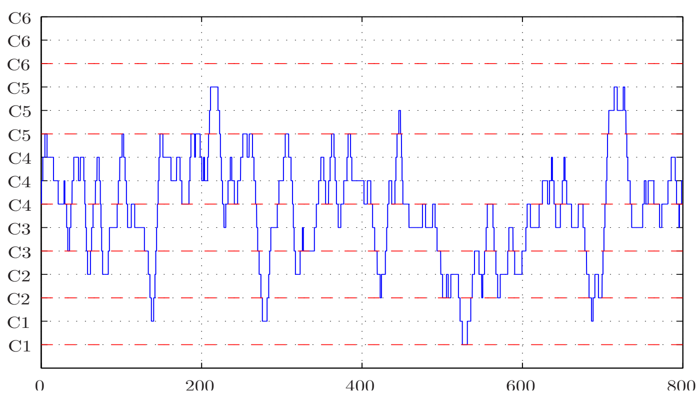


**Figure 6.12:** Controller selection sequence

## Paper B References


[And10] Peter Bjørn Andersen. *Advanced Load Alleviation for Wind Turbines using Adaptive Trailing Edge Flaps: Sensoring and Control.* PhD thesis, Technical University of Denmark, Denmark, 2010.

[BBM06] Fernando D. Bianchi, Hernan De Battista, and Ricardo J. Mantz. *Wind Turbine Control Systems: Principles, Modelling and Gain Scheduling Design.* Springer, 2006.

[BDG+01] Gary J. Balas, John C. Doyle, Keith Glover, Andy Packard, and Roy Smith. *Robust Control Toolbox.* The MathWorks, Inc., June 2001.

[GC08] M. Geyler and P. Caselitz. Robust multivariable pitch control design for load reduction on large wind turbines. *Journal of Solar Energy Engineering*, 130, 2008.

[Han08] Martin O. L. Hansen. *Aerodynamics of Wind Turbines.* Earthscan, 2008.

[Hen07] Lars Christian Henriksen. Model predictive control of a wind turbine. Master's thesis, Technical University of Denmark, Informatics and Mathematical Modelling, 2007.

[HHW06] M. Harris, M. Hand, and A. Wright. LIDAR for turbine control. Technical report, National Renewable Energy Laboratory, 2006.

[JBMS09] J. Jonkman, S. Butterfield, W. Musial, and G. Scott. Definition of a 5MW reference wind turbine for offshore system development. Technical report, National Renewable Energy Laboratory,, 1617 Cole Boulevard, Golden, Colorado 80401-3393 303-275-3000, 2009.

[JF08] Johnson and Fingersh. Adaptive pitch control of variable-speed wind turbines. *J. Sol. Energy Eng. (USA)*, 130(3):031012–1–7, 2008.

[JJ05] Jason M. Jonkman and Marshall L. Buhl Jr. Fast user's guide. Technical Report NREL/EL-500-38230, National Renewable Energy Laboratory, Golden, CO, August 2005.

[JLSM06] Allan Juul Larsen and Thomas Stampe Mogensen. Individuel pitchregulering af vindmølle. Master's thesis, Technical University of Denmark, Informatics and Mathematical Modelling, Lyngby, Denmark, 2006.

[LC00] W.E. Leithead and Bill Connor. Control of variable speed wind turbines: Design task. *Int J Control*, 73(13):1189–1212, 2000.

[LPW09] J.H. Laks, L.Y. Pao, and A.D. Wright. Control of wind turbines: Past, present, and future. *Proceedings of the American Control Conference*, pages 2096–2103, 2009.

[Mat] The MathWorks, Inc. *Robust Control Toolbox*.

[MNP11] Mahmood Mirzaei, Hans Henrik Niemann, and Niels Kjølstad Poulsen. DK-iteration robust control design of a wind turbine. In *IEEE Multi-Conference on Systems and Control*, pages 1493–1498, Denver, CO, USA, 2011.

[Øst08] Kasper Zinck Østergaard. *Robust, Gain-Scheduled Control of Wind Turbines*. PhD thesis, Automation and Control Department of Electronic Systems, Aalborg University, 2008.

[SP01] Sigurd Skogestad and Ian Postlethwaite. *Multivariable Feedback Control Analysis and design*. JOHN WILEY & SONS, Second Edition, 2001.

[Tho06] Sven Creutz Thomsen. Nonlinear control of a wind turbine. Master's thesis, Technical University of Denmark, Informatics and Mathematical Modelling, Lyngby, Denmark, 2006.

Paper C

# Model Predictive Control of a Nonlinear System with Known Scheduling Variable

**Authors:**
M. Mirzaei, N. K. Poulsen and H. H. Niemann

**Published in:**
Proceedings of the 17th Nordic Process Control Workshop, 2012

**Model Predictive Control of a Nonlinear System with Known Scheduling Variable**[1]

Mahmood Mirzaei[2], Niels Kjølstad Poulsen[2] and Hand Henrik Niemann[3]

**Abstract**

Model predictive control (MPC) of a class of nonlinear systems is considered in this paper. We will use Linear Parameter Varying (LPV) model of the nonlinear system. By taking the advantage of having future values of the scheduling variable, we will simplify state prediction. Consequently the control problem of the nonlinear system is simplified into a quadratic programming. Wind turbine is chosen as the case study and we choose wind speed as the scheduling variable. Wind speed is measurable ahead of the turbine, therefore the scheduling variable is known for the entire prediction horizon.

# 7.1 Introduction

Model predictive control (MPC) has been an active area of research and has been successfully applied on different applications in the last decades ([QB96]). The reason for its success is its straightforward ability to handle constraints. Moreover it can employ feedforward measurements in its formulation and can easily be extended to MIMO systems. However the main drawback of MPC was its on-line computational complexity which kept its application to systems with relatively slow dynamics for a while. Fortunately with the rapid progress of fast computations, better optimization algorithms, off-line computations using multi-parametric programming ([Bao05]) and dedicated algorithms and hardware, its applications have been extended to even very fast dynamical systems such as DC-DC converters ([Gey05]). Basically MPC uses a *model* of the plant to *predict* its future behavior in order to compute appropriate control signals to *control* outputs/states of the plant. To do so, at each sample time MPC uses the current measurement of outputs/states and solves an optimization problem. The result of the optimization problem is a sequence of control inputs of which

[1]This work is supported by the CASED Project funded by grant DSF-09- 063197 of the Danish Council for Strategic Research.

[2]DTU Informatics, Technical University of Denmark, Asmussens Alle, building 305, DK-2800 Kgs. Lyngby, Denmark

[3]Department of Electrical Engineering, Technical University of Denmark, Ørsteds Plads, Building 349, DK-2800 Kgs. Lyngby, Denmark

only the first element is applied to the plant and the procedure is repeated at the next sample time with new measurements ([Mac02]). This approach is called receding horizon control. Therefore basic elements of MPC are: a model of the plant to predict its future, a cost function which reflects control objectives, constraints on inputs and states/outputs, an optimization algorithm and the receding horizon principle. Depending on the type of the model, the control problem is called linear MPC, hybrid MPC, nonlinear MPC etc. Nonlinear MPC is normally computationally very expensive and generally there is no guarantee that the solution of the optimization problem is a global optimum. In this work we extend the idea of linear MPC using linear parameter varying (LPV) systems to formulate a tractable predictive control of nonlinear systems. To do so, we use future values of a disturbance to the system that acts as a scheduling variable in the model. However there are some assumptions that restrict our solution to a specific class of problems. The scheduling variable is assumed to be known for the entire prediction horizon. And the operating point of the system mainly depends on the scheduling variable.

## 7.2 Proposed method

Generally the nonlinear dynamics of a plant could be modeled as the following difference equation:

$$x_{k+1} = f(x_k, u_k, d_k) \tag{7.1}$$

With $x_k, u_k$ and $d_k$ as states, inputs and disturbances respectively. Using the nonlinear model, the nonlinear MPC problem could be formulated as:

$$\min_{u} \quad \ell(x_N) + \sum_{i=0}^{N-1} \ell(x_{k+i|k}, u_{k+i|k}) \tag{7.2}$$

$$\text{Subject to} \quad x_{k+1} = f(x_k, u_k, d_k) \tag{7.3}$$

$$u_{k+i|k} \in \mathbb{U} \tag{7.4}$$

$$\hat{x}_{k+i|k} \in \mathbb{X} \tag{7.5}$$

Where $\ell$ denotes some arbitrary norm and $\mathbb{U}$ and $\mathbb{X}$ show the set of acceptable inputs and states. As it was mentioned because of the nonlinear model, this problem is computationally too expensive. One way to avoid this problem is to linearize around an equilibrium point of the system and use linearized model instead of the nonlinear model. However for some plants assumption of linear model does not hold for long prediction horizons as the plant operating point changes, for example based on some disturbances that act as a scheduling variable. An example could be a wind turbine for which wind speed acts as a scheduling variable and changes the operating point of the system.

### 7.2.1 Linear MPC formulation

The problem of linear MPC could be formulated as:

$$\min_{u_0,u_1,\ldots,u_{N-1}} \|x_N\|_{Q_f} + \sum_{i=0}^{N-1} \|x_{k+i|k}\|_Q + \|u_{k+i|k}\|_R \tag{7.6}$$

$$\text{Subject to} \quad x_{k+1} = Ax_k + Bu_k \tag{7.7}$$

$$u_{k+i|k} \in \mathbb{U} \tag{7.8}$$

$$\hat{x}_{k+i|k} \in \mathbb{X} \tag{7.9}$$

Assuming that we use norms $1, 2$ and $\infty$ the optimization problem becomes convex providing that the sets $\mathbb{U}$ and $\mathbb{X}$ are convex. Convexity of the optimization problem makes it tractable and guarantees that the solution is the global optimum. The problem above is based on a single linear model of the plant around one operating point. However below we formulate our problem using linear parameter varying systems (LPV) in which the scheduling variable is known for the entire prediction horizon.

### 7.2.2 Linear Parameter Varying systems

Linear Parameter Varying (LPV) systems are a class of linear systems whose parameters change based on a scheduling variable. Study of LPV systems was motivated by their use in gain-scheduling control of nonlinear systems ([AGB95]). LPV systems are able to handle changes in the dynamics of the system by parameter varying matrices.

**Definition 7.1 (LPV systems)** let $k \in Z$ denote discrete time. We define the following LPV systems:

$$x_{k+1} = A(\gamma_k)x_k + B(\gamma_k)u_k \tag{7.10}$$

$$A(\gamma_k) = \sum_{j=1}^{n_\gamma} A_j \gamma_{k,j} \quad B(\gamma_k) = \sum_{j=1}^{n_\gamma} B_j \gamma_{k,j} \tag{7.11}$$

Which $A(\gamma_k)$ and $B(\gamma_k)$ are functions of the scheduling variable $\gamma_k$. The variables $x_k \in \mathbb{R}^{n_x}, u_k \in \mathbb{R}^{n_u}$, and $\gamma_k \in \mathbb{R}^{n_\gamma}$ are the state, the control input and the scheduling variable respectively.

### 7.2.3 Problem formulation

Using the above definition, the linear parameter varying (LPV) model of the nonlinear system with disturbances is of the following form:

$$\tilde{x}_{k+1} = A(\gamma_k)\tilde{x}_k + B(\gamma_k)\tilde{u}_k + B_d(\gamma_k)\tilde{d}_k \tag{7.12}$$

This model is formulated based on deviations from the operating point. However we need the model to be formulated in absolute values of inputs, states and disturbances. Because in our problem the steady state point changes as a function of the scheduling variable and we need to introduce a variable to capture its bahavior. In order to rewrite the state space model in the absolute form we use:

$$\tilde{x}_k = x_k - x_k^* \tag{7.13}$$

$$\tilde{u}_k = u_k - u_k^* \tag{7.14}$$

$$\tilde{d}_k = d_k - d_k^* \tag{7.15}$$

$x_k^*, u_k^*$ and $d_k^*$ are values of states, inputs and disturbances at the operating point. Therefore the LPV model becomes:

$$\begin{aligned} x_{k+1} = {} & A(\gamma_k)(x_k - x_k^*) + B(\gamma_k)(u_k - u_k^*) \\ & + B_d(\gamma_k)(d_k - d_k^*) + x_{k+1}^* \end{aligned} \tag{7.16}$$

Which could be written as:

$$x_{k+1} = A(\gamma_k)x_k + B(\gamma_k)u_k + B_d(\gamma_k)d_k + \lambda_k \tag{7.17}$$

with

$$\lambda_k = x_{k+1}^* - A(\gamma_k)x_k^* - B(\gamma_k)u_k^* - B_d(\gamma_k)d_k^* \tag{7.18}$$

Now having the LPV model of the system we proceed to compute state predictions. In linear MPC predicted states at step $n$ is:

$$\begin{aligned} x_{k+n} = A^n x_k + \sum_{i=0}^{n-1} A^i B u_{k+(n-1)-i} \\ \text{for} \quad n = 1, 2, \ldots, N \end{aligned} \tag{7.19}$$

However in our method the predicted state is also a function of scheduling variable $\Gamma_n = \left(\gamma_{k+1}, \gamma_{k+2}, \ldots \gamma_{k+n}\right)^T$ for $n = 1, 2, \ldots, N-1$ and we assume that the scheduling variable is known for the entire prediction. Therefore the predicted state could be written as:

$$x_{k+1}(\gamma_k) = A(\gamma_k)x_k + B(\gamma_k)u_k + B_d(\gamma_k)d_k + \lambda_k \tag{7.20}$$

And for $n \in \mathbb{Z}, n \geq 1$:

$$\begin{aligned} x_{k+n+1}(\Gamma_n) = & \prod_{i=n}^{0} A(\gamma_{k+i}) x_k \\ & + \sum_{j=0}^{n-1} \left( \prod_{i=n-j}^{1} A(\gamma_{k+i}) \right) B(\gamma_{k+j}) u_{k+j} \\ & + \sum_{j=0}^{n-1} \left( \prod_{i=n-j}^{1} A(\gamma_{k+i}) \right) B_d(\gamma_{k+j}) d_{k+j} \\ & + \sum_{j=0}^{n-1} \left( \prod_{i=n-j}^{0} A(\gamma_{k+i}) \right) \lambda_{k+(n-1)-j} \\ & + B(\gamma_{k+n}) u_{k+n} + B_d(\gamma_{k+n}) d_{k+n} + \lambda_{k+n} \end{aligned} \tag{7.21}$$

Using the above formulas we write down the stacked predicted states which becomes:

$$X = \Phi(\Gamma) x_k + \mathcal{H}_u(\Gamma) U + \mathcal{H}_d(\Gamma) D + \Phi_\lambda(\Gamma) \Lambda \tag{7.22}$$

with

$$X = \begin{pmatrix} x_{k+1} & x_{k+2} & \dots & x_{k+N} \end{pmatrix}^T \tag{7.23}$$

$$U = \begin{pmatrix} u_k & u_{k+1} & \dots & u_{k+N-1} \end{pmatrix}^T \tag{7.24}$$

$$D = \begin{pmatrix} d_k & d_{k+1} & \dots & d_{k+N-1} \end{pmatrix}^T \tag{7.25}$$

$$\Gamma = \begin{pmatrix} \gamma_k & \gamma_{k+1} & \dots & \gamma_{k+N-1} \end{pmatrix}^T \tag{7.26}$$

$$\Lambda = \begin{pmatrix} \lambda_k & \lambda_{k+1} & \dots & \lambda_{k+N-1} \end{pmatrix}^T \tag{7.27}$$

In order to summarize formulas for matrices $\Phi, \Phi_\lambda, \mathcal{H}_u$ and $\mathcal{H}_d$, we define a new function as:

$$\psi(m, n) = \prod_{i=m}^{n} A(\gamma_{k+i}) \tag{7.28}$$

Therefore the matrices become:

$$\Phi(\Gamma) = \begin{pmatrix} \psi(1,1) \\ \psi(2,1) \\ \psi(3,1) \\ \vdots \\ \psi(N,1) \end{pmatrix}$$

$$\Phi_\lambda(\Gamma) = \begin{pmatrix} I & 0 & 0 & \dots & 0 \\ \psi(1,1) & I & 0 & \dots & 0 \\ \psi(2,1) & \psi(2,2) & I & \dots & 0 \\ \vdots & \vdots & \vdots & \ddots & \vdots \\ \psi(N-1,1) & \psi(N-1,2) & \psi(N-1,3) & \dots & I \end{pmatrix}$$

$$\mathcal{H}_u(\Gamma) = \begin{pmatrix} B(\gamma_k) & 0 & \dots & 0 \\ \psi(1,1)B(\gamma_k) & B(\gamma_{k+1}) & \dots & 0 \\ \psi(2,1)B(\gamma_k) & \psi(2,2)B(\gamma_{k+1}) & \dots & 0 \\ \vdots & \vdots & \ddots & \vdots \\ \psi(N-1,1)B(\gamma_k) & \psi(N-1,2)B(\gamma_{k+1}) & \dots & B(\gamma_{N-1}) \end{pmatrix}$$

$$\mathcal{H}_d(\Gamma) = \begin{pmatrix} B_d(\gamma_k) & 0 & \dots & 0 \\ \psi(1,1)B_d(\gamma_k) & B_d(\gamma_{k+1}) & \dots & 0 \\ \psi(2,1)B_d(\gamma_k) & \psi(2,2)B_d(\gamma_{k+1}) & \dots & 0 \\ \vdots & \vdots & \ddots & \vdots \\ \psi(N-1,1)B_d(\gamma_k) & \psi(N-1,2)B_d(\gamma_{k+1}) & \dots & B_d(\gamma_{N-1}) \end{pmatrix}$$

After computing the state predictions as functions of control inputs (7.22), we can write down the optimization problem similar to a linear MPC problem as a quadratic program:

$$\boxed{\begin{aligned} \min_{U} \quad & X^T Q X + U^T R U \\ \text{Subject to:} \quad & U \in \mathbb{U} \\ & X \in \mathbb{X} \end{aligned}} \tag{7.29}$$

## 7.3 Case study

The case study here is a wind turbine. Wind turbine control is a challenging problem as the dynamics of the system changes based on wind speed which has a stochastic nature. The method that we propose here is to use wind speed as a scheduling variable. With the advances in LIDAR technology ([HHW06]) it is possible to measure wind speed ahead of the turbine and this enables us to have the scheduling variable of the plant for the entire prediction horizon.

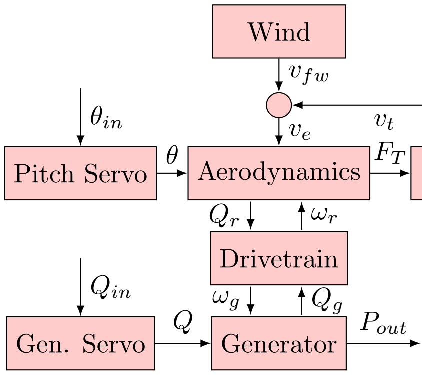


**Figure 7.1:** Wind turbine subsystems

### 7.3.1 Modeling

#### 7.3.1.1 Nonlinear model

For modeling purposes, the whole wind turbine can be divided into 4 subsystems: Aerodynamics subsystem, mechanical subsystem, electrical subsystem and actuator subsystem. The aerodynamic subsystem converts wind forces into mechanical torque and thrust on the rotor. The mechanical subsystem consists of drivetrain, tower and blades. Drivetrain transfers rotor torque to electrical generator. Tower holds the nacelle and withstands the thrust force. And blades transform wind forces into toque and thrust. The generator subsystem converts mechanical energy to electrical energy and finally the blade-pitch and generator-torque actuator subsystems are part of the control system. To model the whole wind turbine, models of these subsystems are obtained and at the end they are connected together. A wind model is obtained and augmented with the wind turbine model to be used for wind speed estimation. Figure 7.1 shows the basic subsystems and their interactions. The dominant dynamics of the wind turbine come from its flexible structure. Several degrees of freedom could be considered to model the flexible structure, but for control design mostly just a few important degrees of freedom are considered. In figure 7.2 basic degrees of freedom which are normally being considered in the design model are shown. However in this work we only consider two degrees of freedom, namely the rotational degree of freedom (DOF) and drivetrain torsion. Nonlinearity of the wind turbines mostly comes from its aerodynamics. Blade element momentum (BEM) theory ([Han08]) is used to numerically calculate aerodynamic torque and thrust on the wind turbine. This theory explains how torque and thrust are related to wind speed, blade pitch angle and rotational speed of the rotor.

In steady state, i.e. disregarding dynamic inflow, the following formulas can be used to calculate aerodynamic torque and thrust.

$$Q_r = \frac{1}{2}\frac{1}{\omega_r}\rho\pi R^2 v_e^3 C_p(\theta, \omega, v_e) \tag{7.30}$$

$$Q_t = \frac{1}{2}\rho\pi R^2 v_e^2 C_t(\theta, \omega, v_e) \tag{7.31}$$

In which $Q_r$ and $Q_t$ are aerodynamic torque and thrust, $\rho$ is the air density, $\omega_r$ is the rotor rotational speed, $v_e$ is the effective wind speed, $C_p$ is the power coefficient and $C_t$ is the thrust force coefficient. The absolute angular position of the rotor and generator are of no interest to us, therefore we use $\psi = \theta_r - \theta_g$ instead which is the drivetrain torsion. Having aerodynamic torque and modeling drivetrain with a simple mass-spring-damper, the whole system equation with 2 degrees of freedom becomes:

$$J_r\dot{\omega}_r = Q_r - c(\omega_r - \frac{\omega_g}{N_g}) - k\psi \tag{7.32}$$

$$(N_g J_g)\dot{\omega}_g = c(\omega_r - \frac{\omega_g}{N_g}) + k\psi - N_g Q_g \tag{7.33}$$

$$\dot{\psi} = \omega_r - \frac{\omega_g}{N_g} \tag{7.34}$$

$$P_e = Q_g \omega_g \tag{7.35}$$

In which $J_r$ and $J_g$ are rotor and generator moments of inertia, $\psi$ is the drivetrain torsion, $c$ and $k$ are the drivetrain damping and stiffness factors respectively lumped in the low speed side of the shaft and $P_e$ is the generated electrical power. For numerical values of these parameters and other parameters given in this paper, we refer to ([JBMS09]).

#### 7.3.1.2 Linearized model

As it was mentioned in the previous section, wind turbines are nonlinear systems. A basic approach to design controllers for nonlinear systems is to linearize them around some operating points. For a wind turbine, the operating points on the quasi-steady $C_p$ and $C_t$ curves are nonlinear functions of rotational speed $\omega_r$, blade pitch $\theta$ and wind speed $v$. To get a linear model of the system we need to linearize around these operating points. Rotational speed and blade pitch are measurable with enough accuracy, however this is not the case for the effect of wind on the rotor. Wind speed changes along the blades and with azimuth angle (angular position) of the rotor. This is because of wind shear and tower shadow and stochastic spatial distribution of the wind field. Therefore a single wind speed does not exist to be used and measured for finding the operating

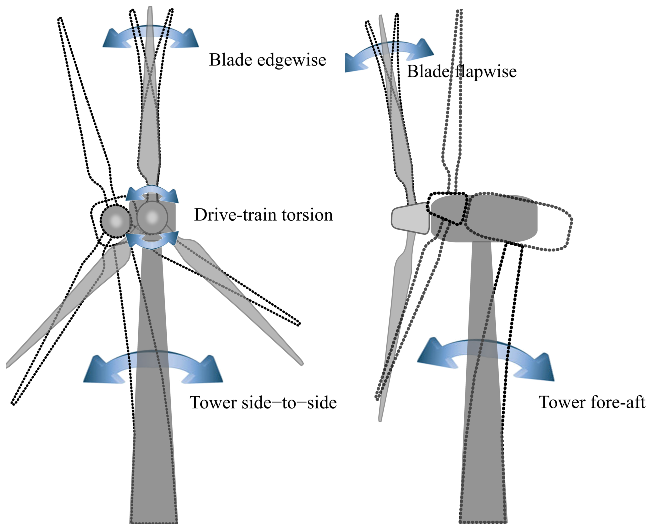


**Figure 7.2:** Basic degrees of freedom

point. We bypass this problem by defining a fictitious variable called effective wind speed ($v_e$) which shows the effect of wind in the rotor disc on the wind turbine. In our two DOFs model only the aerodynamic torque ($Q_r$) and electric power ($P_e$) are nonlinear. Taylor expansion is used to linearize them.

$$\Delta Q_r(\omega, \theta, v_e) = \underbrace{\frac{\partial Q_r}{\partial \omega}}_{a} \Delta\omega + \underbrace{\frac{\partial Q_r}{\partial \theta}}_{b_1} \Delta\theta + \underbrace{\frac{\partial Q_r}{\partial v_e}}_{b_2} \Delta v_e \tag{7.36}$$

$$\Delta P_e = \underbrace{\frac{\partial P_e}{\partial \omega_g}}_{Q_{g_0}} \Delta\omega_g + \underbrace{\frac{\partial P_e}{\partial Q_g}}_{\omega_{g_0}} \Delta Q_g \tag{7.37}$$

For the sake of simplicity in notations we use $Q_r$, $P_e$, $\theta$, $\omega$ and $v_e$ instead of $\Delta Q_r$, $\Delta P_e$, $\Delta\theta$, $\Delta\omega$ and $\Delta v_e$ around the operating points from now on. Using the linearized aerodynamic torque, the 2 DOFs linearized model becomes:

$$\dot{\omega}_r = \frac{a-c}{J_r}\omega_r + \frac{c}{J_r}\omega_g - \frac{k}{J_r}\psi + b_1\theta + b_2 v_e \tag{7.38}$$

$$\dot{\omega}_g = \frac{c}{N_g J_g}\omega_r - \frac{c}{N_g^2 J_g}\omega_g + \frac{k}{N_g J_g}\psi - \frac{Q_g}{J_g} \tag{7.39}$$

$$\dot{\psi} = \omega_r - \frac{\omega_g}{N_g} \tag{7.40}$$

$$P_e = Q_{g_0}\omega_g + \omega_{g_0} Q_g \tag{7.41}$$

A more detailed description of the model and linearization is given in ([MNP11]).

#### 7.3.1.3 LPV model

Collecting all the discussed models, matrices of the state space model become:

$$A(\gamma) = \begin{pmatrix} \frac{a(\gamma)-c}{J_r} & \frac{c}{J_r} & -\frac{k}{J_r} \\ \frac{c}{N_g J_g} & -\frac{c}{N_g^2 J_g} & \frac{k}{N_g J_g} \\ 1 & -1 & 0 \end{pmatrix} \qquad C = \begin{pmatrix} 1 & 0 & 0 \\ 0 & 1 & 0 \\ 0 & Q_{g_0} & 0 \end{pmatrix} \tag{7.42}$$

$$B(\gamma) = \begin{pmatrix} b_1(\gamma) & 0 \\ 0 & -\frac{1}{J_g} \\ 0 & 0 \end{pmatrix} \qquad D = \begin{pmatrix} 0 & 0 \\ 0 & 0 \\ 0 & \omega_{g_0} \end{pmatrix} \tag{7.43}$$

In which $x = \begin{pmatrix} \omega_r & \omega_g & \psi \end{pmatrix}^T$, $u = \begin{pmatrix} \theta & Q_g \end{pmatrix}^T$ and $y = \begin{pmatrix} \omega_r & \omega_g & P_e \end{pmatrix}^T$ are states, inputs and outputs respectively. In the matrix $B$, parameter $b_1$ is uncertain. Therefore the uncertain linear state space model becomes:

$$\begin{aligned} \dot{x} &= A(\gamma)x + B(\gamma)u \\ y &= Cx + Du \end{aligned}$$

### 7.3.2 Control objectives

The most basic control objective of a wind turbine is to maximize captured power during the life time of the wind turbine. This means trying to maximize captured power when wind speed is below its rated value. This is also called maximum power point tracking (MPPT). However when wind speed is above rated, control objective becomes regulation of the outputs around their rated values while trying to minimize dynamic loads on the structure. These objectives should be achieved against fluctuations in wind speed which acts as a disturbance to the system. In this work we have considered operation of the wind turbine in above rated (full load region). Therefore we try to regulate rotational speed and generated power around their rated values and remove the effect of wind speed fluctuations.

### 7.3.3 Offset free control

Persistent disturbances and modeling error can cause an offset between measured outputs and desired outputs. To avoid this problem we have employed an offset free reference tracking approach (see [MB02] and [PR03]). Our RMPC solves the regulation problem around the operating point. However we regulate around the operating point ($x_k^*$ and $u_k^*$) which results in offset from desired outputs. To avoid this problem in our control algorithm we shift origin in our regulation problem to $x_k^0$ and $u_k^0$ instead. In order to find new origins, we have augmented linear model of the plant with a disturbance model that adds fictitious disturbances to the system. The fictitious disturbances compensate the difference between measured outputs and desired outputs. State space model of the augmented system is:

$$\tilde{x}_{k+1} = \tilde{A}\tilde{x}_k + \tilde{B}u_k \tag{7.44}$$

$$y_k = \tilde{C}\tilde{x}_k + Du_k \tag{7.45}$$

in which the augmented state and matrices are:

$$\tilde{x}_k = \begin{pmatrix} \hat{x}_{k+1} \\ \hat{d}_{k+1} \\ \hat{p}_{k+1} \end{pmatrix} \qquad \tilde{A} = \begin{pmatrix} A & B_d & 0 \\ 0 & A_d & 0 \\ 0 & 0 & A_p \end{pmatrix} \tag{7.46}$$

$$\tilde{B} = \begin{pmatrix} B & 0 & 0 \end{pmatrix}^T \qquad \tilde{C} = \begin{pmatrix} C & 0 & C_p \end{pmatrix} \tag{7.47}$$

$\hat{x}_k, \hat{d}_k$ and $\hat{p}_k$ are system states, input/state and output disturbances respectively. $(A, B, C, D)$ are matrices of the linearized model, $B_d$ and $C_p$ show effect of disturbances on states and outputs respectively. $A_d$ and $A_p$ show dynamics of input/state and output disturbances. For more information and how to choose these matrices we refer to ([MB02]) and ([PR03]). Since the disturbances are not measurable, an extended Kalman filter is designed to estimate them. The estimated disturbances are used to remove any offset between desired outputs and measured outputs. Based on this model and estimated disturbances, $x_k^0$ and $u_k^0$ which are offset free steady state input and states can be calculated:

$$\begin{pmatrix} A - I & B \\ C & D \end{pmatrix} \begin{pmatrix} x_k^0 \\ u_k^0 \end{pmatrix} = \begin{pmatrix} -B_d\hat{d}_k \\ -C_p\hat{p}_k \end{pmatrix} \tag{7.48}$$

After calculating these values, we simply replace $x_k^*$ and $u_k^*$ in (7.18) with $x_k^0$ and $u_k^0$ which results in:

$$\lambda_k = x_{k+1}^0 - A(\gamma_k)x_k^0 - B(\gamma_k)u_k^0 - B_d(\gamma_k)d_k^* \tag{7.49}$$

## 7.4 Simulations

In this section simulation results for the obtained controller are presented. The controller is implemented in MATLAB and is tested on a full complexity FAST

**Table 7.1:** Performance comparison between gain scheduling approach and linear MPC

| Parameters | Proposed approach | Linear MPC |
|---|---|---|
| SD of $\omega_r$ (RPM) | 0.111 | 0.212 |
| SD of $P_e$ (Watts) | $4.686 \times 10^4$ | $8.048 \times 10^4$ |
| Mean value of $P_e$ (Watts) | $4.998 \times 10^6$ | $4.998 \times 10^6$ |
| SD of pitch (degrees) | 2.67 | 2.95 |
| SD of shaft moment (N.M.) | 256 | 293 |

([JJ05]) model of the reference wind turbine ([JBMS09]). Simulations are done with realistic turbulent wind speed, with Kaimal model ([iec05]) as the turbulence model and TurbSim ([Jon09]) is used to generate wind profile. In order to stay in the full load region, a realization of turbulent wind speed is used from category $C$ of the turbulence categories of the IEC 61400-1 ([iec05]) with $18m/s$ as the mean wind speed.

### 7.4.1 Stochastic simulations

In this section simulation results for a stochastic wind speed is presented. Control inputs which are pitch reference $\theta_{in}$ and generator reaction torque reference $Q_{in}$ along with system outputs which are rotor rotational speed $\omega_r$ and electrical power $P_e$ are plotted in figures 7.3-7.6 (red-dashed lines are results of linear MPC and solid blue lines show the results of the proposed approach.) Simulation results show good regulations of generated power and rotational speed. Table 7.1 shows a comparison of the results between the proposed approach and MPC approach based on linearization at each sample point ([Hen07]). As it could be seen from the table and figures, the proposed approach gives better regulation on rotational speed and generated power (smaller standard deviations) while maintaining a smaller shaft moment and pitch activity.

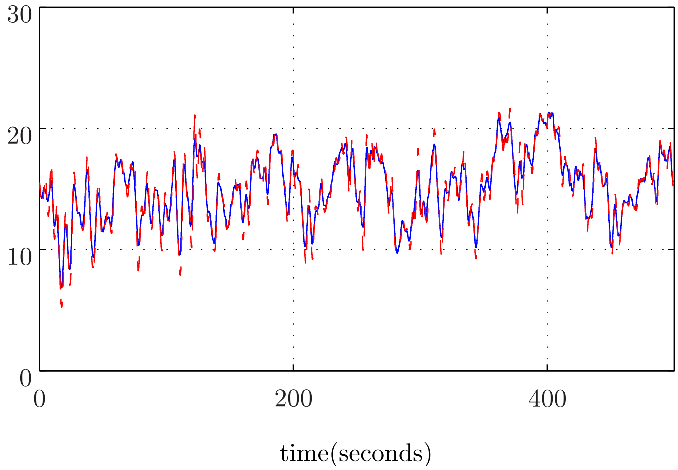


**Figure 7.3:** Blade-pitch reference (degrees, red-dashed line is linear MPC and solid blue line is the proposed approach)

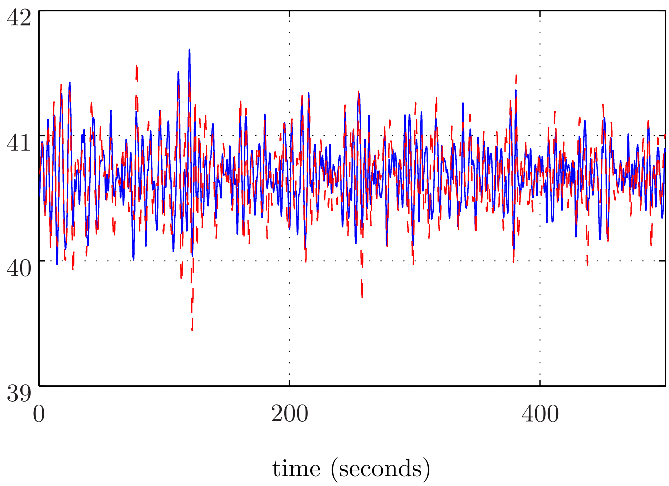


**Figure 7.4:** Generator-torque reference (kNM, red-dashed line is linear MPC and solid blue line is the proposed approach)

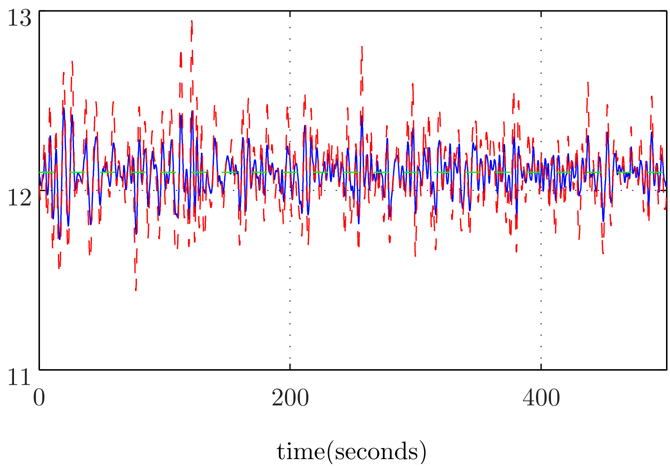


**Figure 7.5:** Rotor rotational speed ($\omega_r$, rpm, red-dashed line is linear MPC and solid blue line is the proposed approach)

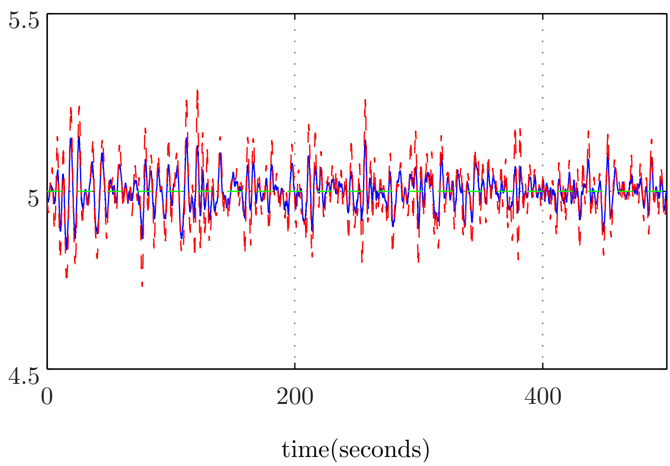


**Figure 7.6:** Electrical power (mega watts, red-dashed line is linear MPC and solid blue line is the proposed approach)

## Paper C References


[AGB95] Pierre Apkarian, Pascal Gahinet, and Greg Becker. Self-scheduled $H_\infty$ control of linear parameter-varying systems: a design example. *Automatica*, 31(9):1251–1261, 1995.

[Bao05] M. Baotic. *Optimal Control of Piecewise Affine Systems – a Multi-parametric Approach*. PhD thesis, March 2005.

[Gey05] T. Geyer. *Low Complexity Model Predictive Control in Power Electronics and Power Systems*. PhD thesis, March 2005.

[Han08] Martin O. L. Hansen. *Aerodynamics of Wind Turbines*. Earthscan, 2008.

[Hen07] Lars Christian Henriksen. Model predictive control of a wind turbine. Master's thesis, Technical University of Denmark, Informatics and Mathematical Modelling, 2007.

[HHW06] M. Harris, M. Hand, and A. Wright. LIDAR for turbine control. Technical report, National Renewable Energy Laboratory, 2006.

[iec05] IEC 61400-1 wind turbines-part 1: Design requirements., August 2005.

[JBMS09] J. Jonkman, S. Butterfield, W. Musial, and G. Scott. Definition of a 5MW reference wind turbine for offshore system development. Technical report, National Renewable Energy Laboratory,, 1617 Cole Boulevard, Golden, Colorado 80401-3393 303-275-3000, 2009.

[JJ05] Jason M. Jonkman and Marshall L. Buhl Jr. Fast user's guide. Technical Report NREL/EL-500-38230, National Renewable Energy Laboratory, Golden, CO, August 2005.

[Jon09] B.J. Jonkman. Turbsim user's guide: Version 1.50. Technical report, National Renewable Energy Laboratory, 1617 Cole Boulevard, Golden, Colorado 80401-3393 303-275-3000, 2009.

[Mac02] J.M. Maciejowski. *Predictive control with constraints*. Pearson Education Lim., Essex, 2002.

[MB02] Kenneth R. Muske and Thomas A. Badgwell. Disturbance modeling for offset-free linear model predictive control. *Journal of Process Control*, 12(5):617–632, 2002.

[MNP11] Mahmood Mirzaei, Hans Henrik Niemann, and Niels Kjølstad Poulsen. A $\mu$-synthesis approach to robust control of a wind turbine. In *the 50th IEEE Conference on Decision and Control and European*

*Control Conference*, pages 645–650, Orlando, Florida, United States, 2011.

[PR03] Gabriele Pannocchia and James B. Rawlings. Disturbance models for offset-free model-predictive control. *AIChE Journal*, 49(2):426–437, 2003.

[QB96] S. Joe Qin and Thomas A. Badgwell. An overview of industrial model predictive control technology. pages –, 1996.

Paper D

# Robust Model Predictive Control of a Wind Turbine

**Authors:**
M. Mirzaei, N. K. Poulsen and H. H. Niemann

**Presented in:**
American Control Conference, 2012.

**Robust Model Predictive Control of a Wind Turbine**[1]

Mahmood Mirzaei[2], Niels Kjølstad Poulsen[2] and Hand Henrik Niemann[3]

**Abstract**

In this work the problem of robust model predictive control (robust MPC) of a wind turbine in the full load region is considered. A minimax robust MPC approach is used to tackle the problem. Nonlinear dynamics of the wind turbine are derived by combining blade element momentum (BEM) theory and first principle modeling of the turbine flexible structure. Thereafter the nonlinear model is linearized using Taylor series expansion around system operating points. Operating points are determined by effective wind speed and an extended Kalman filter (EKF) is employed to estimate this. In addition, a new sensor is introduced in the EKF to give faster estimations. Wind speed estimation error is used to assess uncertainties in the linearized model. Significant uncertainties are considered to be in the gain of the system (B matrix of the state space model). Therefore this special structure of the uncertain system is employed and a norm-bounded uncertainty model is used to formulate a minimax model predictive control. The resulting optimization problem is simplified by semidefinite relaxation and the controller obtained is applied on a full complexity, high fidelity wind turbine model. Finally simulation results are presented. First a comparison between PI and robust MPC is given. Afterwards simulations are done for a realization of turbulent wind with uniform profile based on the IEC standard.

# 8.1 Introduction

## 8.1.1 Wind turbine control

In recent decades there has been an increasing interest in green energies, of which wind energy is one of the most important. Wind turbines are the most

[1]This work is supported by the CASED Project funded by grant DSF-09- 063197 of the Danish Council for Strategic Research.

[2]DTU Informatics, Technical University of Denmark, Asmussens Alle, building 305, DK-2800 Kgs. Lyngby, Denmark

[3]Department of Electrical Engineering, Technical University of Denmark, Ørsteds Plads, Building 349, DK-2800 Kgs. Lyngby, Denmark

common wind energy conversion systems (WECS) and are hoped to be able to compete economically with fossil fuel power plants in near future. However this demands better technology to reduce the price of electricity production. Control can play an essential part in this context because, on the one hand, control methods can decrease the cost of energy by keeping the turbine close to its maximum efficiency. On the other hand, they can reduce structural fatigue and therefore increase the lifetime of the wind turbine. There are several methods for wind turbine control ranging from classical control methods [LC00] which are the most used methods in real applications, to advanced control methods which have been the focus of research in the past few years [LPW09]; gain scheduling [BBM06], adaptive control [JF08], MIMO methods [GC08], nonlinear control [Tho06], robust control [Øst08], model predictive control [Hen07], $\mu$-Synthesis design [MNP11] are just a few. Advanced model based control methods are thought to be the future of wind turbine control as they can conveniently employ new generations of sensors on wind turbines (e.g. LIDAR [HHW06]), new generation of actuators (e.g. trailing edge flaps [And10]) and also treat the turbine as a MIMO system. The last feature seems to be becoming more important than before, as wind turbines are becoming bigger and more flexible. This trend makes decoupling different modes, specifying different objectives and designing controllers based on paired input/output channels more difficult. Model predictive control (MPC) has proved to be an effective tool to deal with multivariable constrained control problems [BM99]. As wind turbines are MIMO systems [GC08] with constraints on inputs and outputs, using MPC seems to be effective. Nominal MPC proved to give satisfactory results for offshore wind turbine control [Hen10] and trailing edge flap control [CPBWH11]. However these works have not taken into account uncertainty in the design model and this problem has been bypassed by trial-error and extensive simulations to get the best performance from the controllers. Based on this argument extending nominal MPC of wind turbines to robust MPC and including model uncertainties in the design seems to be natural. The wind turbine in this paper is treated as a MIMO system with pitch ($\theta_{in}$) and generator reaction torque ($Q_{in}$) as inputs and rotor rotational speed ($\omega_r$), generator rotational speed ($\omega_g$) and generated power ($P_e$) as outputs. This paper is organized as follows: In section 8.2 modeling of the wind turbine including modeling for wind speed estimation, linearization and uncertainty modeling are addressed. In section 8.3 robust MPC design is explained. Finally in section 8.4 simulation results are presented.

## 8.2 Modeling

### 8.2.1 Wind model

Wind can be modeled as a complicated nonlinear stochastic process. However for practical control purposes it could be approximated by a linear model [JLSM06]. In this model the wind has two elements, mean value term ($v_m$) and turbulent term ($v_t$): $v_e = v_m + v_t$. The turbulent term could be modeled by the following transfer function:

$$v_t = \frac{k}{(p_1 s + 1)(p_2 s + 1)} e; \quad e \in N(0, 1)$$

And in the state space form:

$$\begin{pmatrix} \dot{v}_t \\ \ddot{v}_t \end{pmatrix} = \begin{pmatrix} 0 & 1 \\ -\frac{1}{p_1 p_2} & -\frac{p_1+p_2}{p_1 p_2} \end{pmatrix} \begin{pmatrix} v_t \\ \dot{v}_t \end{pmatrix} + \begin{pmatrix} 0 \\ \frac{k}{p_1 p_2} \end{pmatrix} e \tag{8.1}$$

The parameters $p_1, p_2$ and $k$ are found by second order approximation of the wind power spectrum [JLSM06] and they depend on the mean wind speed $v_m$. For wind speed estimation, a one degree of freedom (DOF) nonlinear model of the wind turbine is augmented with the wind model given above. An extended Kalman filter uses this model to estimate the effective wind speed. This wind speed is used to find the operating point of the wind turbine and consequently calculate appropriate control signals.

### 8.2.2 Nonlinear model

For modeling purposes, the whole wind turbine can be divided into 4 subsystems: aerodynamics subsystem, mechanical subsystem, electrical subsystem and actuator subsystem. The aerodynamic subsystem converts wind forces into mechanical torque and thrust on the rotor. The mechanical subsystem consists of the drivetrain, tower and blades. The drivetrain transfers rotor torque to the electrical generator. The ower holds the nacelle and withstands the thrust force and the aerodynamically shaped blades transform wind speed into torque and thrust. The generator subsystem converts mechanical energy to electrical energy and finally the blade-pitch and generator-torque actuator subsystems are part of the control system. To model the whole wind turbine, models of these subsystems are obtained and at the end they are connected together. A wind model is obtained and augmented with the wind turbine model to be used for wind speed estimation. The dominant dynamics of the wind turbine come from its flexible structure. Several degrees of freedom could be considered to model the flexible structure, but for control design just a few important degrees of freedom are usually considered.

In this work we only consider two degrees of freedom, namely the rotational DOF and the drivetrain torsion.

Nonlinearity of the wind turbine mostly comes from its aerodynamics. Blade element momentum (BEM) theory [Han08] is used to calculate aerodynamic torque and thrust on the wind turbine. This theory explains how torque and thrust are related to wind speed, blade pitch angle and rotational speed of the rotor. In steady state, i.e. disregarding dynamic inflow, the following formulas can be used to calculate aerodynamic torque and thrust.

$$Q_r = \frac{1}{2}\frac{1}{\omega_r}\rho\pi R^2 v_e^3 C_p(\theta,\omega,v_e) \tag{8.2}$$

$$Q_t = \frac{1}{2}\rho\pi R^2 v_e^2 C_t(\theta,\omega,v_e) \tag{8.3}$$

In which $Q_r$ and $Q_t$ are aerodynamic torque and thrust, $\rho$ is the air density, $\omega_r$ is the rotor rotational speed, $v_e$ is the effective wind speed, $C_p$ is the power coefficient and $C_t$ is the thrust force coefficient.

The absolute angular position of the rotor and generator are of no interest to us, therefore we use $\psi = \theta_r - \theta_g$ instead which is the drivetrain torsion. Having aerodynamic torque and modeling the drivetrain with a simple mass-spring-damper, the whole system equation with two DOFs becomes:

$$J_r\dot{\omega}_r = Q_r - c(\omega_r - \frac{\omega_g}{N_g}) - k\psi \tag{8.4}$$

$$(N_g J_g)\dot{\omega}_g = c(\omega_r - \frac{\omega_g}{N_g}) + k\psi - N_g Q_g \tag{8.5}$$

$$\dot{\psi} = \omega_r - \frac{\omega_g}{N_g} \tag{8.6}$$

$$P_e = Q_g\omega_g \tag{8.7}$$

In which $J_r$ and $J_g$ are rotor and generator moments of inertia, $\psi$ is the drivetrain torsion, $c$ and $k$ are the drivetrain damping and stiffness factors, respectively lumped in the low speed side of the shaft, and $P_e$ is the electrical power generated. For numerical values of these parameters and other parameters given in this paper, refer to [JBMS09].

### 8.2.3 Uncertain Linear Model

#### 8.2.3.1 Linearized model

As mentioned in the previous section, wind turbines are nonlinear systems. A basic approach to design controllers for nonlinear systems is to linearize them around some operating points. For a wind turbine, the operating points on the quasi-steady $C_p$ and $C_t$ curves are nonlinear functions of rotational speed $\omega_r$, blade pitch $\theta$ and wind speed $v$. To get a linear model of the system we need to linearize around these operating points. Rotational speed and blade pitch are measurable with enough accuracy, however this is not the case for the effect of wind on the rotor. Wind speed changes along the blades and with the azimuth angle (angular position) of the rotor. This is because of wind shear and tower shadow as well as the stochastic spatial distribution of the wind field. Therefore a single wind speed does not exist which can be used and measured for finding the operating point. We bypass this problem by defining a fictitious variable called effective wind speed ($v_e$), which shows the effect of wind in the rotor disc on the wind turbine.

In our two DOFs model only the aerodynamic torque ($Q_r$) and electric power ($P_e$) are nonlinear and Taylor expansion is used to linearize them. For the sake of simplicity in notations we will use $Q_r$, $P_e$, $\theta$, $\omega$ and $v_e$ instead of $\Delta Q_r$, $\Delta P_e$, $\Delta\theta$, $\Delta\omega$ and $\Delta v_e$ around the operating points from now on. Using the linearized aerodynamic torque, the two DOFs linearized model becomes:

$$\dot{\omega}_r = \frac{a-c}{J_r}\omega_r + \frac{c}{J_r}\omega_g - \frac{k}{J_r}\psi + \frac{b_1}{J_r}\theta + \frac{b_2}{J_r}v_e \tag{8.8}$$

$$\dot{\omega}_g = \frac{c}{N_g J_g}\omega_r - \frac{c}{N_g^2 J_g}\omega_g + \frac{k}{N_g J_g}\psi - \frac{Q_g}{J_g} \tag{8.9}$$

$$\dot{\psi} = \omega_r - \frac{\omega_g}{N_g} \tag{8.10}$$

$$P_e = Q_{g_0}\omega_g + \omega_{g_0}Q_g \tag{8.11}$$

#### 8.2.3.2 The uncertain model

As mentioned previously, effective wind speed is not measurable and we need to use an estimation of it instead. An extended Kalman filter (EKF) is used to estimate the wind speed, for more details see section 8.4.1. The estimated $v_e$ has uncertainties and as we use this estimation to linearize the aerodynamics of the wind turbine, we end up with an uncertain linear model. The uncertainty is only in the equation (8.8). The uncertain linear model could be written as:

$$\dot{\omega}_r = \alpha(\delta_1)\omega_r + \frac{c}{J_r}\omega_g - \frac{k}{J_r}\psi + \beta_1(\delta_2)\theta + \beta_2(\delta_3)v_e$$

In which $\alpha(\delta_1), \beta_1(\delta_2)$ and $\beta_2(\delta_3)$ could be written as:

$$\alpha(\delta_1) = \quad \bar{\alpha}(1 + p_1\delta_1) \qquad |\delta_1| \leq 1 \tag{8.12}$$
$$\beta_1(\delta_2) = \quad \bar{\beta}_1(1 + p_2\delta_2) \qquad |\delta_2| \leq 1 \tag{8.13}$$
$$\beta_2(\delta_3) = \quad \bar{\beta}_2(1 + p_3\delta_3) \qquad |\delta_3| \leq 1 \tag{8.14}$$

$\bar{\alpha}, \bar{\beta}_1$ and $\bar{\beta}_2$ are nominal values and $p$'s show relative uncertainties. To get numerical values for relative uncertainty variables ($p_1, p_2$ and $p_3$) we have assumed $1m/s$ wind speed estimation error. Figure 8.1 shows a mapping from this estimation error to errors in the parameters of the linearized model ($\alpha$ and $\beta_1$) for different wind speeds. It can be seen in figures 8.1 that wind speed estimation error gives less than 5% error in $\alpha$, however this value is more than 20% for $\beta_1$. Using this argument and in order to simplify the optimization problem we neglect uncertainty in the dynamics of the system (which is determined by $\alpha$) and consider the uncertainty only to be in the gain of the system. Collecting all the discussed models, matrices of the state space model become:

$$A = \begin{pmatrix} \frac{a-c}{J_r} & \frac{c}{J_r} & -\frac{k}{J_r} \\ \frac{c}{N_g J_g} & -\frac{c}{N_g^2 J_g} & \frac{k}{N_g J_g} \\ 1 & -1 & 0 \end{pmatrix} \qquad B = \begin{pmatrix} \frac{b_1(\delta_2)}{J_r} & 0 \\ 0 & -\frac{1}{J_g} \\ 0 & 0 \end{pmatrix} \tag{8.15}$$

$$C = \begin{pmatrix} 1 & 0 & 0 \\ 0 & 1 & 0 \\ 0 & Q_{g0} & 0 \end{pmatrix} \qquad D = \begin{pmatrix} 0 & 0 \\ 0 & 0 \\ 0 & \omega_{g0} \end{pmatrix} \tag{8.16}$$

In which $x = \begin{pmatrix} \omega_r & \omega_g & \psi \end{pmatrix}^T$, $u = \begin{pmatrix} \theta & Q_g \end{pmatrix}^T$ and $y = \begin{pmatrix} \omega_r & \omega_g & P_e \end{pmatrix}^T$ are states, inputs and outputs respectively. In the matrix $B$, parameter $b_1$ is uncertain.

## 8.3 Control

### 8.3.1 Control objectives

The most basic control objective of a wind turbine is to maximize captured power during the life time of the machine. This means trying to maximize captured power when wind speed is below its rated value which is called maximum power point tracking (MPPT). Rated wind speed is a value where the turbine

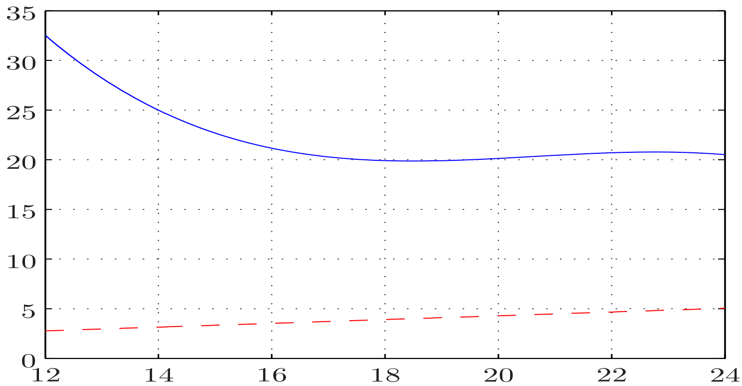


**Figure 8.1:** Relative uncertainties of the parameters (percent), $\beta_1$ solid-blue and $\alpha$ red-dashed

starts to operate at its rated speed and power. When the wind speed is above rated, the control objectives become regulation of the outputs around their rated values while trying to minimize dynamic loads on the structure. These objectives should be achieved against fluctuations in wind speed which acts as a disturbance to the system. In this work we have considered operation of the wind turbine in the above rated wind speed (full load region). Therefore we try to regulate rotational speed and generated power around their rated values and remove the effect of wind speed fluctuations.

### 8.3.2 Minimax MPC formulation

MPC uses a model of the system (to be controlled) to predict its future behavior. In nominal MPC the prediction of the output ($\hat{y}_{k+N|k}$) is a single value and it is calculated based on one model. However in robust MPC because the model is uncertain, this prediction is no longer a unique value but it is a set instead. An approach to tackle the problem with an uncertain model is to try to consider the most pessimistic situation with respect to uncertainties. This means maximizing the cost function on the uncertainty set. After maximization, we minimize the obtained cost function over control inputs as we do in nominal MPC. This approach is called minimax MPC and it is a common solution to robust MPC problems [LÖ3]. As explained in 8.2.3.2 the model obtained from our system only has uncertainties in the $B$ matrix. The special structure of our problem can help us in simplification of the minimax MPC problem. Therefore we formulate robust MPC of the wind turbine in the form of minimax MPC of a system with uncertain gain [LÖ3]:

$$x_{k+1} = Ax_k + B(\Delta_k)u_k \tag{8.17}$$
$$y_k = Cx_k + Du_k \tag{8.18}$$

Polytopic uncertainty and additive disturbances are common ways to include uncertainties in robust MPC formulation [BM99]. However here we have employed norm-bounded uncertainty to model our system [BEGFB94]:

$$B(\Delta_k) = B_0 + B_p\Delta_k C_p, \quad \Delta_k \in \boldsymbol{\Delta} \tag{8.19}$$
$$\boldsymbol{\Delta} = \{\Delta : \|\Delta\| \leq 1\} \tag{8.20}$$

With norm-bounded uncertain model of the system, we formulate the minimax MPC with quadratic performance and soft constraints. In order to simplify notations, we use stacked variables from now on and we define the following matrices:

$$\Phi_x = \begin{pmatrix} CA & CA^2 & \dots & CA^{N-1} \end{pmatrix}^T \tag{8.21}$$
$$\Gamma = \begin{pmatrix} CB(\Delta_1) & D & \dots & 0 \\ CAB(\Delta_2) & CB(\Delta_1) & \dots & 0 \\ \vdots & \vdots & \ddots & \vdots \\ CA^{N-1}B(\Delta_N) & CA^{N-2}B(\Delta_{N-1}) & \dots & D \end{pmatrix} \tag{8.22}$$

By using these matrices, the predicted output vector could be written as:

$$Y = \Phi_x \hat{x}_{k|k-1} + \Gamma U \tag{8.23}$$
$$\Gamma = \Gamma_0 + \Gamma_\Delta(\Delta^N) \tag{8.24}$$
$$\Delta^N = \begin{pmatrix} \Delta_1 & \Delta_2 & \dots & \Delta_N \end{pmatrix}^T \tag{8.25}$$

And the minimax optimization problem becomes:

$$\min_{U} \max_{\Delta^N} \quad Y^TQY + U^TRU + \Upsilon^T S_1 \Upsilon + \Xi^T S_2 \Xi \tag{8.26}$$
$$\text{subject to} \quad U \leq U_{max} + \Upsilon \tag{8.27}$$
$$U \geq U_{min} - \Upsilon \tag{8.28}$$
$$\Delta U \leq \Delta U_{max} + \Xi \tag{8.29}$$
$$\Delta U \geq \Delta U_{min} - \Xi \tag{8.30}$$
$$\Upsilon \geq 0 \tag{8.31}$$
$$\Xi \geq 0 \tag{8.32}$$

We use $\Delta U = \Psi U - I_0 u_{k-1}$ to rewrite constraints on $\Delta U$ in the form of constraints on $U$ in which:

$$\Psi = \begin{pmatrix} 1 & 0 & 0 & \dots & 0 \\ -1 & 1 & 0 & \dots & 0 \\ 0 & -1 & 1 & \dots & 0 \\ \vdots & \vdots & \vdots & \ddots & \vdots \\ 0 & 0 & 0 & \dots & 1 \end{pmatrix} \qquad I_0 = \begin{pmatrix} 1 \\ 0 \\ 0 \\ \vdots \\ 0 \end{pmatrix} \tag{8.33}$$

Now we use semidefinite relaxation and apply the Schur complement to the optimization problem to get the following optimization problem with LMI constraints:

$$\min_{t,U} \quad t \tag{8.34}$$

$$\text{s.t.} \begin{pmatrix} t & Y^T & U^T & \Upsilon^T & \Xi^T \\ \star & Q^{-1} & 0 & 0 & 0 \\ \star & \star & R^{-1} & 0 & 0 \\ \star & \star & \star & S_1^{-1} & 0 \\ \star & \star & \star & \star & S_2^{-1} \end{pmatrix} \succeq 0 \tag{8.35}$$

$$\begin{pmatrix} I \\ -I \\ \Psi \\ -\Psi \end{pmatrix} U - \begin{pmatrix} U_{max} + \Upsilon \\ -U_{min} + \Upsilon \\ \Delta U_{max} + I_0 u_{k-1} + \Xi \\ -\Delta U_{min} - I_0 u_{k-1} + \Xi \end{pmatrix} \leq 0 \tag{8.36}$$

$$\Upsilon \geq 0 \qquad \Xi \geq 0 \tag{8.37}$$

However in the above formulation $Y$ is of the form:

$$\begin{aligned} Y &= \Phi_x \hat{x}_{k|k-1} + \Gamma_0 U + \sum_{j=1}^{N} V_j \Delta_j W_j U, \ \Delta_j \in \boldsymbol{\Delta} \\ V_1 &= \begin{pmatrix} B_p & AB_p & \dots & A^{N-1}B_p \end{pmatrix}^T \\ V_2 &= \begin{pmatrix} 0 & B_p & AB_p & \dots & A^{N-2}B_p \end{pmatrix}^T \\ &\vdots \\ V_N &= \begin{pmatrix} 0 & 0 & 0 & \dots & B_p \end{pmatrix}^T \\ W_1 &= \begin{pmatrix} C_p & 0 & \dots & 0 \end{pmatrix} \\ W_2 &= \begin{pmatrix} 0 & C_p & \dots & 0 \end{pmatrix} \\ &\vdots \\ W_N &= \begin{pmatrix} 0 & 0 & \dots & C_p \end{pmatrix} \end{aligned}$$

and it contains uncertain elements. Based on results from [LÖ3], we use the following theorem to eliminate uncertainties [EGL97].

**Theorem 1:** Robust satisfaction of the uncertain LMI

$$F + L\Delta(I - D\Delta)^{-1}R + R^T(I - \Delta^T D^T)^{-1}\Delta^T L^T \succeq 0$$

is equivalent to the LMI

$$\begin{bmatrix} F & L \\ L^T & 0 \end{bmatrix} \succeq \begin{bmatrix} R & D \\ 0 & I \end{bmatrix}^T \begin{bmatrix} \tau I & 0 \\ 0 & -\tau I \end{bmatrix} \begin{bmatrix} R & D \\ 0 & I \end{bmatrix}$$
$$\tau \geq 0$$

Now we pull out the first uncertain element ($\Delta_1$) from $Y$ in the LMI constraint. To do so we define the following variable:

$$\gamma_i = \Phi_x \hat{x}_{k|k-1} + \Gamma_0 U + \sum_{j=i}^{N} V_j \Delta_j W_j U, \quad i = 1, \ldots, N \tag{8.38}$$

Using theorem 1, and collecting the matrices on the left hand side we get the following LMI:

$$\begin{pmatrix} t & \gamma_2^T & U^T & U^T W_1^T & \Upsilon^T & \Xi^T \\ \star & Q^{-1} - \tau_1 V_1 V_1^T & 0 & 0 & 0 & 0 \\ \star & \star & R^{-1} & 0 & 0 & 0 \\ \star & \star & \star & \tau_1 I & 0 & 0 \\ \star & \star & \star & \star & S_1^{-1} & 0 \\ \star & \star & \star & \star & \star & S_2^{-1} \end{pmatrix} \succeq 0 \tag{8.39}$$

We pulled out $\Delta_1$, and now we repeat the same procedure until we pull out all the uncertainties $\Delta_i$ for $i = 2, \ldots, N$. Afterwards we apply the Schur complement to write the final LMI in the form of smaller LMIs. Finally the optimization problem can be written in the following form:

$$\min_{t,\tau,U} \quad t_x + t_u + t_\upsilon + \sum_{j=0}^{N-1} t_j \tag{8.40}$$

$$\text{subject to} \quad \begin{pmatrix} t_x & \hat{x}_{k|k-1}^T \Phi_x^T + U^T \Gamma_0^T \\ \star & Q^{-1} - \sum_{j=0}^{N-1} \tau_j V_j V_j^T \end{pmatrix} \succeq 0 \tag{8.41}$$

$$\begin{pmatrix} t_u & U^T \\ \star & R^{-1} \end{pmatrix} \succeq 0 \; \begin{pmatrix} t_\upsilon & \Upsilon^T \\ \star & S^{-1} \end{pmatrix} \succeq 0 \; \begin{pmatrix} t_j & U^T W_j^T \\ \star & \tau_j I \end{pmatrix} \succeq 0 \tag{8.42}$$

$$\begin{pmatrix} I \\ -I \\ \Psi \\ -\Psi \end{pmatrix} U - \begin{pmatrix} U_{max} + \Upsilon \\ -U_{min} + \Upsilon \\ \Delta U_{max} + I_0 u_{k-1} + \Xi \\ -\Delta U_{min} - I_0 u_{k-1} + \Xi \end{pmatrix} \leq 0 \tag{8.43}$$

$$\tau_j \geq 0 \qquad \Upsilon \geq 0 \qquad \Xi \geq 0 \tag{8.44}$$

We have used SeDuMi [Stu99] to solve this optimization problem. SeDuMi is a program that solves optimization problems with linear, quadratic and semidefinite constraints.

### 8.3.3 Offset free reference tracking and constraint handling

Persistent disturbances and modeling error can cause an offset between measured outputs and desired outputs. To avoid this problem, we have employed an offset free reference tracking approach (see [MB02] and [PR03]). Our RMPC solves the regulation problem around the operating point. However we regulate around the operating points extracted from wind speed estimation which might be erroneous and results in offset from desired outputs. Besides, the difference between linear model and nonlinear model accounts for some of the differences between the measured outputs and the desired outputs as well. To avoid this problem, in our control algorithm we shift origin in our regulation problem to new operating points which ensures offset free reference tracking. It is clear that they should be included in the constraints of the robust MPC formulation.

## 8.4 Simulations

In this section firstly wind speed estimation is explained. Afterwards simulation results for the obtained controllers are presented. The controllers are implemented in MATLAB and are tested on a full complexity FAST [JJ05] model of the reference wind turbine [JBMS09]. Simulations are done with realistic turbulent wind speed using the Kaimal turbulence model [iec05]. TurbSim [Jon09] is used to generate a time marching hub-height wind profile. In order to stay in the full load region, a realization of turbulent wind speed is used from category $C$ of the turbulence categories of the IEC 61400-1 [iec05], with $18m/s$ as the mean wind speed.

### 8.4.1 Wind speed estimation

Wind speed estimation is essential in our control algorithm and in order to get a faster estimator we have introduced a sensor that measures rotor acceleration. This could be done using rotor speed and generator speed measurements [LD05]. A one DOF model of the wind turbine, including only rotor rotational degree of freedom is used for wind speed estimation. The first order nonlinear equations used in the extended Kalman filter are:

$$\dot{\omega} = \frac{1}{J_r} Q_r(\omega, \theta, v_e) - \frac{1}{J_r} Q_g \tag{8.45}$$

$$y = \begin{pmatrix} \omega & P_e & Q_r - Q_g \end{pmatrix}^T \tag{8.46}$$

| Parameters | RMPC | PI |
|---|---|---|
| $\omega_r$ standard deviation (RMP) | 0.389 | 0.728 |
| $P_e$ standard deviation (Watts) | $6.598 \times 10^4$ | $9.050 \times 10^4$ |
| $P_e$ mean value(Watts) | $4.997 \times 10^6$ | $4.999 \times 10^6$ |
| Pitch standard deviation (degrees) | 10.261 | 8.623 |
| Shaft moment standard deviation (N.M.) | $0.840 \times 10^3$ | $2.376 \times 10^3$ |

**Table 8.1:** RMPC and PI performance comparison

Using the nonlinear equations above and wind model (8.1) an extended Kalman filter is designed to estimate the effective wind speed. Figure 8.2 shows wind speed and its estimation.

### 8.4.2 Stochastic simulations

In this section simulation results for a stochastic wind speed are presented. Control inputs, which are pitch reference $\theta_{in}$ and generator reaction torque reference $Q_{in}$ along with system outputs, which are rotor rotational speed $\omega_r$ and electrical power $P_e$, are plotted in figures 8.3-8.6. The estimated wind speed is inaccurate and the controller is designed such that it can handle the uncertainties which arise from this inaccuracy. Simulation results show good regulations of generated power and rotational speed. Table 8.1 shows a comparison of the results between RMPC and a standard PI controller. The PI controller configuration and parameter values are taken from [JBMS09]. As could be seen from the table, the RMPC controller gives better regulation on rotational speed and generated power (smaller standard deviations) than the PI controller, while keeping the shaft moment less. However when it comes to pitch activity (here we have used pitch standard deviation), it has more pitch activity.

## 8.5 Conclusions

In this paper we found a second order nonlinear model of a wind turbine, using blade element momentum theory (BEM) and first principle modeling of the drivetrain. Our control methodology is based on linear models, therefore we have used Taylor series expansion to linearize the obtained nonlinear model around system operating point. The operating point is a direct function of rotor rotational speed, pitch angle and wind speed. Wind speed estimation is used to find the operating point and we showed that this will result in an uncertain $B$ matrix in our linear model. Special minimax model predictive

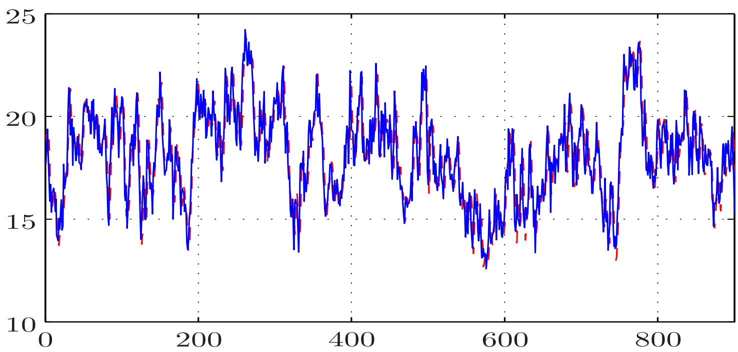


**Figure 8.2:** Wind speed (blue-solid), Estimated wind speed (red-dashed) $(m/s)$

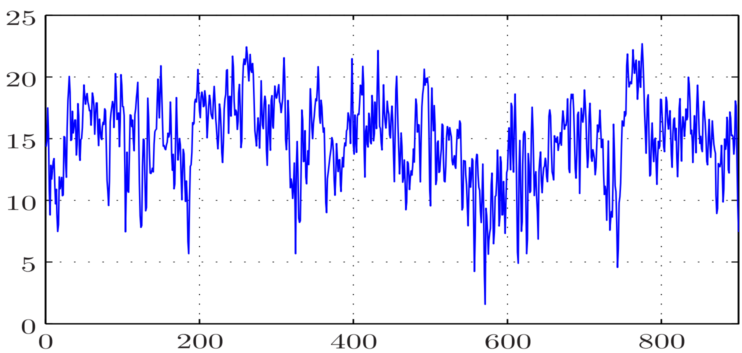


**Figure 8.3:** Blade-pitch reference (degrees)

control formulation was derived to take into account the assumed uncertainties. The final controller was applied on a full complexity FAST [JJ05] model and compared with a standard PI controller.

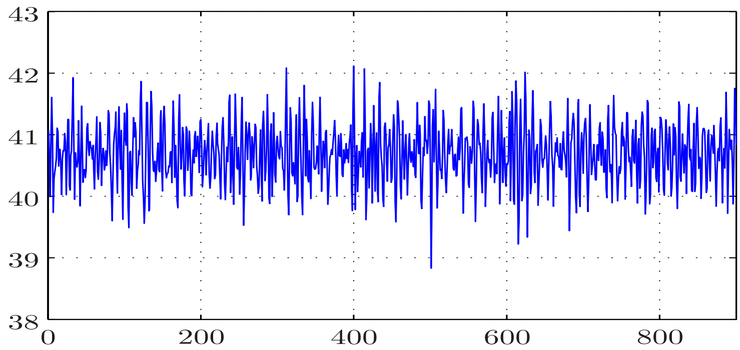


**Figure 8.4:** Generator-torque reference (kilo N.M.)

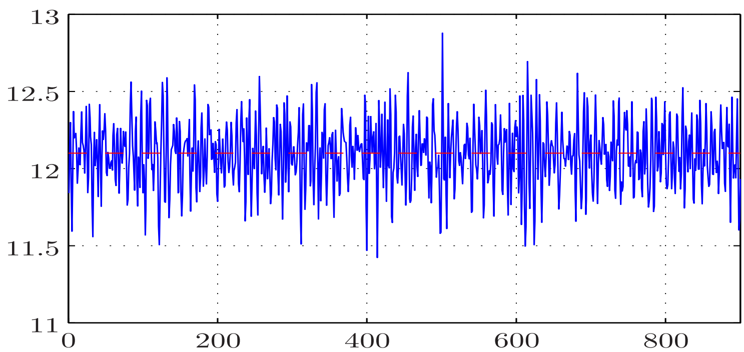


**Figure 8.5:** Rotor rotational speed ($\omega_r$) (rpm)

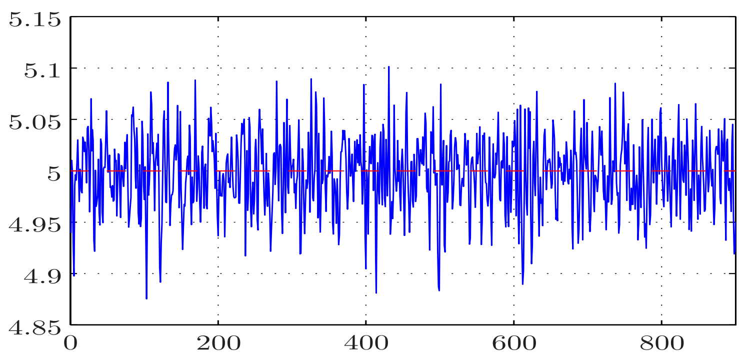


**Figure 8.6:** Electrical power (mega watts)

## Paper D References


[And10] Peter Bjørn Andersen. *Advanced Load Alleviation for Wind Turbines using Adaptive Trailing Edge Flaps: Sensoring and Control.* PhD thesis, Technical University of Denmark, Denmark, 2010.

[BBM06] Fernando D. Bianchi, Hernan De Battista, and Ricardo J. Mantz. *Wind Turbine Control Systems: Principles, Modelling and Gain Scheduling Design.* Springer, 2006.

[BEGFB94] S Boyd, L El-Ghaoui, E Feron, and V Balakrishnan. *Linear Matrix Inequalities in Systems and Control Theory.* SIAM, Philadelphia,Pa., 1994.

[BM99] A Bemporad and M Morari. Robust model predictive control: A survey. *Lecture Notes in Control and Information Sciences*, 245:207–226, 1999.

[CPBWH11] Damien Castaignet, Niels K. Poulsen, Thomas Buhl, and Jens Jakob Wedel-Heinen. Model predictive control of trailing edge flaps on a wind turbine blade. *Proceedings of the American Control Conference*, pages 4398–4403, 2011.

[EGL97] Laurent El Ghaoui and Hervé Lebret. Robust solutions to least-squares problems with uncertain data. *SIAM journal on matrix analysis and applications*, 18(4):1035–1064, 1997.

[GC08] M. Geyler and P. Caselitz. Robust multivariable pitch control design for load reduction on large wind turbines. *Journal of solar energy engineering*, 130(3):–, 2008.

[Han08] Martin O. L. Hansen. *Aerodynamics of Wind Turbines.* Earthscan, 2008.

[Hen07] Lars Christian Henriksen. Model predictive control of a wind turbine. Master's thesis, Technical University of Denmark, Informatics and Mathematical Modelling, 2007.

[Hen10] Lars Christian Henriksen. *Model Predictive Control of Wind Turbines.* PhD thesis, Department of Informatics, Technical University of Denmark (DTU), Kgs. Lyngby, Denmark, 2010.

[HHW06] M. Harris, M. Hand, and A. Wright. LIDAR for turbine control. Technical report, National Renewable Energy Laboratory, 2006.

[iec05] IEC 61400-1 wind turbines-part 1: Design requirements., August 2005.

[JBMS09] J. Jonkman, S. Butterfield, W. Musial, and G. Scott. Definition of a 5MW reference wind turbine for offshore system development. Technical report, National Renewable Energy Laboratory,, 1617 Cole Boulevard, Golden, Colorado 80401-3393 303-275-3000, 2009.

[JF08] Johnson and Fingersh. Adaptive pitch control of variable-speed wind turbines. *J. Sol. Energy Eng. (USA)*, 130(3):031012–1–7, 2008.

[JJ05] Jason M. Jonkman and Marshall L. Buhl Jr. Fast user's guide. Technical Report NREL/EL-500-38230, National Renewable Energy Laboratory, Golden, CO, August 2005.

[JLSM06] Allan Juul Larsen and Thomas Stampe Mogensen. Individuel pitchregulering af vindmølle. Master's thesis, Technical University of Denmark, Informatics and Mathematical Modelling, Lyngby, Denmark, 2006.

[Jon09] B.J. Jonkman. Turbsim user's guide: Version 1.50. Technical report, National Renewable Energy Laboratory, 1617 Cole Boulevard, Golden, Colorado 80401-3393 303-275-3000, 2009.

[LÖ3] Johan Löfberg. *Minimax approaches to robust model predictive control*. PhD thesis, Department of Electrical Engineering, Linköping University, 2003.

[LC00] W.E. Leithead and Bill Connor. Control of variable speed wind turbines: Design task. *Int J Control*, 73(13):1189–1212, 2000.

[LD05] W.E. Leithead and S. Dominguez. Wind turbine rotor acceleration : identification using gaussian regression. In *Proceedings of International Conference on Informatics in Control, Automation*, Barcelona, 2005.

[LPW09] J.H. Laks, L.Y. Pao, and A.D. Wright. Control of wind turbines: Past, present, and future. *Proceedings of the American Control Conference*, pages 2096–2103, 2009.

[MB02] Kenneth R. Muske and Thomas A. Badgwell. Disturbance modeling for offset-free linear model predictive control. *Journal of Process Control*, 12(5):617–632, 2002.

[MNP11] Mahmood Mirzaei, Hans Henrik Niemann, and Niels Kjølstad Poulsen. A $\mu$-synthesis approach to robust control of a wind turbine. In *the 50th IEEE Conference on Decision and Control and European Control Conference*, pages 645–650, Orlando, Florida, United States, 2011.

[Øst08] Kasper Zinck Østergaard. *Robust, Gain-Scheduled Control of Wind Turbines.* PhD thesis, Automation and Control Department of Electronic Systems, Aalborg University, 2008.

[PR03] Gabriele Pannocchia and James B. Rawlings. Disturbance models for offset-free model-predictive control. *AIChE Journal*, 49(2):426–437, 2003.

[Stu99] JF Sturm. Using sedumi 1.02, a matlab toolbox for optimization over symmetric cones. *Optim. Method Softw.*, 11-2(1-4):625–653, 1999.

[Tho06] Sven Creutz Thomsen. Nonlinear control of a wind turbine. Master's thesis, Technical University of Denmark, Informatics and Mathematical Modelling, Lyngby, Denmark, 2006.

# Paper E

# Robust Model Predictive Control of a Nonlinear System with Known Scheduling Variable and Uncertain Gain

**Authors:**
M. Mirzaei, N. K. Poulsen and H. H. Niemann

**Presented in:**
The 7th IFAC Symposium on Robust Control Design, 2012.

# Robust Model Predictive Control of a Nonlinear System with Known Scheduling Variable and Uncertain Gain[1]

Mahmood Mirzaei[2], Niels Kjølstad Poulsen[2] and Hand Henrik Niemann[3]

**Abstract**

Robust model predictive control (RMPC) of a class of nonlinear systems is considered in this paper. We will use Linear Parameter Varying (LPV) model of the nonlinear system. By taking the advantage of having future values of the scheduling variable, we will simplify state prediction. Because of the special structure of the problem, uncertainty is only in the $B$ matrix (gain) of the state space model. Therefore by taking advantage of this structure, we formulate a tractable minimax optimization problem to solve robust model predictive control problem. Wind turbine is chosen as the case study and we choose wind speed as the scheduling variable. Wind speed is measurable ahead of the turbine, therefore the scheduling variable is known for the entire prediction horizon.

## 9.1 Introduction

Model predictive control (MPC) has been an active area of research and has been successfully applied on different applications in the last decades ([QB96]). The reason for its success is its straightforward ability to handle constraints. Moreover it can employ feedforward measurements in its formulation and can easily be extended to MIMO systems. However the main drawback of MPC was its on-line computational complexity which kept its application to systems with relatively slow dynamics for a while. Fortunately with the rapid progress of fast computations, off-line computations using multi-parametric programming ([Bao05]) and dedicated algorithms and hardware, its applications have been extended to even very fast dynamical systems such as DC-DC converters ([Gey05]). Basically MPC uses a *model* of the plant to *predict* its future behavior in order to compute appropriate control signals to *control* outputs/states of the plant. To do so, at each sample time MPC uses the current measurement

[1]This work is supported by the CASED Project funded by grant DSF-09- 063197 of the Danish Council for Strategic Research.
[2]DTU Informatics, Technical University of Denmark, Asmussens Alle, building 305, DK-2800 Kgs. Lyngby, Denmark
[3]Department of Electrical Engineering, Technical University of Denmark, Ørsteds Plads, Building 349, DK-2800 Kgs. Lyngby, Denmark

of outputs and solves an optimization problem. The result of the optimization problem is a sequence of control inputs of which only the first element is applied to the plant and the procedure is repeated at the next sample time with new measurements ([Mac02]). This approach is called receding horizon control. Therefore basic elements of MPC are: a model of the plant to predict its future, a cost function which reflects control objectives, constraints on inputs and states/outputs, an optimization algorithm and the receding horizon principle. Depending on the type of the model, the control problem is called linear MPC, hybrid MPC, nonlinear MPC etc. Nonlinear MPC is normally computationally very expensive and generally there is no guarantee that the solution of the optimization problem is a global optimum. In this work we extend the idea of linear MPC using linear parameter varying (LPV) systems to formulate a tractable predictive control of nonlinear systems. MPC problem of LPV systems has been considered in ([CGM99]) and min-max MPC of LPV systems has been addressed in ([CFF03]), however in this work we use future values of the scheduling variable to simplify the optimization problem. To do so, we use future values of a disturbance to the system that acts as a scheduling variable in the model. However there are some assumptions that restrict our solution to a specific class of problems. The scheduling variable is assumed to be known for the entire prediction horizon. And the nonlinear dynamics of the system is determined by the scheduling variable.

## 9.2 Proposed method

Generally the nonlinear dynamics of a plant could be modeled as the following difference equation:

$$x_{k+1} = f(x_k, u_k) \tag{9.1}$$

With $x_k$ and $u_k$ as states and inputs respectively. Using the nonlinear model, the nonlinear MPC problem could be formulated as:

$$\begin{aligned}
\min_{u} \quad & p(x_N) + \sum_{i=0}^{N-1} q(x_{k+i|k}, u_{k+i|k}) && (9.2)\\
\text{Subject to} \quad & x_{k+1} = f(x_k, u_k) && (9.3)\\
& u_{k+i|k} \in \mathbb{U} && (9.4)\\
& \hat{x}_{k+i|k} \in \mathbb{X} && (9.5)
\end{aligned}$$

Where $p(x_N)$ and $q(x_{k+i|k}, u_{k+i|k})$ are called terminal cost and stage cost respectively and are assumed to be positive definite. $\mathbb{U}$ and $\mathbb{X}$ show the set of acceptable inputs and states. As it was mentioned because of the nonlinear model, this problem is computationally too expensive. One way to avoid this problem is to linearize around an equilibrium point of the system and use linearized model instead of the nonlinear model. However for some plants assumption of linear model does not hold for long prediction horizons. Because the plant operating point changes for example based on some disturbances that act as a scheduling variable. An example could be a wind turbine for which wind speed acts as a scheduling variable and changes the operating point of the system.

### 9.2.1 Linear MPC formulation

The problem of linear MPC could be formulated as:

$$\min_{u_0,u_1,\ldots,u_{N-1}} \|x_N\|_{Q_f} + \sum_{i=0}^{N-1} \|x_{k+i|k}\|_Q + \|u_{k+i|k}\|_R \tag{9.6}$$

$$\text{Subject to} \quad x_{k+1} = Ax_k + Bu_k \tag{9.7}$$

$$u_{k+i|k} \in \mathbb{U} \tag{9.8}$$

$$\hat{x}_{k+i|k} \in \mathbb{X} \tag{9.9}$$

Assuming that we use norms $1, 2$ and $\infty$ the optimization problem becomes convex providing that the sets $\mathbb{U}$ and $\mathbb{X}$ are convex. Convexity of the optimization problem makes it tractable and guarantees that the solution is the global optimum. The problem above is based on a single linear model of the plant around one operating point. However below we formulate our problem using linear parameter varying systems (LPV) in which the scheduling variable is known for the entire prediction horizon.

### 9.2.2 Linear Parameter Varying systems

Linear Parameter Varying (LPV) systems are a class of linear systems whose parameters change based on a scheduling variable. Study of LPV systems was motivated by their use in gain-scheduling control of nonlinear systems ([AGB95]). LPV systems are able to handle changes in the dynamics of the system by parameter varying matrices.

**Definition 9.1 (LPV systems)** let $k \in Z$ denote discrete time. We define the following LPV systems:

$$x_{k+1} = A(\gamma_k)x_k + B(\gamma_k)u_k \tag{9.10}$$

$$A(\gamma_k) = \sum_{j=1}^{n_\gamma} A_j \gamma_{k,j} \quad B(\gamma_k) = \sum_{j=1}^{n_\gamma} B_j \gamma_{k,j} \tag{9.11}$$

Which $A(\gamma_k)$ and $B(\gamma_k)$ are functions of the scheduling variable $\gamma_k$. The variables $x_k \in \mathbb{R}^{n_x}, u_k \in \mathbb{R}^{n_u}$, and $\gamma_k \in \mathbb{R}^{n_\gamma}$ are the state, the control input and the scheduling variable respectively.

### 9.2.3 Problem formulation

Using the above definition, the linear parameter varying (LPV) model of the nonlinear system is of the following form:

$$\tilde{x}_{k+1} = A(\gamma_k)\tilde{x}_k + B(\gamma_k)\tilde{u}_k \tag{9.12}$$

This model is formulated based on deviations from the operating point. However we need the model to be formulated in absolute values of inputs and states. Because in our problem the steady state point changes as a function of the scheduling variable, we need to introduce a variable to capture its bahavior. In order to rewrite the state space model in the absolute form we use:

$$\tilde{x}_k = x_k - x_k^* \tag{9.13}$$

$$\tilde{u}_k = u_k - u_k^* \tag{9.14}$$

$x_k^*$ and $u_k^*$ are values of states and inputs at the operating point. Therefore the LPV model becomes:

$$x_{k+1} = A(\gamma_k)(x_k - x_k^*) + B(\gamma_k)(u_k - u_k^*) + x_{k+1}^* \tag{9.15}$$

Which could be written as:

$$x_{k+1} = A(\gamma_k)x_k + B(\gamma_k)u_k + \lambda_k \tag{9.16}$$

with

$$\lambda_k = x_{k+1}^* - A(\gamma_k)x_k^* - B(\gamma_k)u_k^* \tag{9.17}$$

Now having the LPV model of the system we proceed to compute state predictions. In linear MPC predicted states at step $n$ is:

$$\begin{aligned} x_{k+n} &= A^n x_k + \sum_{i=0}^{n-1} A^i B u_{k+(n-1)-i} \\ &\text{for} \quad n = 1, 2, \ldots, N \end{aligned} \tag{9.18}$$

However in our method the predicted state is also a function of scheduling variable $\Gamma_n = \left(\gamma_{k+1}, \gamma_{k+2}, \dots \gamma_{k+n}\right)^T$ for $n = 1, 2, \dots, N-1$ and we assume that the scheduling variable is known for the entire prediction. Therefore the predicted state could be written as:

$$x_{k+1}(\gamma_k) = A(\gamma_k)x_k + B(\gamma_k)u_k + \lambda_k \tag{9.19}$$

And for $n \in \mathbb{Z}, n \geq 1$:

$$\begin{aligned} x_{k+n+1}(\Gamma_n) = &\left(\prod_{i=0}^{n} A^T(\gamma_{k+i})x_k\right)^T \\ &+ \sum_{j=0}^{n-1}\left(\prod_{i=1}^{n-j} A^T(\gamma_{k+i})\right)^T B(\gamma_{k+j})u_{k+j} \\ &+ \sum_{j=0}^{n-1}\left(\prod_{i=0}^{n-j} A^T(\gamma_{k+i})\right)^T \lambda_{k+(n-1)-j} \\ &+ B(\gamma_{k+n})u_{k+n} + \lambda_{k+n} \end{aligned} \tag{9.20}$$

Using the above formulas we write down the stacked predicted states which becomes:

$$X = \Phi(\Gamma)x_k + \mathcal{H}_u(\Gamma)U + \Phi_\lambda(\Gamma)\Lambda \tag{9.21}$$

with

$$X = \begin{pmatrix} x_{k+1} & x_{k+2} & \dots & x_{k+N} \end{pmatrix}^T \tag{9.22}$$

$$U = \begin{pmatrix} u_k & u_{k+1} & \dots & u_{k+N-1} \end{pmatrix}^T \tag{9.23}$$

$$\Gamma = \begin{pmatrix} \gamma_k & \gamma_{k+1} & \dots & \gamma_{k+N-1} \end{pmatrix}^T \tag{9.24}$$

$$\Lambda = \begin{pmatrix} \lambda_k & \lambda_{k+1} & \dots & \lambda_{k+N-1} \end{pmatrix}^T \tag{9.25}$$

In order to summarize formulas for matrices $\Phi, \Phi_\lambda$ and $\mathcal{H}_u$, we define a new function as:

$$\psi(m,n) = \left(\prod_{i=n}^{m} A^T(\gamma_{k+i})\right)^T \tag{9.26}$$

Therefore the matrices become:

$$\Phi(\Gamma) = \begin{pmatrix} \psi(1,1) \\ \psi(2,1) \\ \psi(3,1) \\ \vdots \\ \psi(N,1) \end{pmatrix}$$

$$\Phi_\lambda(\Gamma) = \begin{pmatrix} I & 0 & 0 & \dots & 0 \\ \psi(1,1) & I & 0 & \dots & 0 \\ \psi(2,1) & \psi(2,2) & I & \dots & 0 \\ \vdots & \vdots & \vdots & \ddots & \vdots \\ \psi(N-1,1) & \psi(N-1,2) & \psi(N-1,3) & \dots & I \end{pmatrix}$$

$$\mathcal{H}_u(\Gamma) = \begin{pmatrix} B(\gamma_k) & 0 & \dots & 0 \\ \psi(1,1)B(\gamma_k) & B(\gamma_{k+1}) & \dots & 0 \\ \psi(2,1)B(\gamma_k) & \psi(2,2)B(\gamma_{k+1}) & \dots & 0 \\ \vdots & \vdots & \ddots & \vdots \\ \psi(N-1,1)B(\gamma_k) & \psi(N-1,2)B(\gamma_{k+1}) & \dots & B(\gamma_{N-1}) \end{pmatrix}$$

After computing the state predictions as functions of control inputs, we can write down the optimization problem similar to a linear MPC problem as a quadratic program.

## 9.3 Minimax Problem

### 9.3.1 Minimax for Linear Model

MPC uses a model of the system (to be controlled) to predict its future behavior. In nominal MPC the prediction of the state ($\hat{x}_{k+N|k}$) is a single value and it is calculated based on one model. However in robust MPC where the model is uncertain, this prediction is no longer a unique value, but it is a set instead. An approach to tackle the problem with uncertain model is to try to optimize the most pessimistic situation with respect to uncertainties. This means maximizing cost function on the uncertainty set. After maximization, we minimize the obtained cost function over control inputs as we do in nominal MPC. This approach is called minimax MPC which is a common solution to robust MPC problems ([LÖ3]). The special structure of our problem (having uncertainty only in the gain of the system) can help us simplifying the minimax MPC problem. Therefore we formulate robust MPC of our system in the form of minimax MPC of a system with uncertain gain ([LÖ3]):

$$x_{k+1} = Ax_k + B(\Delta_k)u_k \tag{9.27}$$
$$y_k = Cx_k + Du_k \tag{9.28}$$

We have employed norm-bounded uncertainty ([BEGFB94]) to model our system:

$$B(\Delta_k) = B_0 + B_p\Delta_k C_p, \quad \Delta_k \in \boldsymbol{\Delta} \tag{9.29}$$
$$\boldsymbol{\Delta} = \{\Delta : \|\Delta\| \le 1\} \tag{9.30}$$

And as the $B$ matrices are dependent on $\gamma$, we have:

$$B(\gamma_k, \Delta_k) = B_0(\gamma_k) + B_p(\gamma_k)\Delta_k C_p(\gamma_k), \quad \Delta_k \in \boldsymbol{\Delta} \tag{9.31}$$
$$\boldsymbol{\Delta} = \{\Delta : \|\Delta\| \le 1\} \tag{9.32}$$

With norm-bounded uncertain model of the system, we can formulate the minimax MPC with quadratic performance and soft constraints on inputs in the following form:

$$
\begin{array}{lrl}
\min\limits_{u} \max\limits_{\Delta} & \sum_{j=0}^{N-1} & \|y_{k+j|k}\|_Q^2 + \|u_{k+j|k}\|_R^2 + \\
 & & \|\upsilon_{k+j|k}\|_{S_1}^2 + \|\xi_{k+j|k}\|_{S_2}^2 \\
\text{subject to} & \hat{x}_{k+1|k} = & A\hat{x}_{k|k} + B(\Delta_k)u_k \\
 & \hat{y}_{k|k} = & C\hat{x}_{k|k} + Du_k \\
 & u_{k+j|k} \le & U_{max} + \upsilon_{k+j|k} \\
 & u_{k+j|k} \ge & U_{min} - \upsilon_{k+j|k} \\
 & \Delta u_{k+j|k} \le & \Delta U_{max} + \xi_{k+j|k} \\
 & \Delta u_{k+j|k} \ge & \Delta U_{min} - \xi_{k+j|k} \\
 & \eta_{k+j|k} \ge & 0 \\
 & \xi_{k+j|k} \ge & 0
\end{array}
$$

In order to simplify notations, we use stacked variables. The stacked output predictions, control sequences and auxiliary variables become:

$$U = \begin{pmatrix} u_{k|k} & u_{k+1|k} & \dots & u_{k+N-1|k} \end{pmatrix}^T \tag{9.33}$$
$$\Delta U = \begin{pmatrix} \Delta u_{k|k} & \Delta u_{k+1|k} & \dots & \Delta u_{k+N-1|k} \end{pmatrix}^T \tag{9.34}$$
$$Y = \begin{pmatrix} \hat{y}_{k|k} & \hat{y}_{k+1|k} & \dots & \hat{y}_{k+N-1|k} \end{pmatrix}^T \tag{9.35}$$
$$\Xi = \begin{pmatrix} \xi_{k|k} & \xi_{k+1|k} & \dots & \xi_{k+N-1|k} \end{pmatrix}^T \tag{9.36}$$
$$\Upsilon = \begin{pmatrix} \upsilon_{k|k} & \upsilon_{k+1|k} & \dots & \upsilon_{k+N-1|k} \end{pmatrix}^T \tag{9.37}$$
$$\Phi_x(\Gamma) = \begin{pmatrix} C\psi(1,0) & C\psi(1,1) & \dots & C\psi(1,N-1) \end{pmatrix}^T \tag{9.38}$$

Which gives:

$$\begin{aligned}
\min_{U}\max_{\Delta^N} \quad & Y^TQY + U^TRU + \Upsilon^T S_1 \Upsilon + \Xi^T S_2 \Xi && (9.39)\\
\text{subject to} \quad & U \leq U_{max} + \Upsilon && (9.40)\\
& U \geq U_{min} - \Upsilon && (9.41)\\
& \Delta U \leq \Delta U_{max} + \Xi && (9.42)\\
& \Delta U \geq \Delta U_{min} - \Xi && (9.43)\\
& \Upsilon \geq 0 && (9.44)\\
& \Xi \geq 0 && (9.45)
\end{aligned}$$

Where:

$$Y = \Phi_x(\Gamma)\hat{x}_{k|k-1} + \mathcal{H}_u(\Gamma)U + \Phi_\lambda(\Gamma)\Lambda \tag{9.46}$$

$$\mathcal{H}_u(\Gamma) = \mathcal{H}_u^0(\Gamma) + \mathcal{H}_u^\Delta(\Gamma, \Delta^N) \tag{9.47}$$

$$\Delta^N = \begin{pmatrix} \Delta_1 & \Delta_2 & \dots & \Delta_N \end{pmatrix}^T \tag{9.48}$$

And

$$\mathcal{H}_u^0(\Gamma) = \begin{pmatrix} CB(\gamma_k) & 0 & \dots & 0 \\ C\psi(1,1)B(\gamma_k) & CB(\gamma_{k+1}) & \dots & 0 \\ C\psi(2,1)B(\gamma_k) & C\psi(2,2)B(\gamma_{k+1}) & \dots & 0 \\ \vdots & \vdots & \ddots & \vdots \\ C\psi(N-1,1)B(\gamma_k) & C\psi(N-1,2)B(\gamma_{k+1}) & \dots & CB(\gamma_{N-1}) \end{pmatrix} \tag{9.49}$$

In above, $Y$ is uncertain and depend on $\Delta^N$. Our next task is to eliminate uncertainties from our optimization problem. To do so, we pull out the $\Delta$ variables. We start by writing the stacked output vector $Y$ in the following form and then use theorem 1 to pull out the uncertainties:

$$\begin{aligned} Y =& \Phi_x(\Gamma)\hat{x}_{k|k-1} + \Phi_\lambda(\Gamma)\Lambda + \mathcal{H}_u^0(\Gamma)U \\ &+ \sum\nolimits_{j=1}^{N} V_j\Delta_j W_j U, \quad \Delta_j \in \mathbf{\Delta} \end{aligned} \tag{9.50}$$

$$
\begin{aligned}
V_1 &= \begin{pmatrix} CB_p(\gamma_k) & C\psi(1,1)B_p(\gamma_k) & \dots & C\psi(N-1,1)B_p(\gamma_k) \end{pmatrix}^T \\
V_2 &= \begin{pmatrix} 0 & CB_p(\gamma_{k+1}) & \dots & C\psi(N-2,2)B_p(\gamma_{k+1}) \end{pmatrix}^T \\
&\vdots \\
V_N &= \begin{pmatrix} 0 & 0 & 0 & \dots & CB_p(\gamma_{k+N-1}) \end{pmatrix}^T \\
W_1 &= \begin{pmatrix} C_p(\gamma_{k+1}) & 0 & \dots & 0 \end{pmatrix}^T \\
W_2 &= \begin{pmatrix} 0 & C_p(\gamma_{k+1}) & \dots & 0 \end{pmatrix}^T \\
&\vdots \\
W_N &= \begin{pmatrix} 0 & 0 & \dots & C_p(\gamma_{k+1}) \end{pmatrix}^T
\end{aligned}
$$

Now we pull out the first uncertain element ($\Delta_1$) from $Y$ in the LMI constraint. To do so we define the following variable:

$$
\begin{aligned}
\gamma_i = \Phi_x(\Gamma)\hat{x}_{k|k-1} + \Phi_\lambda(\Gamma)\Lambda + \mathcal{H}_u^0(\Gamma)U \\
+ \sum\nolimits_{j=i}^{N} V_j \Delta_j W_j U, \quad i = 1, \dots, N
\end{aligned}
\tag{9.51}
$$

And afterwards we have:

$$
\begin{aligned}
&\begin{pmatrix} t & \gamma_2^T & U^T & \Upsilon^T & \Xi^T \\ \star & Q^{-1} & 0 & 0 & 0 \\ \star & \star & R^{-1} & 0 & 0 \\ \star & \star & \star & S_1^{-1} & 0 \\ \star & \star & \star & \star & S_2^{-1} \end{pmatrix} + \begin{pmatrix} U^T W_1^T \\ 0 \\ 0 \\ 0 \\ 0 \end{pmatrix} \Delta_1^T \begin{pmatrix} 0 \\ V_1 \\ 0 \\ 0 \\ 0 \end{pmatrix}^T \\
&+ \begin{pmatrix} 0 \\ V_1 \\ 0 \\ 0 \\ 0 \end{pmatrix} \Delta_1 \begin{pmatrix} U^T W_1^T \\ 0 \\ 0 \\ 0 \\ 0 \end{pmatrix}^T \succeq 0
\end{aligned}
\tag{9.52}
$$

After pulling out the first uncertain element, we use the following theorem to find its equivalent certain LMI:

**Theorem 1:** Robust satisfaction of the uncertain LMI:

$$
F + L\Delta(I - D\Delta)^{-1}R + R^T(I - \Delta^T D^T)^{-1}\Delta^T L^T \succeq 0
$$

is equivalent to the LMI

$$
\begin{aligned}
\begin{bmatrix} F & L \\ L^T & 0 \end{bmatrix} \succeq \begin{bmatrix} R & D \\ 0 & I \end{bmatrix}^T \begin{bmatrix} \tau I & 0 \\ 0 & -\tau I \end{bmatrix} \begin{bmatrix} R & D \\ 0 & I \end{bmatrix} \\
\tau \geq 0
\end{aligned}
$$

Using theorem 1, it could be seen that the above LMI is equivalent to the following LMI:

$$\begin{pmatrix} t & \gamma_2^T & U^T & U^T W_1^T & \Upsilon^T & \Xi^T \\ \star & Q^{-1} & 0 & 0 & 0 & 0 \\ \star & \star & R^{-1} & 0 & 0 & 0 \\ \star & \star & \star & 0 & 0 & 0 \\ \star & \star & \star & \star & S_1^{-1} & 0 \\ \star & \star & \star & \star & \star & S_2^{-1} \end{pmatrix} \succeq \begin{pmatrix} 0 & 0 \\ V_1 & 0 \\ 0 & 0 \\ 0 & I \\ 0 & 0 \\ 0 & 0 \end{pmatrix} \begin{pmatrix} \tau_1 I & 0 \\ 0 & -\tau_1 I \end{pmatrix} \begin{pmatrix} 0 & 0 \\ V_1 & 0 \\ 0 & 0 \\ 0 & I \\ 0 & 0 \\ 0 & 0 \end{pmatrix}^T \tag{9.53}$$

Which is equivalent to:

$$\begin{pmatrix} t & \gamma_2^T & U^T & U^T W_1^T & \Upsilon^T & \Xi^T \\ \star & Q^{-1} - \tau_1 V_1 V_1^T & 0 & 0 & 0 & 0 \\ \star & \star & R^{-1} & 0 & 0 & 0 \\ \star & \star & \star & \tau_1 I & 0 & 0 \\ \star & \star & \star & \star & S_1^{-1} & 0 \\ \star & \star & \star & \star & \star & S_2^{-1} \end{pmatrix} \succeq 0 \tag{9.54}$$

We pulled out $\Delta_1$, and now we repeat the same procedure until we pull out all the uncertainties $\Delta_i$ for $i = 2, \ldots, N$. Afterwards we apply Schur complement to write the final LMI in the form of smaller LMIs. Finally the optimization problem can be written in the following form:

$$\begin{aligned} &\min_{t,\tau,U} \quad t_x + t_u + t_v + \sum\nolimits_{j=0}^{N-1} t_j \\ &\text{subject to} \\ &\begin{pmatrix} t_x & \hat{x}_{k|k-1}^T \Phi_x(\Gamma)^T + \Phi_\lambda(\Gamma)\Lambda + U^T \mathcal{H}_u^0(\Gamma)^T \\ \star & Q^{-1} - \sum_{j=0}^{N-1} \tau_j V_j V_j^T \end{pmatrix} \succeq 0 \\ &\begin{pmatrix} t_u & U^T \\ \star & R^{-1} \end{pmatrix} \succeq 0 \ \begin{pmatrix} t_v & \Upsilon^T \\ \star & S^{-1} \end{pmatrix} \succeq 0 \ \begin{pmatrix} t_j & U^T W_j^T \\ \star & \tau_j I \end{pmatrix} \succeq 0 \\ &\begin{pmatrix} I \\ -I \\ \Psi \\ -\Psi \end{pmatrix} U - \begin{pmatrix} U_{max} + \Upsilon \\ -U_{min} + \Upsilon \\ \Delta U_{max} + I_0 u_{k-1} + \Xi \\ -\Delta U_{min} - I_0 u_{k-1} + \Xi \end{pmatrix} \leq \ 0 \\ &\tau_j \geq 0 \qquad \Upsilon \geq \ 0 \qquad \Xi \geq \ 0 \end{aligned} \tag{9.55}$$

We have used SeDuMi ([Stu99]) to solve this optimization problem. SeDuMi is a program that solves optimization problems with linear, quadratic and semidefinite constraints.

## 9.4 Case study

The case study here is a wind turbine. Wind turbine control is a challenging problem as the dynamics of the system change based on wind speed which has a stochastic nature. The method that we propose here is to use wind speed as a scheduling variable. With the advances in LIDAR technology ([HHW06]) it is possible to measure wind speed ahead of the turbine and this enables us to have the scheduling variable of the plant for the entire prediction horizon.

### 9.4.1 Modeling

In this section modeling of a wind turbine is explained. For detailed explanation on the modeling see ([MPN12a]).

#### 9.4.1.1 Nonlinear model

For modeling purposes, the whole wind turbine can be divided into 4 subsystems: Aerodynamics subsystem, mechanical subsystem, electrical subsystem and actuator subsystem. To model the whole wind turbine, models of these subsystems are obtained and at the end they are connected together. The dominant dynamics of the wind turbine come from its flexible structure. Several degrees of freedom could be considered to model the flexible structure, but for control design mostly just a few important degrees of freedom are considered. In this work we only consider two degrees of freedom, namely the rotational degree of freedom (DOF) and drivetrain torsion. Nonlinearity of the wind turbines mostly comes from its aerodynamics. Blade element momentum (BEM) theory ([Han08]) is used to numerically calculate aerodynamic torque and thrust on the wind turbine. This theory explains how torque and thrust are related to wind speed, blade pitch angle and rotational speed of the rotor. Having aerodynamic torque and modeling drivetrain with a simple mass-spring-damper, the whole system equation with 2 degrees of freedom becomes:

$$J_r\dot{\omega}_r = Q_r - c(\omega_r - \frac{\omega_g}{N_g}) - k\psi \tag{9.56}$$

$$(N_g J_g)\dot{\omega}_g = c(\omega_r - \frac{\omega_g}{N_g}) + k\psi - N_g Q_g \tag{9.57}$$

$$\dot{\psi} = \omega_r - \frac{\omega_g}{N_g} \tag{9.58}$$

$$P_e = Q_g\omega_g \tag{9.59}$$

In which $Q_r$ is aerodynamic torque, $J_r$ and $J_g$ are rotor and generator moments of inertia, $\psi$ is the drivetrain torsion, $c$ and $k$ are the drivetrain damping and stiffness factors respectively lumped in the low speed side of the shaft and $P_e$ is the generated electrical power. For numerical values of these parameters and other parameters given in this paper, we refer to ([JBMS09]).

#### 9.4.1.2 Linearized model

To get a linear model of the system we need to linearize around some operating points. In our two DOFs model only the aerodynamic torque ($Q_r$) and electric power ($P_e$) are nonlinear. Taylor expansion is used to linearize them. Uncertainty in the measured wind speed and also in pitch actuator leads to uncertainty in the $B$ matrix, yet the $A$ matrix is known with enough accuracy. For more details on the uncertain state space model see ([MPN12b]). Collecting all the discussed models, matrices of the state space model become:

$$A(\gamma) = \begin{pmatrix} \frac{a(\gamma)-c}{J_r} & \frac{c}{J_r} & -\frac{k}{J_r} \\ \frac{c}{N_g J_g} & -\frac{c}{N_g^2 J_g} & \frac{k}{N_g J_g} \\ 1 & -1 & 0 \end{pmatrix} \qquad C = \begin{pmatrix} 1 & 0 & 0 \\ 0 & 1 & 0 \\ 0 & Q_{g0} & 0 \end{pmatrix} \tag{9.60}$$

$$B(\gamma,\delta) = \begin{pmatrix} b_1(\gamma,\delta) & 0 \\ 0 & -\frac{1}{J_g} \\ 0 & 0 \end{pmatrix} \qquad D = \begin{pmatrix} 0 & 0 \\ 0 & 0 \\ 0 & \omega_{g0} \end{pmatrix} \tag{9.61}$$

In which $x = \begin{pmatrix}\omega_r & \omega_g & \psi\end{pmatrix}^T$, $u = \begin{pmatrix}\theta & Q_g\end{pmatrix}^T$ and $y = \begin{pmatrix}\omega_r & \omega_g & P_e\end{pmatrix}^T$ are states, inputs and outputs respectively. In the matrix $B$, parameter $b_1$ is uncertain. Therefore the uncertain linear state space model becomes:

$$\dot{x} = A(\gamma)x + B(\gamma,\Delta)u$$
$$y = Cx + Du$$

### 9.4.2 Control objectives

The most basic control objective of a wind turbine is to maximize captured power during the life time of the wind turbine. This means trying to maximize captured power when wind speed is below its rated value. This is also called maximum power point tracking (MPPT). However when wind speed is above rated, control objective becomes regulation of the outputs around their rated values while trying to minimize dynamic loads on the structure. These objectives should be achieved against fluctuations in wind speed which acts as a disturbance to the system. In this work we have considered operation of the wind turbine in above rated (full load region). Therefore we try to regulate rotational speed and generated power around their rated values and remove the effect of wind speed fluctuations.

## 9.5 Simulations

In this section simulation results for the obtained controllers are presented. The controllers are implemented in MATLAB and are tested on a full complexity FAST ([JJ05]) model of the reference wind turbine ([JBMS09]). Simulations are done with realistic turbulent wind speed, with Kaimal model ([iec05]) as the turbulence model and TurbSim ([Jon09]) is used to generate wind profile. In order to stay in the full load region, a realization of turbulent wind speed is used from category $C$ of the turbulence categories of the IEC 61400-1 ([iec05]) with $18m/s$ as the mean wind speed. Control inputs which are pitch reference $\theta_{in}$ and generator reaction torque reference $Q_{in}$ along with system outputs which are rotor rotational speed $\omega_r$ and electrical power $P_e$ are shown in figures 9.1-9.4. Sampling time and prediction horizon are chosen to be 0.1 and 10 respectively. Uncertainty is multiplicative and chosen to be %20 of the nominal value. Simulation results show good regulations of generated power and rotational speed. Table 9.1 shows a comparison of the results between the proposed approach and MPC with linearization at each sample point ([Hen07]). As it could be seen from the table, the proposed approach gives better regulation on rotational speed and generated power (smaller standard deviations) than MPC, while keeping the shaft moment and pitch activity less. In all the figures 9.1-9.4 x-axis is time in seconds.

**Table 9.1:** Performance comparison between gain scheduling approach and linear MPC

| Parameters | Proposed approach | Linear MPC |
|---|---|---|
| SD of $\omega_r$ (RPM) | 0.042 | 0.103 |
| SD of $P_e$ (Watts) | $4.158 \times 10^4$ | $9.975 \times 10^4$ |
| Mean value of $P_e$ (Watts) | $4.998 \times 10^6$ | $4.998 \times 10^6$ |
| SD of pitch (degrees) | 2.781 | 3.005 |
| SD of shaft moment (kNM) | 295.26 | 482.49 |

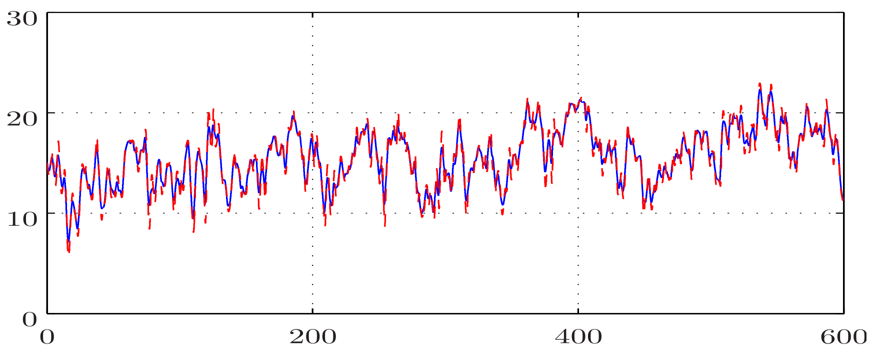


**Figure 9.1:** Blade-pitch reference (degrees, red-dashed line is linear MPC and solid-blue line is the proposed approach)

## 9.6 Conclusions

A method for dealing with robust MPC of nonlinear systems whose scheduling variable is known for the entire prediction horizon is proposed. The method is used for wind turbine control and the results are compared with a linear MPC that uses linearized model of the system at each sample time. Stability of the closed loop and recursive feasibility of the optimization problem are important issues that will be dealt with in future.

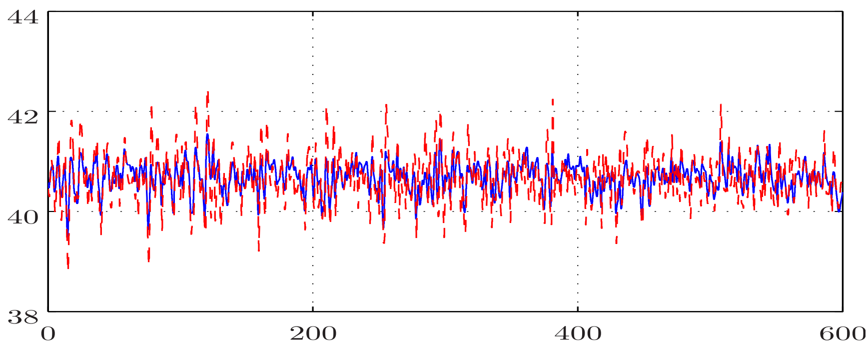


**Figure 9.2:** Generator-torque reference (kNM, red-dashed line is linear MPC and solid-blue line is the proposed approach)

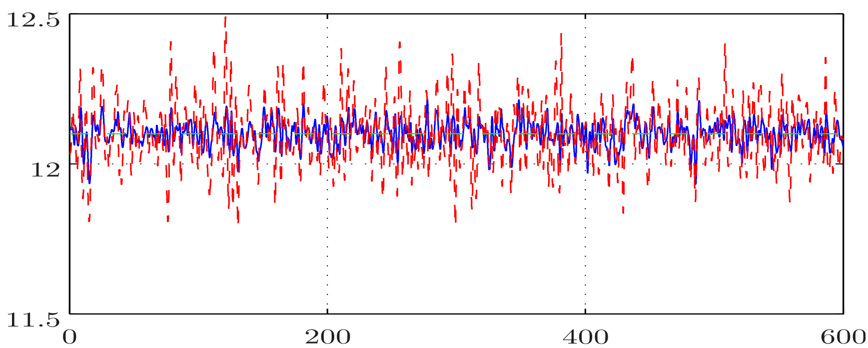


**Figure 9.3:** Rotor rotational speed ($\omega_r$, rpm, red-dashed line is linear MPC and solid-blue line is the proposed approach)

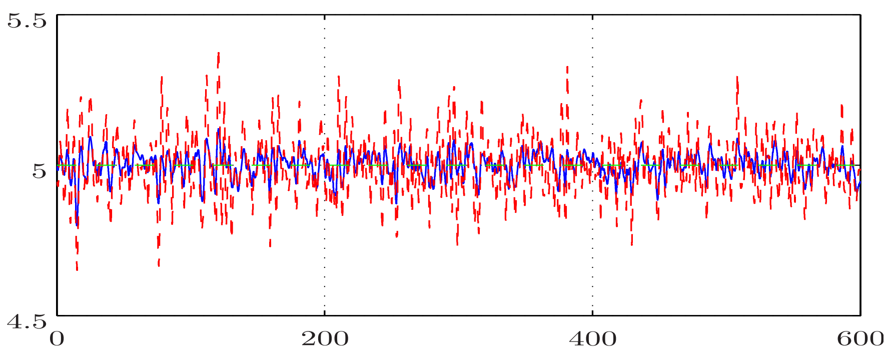


**Figure 9.4:** Electrical power (mega watts, red-dashed line is linear MPC and solid-blue line is the proposed approach)

## Paper E References


[AGB95] Pierre Apkarian, Pascal Gahinet, and Greg Becker. Self-scheduled $H_\infty$ control of linear parameter-varying systems: a design example. *Automatica*, 31(9):1251–1261, 1995.

[Bao05] M. Baotic. *Optimal Control of Piecewise Affine Systems – a Multiparametric Approach*. PhD thesis, March 2005.

[BEGFB94] S Boyd, L El-Ghaoui, E Feron, and V Balakrishnan. *Linear Matrix Inequalities in Systems and Control Theory*. SIAM, Philadelphia,Pa., 1994.

[CFF03] Alessandro Casavola, Domenico Famularo, and Giuseppe Franza. Predictive control of constrained nonlinear systems via lpv linear embeddings. *International Journal of Robust and Nonlinear Control*, 13:281–294, 2003.

[CGM99] Alessandro Casavola, Monica Giannelli, and Edoardo Mosca. Robust predictive control of input-saturated uncertain systems. *Proc IEEE Conf Decis Control*, 3:2768–2773, 1999.

[Gey05] T. Geyer. *Low Complexity Model Predictive Control in Power Electronics and Power Systems*. PhD thesis, March 2005.

[Han08] Martin O. L. Hansen. *Aerodynamics of Wind Turbines*. Earthscan, 2008.

[Hen07] Lars Christian Henriksen. Model predictive control of a wind turbine. Master's thesis, Technical University of Denmark, Informatics and Mathematical Modelling, 2007.

[HHW06] M. Harris, M. Hand, and A. Wright. LIDAR for turbine control. Technical report, National Renewable Energy Laboratory, 2006.

[iec05] IEC 61400-1 wind turbines-part 1: Design requirements., August 2005.

[JBMS09] J. Jonkman, S. Butterfield, W. Musial, and G. Scott. Definition of a 5MW reference wind turbine for offshore system development. Technical report, National Renewable Energy Laboratory,, 1617 Cole Boulevard, Golden, Colorado 80401-3393 303-275-3000, 2009.

[JJ05] Jason M. Jonkman and Marshall L. Buhl Jr. Fast user's guide. Technical Report NREL/EL-500-38230, National Renewable Energy Laboratory, Golden, CO, August 2005.

[Jon09] B.J. Jonkman. Turbsim user's guide: Version 1.50. Technical report, National Renewable Energy Laboratory, 1617 Cole Boulevard, Golden, Colorado 80401-3393 303-275-3000, 2009.

[LÖ3] Johan Löfberg. *Minimax approaches to robust model predictive control.* PhD thesis, Department of Electrical Engineering, Linköping University, 2003.

[Mac02] J.M. Maciejowski. *Predictive control with constraints.* Pearson Education Lim., Essex, 2002.

[MPN12a] Mahmood Mirzaei, Niels Kjølstad Poulsen, and Hans Henrik Niemann. Model predictive control of a nonlinear system with known scheduling variable. *Proceedings of the 17th Nordic Process Control Workshop*, pages 163–168, 2012.

[MPN12b] Mahmood Mirzaei, Niels Kjølstad Poulsen, and Hans Henrik Niemann. Robust model predictive control of a nonlinear system with known scheduling variable and uncertain gain. In *7th IFAC Symposium on Robust Control Design*, Aalborg, Denmark, 2012.

[QB96] S. Joe Qin and Thomas A. Badgwell. An overview of industrial model predictive control technology. pages –, 1996.

[Stu99] JF Sturm. Using sedumi 1.02, a matlab toolbox for optimization over symmetric cones. *Optim. Method Softw.*, 11-2(1-4):625–653, 1999.

Paper F

# Individual Pitch Control Using LIDAR Measurements

**Authors:**
M. Mirzaei, L. C. Henriksen, N. K. Poulsen, H. H. Niemann and M. H. Hansen

**Presented in:**
IEEE Multiconference on Systems and Control, 2012.

# Individual Pitch Control Using LIDAR Measurements[1]

Mahmood Mirzaei[2], Lars C. Henriksen[3], Niels K. Poulsen[2], Hand H. Niemann[4] and Morten H. Hansen[3]

**Abstract**

In this work the problem of individual pitch control of a variable-speed variable-pitch wind turbine in the full load region is considered. Model predictive control (MPC) is used to solve the problem. However as the plant is nonlinear and time varying, a new approach is proposed to simplify the optimization problem. Nonlinear dynamics of the wind turbine is derived by combining blade element momentum (BEM) theory and first principle modeling of the flexible structure. Then the nonlinear model of the system is linearized using Taylor series expansion around its operating points and a family of linear models are obtained. The operating points are determined by LIDAR measurements both for the current and predicted future operating points. The obtained controller is applied on a full complexity, high fidelity wind turbine model. Finally simulation results show improved load reduction on out-of-plane blade root bending moments and a better transient response compared to a benchmark PI individual pitch controller.

## 10.1 Introduction

### 10.1.1 Wind turbine control

In the recent decades there has been an increasing interest in green energies of which wind energy is one of the most important ones. Wind turbines are the most common wind energy conversion systems (WECS) and are hoped to be able to compete with fossil fuel power plants on the energy price in near future. However this demands better technology to reduce electricity production price. Control can play an essential part in this context. Because, on the one hand

[1]This work is supported by the CASED Project funded by grant DSF-09- 063197 of the Danish Council for Strategic Research.
[2]DTU Informatics, Technical University of Denmark, Asmussens Alle, building 305, DK-2800 Kgs. Lyngby, Denmark
[3]Department of Wind Energy, Technical University of Denmark, 4000 Roskilde, Denmark
[4]Department of Electrical Engineering, Technical University of Denmark, Ørsteds Plads, Building 349, DK-2800 Kgs. Lyngby, Denmark

control methods can decrease the cost of energy by keeping the turbine close to its maximum efficiency. On the other hand they can reduce structural fatigue and therefore increase lifetime of the wind turbine. There are several methods for wind turbine control ranging from classical control methods [LC00] which are the most used methods in real applications to advanced control methods which have been the focus of research in the past few years [LPW09]. Gain scheduling [BBM06], adaptive control [JF08], MIMO methods [GC08], nonlinear control [Tho06], robust control [Øst08], model predictive control [Hen07], $\mu$-Synthesis design [MNP11] are just to mention a few. Advanced model based control methods are thought to be the future of wind turbine control as they can conveniently employ new generations of sensors on wind turbines (e.g. LIDAR [HHW06]), new generation of actuators (e.g. trailing edge flaps [And10]) and also treat the turbine as a MIMO system. The last feature seems to become more important than before as wind turbines are becoming bigger and more flexible. This trend makes decoupling different modes, specifying different objectives and designing controllers based on paired input/output channels more difficult. Model predictive control (MPC) has proved to be an effective tool to deal with multivariable constrained control problems [BM99]. As wind turbines are MIMO systems [GC08] with constraints on inputs and outputs, using MPC seems to be effective. Individual pitch control in which each blade is given a specific pitch reference versus collective pitch in which all the blades receive the same pitch reference has given promising results in reducing fatigue loads [Bos03]. There have been a number of works addressing individual pitch control using LIDAR measurements [SK08], [SSG+10] and [LPS+11].

### 10.1.2 Model predictive control approach

Model predictive control (MPC) has been an active area of research and has been successfully applied on different applications in the last decades [QB96]. Basic elements of MPC are: a model of the plant to predict its future, a cost function which reflects control objectives, constraints on inputs and states/outputs, an optimization algorithm and the receding horizon principle. Depending on the type of the model, the control problem is called linear MPC, hybrid MPC, nonlinear MPC etc. Nonlinear MPC is normally computationally very expensive and generally there is no guarantee that the solution of the optimization problem is a global optimum. In this work we extend the idea of linear MPC using linear parameter varying (LPV) systems to formulate a tractable predictive control of nonlinear systems. MPC problem of LPV systems has been considered in [CGM99], however the difference here is that we use future values of the scheduling variable to simplify the optimization problem. To do so, we use future values of an input to the system that acts as a scheduling variable in the model. However there are some assumptions that restrict our solution to a specific class of problems. The scheduling variable is assumed to be known for the entire prediction horizon. And the operating point of the system mainly depends on the scheduling variable. The paper is organized as follows. In 10.2 modeling of the wind turbine is explained, the nonlinear model is derived and linear parameter varying model is given. In 10.3 our proposed method for solving model predictive control of the system is presented. In 10.4 control design is explained. Firstly control objectives are discussed and afterwards collective and individual pitch controllers are presented. In this section appropriate references are given for the benchmark individual pitch controller. Finally in 10.5 simulation results are given.

## 10.2 Modeling

### 10.2.1 Nonlinear model

For modeling purposes, the whole wind turbine can be divided into 4 subsystems: Aerodynamics subsystem, mechanical subsystem, electrical subsystem and actuator subsystem. The aerodynamic subsystem converts wind forces into mechanical torque and thrust on the rotor. The mechanical subsystem consists of drivetrain, tower and blades. Drivetrain transfers rotor torque to electrical generator. Tower holds the nacelle and withstands the thrust force. And blades transform wind forces into toque and thrust. The generator subsystem converts mechanical energy to electrical energy and finally the blade-pitch and generator-torque actuator subsystems are part of the control system. To model the whole wind turbine, models of these subsystems are obtained and at the end they are connected together. Figure 10.1 shows the basic subsystems and their interactions. The dominant dynamics of the wind turbine come from its flexible structure. Several degrees of freedom could be considered to model the flexible structure, but for control design mostly just a few important degrees of freedom are considered. In figure 10.2 basic degrees of freedom which are normally being considered in the design model are shown. In this work we have considered three degrees of freedom, namely the rotational degree of freedom (DOF), drivetrain torsion and tower fore-aft motion. Nonlinearity of the wind turbines mostly comes from its aerodynamics. Blade element momentum (BEM) theory [Han08] is used to numerically calculate aerodynamic torque and thrust on the wind turbine. This theory explains how torque and thrust are related to wind speed, blade pitch angle and rotational speed of the rotor. In steady state, i.e. disregarding dynamic inflow, the following formulas can be used to calculate

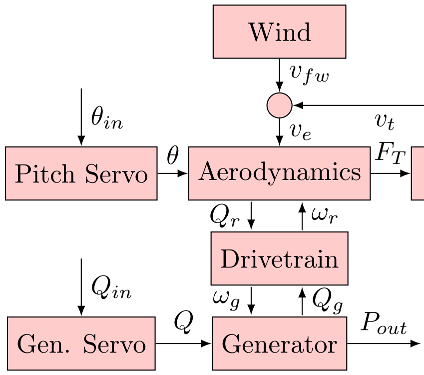


**Figure 10.1:** Wind turbine subsystems

aerodynamic torque and thrust.

$$Q_r = \frac{1}{2}\frac{1}{\omega_r}\rho\pi R^2 v_e^3 C_p(\theta, \omega, v_e) \tag{10.1}$$

$$Q_t = \frac{1}{2}\rho\pi R^2 v_e^2 C_t(\theta, \omega, v_e) \tag{10.2}$$

In which $Q_r$ and $Q_t$ are aerodynamic torque and thrust, $\rho$ is the air density, $\omega_r$ is the rotor rotational speed, $v_e$ is the effective wind speed, $C_p$ is the power coefficient and $C_t$ is the thrust force coefficient. The absolute angular position of the rotor and generator are of no interest to us, therefore we use $\psi = \theta_r - \theta_g$ instead which is the drivetrain torsion. Having aerodynamic torque and modeling drivetrain and tower with simple mass-spring-damper, the whole system equation with 3 degrees of freedom becomes:

$$J_r\dot{\omega}_r = Q_r - C_d(\omega_r - \frac{\omega_g}{N_g}) - K_d\psi \tag{10.3}$$

$$(N_g J_g)\dot{\omega}_g = C_d(\omega_r - \frac{\omega_g}{N_g}) + K_d\psi - N_g Q_g \tag{10.4}$$

$$\dot{\psi} = \omega_r - \frac{\omega_g}{N_g} \tag{10.5}$$

$$M\ddot{x}_t = Q_t - C_t\dot{x}_t - K_t x_t \tag{10.6}$$

$$P_e = Q_g\omega_g \tag{10.7}$$

In which $J_r$ and $J_g$ are rotor and generator moments of inertia, $\psi$ is the drivetrain torsion, $C_d$ and $K_d$ are the drivetrain damping and stiffness factors respectively lumped in the low speed side of the shaft. $C_t$ and $K_t$ are the tower damping and stiffness factors respectively. $x_t$ and $P_e$ are the generated electrical power and tower displacement respectively. For numerical values of these parameters and other parameters given in this paper, we refer to [JBMS09].

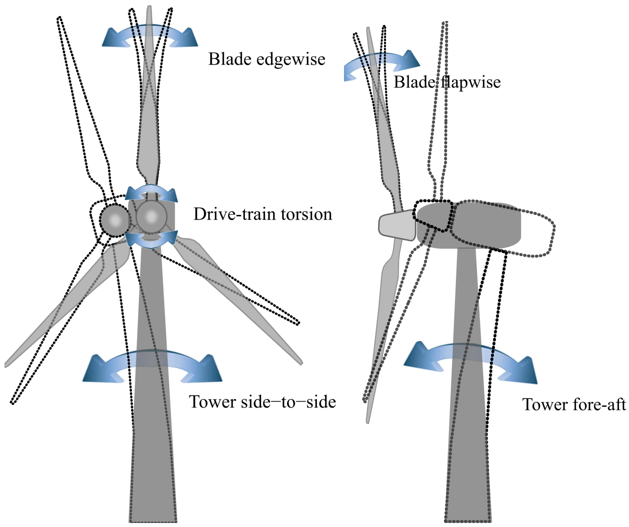


**Figure 10.2:** Basic degrees of freedom

### 10.2.2 Linearized model

To get a linear model of the system we need to linearize around its operating points which are determined by wind speed on the rotor area. Wind speed changes along the blades and with azimuth angle (angular position) of the rotor. This is because of wind shear, tower shadow and stochastic spatial distribution of the wind field. Therefore a single wind speed does not exist to be used and measured for finding the operating point. We bypass this problem by defining a fictitious variable called effective wind speed ($v_e$) which shows the effect of wind in the rotor disc on the wind turbine. Using the linearized aerodynamic torque and thrust, state space matrices for the 3 DOFs linearized model becomes:

$$\dot{\omega}_r = \frac{\alpha_1(v_e) - c}{J_r}\omega_r + \frac{c}{J_r}\omega_g - \frac{k}{J_r}\psi \tag{10.8}$$

$$+ \beta_{11}(v_e)\theta + \beta_{12}(v_e)v_e \tag{10.9}$$

$$\dot{\omega}_g = \frac{c}{N_g J_g}\omega_r - \frac{c}{N_g^2 J_g}\omega_g + \frac{k}{N_g J_g}\psi - \frac{Q_g}{J_g} \tag{10.10}$$

$$\dot{\psi} = \omega_r - \frac{\omega_g}{N_g} \tag{10.11}$$

$$M\ddot{x}_t = \alpha_2(v_e) + \beta_{21}(v_e)\theta + \beta_{22}(v_e)v_e \tag{10.12}$$

$$- C_t\dot{x}_t - K_t x_t \tag{10.13}$$

$$P_e = Q_{g_0}\omega_g + \omega_{g_0}Q_g \tag{10.14}$$

And as it could be seen the parameters of the linearzied model are functions of wind speed which in our approach acts as a scheduling variable. A more detailed description of the model and linearization is given in ([MNP11]).

## 10.3 MPC of a LPV System with Known Scheduling Variable

Generally the nonlinear dynamics of a plant could be modeled as the following difference equation:

$$x_{k+1} = f(x_k, u_k, d_k) \tag{10.15}$$

With $x_k, u_k$ and $d_k$ as states, inputs and disturbances respectively. Using the nonlinear model, the nonlinear MPC problem could be formulated as:

$$\begin{aligned}
\min_{u} \quad & \ell(x_N) + \sum_{i=0}^{N-1} \ell(x_{k+i|k}, u_{k+i|k}) && (10.16)\\
\text{Subject to} \quad & x_{k+1} = f(x_k, u_k, d_k) && (10.17)\\
& u_{k+i|k} \in \mathbb{U} && (10.18)\\
& \hat{x}_{k+i|k} \in \mathbb{X} && (10.19)
\end{aligned}$$

Where $\ell$ denotes some arbitrary norm and $\mathbb{U}$ and $\mathbb{X}$ show the set of acceptable inputs and states. As it was mentioned because of the nonlinear model, this problem is computationally too expensive. One way to avoid this problem is to linearize around an equilibrium point of the system and use linearized model instead of the nonlinear model. However for some plants assumption of linear model does not hold for long prediction horizons as the plant operating point changes, for example based on some inputs to the system that act as a scheduling variable. An example could be a wind turbine for which wind speed acts as a scheduling variable and changes the operating point of the system.

### 10.3.1 Linear MPC formulation

The problem of linear MPC could be formulated as:

$$\min_{u_0,u_1,\ldots,u_{N-1}} \|x_N\|_{Q_f} + \sum_{i=0}^{N-1} \|x_{k+i|k}\|_Q + \|u_{k+i|k}\|_R \tag{10.20}$$

$$\text{Subject to} \quad x_{k+1} = Ax_k + Bu_k \tag{10.21}$$

$$u_{k+i|k} \in \mathbb{U} \tag{10.22}$$

$$\hat{x}_{k+i|k} \in \mathbb{X} \tag{10.23}$$

Assuming that we use norms $1, 2$ and $\infty$ the optimization problem becomes convex providing that the sets $\mathbb{U}$ and $\mathbb{X}$ are convex. Convexity of the optimization problem makes it tractable and guarantees that the solution is the global optimum. The problem above is based on a single linear model of the plant around one operating point. However below we formulate our problem using linear parameter varying systems (LPV) in which the scheduling variable is known for the entire prediction horizon.

### 10.3.2 Linear Parameter Varying systems

Linear Parameter Varying (LPV) systems are a class of linear systems whose parameters change based on a scheduling variable. Study of LPV systems was motivated by their use in gain-scheduling control of nonlinear systems ([AGB95]). LPV systems are able to handle changes in the dynamics of the system by parameter varying matrices.

**(LPV systems)** let $k \in Z$ denote discrete time. We define the following LPV systems:

$$x_{k+1} = A(\gamma_k)x_k + B(\gamma_k)u_k \tag{10.24}$$

$$A(\gamma_k) = \sum_{j=1}^{n_\gamma} A_j\gamma_{k,j} \quad B(\gamma_k) = \sum_{j=1}^{n_\gamma} B_j\gamma_{k,j} \tag{10.25}$$

Which $A(\gamma_k)$ and $B(\gamma_k)$ are functions of the scheduling variable $\gamma_k$. The variables $x_k \in \mathbb{R}^{n_x}, u_k \in \mathbb{R}^{n_u}$, and $\gamma_k \in \mathbb{R}^{n_\gamma}$ are the state, the control input and the scheduling variable respectively.

### 10.3.3 Problem formulation

Using the above definition, the linear parameter varying (LPV) model of the nonlinear system with disturbances is of the following form:

$$\tilde{x}_{k+1} = A(\gamma_k)\tilde{x}_k + B(\gamma_k)\tilde{u}_k + B_d(\gamma_k)\tilde{d}_k \tag{10.26}$$

This model is formulated based on deviations from the operating point. However we need the model to be formulated in absolute values of inputs, states and disturbances. Therefore the LPV model becomes:

$$\begin{aligned} x_{k+1} = A(\gamma_k)(x_k - x_k^*) + B(\gamma_k)(u_k - u_k^*) \\ + B_d(\gamma_k)(d_k - d_k^*) + x_{k+1}^* \end{aligned} \tag{10.27}$$

which $x_k^*$, $u_k^*$ and $d_k^*$ are values of states, inputs and disturbances at the operating point. Which could be written as:

$$x_{k+1} = A(\gamma_k)x_k + B(\gamma_k)u_k + B_d(\gamma_k)d_k + \lambda_k \tag{10.28}$$

with

$$\lambda_k = x_{k+1}^* - A(\gamma_k)x_k^* - B(\gamma_k)u_k^* - B_d(\gamma_k)d_k^* \tag{10.29}$$

Now having the LPV model of the system we proceed to compute state predictions. In linear MPC predicted states at step $n$ is:

$$\begin{aligned} x_{k+n} = A^n x_k + \sum_{i=0}^{n-1} A^i B u_{k+(n-1)-i} \\ \text{for} \quad n = 1, 2, \ldots, N \end{aligned} \tag{10.30}$$

However in our method the predicted state is also a function of scheduling variable $\Gamma_n = \left(\gamma_{k+1}, \gamma_{k+2}, \ldots \gamma_{k+n}\right)^T$ for $n = 1, 2, \ldots, N-1$ and we assume that the scheduling variable is known for the entire prediction. Therefore the predicted state could be written as:

$$x_{k+1}(\gamma_k) = A(\gamma_k)x_k + B(\gamma_k)u_k + B_d(\gamma_k)d_k + \lambda_k \tag{10.31}$$

And for $n \in \mathbb{Z}, n \geq 1$:

$$\begin{aligned} x_{k+n+1}(\Gamma_n) = &\left(\prod_{i=0}^{n} A^T(\gamma_{k+i}) x_k\right)^T \\ &+ \sum_{j=0}^{n-1} \left(\prod_{i=1}^{n-j} A^T(\gamma_{k+i})\right)^T B(\gamma_{k+j}) u_{k+j} \\ &+ \sum_{j=0}^{n-1} \left(\prod_{i=1}^{n-j} A^T(\gamma_{k+i})\right)^T B_d(\gamma_{k+j}) d_{k+j} \\ &+ \sum_{j=0}^{n-1} \left(\prod_{i=1}^{n-j} A^T(\gamma_{k+i})\right)^T \lambda_{k+(n-1)-j} \\ &+ B(\gamma_{k+n}) u_{k+n} + B_d(\gamma_{k+n}) d_{k+n} + \lambda_{k+n} \end{aligned} \tag{10.32}$$

Using the above formulas we write down the stacked predicted states which becomes:

$$X(\Gamma) = \Phi(\Gamma) x_k + \mathcal{H}_u(\Gamma) U + \mathcal{H}_d(\Gamma) D + \Phi_\lambda(\Gamma) \Lambda \tag{10.33}$$

with

$$X = \begin{pmatrix} x_{k+1} & x_{k+2} & \dots & x_{k+N} \end{pmatrix}^T \tag{10.34}$$

$$U = \begin{pmatrix} u_k & u_{k+1} & \dots & u_{k+N-1} \end{pmatrix}^T \tag{10.35}$$

$$D = \begin{pmatrix} d_k & d_{k+1} & \dots & d_{k+N-1} \end{pmatrix}^T \tag{10.36}$$

$$\Gamma = \begin{pmatrix} \gamma_k & \gamma_{k+1} & \dots & \gamma_{k+N-1} \end{pmatrix}^T \tag{10.37}$$

$$\Lambda = \begin{pmatrix} \lambda_k & \lambda_{k+1} & \dots & \lambda_{k+N-1} \end{pmatrix}^T \tag{10.38}$$

In order to summarize formulas for matrices $\Phi, \Phi_\lambda, \mathcal{H}_u$ and $\mathcal{H}_d$, we define a new function as:

$$\psi(m, n) = \left(\prod_{i=m}^{n} A^T(\gamma_{k+i})\right)^T \tag{10.39}$$

Therefore the matrices become:

$$\Phi(\Gamma) = \begin{pmatrix} \psi(1,1) \\ \psi(2,1) \\ \psi(3,1) \\ \vdots \\ \psi(N,1) \end{pmatrix}$$

$$\Phi_\lambda(\Gamma) = \begin{pmatrix} I & 0 & 0 & \dots & 0 \\ \psi(1,1) & I & 0 & \dots & 0 \\ \psi(2,1) & \psi(2,2) & I & \dots & 0 \\ \vdots & \vdots & \vdots & \ddots & \vdots \\ \psi(N-1,1) & \psi(N-1,2) & \psi(N-1,3) & \dots & I \end{pmatrix}$$

$$\mathcal{H}_u(\Gamma) = \begin{pmatrix} B(\gamma_k) & 0 & \dots & 0 \\ \psi(1,1)B(\gamma_k) & B(\gamma_{k+1}) & \dots & 0 \\ \psi(2,1)B(\gamma_k) & \psi(2,2)B(\gamma_{k+1}) & \dots & 0 \\ \vdots & \vdots & \ddots & \vdots \\ \psi(N-1,1)B(\gamma_k) & \psi(N-1,2)B(\gamma_{k+1}) & \dots & B(\gamma_{N-1}) \end{pmatrix}$$

$$\mathcal{H}_d(\Gamma) = \begin{pmatrix} B_d(\gamma_k) & 0 & \dots & 0 \\ \psi(1,1)B_d(\gamma_k) & B_d(\gamma_{k+1}) & \dots & 0 \\ \psi(2,1)B_d(\gamma_k) & \psi(2,2)B_d(\gamma_{k+1}) & \dots & 0 \\ \vdots & \vdots & \ddots & \vdots \\ \psi(N-1,1)B_d(\gamma_k) & \psi(N-1,2)B_d(\gamma_{k+1}) & \dots & B_d(\gamma_{N-1}) \end{pmatrix}$$

After computing the state predictions as functions of control inputs (10.33), we can write down the optimization problem similar to a linear MPC problem as a quadratic program:

$$\min_U \quad X^T(\Gamma)QX(\Gamma) + U^TRU \tag{10.40}$$

# 10.4 Control

## 10.4.1 Control objectives

The most basic control objective of a wind turbine is to maximize captured power during the life time of the wind turbine. Which is producing electricity as close to the rated value as possible and reducing fatigue loads in order to increase life time of the turbine. To achieve these objectives wind turbine operations can be divided into two basic regions, partial load region and full load region.

In partial load region the objective is to maximize captured power when wind speed is below its rated value. This is also called maximum power point tracking (MPPT). However in full load region in which wind speed is above rated, control objective becomes regulation of the outputs around their rated values while trying to minimize dynamic loads on the structure. These objectives should be achieved against fluctuations in wind speed which act as a disturbance to the system. In this work we have considered operation of the wind turbine in above rated (full load region). Therefore we try to regulate rotational speed and generated power around their rated values and remove the effect of wind speed fluctuations.

### 10.4.2 Implementation

Two controllers are implemented in this work. One controller produces the collective pitch and regulates power and rotational speed and the other controller produces $\Delta\theta_i, i = 1, 2, 3$ for fatigue load reduction by adjusting individual blade pitch based on wind speed measurements. Both of the controllers take the advantage of having wind speed for the entire prediction horizon. These are fed to the controllers through 4 vectors, $V_{hh}, V_1, V_2$ and $V_3$ which are vector of wind speeds at hub height and 75% of the blades $1, 2$ and $3$ respectively.

#### 10.4.2.1 Collective pitch controller

The first controller uses the linearized model which was explained in section 10.2.2 augmented with a second order system modeling actuator dynamics. Measured outputs that are fed to this controller are:

$$\begin{pmatrix} \omega_r \\ \omega_g \\ P_e \\ a_t \\ \theta_c \\ V_{hh} \end{pmatrix} \begin{array}{l} \text{Rotor rotational speed} \\ \text{Generator rotational speed} \\ \text{Generated power} \\ \text{Tower top acceleration} \\ \text{Measured collective pitch} \\ \text{Hub height wind speed vector} \end{array} \tag{10.41}$$

#### 10.4.2.2 Individual pitch controller

Objective of this controller is to reduce fluctuations on blade root bending moments by adjusting pitch angle based on measured wind speeds. This will reduce 1P fluctuations of bending moments on the blade roots. Taking into account blade dynamics, the out-of-plane root bending moments can be modeled as a second order system with pitch and wind speed as their inputs:

$$\tilde{M}_i(s) = H_1(s)\tilde{\theta}_i(s) + H_2(s)\tilde{v}_i(s) \tag{10.42}$$

The fluctuations in the blade root bending moments are considered to be from $M_{hh}$ which is the bending moment produced by hub height wind speed. $H_1(s)$ and $H_2(s)$ are found using system identification on FAST [JJ05] simulation results. In steady state $\tilde{M}$ should be zero, therefore we can find steady state values for $\tilde{\theta}$ having $\tilde{v}$. This steady state value is taken to be reference value of the pitch actuator which was modeled as a second order system. This model is used in the controller design, therefore at this stage we have disregarded blade dynamics and only used pitch actuator dynamics. The objective of the individual pitch controller is to follow a reference point which is changing as a function of wind speed. Measurements that are fed to this controller are:

$$\begin{pmatrix} \theta_1 \\ \theta_2 \\ \theta_3 \\ V_1 \\ V_2 \\ V_3 \end{pmatrix} \begin{array}{l} \text{Measured pitch on blade 1} \\ \text{Measured pitch on blade 2} \\ \text{Measured pitch on blade 3} \\ \text{Wind speed vector for blade 1} \\ \text{Wind speed vector for blade 2} \\ \text{Wind speed vector for blade 3} \end{array} \tag{10.43}$$

### 10.4.3 Benchmark controller

The benchmark controller used in this work is a collective pitch controller based on the one found in [JBMS09]. The controller has a gain scheduled feedback from rotor speed to collective pitch angle and controls the generator torque to achieve constant power. The collective pitch controller is augmented with an individual pitch control (IPC) system that uses the flapwise blade root bending moments via the Coleman transform to determine cyclic behavior of the pitch angles. The cyclic pitch terms are then added to the collective pitch angle. Details regarding the tuning and implementation of the IPC can be found in [bMHHZ11].

## 10.5 Simulations

In this section simulation results for the obtained controllers which are denoted as MPC IPC (the proposed approach) and PI IPC (the benchmark controller) are presented. The controllers are implemented in MATLAB and are tested on

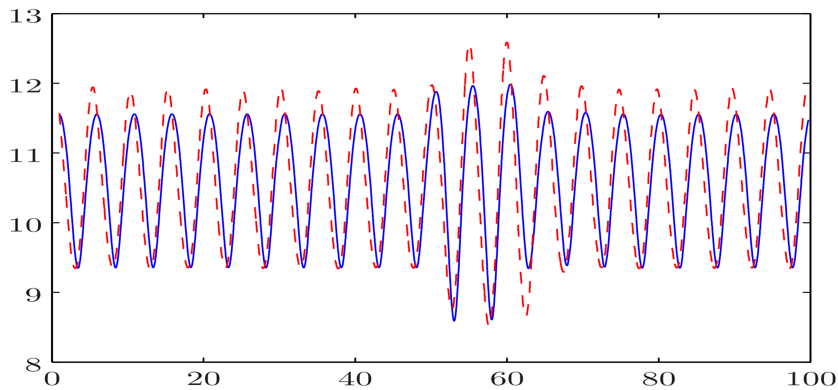


**Figure 10.3:** Pitch of one of the blades, (MPC IPC is solid-blue and PI IPC is red-dashed, degrees)

a full complexity FAST [JJ05] model of the reference wind turbine [JBMS09]. MPC IPC and PI IPC performed almost equally well in stochastic wind speeds and also step up and down with wind shear. However the advantage of using MPC IPC based on LIDAR measurements expressed itself in the transition situations. To show the advantage we have done a comparison of the simulation results of the two controllers for the extreme wind shear (EWS). The EWS simulation is inspired from the IEC standard [iec05].

### 10.5.1 Extreme wind shear simulations

In this section simulation results for a vertical extreme wind shear (EWS) event are presented. Power law wind profile is used to demonstrate wind shear. In the vertical EWS event, the power law exponent ramps up from a normal value of 0.2 to an extreme value of 0.3 in 2 seconds and after 10 seconds ramps down to the normal situation. Controller performance for the MPC IPC and PI IPC are compared for this event. A comparison of blade pitch are given in 10.3 as it could be seen, the MPC IPC gives a smoother increase in blade pitch while PI IPC has an overshoot. Out-of-plane blade root bending moments of one of the blades are given in 10.4. Clearly the MPC IPC gives better performance in reducing both steady state and transient fluctuations. In order to simplify comparison of the signals, Coleman transformation [CF61] of the three out-of-plane blade root bending moments are calculated and the results, namely yaw and tilt signals, for both controllers are given in 10.5 and 10.6 respectively.

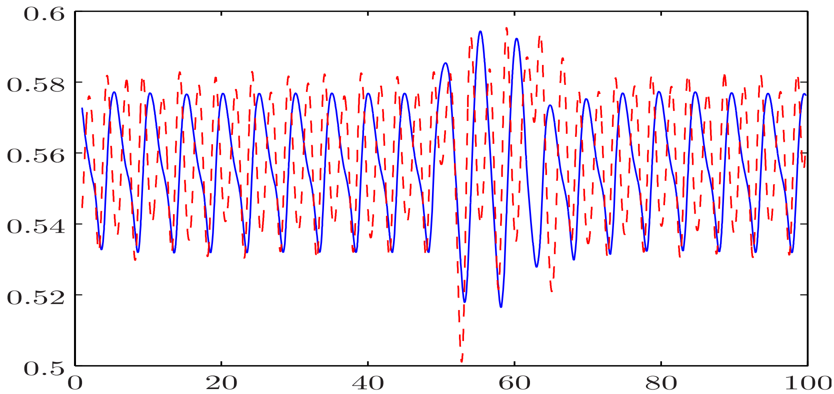


**Figure 10.4:** Out-of-plane blade root bending moment, (MPC IPC is solid-blue and PI IPC is red-dashed, Mega N.m)

## 10.6 Conclusions

In this paper firstly nonlinear model of a wind turbine, using blade element momentum theory (BEM) and first principle modeling of the flexible drive train and tower was found. Our control methodology is based on a family of linear models, therefore we have used Taylor series expansion to linearize the obtained nonlinear model around system operating points. Operating points are functions of wind speed, therefore wind speed is used as a scheduling variable. A model predictive control approach for the parameter varying systems was suggested. The approach employs known scheduling variable which is the effective wind speed. The effective wind speed is calculated by measuring and processing wind speed profile ahead of the wind turbine. The final controller was applied on a full complexity FAST [JJ05] model and was compared with a benchmark controller.

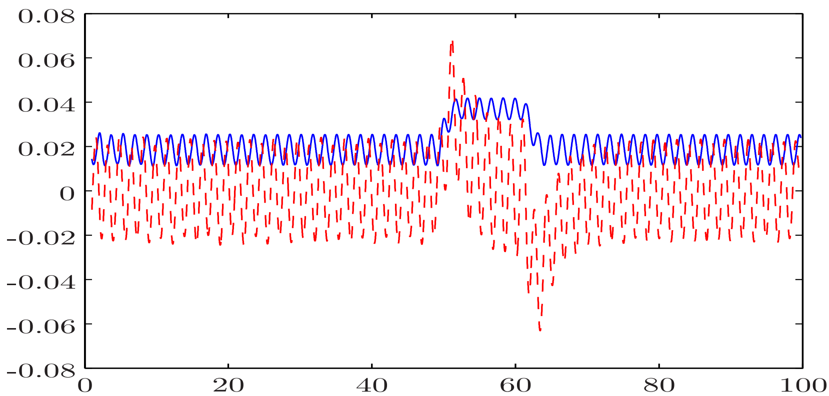


**Figure 10.5:** Tilt signal, (MPC IPC is solid-blue and PI IPC is red-dashed, Mega N.m)

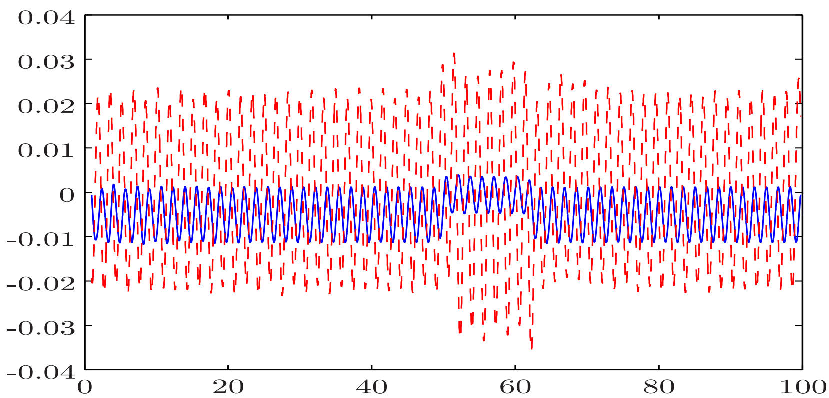


**Figure 10.6:** Yaw signal, (MPC IPC is solid-blue and PI IPC is red-dashed, Mega N.m)

## Paper F References


[AGB95] Pierre Apkarian, Pascal Gahinet, and Greg Becker. Self-scheduled $H_\infty$ control of linear parameter-varying systems: a design example. *Automatica*, 31(9):1251–1261, 1995.

[And10] Peter Bjørn Andersen. *Advanced Load Alleviation for Wind Turbines using Adaptive Trailing Edge Flaps: Sensoring and Control.* PhD thesis, Technical University of Denmark, Denmark, 2010.

[BBM06] Fernando D. Bianchi, Hernan De Battista, and Ricardo J. Mantz. *Wind Turbine Control Systems: Principles, Modelling and Gain Scheduling Design.* Springer, 2006.

[BM99] A Bemporad and M Morari. Robust model predictive control: A survey. *Lecture Notes in Control and Information Sciences*, 245:207–226, 1999.

[bMHHZ11] Edited by Morten Hartvig Hansen and Frederik Zahle. Aeroelastic optimization of mw wind turbines. Technical Report Risø-R-1803, Risø National Laboratory for Sustainable Energy, Technical University of Denmark, December 2011.

[Bos03] E. A. Bossanyi. Individual blade pitch control for load reduction. *Wind Energy*, 6(2):119–128, 2003.

[CF61] Robert P Coleman and Arnold M Feingold. Theory of self-excited mechanical oscillations of helicopter rotors with hinged blades. *CASI*, pages –, 1961.

[CGM99] Alessandro Casavola, Monica Giannelli, and Edoardo Mosca. Robust predictive control of input-saturated uncertain systems. *Proc IEEE Conf Decis Control*, 3:2768–2773, 1999.

[GC08] M. Geyler and P. Caselitz. Robust multivariable pitch control design for load reduction on large wind turbines. *Journal of solar energy engineering*, 130(3):–, 2008.

[Han08] Martin O. L. Hansen. *Aerodynamics of Wind Turbines.* Earthscan, 2008.

[Hen07] Lars Christian Henriksen. Model predictive control of a wind turbine. Master's thesis, Technical University of Denmark, Informatics and Mathematical Modelling, 2007.

[HHW06] M. Harris, M. Hand, and A. Wright. LIDAR for turbine control. Technical report, National Renewable Energy Laboratory, 2006.

[iec05] IEC 61400-1 wind turbines-part 1: Design requirements., August 2005.

[JBMS09] J. Jonkman, S. Butterfield, W. Musial, and G. Scott. Definition of a 5MW reference wind turbine for offshore system development. Technical report, National Renewable Energy Laboratory,, 1617 Cole Boulevard, Golden, Colorado 80401-3393 303-275-3000, 2009.

[JF08] Johnson and Fingersh. Adaptive pitch control of variable-speed wind turbines. *J. Sol. Energy Eng. (USA)*, 130(3):031012–1–7, 2008.

[JJ05] Jason M. Jonkman and Marshall L. Buhl Jr. Fast user's guide. Technical Report NREL/EL-500-38230, National Renewable Energy Laboratory, Golden, CO, August 2005.

[LC00] W.E. Leithead and Bill Connor. Control of variable speed wind turbines: Design task. *Int J Control*, 73(13):1189–1212, 2000.

[LPS+11] Jason Laks, Lucy Y. Pao, Eric Simley, Alan Wright, Neil Kelley, and Bonnie Jonkman. Model predictive control using preview measurements from lidar. In *49th AIAA Aerospace Sciences Meeting including the New Horizons Forum and Aerospace Exposition*, Orlando, Florida, January 2011.

[LPW09] J.H. Laks, L.Y. Pao, and A.D. Wright. Control of wind turbines: Past, present, and future. *Proceedings of the American Control Conference*, pages 2096–2103, 2009.

[MNP11] Mahmood Mirzaei, Hans Henrik Niemann, and Niels Kjølstad Poulsen. A $\mu$-synthesis approach to robust control of a wind turbine. In *the 50th IEEE Conference on Decision and Control and European Control Conference*, pages 645–650, Orlando, Florida, United States, 2011.

[Øst08] Kasper Zinck Østergaard. *Robust, Gain-Scheduled Control of Wind Turbines*. PhD thesis, Automation and Control Department of Electronic Systems, Aalborg University, 2008.

[QB96] S. Joe Qin and Thomas A. Badgwell. An overview of industrial model predictive control technology. pages –, 1996.

[SK08] D Schlipf and M. Kühn. Prospects of a collective pitch control by means of predictive disturbance compensation assisted by wind speed measurements. In *Proceedings of the German Wind Energy Conference, DEWEK*, 2008.

[SSG+10] D. Schlipf, S. Schuler, P. Grau, F. Allgöwer, and M. Kühn. Look-ahead cyclic pitch control using lidar. In *the Science of making Torque from Wind (TORQUE)*, 2010.

[Tho06] Sven Creutz Thomsen. Nonlinear control of a wind turbine. Master's thesis, Technical University of Denmark, Informatics and Mathematical Modelling, Lyngby, Denmark, 2006.

Paper G

# Robust Control Design of Wind Turbines using $\mu$-Synthesis

**Authors:**
M. Mirzaei, H. H. Niemann, N. K. Poulsen

**Submitted to:**
IET Control Theory and Applications (journal)

**Robust Control Design of Wind Turbines using $\mu$-Synthesis[1]**

Mahmood Mirzaei[2], Hand Henrik Niemann[3] and Niels Kjølstad Poulsen[2]

**Abstract**

The problem of robust control of a wind turbine is considered in this paper. A controller is designed based on a 2 degrees of freedom linearized model of a wind turbine. Due to approximate aerodynamics calculations and linearization of the nonlinear model, uncertainty in the obtained linear model is considered. We include these uncertainties as parametric uncertainties in the model and design a robust controller using the $\mu$-synthesis method. The resulting controller is applied on a high fidelity simulation model and simulations are performed with stochastic wind speeds.

## 11.1 Introduction

In recent decades there has been increasing interest in green energies of which wind energy is one of the most important. Wind turbines are the most common wind energy conversion systems (WECS) and are hoped to be able to compete with fossil fuel power plants on energy price in the near future. However this demands better technology to reduce the electricity production price. Control can play an essential part in this context, because on the one hand control methods can decrease the cost of energy by keeping the turbine close to its maximum efficiency. On the other hand they can reduce structural fatigue and therefore increase the lifetime of the wind turbine. There are several methods of wind turbine control ranging from classical control methods [LC00] which are the most commonly used methods in real applications, to advanced control methods, which have been the focus of research recently [LPW09]. Gain scheduling [BBM06], adaptive control [JF08], MIMO methods [GC08], nonlinear control [Tho06], robust control [Øst08], model predictive control [Hen07] and $DK$-iteration [MNP11] to mention a just few. Advanced control methods are thought to be the future of wind turbine control as they can employ new

[1]This work is supported by the CASED Project funded by grant DSF-09- 063197 of the Danish Council for Strategic Research.
[2]DTU Informatics, Technical University of Denmark, Asmussens Alle, building 305, DK-2800 Kgs. Lyngby, Denmark
[3]Department of Electrical Engineering, Technical University of Denmark, Ørsteds Plads, Building 349, DK-2800 Kgs. Lyngby, Denmark

generations of sensors on wind turbines (e.g. LIDAR [HHW06]), new generation of actuators (e.g. trailing edge flaps [And10]) and also conveniently treat the turbine as a MIMO system. The last feature seems to be becoming more important than before, as wind turbines are becoming bigger and more flexible, which makes decoupling different modes and designing a controller for each mode more difficult. The wind turbine in this paper is treated as a MIMO system with pitch ($\Theta$) and generator reaction torque ($\mathcal{Q}$) as inputs and rotor rotational speed ($\Omega$), generated power ($\mathcal{P}_e$) and tower fore-aft rate ($\mathcal{V}_t$) as outputs. Parametric uncertainties are considered and the $\mu$-synthesis method [SP01] is used to solve the control problem. $\mu$-synthesis is a method that takes structured uncertainty into account in order to reduce the conservativeness of the $\mathcal{H}_\infty$ procedure. This paper is organized as follows: In section 11.2 modeling of the wind turbine including linearization and uncertainty modeling is addressed. In section 11.3 controller design is explained. Finally in section 11.4 simulation results are presented.

## 11.2 Modeling of the Wind Turbine

For modeling purposes, the whole wind turbine can be divided into four subsystems: Structural subsystem, aerodynamics subsystem, electrical subsystem and actuator subsystem. The dominant dynamics of the wind turbine come from its structure, which includes the drivetrain, tower and blades. Several degrees of freedom could be considered to model the structure, but for control design just a few important degrees of freedom are usually considered. In this work we only consider two degrees of freedom, namely the rotational degree of freedom (DOF) and tower fore-aft movement. The aerodynamics subsystem gets effective wind speed ($\mathcal{V}_e$), pitch angle ($\Theta$) and rotational speed of the rotor ($\Omega$) and returns aerodynamic torque ($\mathcal{Q}_r$) and thrust ($\mathcal{Q}_t$). The aerodynamic subsystem is responsible for the nonlinearity in the wind turbine model. More details are presented in section 11.2.1.

### 11.2.1 Nonlinear Model

As mentioned earlier, for modeling purposes, the whole wind turbine can be divided into four subsystems (see figure 11.1). The aerodynamic subsystem converts wind forces into mechanical torque and thrust on the rotor. The mechanical subsystem consists of the drivetrain, tower and blades. The drivetrain transfers rotor torque to the electrical generator. The tower holds the nacelle and withstands the thrust force. Finally blades transform wind forces into torque and thrust. The generator subsystem converts mechanical energy to electrical

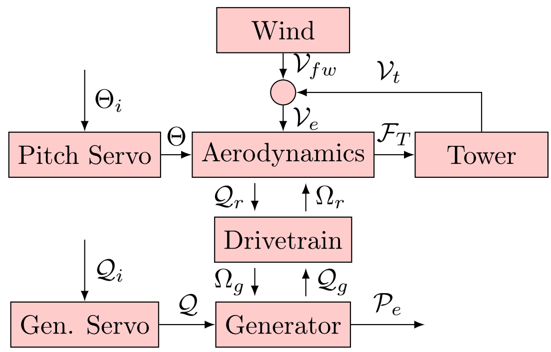


**Figure 11.1:** Wind turbine subsystems

energy and finally the blade-pitch and generator-torque actuator subsystems are part of the control system. To model the whole wind turbine, models of these subsystems are obtained and at the end they are connected together. Figure 11.1 shows the basic subsystems and their interactions. The dominant dynamics of the wind turbine comes from its flexible structure. Several degrees of freedom could be considered to model the flexible structure, but for control design, mostly just a few important degrees of freedom are considered. In figure 11.2 basic degrees of freedom which are normally being considered in a wind turbine model are shown. However in this work we only consider two degrees of freedom, namely the rotation of the rotor and fore-aft movement of the tower. Nonlinearity of a wind turbine mostly comes from its aerodynamics. Blade element momentum (BEM) theory [Han08] is used to numerically calculate aerodynamic torque and thrust on the wind turbine. This theory explains how torque and thrust are related to wind speed, blade pitch angle and rotational speed of the rotor. In the quasi-steady state, i.e. disregarding unsteady aerodynamic effects, the following formulas can be used to calculate aerodynamic torque and thrust.

$$\mathcal{Q}_r = \frac{1}{2}\frac{1}{\Omega}\rho\pi R^2 \mathcal{V}_e^3 C_p(\Theta, \Omega, \mathcal{V}_e) \tag{11.1}$$

$$\mathcal{Q}_t = \frac{1}{2}\rho\pi R^2 \mathcal{V}_e^2 C_t(\Theta, \Omega, \mathcal{V}_e) \tag{11.2}$$

In which $\mathcal{Q}_r$ and $\mathcal{Q}_t$ are aerodynamic torque and thrust, $\rho$ is the air density, $R$ is the rotor radius, $\omega$ is the rotor rotational speed, $\mathcal{V}_e$ is the effective wind speed, $C_p$ is the power coefficient and $C_t$ is the thrust force coefficient. $C_p$ and $C_t$ are found using BEM algorithm and stored as look-up tables. Figure 11.3 shows $C_p$ and $C_t$ curves. Having aerodynamic torque and thrust, and modeling tower fore-aft dynamics with a simple mass-spring-damper, the whole system

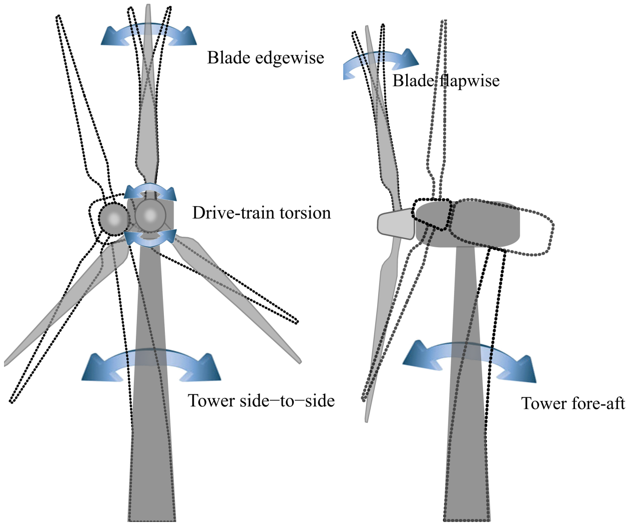


**Figure 11.2:** Basic degrees of freedom

equation with 2 degrees of freedom becomes:

$$J_t\dot{\Omega} = \mathcal{Q}_r(\Theta, \Omega, \mathcal{V}_e) - N_g\mathcal{Q}_g \tag{11.3}$$

$$M_t\ddot{\mathcal{X}}_t = \mathcal{Q}_t(\Theta, \Omega, \mathcal{V}_e) - c_t\dot{\mathcal{X}}_t + k_t\mathcal{X}_t \tag{11.4}$$

$$\mathcal{P}_e = \mathcal{Q}_g N_g \Omega \tag{11.5}$$

In which $J_t$ is the rotor moments of inertia, $c_t$ and $k_t$ are the tower fore-aft damping and stiffness factors, $\mathcal{X}_t$ is the tower fore-aft displacement and $\mathcal{P}_e$ is the generated electrical power. For numerical values of these parameters and other parameters given in this paper, we refer to [JBMS09].

### 11.2.2 Linearization

Our control design method is based on linear models, therefore we need to linearize the nonlinear model of the system obtained in the previous section. This is done by first finding the operating point, which is a function of effective wind speed ($\mathcal{V}_e$). Thereafter Taylor series expansion is used to find aerodynamic torque ($Q_r$), aerodynamic thrust ($Q_t$) and generated power ($P_e$) as linear functions of $\theta$, $\omega$ and $v_e$ which are deviations from the operating points.

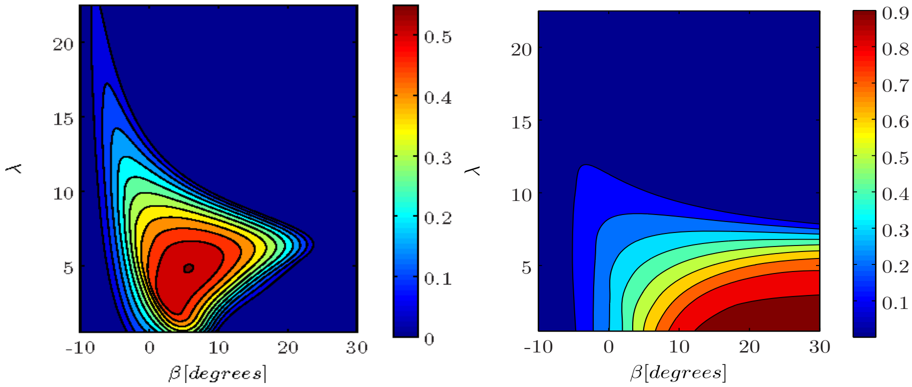


**Figure 11.3:** $C_p$ curve (left) and $C_t$ curve (right)

### 11.2.3 Uncertain model

As mentioned previously, for control design we need to have a linear model of the system and the following model of the wind turbine is used:

$$\begin{pmatrix} \dot{x} \\ y_\Delta \\ y \end{pmatrix} = \left(\begin{array}{c|cc} A & B_1 & B_2 \\ \hline C_1 & D_{11} & D_{12} \\ C_2 & D_{21} & D_{22} \end{array}\right) \begin{pmatrix} x \\ u_\Delta \\ u \end{pmatrix} \tag{11.6}$$

In which states, inputs and outputs are:

$$\begin{aligned} x &= \begin{pmatrix} \omega & x_t & \dot{x}_t \end{pmatrix}^T \\ u &= \begin{pmatrix} \theta & Q_g \end{pmatrix}^T \\ y &= \begin{pmatrix} \omega & \dot{x}_t \end{pmatrix}^T \end{aligned} \tag{11.7}$$

$\omega$ is the rotational speed of the rotor, $x_t$ and $\dot{x}_t$ are the tower fore-aft displacement and velocity, respectively, $\theta$ is the pitch of the blade, $Q_g$ is the generator reaction torque and $P_e$ is the electrical power. Having all the equations, system equations become:

$$\dot{\omega} = \frac{a_1}{J_t}\omega + \frac{b_{11}}{J_t}\theta + \frac{b_{12}}{J_t}(v_e - \dot{x}_t) - \frac{N_g}{J_t}Q_g \tag{11.8}$$

$$\ddot{x}_t = \frac{a_2}{M_t}\omega + \frac{b_{21}}{M_t}\theta + \frac{b_{22}}{M_t}(v_e - \dot{x}_t) - \frac{c_t}{M_t}\dot{x}_t - \frac{k_t}{M_t}x_t \tag{11.9}$$

$$P_e = Q_{g_0}N_g\omega + N_g\omega_0 Q_g \tag{11.10}$$

In the equation (11.3) we consider $Q_g$ to be approximately constant in comparison to the disturbances of the aerodynamic torque $Q_r$. $Q_g$ is mainly used in the equation (11.10) for trimming the output power. By neglecting the effect of $Q_g$ in the equation (11.8), we basically use the pitch of the blades for regulating the rotation of the rotor and damping tower fore-aft oscillations in the equations (11.8) and (11.9), and the torque of the generator for regulating the generated power in the equation (11.10). Using the blade pitch ($\theta$) for regulating the rotational speed and damping the tower fore aft oscillations is inspired by the standard PI controller [JBMS09]. Based on this argument, we can consider the wind turbine both a SIMO (Single Input, Multi Output) and a MIMO (Multi Input, Multi Output) system. In the SIMO case, we only use blade pitch in the equation (11.10) to control rotation of the rotor, and neglect the effect of generator torque. Then another controller is designed which uses generator torque $Q_g$ to control generated power. In the MIMO case (presented in this work), one controller is designed to control both the rotation of the rotor and the generated power using blade pitch ($\theta$) and generator torque ($Q_g$). Uncertainties for the parameters of the equations (11.8)-(11.10) are:

$$\begin{array}{lll} a_1 & = \bar{a}_1(1 + p_{a2}\delta_{a1}) & \text{Linearized model} \\ b_{11} & = \bar{b}_{11}(1 + p_{11}\delta_{b11}) & \text{Linearized model} \\ a_2 & = \bar{a}_2(1 + p_{a1}\delta_{a2}) & \text{Linearized model} \\ b_{21} & = \bar{b}_{21}(1 + p_{21}\delta_{b21}) & \text{Linearized model} \end{array} \tag{11.11}$$

In which:

$$|\delta_{a1}| \leq 1, \quad |\delta_{b11}| \leq 1, \quad |\delta_{a2}| \leq 1, \quad |\delta_{b21}| \leq 1, \tag{11.12}$$

$\bar{a}_1, \bar{b}_{11}, \bar{a}_2$ and $\bar{b}_{21}$, are the nominal values and $p_{a1}, p_{b11}, p_{a2}$ and $p_{b21}$ represent the relative perturbations. Uncertainty in the linearized model could be a result of approximate $C_P$ curve calculations, wrong wind speed estimation, which results in picking the wrong operating point, or aerodynamic changes due to blade flexibility or ice coatings on the blades. Using equation (11.11) to represent uncertainties, the uncertainty matrix ($\Delta$) becomes a diagonal matrix which connects $y_\Delta$ and $u_\Delta$:

$$\begin{aligned} u_\Delta &= \text{diag}(\delta_{a1}, \delta_{b11}, \delta_{a2}, \delta_{b21}) y_\Delta \\ y_\Delta &= \begin{pmatrix} y_{a1} & y_{b11} & y_{a2} & y_{b21} \end{pmatrix}^T \\ u_\Delta &= \begin{pmatrix} u_{a1} & u_{b11} & u_{a2} & u_{b21} \end{pmatrix}^T \end{aligned} \tag{11.13}$$

### 11.2.4 Simulation Model

The FAST (Fatigue, Aerodynamics, Structures, and Turbulence) code [JJ05] is used as the simulation model and the 5MW reference wind turbine is used as the plant [JBMS09]. In the simulation model 10 degrees of freedom are enabled

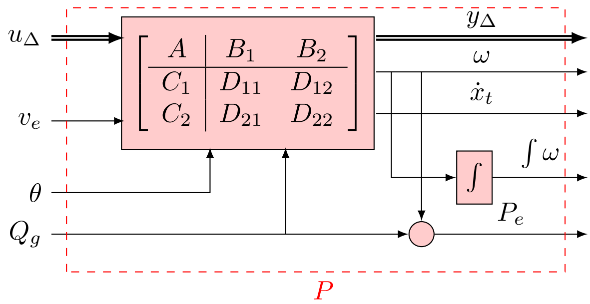


**Figure 11.4:** System interconnections

which are: generator, drivetrain torsion, 1st and 2nd tower fore-aft, 1st and 2nd tower side-side, 1st and 2nd blade flapwise, 1st blade edgewise degrees of freedom.

## 11.3 Controller Design

In this section we first explain basic wind turbine control objectives. Thereafter we show how to express the control objectives in the form of weighting functions of frequency on input disturbances and exogenous outputs. Afterwards we design two controllers, one based on $\mathcal{H}_\infty$ controller design procedure which results in a controller for the nominal performance problem and one using $DK$-iteration which results in a controller for the robust performance problem. At the end of the section we present some analysis on robust stability and robust performance of the controllers.

### 11.3.1 Control Objectives

The most basic control objective of a wind turbine is to maximize produced power for the entire life time of the machine which means maximizing captured power (up until rated power) and prolonging its life time. The second objective is achieved by minimizing the dynamics loads on the turbine. Generally maximizing power is considered in the partial load and minimizing fatigue loads is mainly considered above rated. As we are operating in the full load region in this work, we have considered the second objective. Control objectives are formulated in the form of weighting functions on input disturbances ($d$) and exogenous outputs ($z$). In order to avoid high frequency activity of the actuators, we have put high pass filters on control signals to penalize high frequency activity, see figures 11.5c and 11.5d. Also we have setup low pass filters to penalize only low frequency of some of the system outputs as their high frequency dynamics are outside our actuator bandwidth and we can not control them, see figures 11.6a and 11.6b. A low pass filter is considered for the input of wind speed as a source of disturbance with limited bandwidth (see figure 11.5a) and high pass filters are considered to show the precision of our measurement sensors in low frequencies and the effect of noise in high frequencies, see figure 11.5b. For regulating power and rotational speed, $P_e$, $\omega$ are penalized using low pass filters. $\int \omega$ is introduced and penalized to achieve offset free regulation. For minimizing fatigue loads on the tower, $\dot{x}_t$ is penalized using low pass filters.

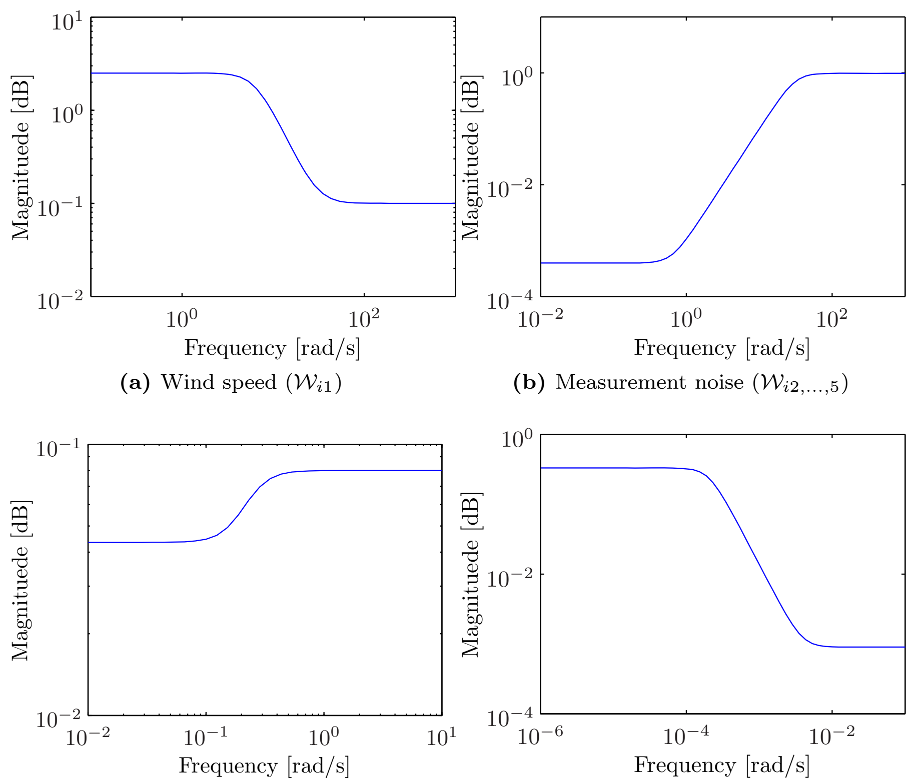


**(a)** Wind speed ($\mathcal{W}_{i1}$)

**(b)** Measurement noise ($\mathcal{W}_{i2,\ldots,5}$)

**(c)** Blade-pitch ($\mathcal{W}_{o1}$)

**(d)** Generator torque ($\mathcal{W}_{o2}$)

**Figure 11.5:** Bode plots of weighting functions (y-axis is in dB and x-axis is in rad/s)

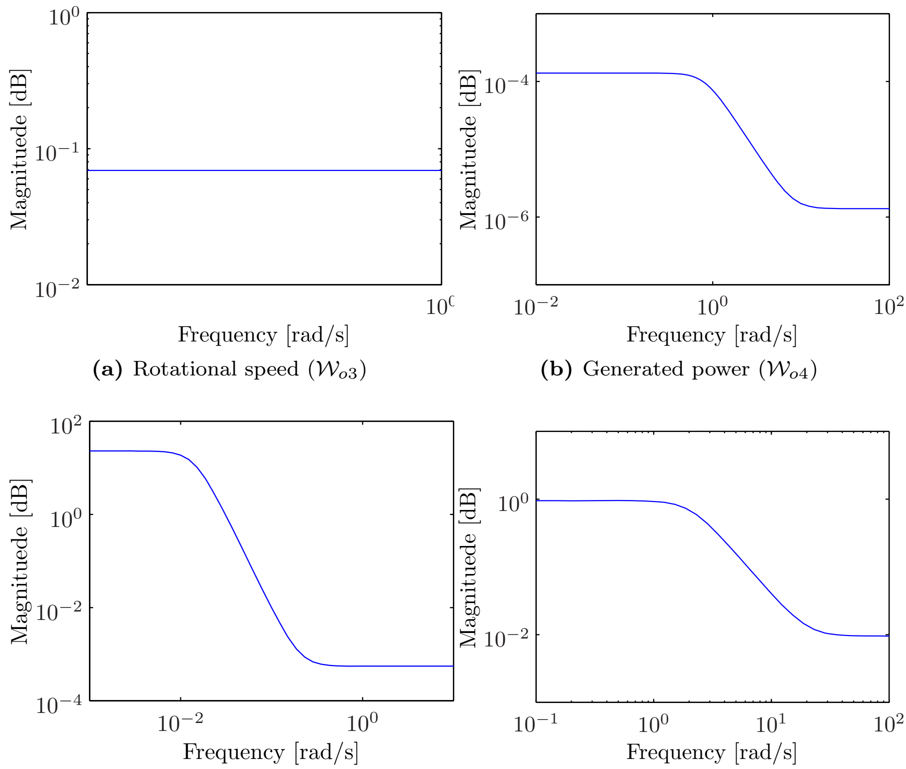


**Figure 11.5:** Bode plots of weighting functions (y-axis is in dB and x-axis is in rad/s)

## 11.3.2 Nominal Performance Problem

### 11.3.2.1 Theory

$\mathcal{H}_\infty$ control theory [SP01] is used to solve the nominal performance problem. In this problem the $\Delta$ matrix is considered zero (no perturbation) and the following problem is solved:

$$K(s) = \arg \min_{K \in \mathcal{K}} \| \mathcal{W}_o F_l(P, K) \mathcal{W}_i(j\omega) \|_{\mathcal{H}_\infty} \tag{11.14}$$

In which $F_l(P, K)$ is the lower LFT of plant $P$ (figure 11.4) and controller $K$. $\mathcal{W}_i$ and $\mathcal{W}_o$ are frequency-dependent weighting matrices on disturbances and

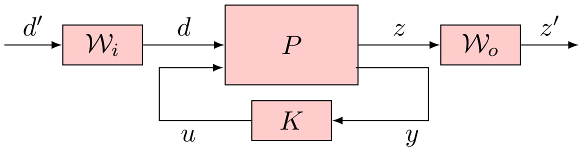


**Figure 11.6:** Nominal performance configuration

exogenous outputs, respectively, of the form:

$$\begin{aligned}\mathcal{W}_o &= diag(\mathcal{W}_{o1}, \ldots, \mathcal{W}_{o6}) \\ \mathcal{W}_i &= diag(\mathcal{W}_{i1}, \ldots, \mathcal{W}_{i5})\end{aligned} \tag{11.15}$$

Bode plots of the weighting functions are given in the figure 11.5. Input disturbance ($d$) and exogenous outputs ($z$) are (see figure 11.4):

$$\begin{array}{ll} d = v_e & \text{Wind Speed} \\ z = \begin{pmatrix} \theta \\ Q_g \\ \omega \\ \dot{x}_t \\ \int \omega \\ P_e \end{pmatrix} & \begin{array}{l} \text{Pitch reference} \\ \text{Generator reaction torque reference} \\ \text{Error on the rotational speed} \\ \text{Tower fore-aft velocity} \\ \text{Integral of rotational speed error} \\ \text{Generated power error} \end{array} \end{array}$$

By the optimization problem we are trying to find a controller in the set of all stabilizing controllers that minimizes the $\mathcal{H}_\infty$-norm of weighted sensitivity function. This means we try to minimize the peak frequency of $\mathcal{W}_o S \mathcal{W}_i(j\omega)$. The resulting controller guarantees nominal performance if:

$$\| \mathcal{W}_o F_l(P,K) \mathcal{W}_i(j\omega) \|_{\mathcal{H}_\infty} < 1 \tag{11.16}$$

#### 11.3.2.2 Implementation

The robust control toolbox [BDG+01] is used to solve the above optimization problem. The controller is found by trying to minimize the transfer function from the disturbances (vector $d$) to the exogenous outputs (vector $z$).

### 11.3.3 Robust Performance Problem

#### 11.3.3.1 Theory

Robust performance means that the performance objective is satisfied for all possible plants in the uncertainty set. The robust performance condition can be cast into a robust stability problem, with an additional perturbation block that defines $\mathcal{H}_\infty$ performance specifications. For a closed loop $M - \Delta$ structure, the robust stability condition is [SP01]:

$$\| M\Delta \|_{\mathcal{H}_\infty} < 1 \tag{11.17}$$

However when we have a structure in the uncertainty block $\Delta$, we can exploit it and reduce the conservativeness of the controller. Structured singular value (also known as $\mu$) is a tool that utilizes structures in the uncertainty block to analyze the robust stability of the system. Here we have used the structured singular value to solve the robust performance problem, as explained above, by transforming it into a robust stability problem. The structured singular value of a complex matrix $M$ with respect to a class of perturbations $\Delta$ is given by.

$$\mu_\Delta(M) \triangleq \frac{1}{\inf\{\sigma_{max}(\Delta) |\det(I - M\Delta) = 0\}}, \qquad \Delta \in \boldsymbol{\Delta} \tag{11.18}$$

The structured singular value $\mu$ is a very powerful tool for analysis of robust performance with a given controller. However in order to design a controller, we need a synthesis tool. To that end, a scaled version of the upper bound of $\mu$ is used for controller synthesis. The problem is formulated in the following form:

$$\mu_\Delta(N(K)) \leq \min_{D\in\mathcal{D}} \sigma(DN(K)D^{-1}) \tag{11.19}$$

Now, the synthesis problem can be cast into the following optimization problem in which one tries to find a controller that minimizes the peak value over the frequency of this upper bound:

$$\min_{K\in\mathcal{K}}(\min_{D\in\mathcal{D}} \| DN(K)D^{-1} \|_\infty) \tag{11.20}$$

This problem is solved by an iterative approach called $DK$-iteration. For detailed explanations of the method and notations, the reader is referred to [SP01].

#### 11.3.3.2 Implementation

We have used the $DK$-Iteration algorithm of the robust control toolbox [Mat] to design controllers. Figure 11.7 shows the robust performance problem setup.

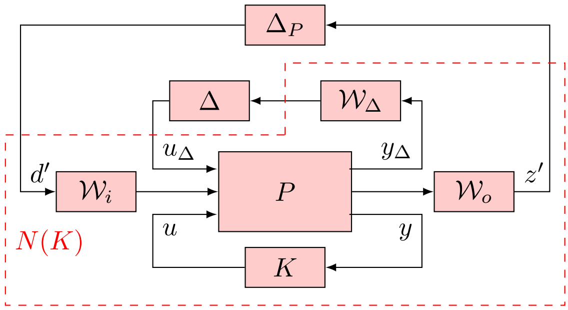


**Figure 11.7:** System setup for robust performance problem

| Iteration number | 1 | 2 | 3 |
|---|---|---|---|
| Controller Order | 32 | 32 | 32 |
| $\gamma$ Acheived | 78125.50 | 0.535 | 0.535 |
| Peak $\mu$-Value | 2.598 | 0.473 | 0.473 |

**Table 11.1:** $DK$-iteration summary for one of the controllers

$\mathcal{W}_\Delta$ is used to scale the $\Delta$ matrix. We have taken uncertainty of 20% for the uncertain parameters, therefore the weighting matrix becomes:

$$\mathcal{W}_\Delta = diag(0.2, 0.2, 0.2, 0.2) \tag{11.21}$$

$\Delta_P$ scaled by $\mathcal{W}_i$ and $\mathcal{W}_o$ matrices defines performance of the system in the form of a complex perturbation matrix. The resulting $\mu$ for the controller is given in figure 11.8 and the iteration summary in table 11.1. The order of the resulting controller is 32, and since high order controllers are problematic in the implementation phase, we have used balanced model reduction to reduce the order of the controller to 15. Table 11.1 shows the $DK$-iteration summary for obtaining the controller after the second iteration $\mu$ value does not improve.

### 11.3.4 Robust Stability Analysis

In this section we determine whether the system remains stable for all the uncertainties we have considered in the plant. To do so we calculate upper and lower bounds on the robust stability margins. Stability margins give us a measure of how much uncertainty the system can tolerate before it becomes unstable. Here we compare the $\mathcal{H}_\infty$ and $\mu$ controllers. The system with the $\mu$ controller can tolerate up to 955% of the modeled uncertainty, while the $\mathcal{H}_\infty$ controller can tolerate up to 878% of the modeled uncertainty. In the robust stability

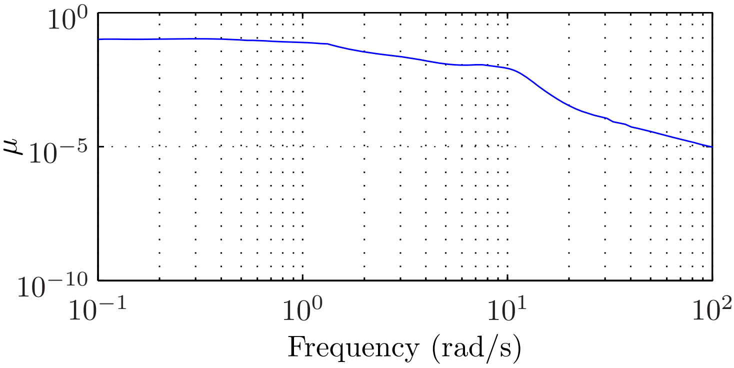


**Figure 11.8:** Robust stability

analysis it was also noted that uncertainty in the linearized parameters of the thrust force (for the specific wind speed of $18m/s$) does not affect the stability of the system. However increasing $a_1$ (aerodynamic damping of the rotational speed) by 25% leads to a 33% decrease in the margin, and increasing $b_{11}$ (aerodynamic gain from pitch to rotational speed) by 25% leads to a 5% decrease in the margin. Figure 11.8 shows the $\mu$ plot for robust stability margins for the $\mu$ controller.

### 11.3.5 Robust Performance Analysis

Often robust stability is not the main goal of robust control design. In the case of wind turbine design, in which wind speed fluctuations are considered as disturbances, we try to reduce the effect of these fluctuations on rotational speed and generated power, while keeping dynamical loads at their minimum. The dynamics from the disturbances to rotational speed, generated power and tower fore-aft velocity are dependent on the uncertainties in the system and it is the robust controller's task to reduce the effect of the uncertainties on the performance of the system. In our problem, before instability occurs the performance has degraded to the level of unacceptable. Therefore robust performance tests are even more important than robust stability tests. The system with the $\mu$ controller can tolerate up to 225% of the modeled uncertainty while the $\mathcal{H}_\infty$ controller can tolerate up to 200% of the modeled uncertainty before it loses the required performance specifications. In the robust stability analysis it was also noted that uncertainty in the linearized parameters of the thrust force (for the specific wind speed of $15m/s$) does not affect performance of the system. However increasing $a_1$ by 25% leads to a 4% decrease in the margin and increasing $b_{11}$ by 25% leads to a 4% decrease in the margin.

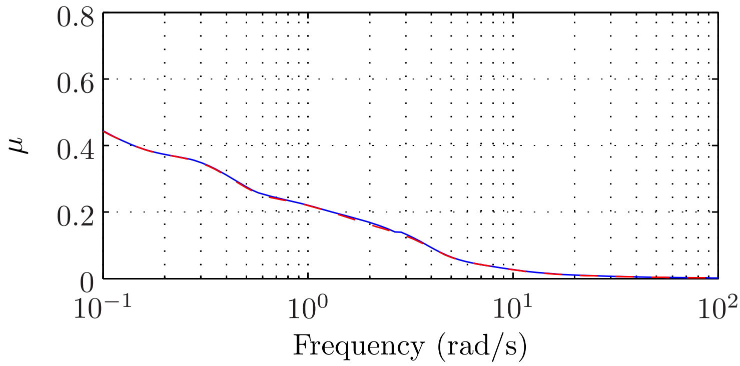


**Figure 11.9:** Robust performance, solid-blue is upper bound and red-dashed is lower bound of $\mu$

## 11.4 Simulation Results

In this section simulation results for a stochastic wind speed with the obtained controller are presented and compared against a standard PI controller. The controllers are implemented in MATLAB and are tested on the full complexity FAST model of the reference wind turbine [JBMS09]. The Kaimal model is used as the turbulence model and in order to stay close to the linearization point, the turbulence intensity has been decreased. Simulation results compare the robust $\mu$ controller with the standard PI controller. The simulations show that the $\mu$ controller achieves better regulation of rotational speed and power and reduced tower fore-aft oscillations, while keeping less generator reaction torque and almost the same pitch activity. Simulations are done both for the nominal plant and the perturbed plant. For the nominal plant, the high fidelity FAST model of the NREL reference wind turbine [JBMS09] is used and for the perturbed system we have increased pitch gain to the system by 20%. Control inputs, which are collective pitch of the blades $\theta$ and generator reaction torque $Q$, along with system outputs, which are rotor rotational speed $\omega$, tower fore-aft velocity $\dot{x}_t$ and electrical power $P_e$, are plotted in figures 11.11a-11.11e for the nominal case and in 11.10a-11.10e for the perturbed case. Table 11.2 shows comparison between the $\mu$-controller and the standard PI for the nominal case and 11.3 shows the result for the perturbed case.

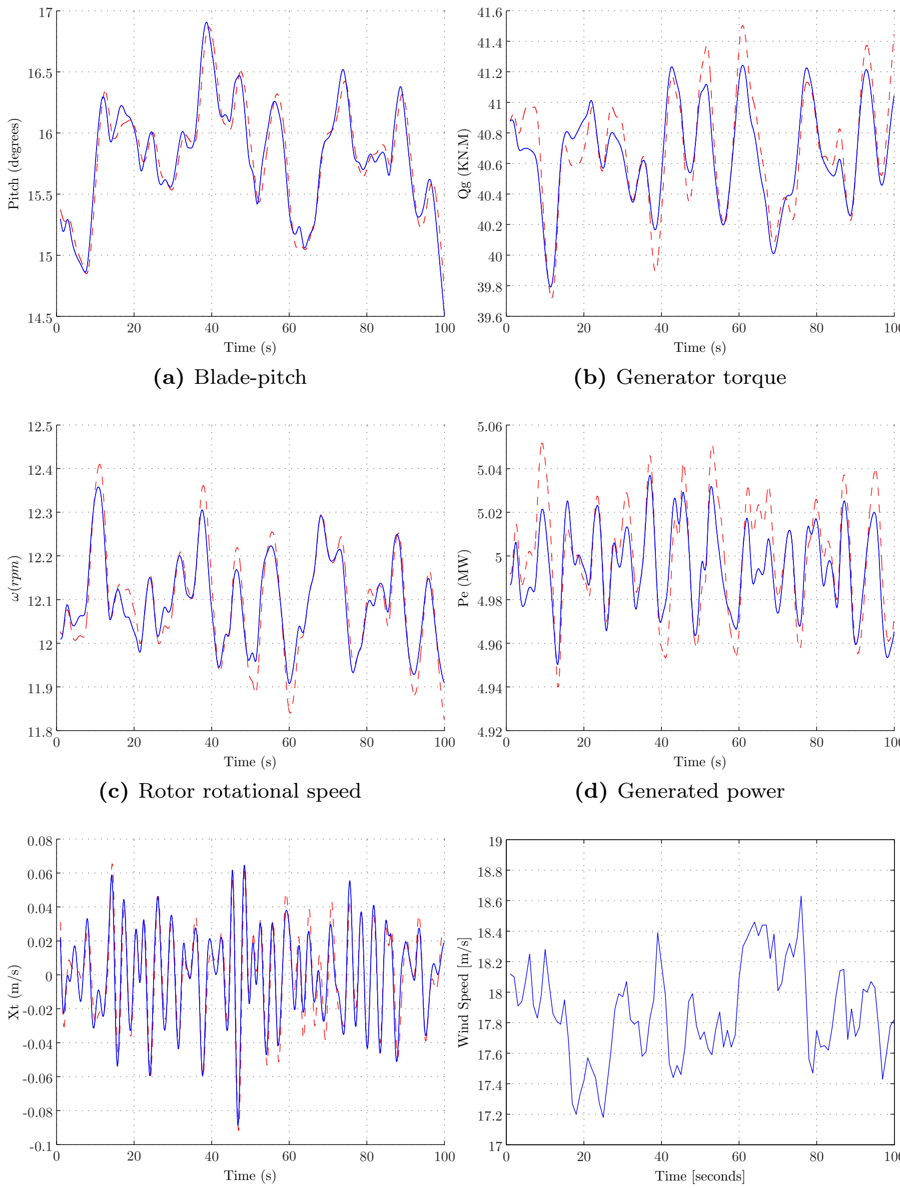


**(a)** Blade-pitch **(b)** Generator torque

**(c)** Rotor rotational speed **(d)** Generated power

**(e)** Tower fore-aft velocity **(f)** Wind speed

**Figure 11.10:** Simulation results for perturbed system, solid-blue $\mu$-controller, red-dashed standard PI controller

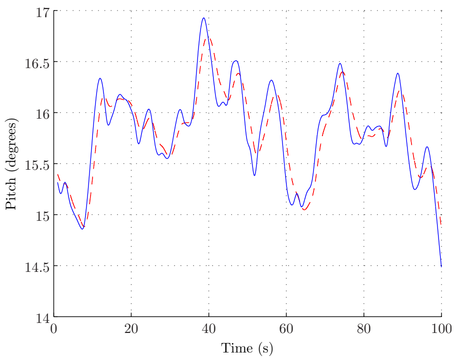


**(a)** Blade-pitch

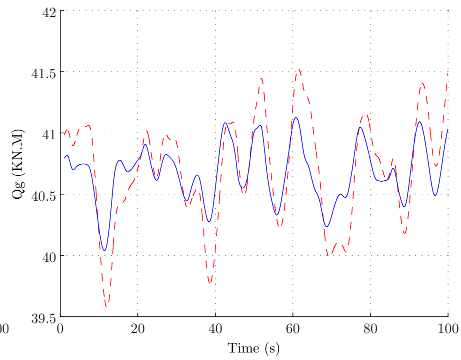


**(b)** Generator torque

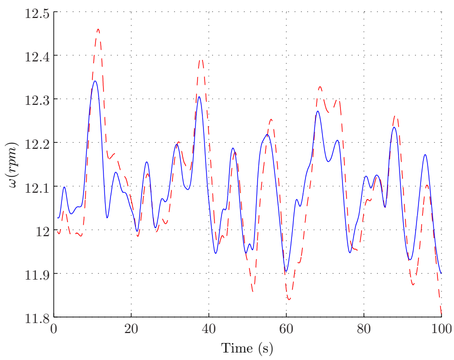


**(c)** Rotor rotational speed

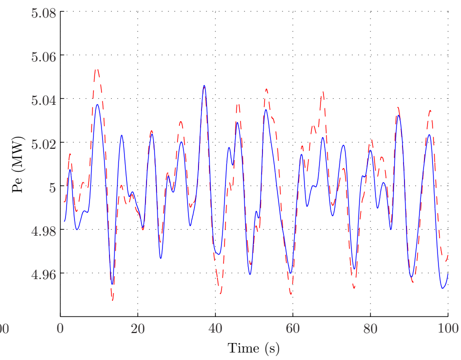


**(d)** Generated power

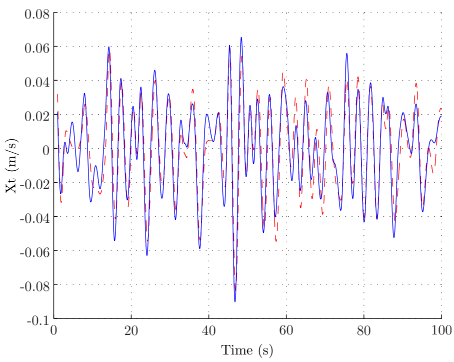


**(e)** Tower fore-aft velocity

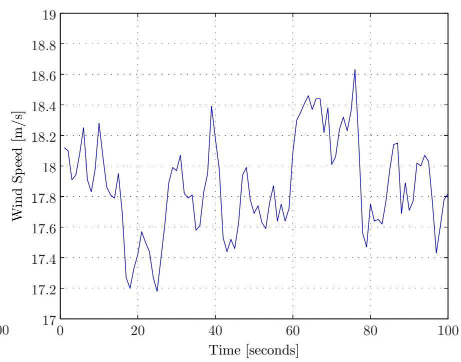


**(f)** Wind speed

**Figure 11.11:** Simulation results for nominal system, solid-blue $\mu$-controller, red-dashed standard PI controller

| Parameters | $\mu$-controller | PI | Improvement |
|---|---|---|---|
| SD of $\omega$ (RMP) | 0.1067 | 0.1564 | 31.77% |
| SD of $P_e$ (kWatts) | 22.25 | 26.29 | 15.36% |
| Pitch travel (degrees) | 0.6028 | 0.5862 | -2.83% |
| SD of Shaft moment (kN.M.) | 0.2754 | 0.5042 | 45.37% |
| SD of Tower fore-aft (m/s) | 0.0322 | 0.0334 | 3.59% |

**Table 11.2:** $\mu$-controller and PI performance comparison for the nominal case (SD stands for standard deviation and DEL stands for damage equivalent load)

| Parameters | $\mu$-controller | PI | Improvement |
|---|---|---|---|
| SD of $\omega$ (RMP) | 0.0934 | 0.1322 | 29.34% |
| SD of $P_e$ (kWatts) | 20.630 | 25.367 | 18.67% |
| Pitch travel (degrees) | 0.6068 | 0.6092 | 0.393% |
| SD of Shaft moment (kN.M.) | 0.2345 | 0.4206 | 44.24% |
| SD of Tower fore-aft (m/s) | 0.0328 | 0.0354 | 7.34% |

**Table 11.3:** $\mu$-controller and PI performance comparison for the perturbed case (SD stands for standard deviation and DEL stands for damage equivalent load)

## 11.5 CONCLUSION

In this paper we solved the problem of robust control of a wind turbine using the $DK$-iteration technique. Parametric uncertainties are considered in the uncertain model and then we have used a $\mu$-synthesis tool to design a robust controller. The final controller is implemented on a FAST simulation model with 10 degrees of freedom and simulation with stochastic wind speed is done. The results show improvement in regulation of generated power and rotational speed over the standard PI controller [JBMS09] with less generator torque activity and almost the same pitch activity, both for a nominal and perturbed system.

## Paper G References


[And10] Peter Bjørn Andersen. *Advanced Load Alleviation for Wind Turbines using Adaptive Trailing Edge Flaps: Sensoring and Control.* PhD thesis, Technical University of Denmark, Denmark, 2010.

[BBM06] Fernando D. Bianchi, Hernan De Battista, and Ricardo J. Mantz. *Wind Turbine Control Systems: Principles, Modelling and Gain Scheduling Design.* Springer, 2006.

[BDG+01] Gary J. Balas, John C. Doyle, Keith Glover, Andy Packard, and Roy Smith. *Robust Control Toolbox.* The MathWorks, Inc., June 2001.

[GC08] M. Geyler and P. Caselitz. Robust multivariable pitch control design for load reduction on large wind turbines. *Journal of Solar Energy Engineering*, 130, 2008.

[Han08] Martin O. L. Hansen. *Aerodynamics of Wind Turbines.* Earthscan, 2008.

[Hen07] Lars Christian Henriksen. Model predictive control of a wind turbine. Master's thesis, Technical University of Denmark, Informatics and Mathematical Modelling, 2007.

[HHW06] M. Harris, M. Hand, and A. Wright. LIDAR for turbine control. Technical report, National Renewable Energy Laboratory, 2006.

[JBMS09] J. Jonkman, S. Butterfield, W. Musial, and G. Scott. Definition of a 5MW reference wind turbine for offshore system development. Technical report, National Renewable Energy Laboratory,, 1617 Cole Boulevard, Golden, Colorado 80401-3393 303-275-3000, 2009.

[JF08] Johnson and Fingersh. Adaptive pitch control of variable-speed wind turbines. *J. Sol. Energy Eng. (USA)*, 130(3):031012–1–7, 2008.

[JJ05] Jason M. Jonkman and Marshall L. Buhl Jr. Fast user's guide. Technical Report NREL/EL-500-38230, National Renewable Energy Laboratory, Golden, CO, August 2005.

[LC00] W.E. Leithead and Bill Connor. Control of variable speed wind turbines: Design task. *Int J Control*, 73(13):1189–1212, 2000.

[LPW09] J.H. Laks, L.Y. Pao, and A.D. Wright. Control of wind turbines: Past, present, and future. *Proceedings of the American Control Conference*, pages 2096–2103, 2009.

[Mat] The MathWorks, Inc. *Robust Control Toolbox.*

[MNP11] Mahmood Mirzaei, Hans Henrik Niemann, and Niels Kjølstad Poulsen. DK-iteration robust control design of a wind turbine. In *IEEE Multi-Conference on Systems and Control*, pages 1493–1498, Denver, CO, USA, 2011.

[Øst08] Kasper Zinck Østergaard. *Robust, Gain-Scheduled Control of Wind Turbines*. PhD thesis, Automation and Control Department of Electronic Systems, Aalborg University, 2008.

[SP01] Sigurd Skogestad and Ian Postlethwaite. *Multivariable Feedback Control Analysis and design*. JOHN WILEY & SONS, Second Edition, 2001.

[Tho06] Sven Creutz Thomsen. Nonlinear control of a wind turbine. Master's thesis, Technical University of Denmark, Informatics and Mathematical Modelling, Lyngby, Denmark, 2006.

## Paper H

# Model Predictive Individual Pitch Control of Wind Turbines Using LIDAR Measurements

**Authors:**
M. Mirzaei, L. C. Henriksen, N. K. Poulsen, H. H. Niemann and M. H. Hansen

**Submitted to:** Journal of Wind Engineering and Industrial Aerodynamics

## Model Predictive Individual Pitch Control of Wind Turbines Using LIDAR Measurements[1]

Mahmood Mirzaei[2], Lars C. Henriksen[3], Niels K. Poulsen[2], Hand H. Niemann[4] and Morten H. Hansen[3]

**Abstract**

Spatial distribution of the wind field contributes to imbalance loads on wind turbine structures and it is shown these loads could be mitigated by controlling each blade's angle individually (individual pitch control). In this work the problem of individual pitch control of a variable-speed variable-pitch wind turbine in the full load region is considered. Model predictive control (MPC) is used to solve the problem. However as the turbine is nonlinear and time varying, a new approach is proposed to simplify the optimization problem of the control problem. Nonlinear dynamics of the wind turbine is derived by combining blade element momentum (BEM) theory and first principle modeling of the flexible structure and system identification. Then the nonlinear model of the system is linearized using Taylor series expansion around its operating points and a family of linear models is obtained. The operating points are determined by LIDAR measurements both for the current and predicted future operating points. The obtained controller is applied on a full complexity, high fidelity wind turbine model. Finally simulation results show improved load reduction on out-of-plane blade root bending moments and a better transient response compared to a benchmark PI individual pitch controller.

# 12.1 Introduction

## 12.1.1 Wind turbine control

In recent decades there has been increasing interest in green energies, of which wind energy is one of the most important. Wind turbines are the most common wind energy conversion systems (WECS) and are hoped to be able to

[1]This work is supported by the CASED Project funded by grant DSF-09- 063197 of the Danish Council for Strategic Research.
[2]DTU Informatics, Technical University of Denmark, Asmussens Alle, building 305, DK-2800 Kgs. Lyngby, Denmark
[3]Department of Wind Energy, Technical University of Denmark, 4000 Roskilde, Denmark
[4]Department of Electrical Engineering, Technical University of Denmark, Ørsteds Plads, Building 349, DK-2800 Kgs. Lyngby, Denmark

compete with fossil fuel power plants on energy price in near future. However this demands better technology to reduce the electricity production price. Control can play an essential part in this context. This is because, on the one hand control methods can decrease the cost of energy by keeping the turbine close to its maximum efficiency. On the other hand they can reduce structural fatigue and therefore increase the lifetime of the wind turbine. There are several methods of wind turbine control, ranging from classical control methods, [LC00] which are the most commonly used methods in real applications, to advanced control methods, which have been the focus of research in the past few years [LPW09]. Gain scheduling [BBM06], adaptive control [JF08], MIMO methods [GC08], nonlinear control [Tho06], robust control [Øst08], model predictive control [Hen07] and $\mu$-Synthesis design [MNP11] are just to mention a few. Advanced model-based control methods are thought to be the future of wind turbine control, as they can conveniently employ new generations of sensors on wind turbines (e.g. LIDAR [HHW06]), new generation, of actuators (e.g. trailing edge flaps [And10]) and they also treat the turbine as a MIMO system. The last feature seems to have become more important than before, as wind turbines are becoming bigger and more flexible. This trend makes decoupling different modes, specifying different objectives and designing controllers based on paired input/output channels more difficult. Model predictive control (MPC) has proved to be an effective tool to deal with multivariable constrained control problems [BM99]. As wind turbines are MIMO systems [GC08] with constraints on inputs and outputs, using MPC seems to be effective. Individual pitch control, in which each blade is given a specific pitch reference, instead of collective pitch in which all the blades receive the same pitch reference, has given promising results in reducing fatigue loads caused by spatial distribution of the wind field [Bos03]. There have been a number of works addressing individual pitch control using LIDAR measurements [SK08], [SSG$^+$10] and [LPS$^+$11].

### 12.1.2 Model Predictive Control Approach

Model predictive control (MPC) has been an active area of research and has been successfully applied on different applications in the last decades ([QB96]). Basic elements of MPC are: a model of the plant to predict its future, a cost function which reflects control objectives, constraints on inputs and states/outputs, an optimization algorithm and the receding horizon principle. Depending on the type of the model, the control problem is called linear MPC, hybrid MPC, nonlinear MPC etc. Nonlinear MPC is normally computationally very expensive and generally there is no guarantee that the solution to its optimization problem is a global optimum. In this work we extend the idea of linear MPC using linear parameter varying (LPV) systems to formulate a tractable predictive control of nonlinear systems. To do so, we use future values of an input to the system that

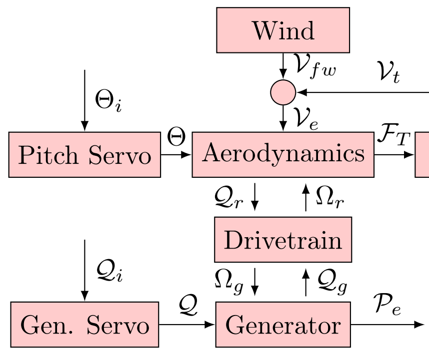


**Figure 12.1:** Wind turbine subsystems

acts as a scheduling variable in the model. However there are some assumptions that restrict our solution to a specific class of problems. The scheduling variable is assumed to be known for the entire prediction horizon. And the operating point of the system mainly depends on the scheduling variable. The paper is organized as follows. In 12.2 modeling of the wind turbine is explained, the nonlinear model is derived and the linear parameter varying model is given. In 12.3 our proposed method for solving model predictive control of the system is presented. In 12.4 control design is explained. Firstly control objectives are discussed and afterwards collective and individual pitch controllers are presented. In this section appropriate references are given for the benchmark individual pitch controller. Finally in 12.5 simulation results are given.

## 12.2 Modeling

### 12.2.1 Nonlinear model

For modeling purposes, the whole wind turbine can be divided into four subsystems: Aerodynamics subsystem, mechanical subsystem, electrical subsystem and actuator subsystem. The aerodynamic subsystem converts wind forces into mechanical torque and thrust on the rotor. The mechanical subsystem consists of the drivetrain, tower and blades. Drivetrain transfers rotor torque to the electrical generator. The tower holds the nacelle and withstands the thrust force. Blades transform wind forces into toque and thrust. The generator subsystem converts mechanical energy to electrical energy and finally the blade-pitch and generator-torque actuator subsystems are part of the control system. To model

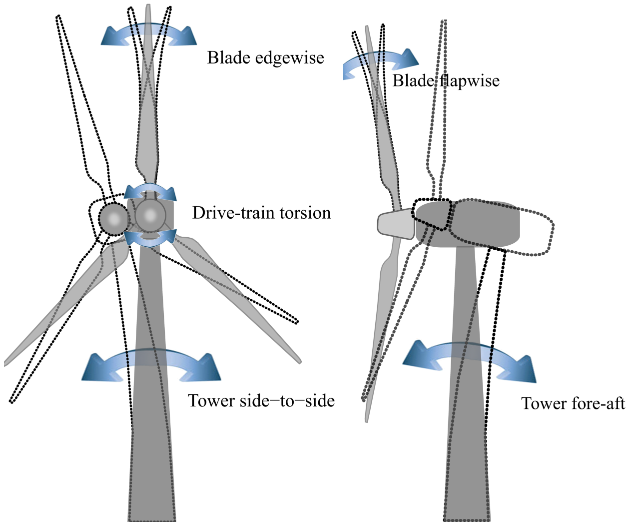


**Figure 12.2:** Basic degrees of freedom

the whole wind turbine, models of these subsystems are obtained and at the end they are connected together. Figure 12.1 shows the basic subsystems and their interactions. The dominant dynamics of the wind turbine come from its flexible structure. Several degrees of freedom could be considered to model the flexible structure, but for control design, just a few important degrees of freedom are usually considered. In figure 12.2 basic degrees of freedom, which are normally being considered in the design model, are shown. In this work we have considered three degrees of freedom, namely the rotational degree of freedom (DOF), drivetrain torsion and tower fore-aft motion. Nonlinearity of a wind turbine mostly comes from its aerodynamics. Blade element momentum (BEM) theory [Han08] is used to numerically calculate aerodynamic torque and thrust on the wind turbine. This theory explains how torque and thrust are related to wind speed, blade pitch angle and rotational speed of the rotor. In steady state, i.e. disregarding dynamic inflow, the following formulas can be used to calculate aerodynamic torque and thrust.

$$\mathcal{Q}_r = \frac{1}{2}\frac{1}{\Omega_r}\rho\pi R^2\mathcal{V}_e^3 C_p(\Theta, \Omega_r, \mathcal{V}_e) \tag{12.1}$$

$$\mathcal{Q}_t = \frac{1}{2}\rho\pi R^2\mathcal{V}_e^2 C_t(\Theta, \Omega_r, \mathcal{V}_e) \tag{12.2}$$

In which $\mathcal{Q}_r$ and $\mathcal{Q}_t$ are aerodynamic torque and thrust, $R$ is the rotor radius, $\rho$ is the air density, $\Omega_r$ is the rotor rotational speed, $\mathcal{V}_e$ is the effective wind speed, $C_p$ is the power coefficient and $C_t$ is the thrust force coefficient. The $C_p$ and $C_t$ are found using BEM algorithm and stored as look-up tables. Figure

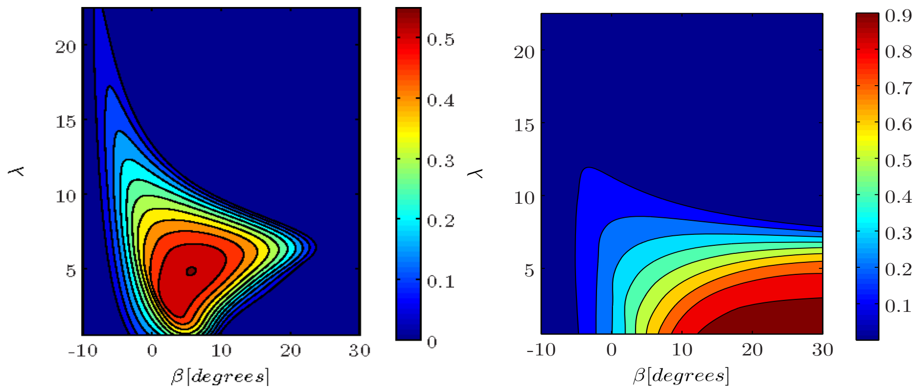


**Figure 12.3:** $C_p$ curve (left) and $C_t$ curve (right)

12.3 shows the $C_p$ and $C_t$ curves. The absolute angular position of the rotor and generator are of no interest to us, therefore we use $\psi$ instead, which is the drivetrain torsion. Having aerodynamic torque and modeling drivetrain and tower with simple mass-spring-damper, the whole system equation with 3 degrees of freedom becomes:

$$J_r\dot{\Omega}_r = \mathcal{Q}_r - C_d(\Omega_r - \frac{\Omega_g}{N_g}) - K_d\psi \tag{12.3}$$

$$(N_g J_g)\dot{\Omega}_g = C_d(\Omega_r - \frac{\Omega_g}{N_g}) + K_d\psi - N_g\mathcal{Q}_g \tag{12.4}$$

$$\dot{\psi} = \Omega_r - \frac{\Omega_g}{N_g} \tag{12.5}$$

$$M\ddot{\mathcal{X}}_t = Q_t - C_t\dot{\mathcal{X}}_t - K_t\mathcal{X}_t \tag{12.6}$$

$$\mathcal{P}_e = \mathcal{Q}_g\Omega_g \tag{12.7}$$

In which $J_r$ and $J_g$ are rotor and generator moments of inertia, $\psi$ is the drivetrain torsion, $C_d$ and $K_d$ are the drivetrain damping and stiffness factors, respectively, lumped in the low speed side of the shaft. $C_t$ and $K_t$ are the tower damping and stiffness factors, respectively. $\mathcal{P}_e$ and $\mathcal{X}_t$ are the generated electrical power and tower displacement, respectively. For numerical values of these parameters and other parameters given in this paper, we refer to [JBMS09].

### 12.2.2 Linearized model

To get a linear model of the system we need to linearize around its operating points, which are determined by wind speed on the rotor area. Wind speed changes along the blades and with the azimuth angle (angular position) of the rotor. This is because of wind shear, tower shadow and stochastic spatial distribution of the wind field. Therefore a single wind speed does not exist to be used and measured in order to find the operating point. We bypass this problem by defining a fictitious variable called effective wind speed ($\mathcal{V}_e$), which shows the effect of wind in the rotor disc on the wind turbine. Using the linearized aerodynamic torque and thrust, state space matrices for the 3 DOFs linearized model become:

$$\dot{\omega}_r = \frac{\alpha_1(v_e) - c}{J_r}\omega_r + \frac{c}{J_r}\omega_g - \frac{k}{J_r}\psi \tag{12.8}$$

$$+ \beta_{11}(v_e)\theta + \beta_{12}(v_e)(v_e - v_t) \tag{12.9}$$

$$\dot{\omega}_g = \frac{c}{N_g J_g}\omega_r - \frac{c}{N_g^2 J_g}\omega_g + \frac{k}{N_g J_g}\psi - \frac{Q_g}{J_g} \tag{12.10}$$

$$\dot{\psi} = \omega_r - \frac{\omega_g}{N_g} \tag{12.11}$$

$$\dot{x}_t = v_t \tag{12.12}$$

$$\dot{v}_t = \frac{\alpha_2(v_e)}{M}\omega_r + \frac{\beta_{21}(v_e)}{M}\theta + \frac{\beta_{22}(v_e)}{M}(v_e - v_t) \tag{12.13}$$

$$- \frac{C_t}{M}v_t - \frac{K_t}{M}x_t \tag{12.14}$$

$$P_e = Q_{g_0}\omega_g + \omega_{g_0}Q_g \tag{12.15}$$

n which the lower-case variables are deviations away from steady state of the upper-case variables given in the equations (12.3-12.7). And as could be seen, the parameters of the linearized model are functions of wind speed, which in our approach acts as a scheduling variable. A more detailed description of the model and linearization is given in [MNP11].

### 12.2.3 Pitch actuator

A second order model is used to model pitch actuator:

$$\dot{\theta}_1 = \theta_2 \tag{12.16}$$

$$\dot{\theta}_2 = -2\zeta_\theta\omega_\theta\theta_2 - \omega_\theta^2\theta_1 + \omega_\theta^2\theta_i \tag{12.17}$$

In which $\theta_i$ is the input to the actuator, and $\omega_\theta$ and $\zeta_\theta$ are natural frequency and damping of the actuator, respectively.

### 12.2.4 Dynamics of the blades

Blade dynamics is simplified as a parameter varying second order dynamical system with two inputs, which are wind speed and pitch angle, and one output, which is out of plane blade root bending moment. The model is considered to be:

$$\tilde{\mathcal{M}}_i(s) = \mathcal{H}_{1,i}(\gamma, s)\tilde{\theta}_i(s) + \mathcal{H}_{2,i}(\gamma, s)\tilde{v}_i(s), \quad i = 1, 2, 3 \tag{12.18}$$

For which the state space matrices become:

$$A(\gamma) = \begin{pmatrix} 0 & 1 \\ -\omega_n(\gamma)^2 & -2\zeta(\gamma)\omega_n(\gamma) \end{pmatrix} \qquad B(\gamma) = \begin{pmatrix} 0 & 0 \\ b_1(\gamma) & b_2(\gamma) \end{pmatrix} \tag{12.19}$$

$$C = \begin{pmatrix} 1 & 0 \end{pmatrix} \qquad D = \begin{pmatrix} 0 & 0 \end{pmatrix} \tag{12.20}$$

The argument $\gamma$ signifies that the linearized model depends on the operating point. Different wind speeds, which result in different operating points are used to identify the system. Prediction error [Lju99] method is used on the above greybox model of the blade and parameters of the state space model are identified. It was observed that $\omega_n$ and $\zeta$ take almost constant values of 6 (rad/s) and 0.6 (Ns/m) respectively. Therefore, for the three blades, the dynamics of the whole system could be written as:

$$\mathcal{A} = \bigoplus_{i=1}^{3} A \quad \mathcal{B}(\gamma_1, \gamma_2, \gamma_3) = \bigoplus_{i=1}^{3} B(\gamma_i) \quad \mathcal{C} = \bigoplus_{i=1}^{3} C \quad \mathcal{D} = \bigoplus_{i=1}^{3} D \tag{12.21}$$

In $\mathcal{B}(\gamma_1, \gamma_2, \gamma_3)$, the three variables $\gamma_1, \gamma_2$ and $\gamma_3$ are determined by the effective wind speed on the corresponding blade.

## 12.3 MPC of a LPV System with Known Scheduling Variable

Generally nonlinear dynamics of a plant could be modeled as the following difference equation:

$$x_{k+1} = f(x_k, u_k) \tag{12.22}$$

With $x_k$ and $u_k$ as states and inputs respectively. Using the nonlinear model, the nonlinear MPC problem could be formulated as:

$$\begin{aligned} \min_{u} \quad & p(x_N) + \sum_{i=0}^{N-1} q(x_{k+i|k}, u_{k+i|k}) && (12.23) \\ \text{Subject to} \quad & x_{k+1} = f(x_k, u_k) && (12.24) \\ & u_{k+i|k} \in \mathbb{U} && (12.25) \\ & \hat{x}_{k+i|k} \in \mathbb{X} && (12.26) \end{aligned}$$

Where $p(x_N)$ and $q(x_{k+i|k}, u_{k+i|k})$ are called terminal cost and stage cost respectively and are assumed to be positive definite. $\mathbb{U}$ and $\mathbb{X}$ show the set of acceptable inputs and states. As mentioned above, because of the nonlinear model, this problem is computationally too expensive. One way to avoid this problem is to linearize around an equilibrium point of the system and use a linearized model instead of the nonlinear model. However, for some plants assumption of a linear model does not hold for long prediction horizons. This is because the plant operating point changes, for example on the basis of disturbances that act as a scheduling variable. An example could be a wind turbine for which wind speed acts as a scheduling variable and changes the operating point of the system.

### 12.3.1 Linear MPC formulation

The problem of linear MPC could be formulated as:

$$\begin{aligned} \min_{u_0, u_1, \ldots, u_{N-1}} \quad & \|x_N\|_{Q_f} + \sum_{i=0}^{N-1} \|x_{k+i|k}\|_Q + \|u_{k+i|k}\|_R && (12.27) \\ \text{Subject to} \quad & x_{k+1} = Ax_k + Bu_k && (12.28) \\ & u_{k+i|k} \in \mathbb{U} && (12.29) \\ & \hat{x}_{k+i|k} \in \mathbb{X} && (12.30) \end{aligned}$$

Assuming that we use norms $1, 2$ and $\infty$, the optimization problem becomes convex providing that the sets $\mathbb{U}$ and $\mathbb{X}$ are convex. Convexity of the optimization problem makes it tractable and guarantees that the solution is the global optimum. The problem above is based on a single linear model of the plant around one operating point. However below we formulate our problem using linear parameter varying systems (LPV) in which the scheduling variable is known for the entire prediction horizon.

### 12.3.2 Linear Parameter Varying systems

Linear Parameter Varying (LPV) systems are a class of linear systems whose parameters change on the basis of a scheduling variable. Study of LPV systems was motivated by their use in gain-scheduling control of nonlinear systems ([AGB95]). LPV systems are able to handle changes in the dynamics of the system by parameter varying matrices. **(LPV systems)** let $k \in Z$ denote discrete time. We define the following LPV systems:

$$x_{k+1} = A(\gamma_k)x_k + B(\gamma_k)u_k \tag{12.31}$$

$$A(\gamma_k) = \sum_{j=1}^{n_\gamma} A_j\gamma_{k,j} \quad B(\gamma_k) = \sum_{j=1}^{n_\gamma} B_j\gamma_{k,j} \tag{12.32}$$

Where $A(\gamma_k)$ and $B(\gamma_k)$ are functions of the scheduling variable $\gamma_k$. The variables $x_k \in \mathbb{R}^{n_x}, u_k \in \mathbb{R}^{n_u}$, and $\gamma_k \in \mathbb{R}^{n_\gamma}$ are the state, the control input and the scheduling variable respectively.

### 12.3.3 Problem formulation

Using the above definition, the linear parameter varying (LPV) model of the nonlinear system is of the following form:

$$\tilde{x}_{k+1} = A(\gamma_k)\tilde{x}_k + B(\gamma_k)\tilde{u}_k \tag{12.33}$$

This model is formulated based on deviations from the operating point. However we need the model to be formulated in absolute values of inputs and states. Because in our problem the steady state point changes as a function of the scheduling variable, we need to introduce a variable to capture its behavior. In order to rewrite the state space model in the absolute form we use:

$$\tilde{x}_k = x_k - x_k^* \tag{12.34}$$

$$\tilde{u}_k = u_k - u_k^* \tag{12.35}$$

Where $x_k^*$ and $u_k^*$ are values of states and inputs at the operating point. Therefore the LPV model becomes:

$$x_{k+1} = A(\gamma_k)(x_k - x_k^*) + B(\gamma_k)(u_k - u_k^*) + x_{k+1}^* \tag{12.36}$$

Which could be written as:

$$x_{k+1} = A(\gamma_k)x_k + B(\gamma_k)u_k + \lambda_k \tag{12.37}$$

with

$$\lambda_k = x^*_{k+1} - A(\gamma_k)x^*_k - B(\gamma_k)u^*_k \tag{12.38}$$

Now having the LPV model of the system we proceed to compute state predictions. In linear MPC predicted state at step $n$ is:

$$\begin{aligned} x_{k+n} &= A^n x_k + \sum_{i=0}^{n-1} A^i B u_{k+(n-1)-i} \\ &\text{for} \quad n = 1, 2, \ldots, N \end{aligned} \tag{12.39}$$

However in our method the predicted state is also a function of the scheduling variable $\Gamma_n = \left(\gamma_{k+1}, \gamma_{k+2}, \ldots \gamma_{k+n}\right)^T$ for $n = 1, 2, \ldots, N-1$ and we assume that the scheduling variable is known for the entire prediction. Therefore the predicted state could be written as:

$$x_{k+1}(\gamma_k) = A(\gamma_k)x_k + B(\gamma_k)u_k + \lambda_k \tag{12.40}$$

And for $n \in \mathbb{Z}, n \geq 1$:

$$\begin{aligned} x_{k+n+1}(\Gamma_n) = {} & \left(\prod_{i=0}^{n} A^T(\gamma_{k+i})x_k\right)^T \\ & + \sum_{j=0}^{n-1} \left(\prod_{i=1}^{n-j} A^T(\gamma_{k+i})\right)^T B(\gamma_{k+j})u_{k+j} \\ & + \sum_{j=0}^{n-1} \left(\prod_{i=0}^{n-j} A^T(\gamma_{k+i})\right)^T \lambda_{k+(n-1)-j} \\ & + B(\gamma_{k+n})u_{k+n} + \lambda_{k+n} \end{aligned} \tag{12.41}$$

Using the above formulas we write down the stacked predicted state which becomes:

$$X = \Phi(\Gamma)x_k + \mathcal{H}_u(\Gamma)U + \Phi_\lambda(\Gamma)\Lambda \tag{12.42}$$

with

$$X = \begin{pmatrix} x_{k+1} & x_{k+2} & \ldots & x_{k+N} \end{pmatrix}^T \tag{12.43}$$

$$U = \begin{pmatrix} u_k & u_{k+1} & \ldots & u_{k+N-1} \end{pmatrix}^T \tag{12.44}$$

$$\Gamma = \begin{pmatrix} \gamma_k & \gamma_{k+1} & \ldots & \gamma_{k+N-1} \end{pmatrix}^T \tag{12.45}$$

$$\Lambda = \begin{pmatrix} \lambda_k & \lambda_{k+1} & \ldots & \lambda_{k+N-1} \end{pmatrix}^T \tag{12.46}$$

In order to summarize formulas for matrices $\Phi, \Phi_\lambda$ and $\mathcal{H}_u$, we define a new function as:

$$\psi(m, n) = \left(\prod_{i=n}^{m} A^T(\gamma_{k+i})\right)^T \tag{12.47}$$

Therefore the matrices become:

$$\Phi(\Gamma) = \begin{pmatrix} \psi(1,1) \\ \psi(2,1) \\ \psi(3,1) \\ \vdots \\ \psi(N,1) \end{pmatrix}$$

$$\Phi_\lambda(\Gamma) = \begin{pmatrix} I & 0 & 0 & \dots & 0 \\ \psi(1,1) & I & 0 & \dots & 0 \\ \psi(2,1) & \psi(2,2) & I & \dots & 0 \\ \vdots & \vdots & \vdots & \ddots & \vdots \\ \psi(N-1,1) & \psi(N-1,2) & \psi(N-1,3) & \dots & I \end{pmatrix}$$

$$\mathcal{H}_u(\Gamma) = \begin{pmatrix} B(\gamma_k) & 0 & \dots & 0 \\ \psi(1,1)B(\gamma_k) & B(\gamma_{k+1}) & \dots & 0 \\ \psi(2,1)B(\gamma_k) & \psi(2,2)B(\gamma_{k+1}) & \dots & 0 \\ \vdots & \vdots & \ddots & \vdots \\ \psi(N-1,1)B(\gamma_k) & \psi(N-1,2)B(\gamma_{k+1}) & \dots & B(\gamma_{N-1}) \end{pmatrix}$$

$$\mathcal{H}_d(\Gamma) = \begin{pmatrix} B_d(\gamma_k) & 0 & \dots & 0 \\ \psi(1,1)B_d(\gamma_k) & B_d(\gamma_{k+1}) & \dots & 0 \\ \psi(2,1)B_d(\gamma_k) & \psi(2,2)B_d(\gamma_{k+1}) & \dots & 0 \\ \vdots & \vdots & \ddots & \vdots \\ \psi(N-1,1)B_d(\gamma_k) & \psi(N-1,2)B_d(\gamma_{k+1}) & \dots & B_d(\gamma_{N-1}) \end{pmatrix}$$

After computing the state predictions as functions of control inputs, we can write down the optimization problem similar to a linear MPC problem as a quadratic program.

## 12.4 Control

### 12.4.1 Control objectives

The most basic control objective of a wind turbine is to maximize captured power during the life time of the wind turbine. This means producing electricity as close to the rated value as possible and reducing fatigue loads in order to increase the life-time of the turbine. To achieve these objectives wind turbine operations can be divided into two basic regions, the partial load region and the full load region. In the partial load region, the objective is to maximize captured power when wind speed is below its rated value. This is also called maximum power point tracking (MPPT). However in the full load region in which wind speed is above rated, the control objective becomes regulation of the outputs around their rated values while trying to minimize dynamic loads on the structure. These objectives should be achieved against fluctuations in wind speed which act as a disturbance to the system. In this work we have considered operation of the wind turbine in the above rated (full load region). Therefore we try to regulate rotational speed and generated power around their rated values and remove the effect of wind speed fluctuations.

### 12.4.2 Implementation

Two controllers are implemented in this work. One controller determines the collective pitch and generator reaction torque and regulates power and rotational speed. The second controller determines $\Delta\theta_i, i = 1, 2, 3$ for fatigue load reduction by adjusting individual blade pitch based on the individual blade's effective wind speed calculations. Both of the controllers take advantage of having the wind speed for the entire prediction horizon. These are fed to the controllers through four vectors, $V_{hh}, V_1, V_2$ and $V_3$, which are vector of wind speeds at hub height and 75% of blades $1, 2$ and 3 respectively.

#### 12.4.2.1 Collective pitch controller

The first controller uses the linearized model which was explained in section 12.2.2 augmented with a second order system modeling actuator dynamics. Measured outputs that are fed to this controller are:

$$\begin{pmatrix} \omega_r \\ P_e \\ a_t \\ \theta_c \\ V_{hh} \end{pmatrix} \begin{array}{l} \text{Rotor rotational speed} \\ \text{Generated power} \\ \text{Tower top acceleration} \\ \text{Measured collective pitch} \\ \text{Hub height wind speed vector} \end{array} \tag{12.48}$$

#### 12.4.2.2 Individual pitch controller

The objective of this controller is to reduce fluctuations on blade root bending moments by adjusting pitch angle based on calculated effective wind speeds and blade root bending moment measurements for each blade individually. The controller will reduce 1P fluctuations of bending moments on the blade roots. The fluctuations in the blade root bending moments are considered to be from

$\mathcal{M}_{hh}$ which is the bending moment produced by the hub height wind speed. In steady state, $\tilde{\mathcal{M}}$ in equation 12.18 should be zero, therefore we can find steady state values for $\tilde{\theta}$ having $\tilde{v}$. This steady state value is taken to be the reference value of the pitch actuator which was modeled as a second order system. Measurements that are fed to the individual pitch controller are out-of-plane blade root bending moments and calculated effective wind speeds:

$$\begin{pmatrix} \tilde{\mathcal{M}}_1 \\ \tilde{\mathcal{M}}_2 \\ \tilde{\mathcal{M}}_3 \\ V_1 \\ V_2 \\ V_3 \end{pmatrix} \begin{array}{l} \text{Out-of-plane blade root bending moment of blade 1} \\ \text{Out-of-plane blade root bending moment of blade 2} \\ \text{Out-of-plane blade root bending moment of blade 3} \\ \text{Wind speed vector for blade 1} \\ \text{Wind speed vector for blade 2} \\ \text{Wind speed vector for blade 3} \end{array} \tag{12.49}$$

### 12.4.3 Benchmark controller

The benchmark controller used in this work is a collective pitch controller based on the one found in [JBMS09]. The controller has a gain-scheduled feedback from rotor speed to collective pitch angle and controls the generator torque to achieve constant power. The collective pitch controller is augmented with an individual pitch control (IPC) system that uses the flapwise blade root bending moments via the Coleman transform to determine cyclic behavior of the pitch angles. The cyclic pitch terms are then added to the collective pitch angle. Details regarding the tuning and implementation of the IPC can be found in [bMHHZ11].

## 12.5 Simulations

In this section simulation results for the obtained controllers which are denoted as MPC IPC (the proposed approach) and PI IPC (the benchmark controller) are presented. The controllers are implemented in MATLAB and are tested on a full complexity FAST [JJ05] model of the reference wind turbine [JBMS09]. Simulation results are shown for two scenarios, one stochastic hub height wind speed with wind shear, and one with extreme wind shear. Both scenarios are taken from the IEC standard [iec05].

| Parameters | MPC-IPC | PI-IPC | Improvement |
|---|---|---|---|
| SD of $\omega_r$ (RMP) | 0.2185 | 0.6802 | 67.87% |
| SD of $P_e$ (KWatts) | 10.402 | 86.826 | 88.01% |
| Pitch travel (degrees) | 886.9 | 829.3 | 6.49% |
| SD of shaft moment (KN.M.) | 0.7237 | 2.2144 | 67.31% |
| Tower base DEL (fore-aft) | $6.063 \times 10^2$ | $1.431 \times 10^3$ | 57.63% |
| Blade root DEL (flapwise) | $2.538 \times 10^3$ | $2.873 \times 10^5$ | 99.1% |

**Table 12.1:** MPC and PI performance comparison for stochastic wind (SD stands for standard deviation and DEL stands for damage equivalent load)

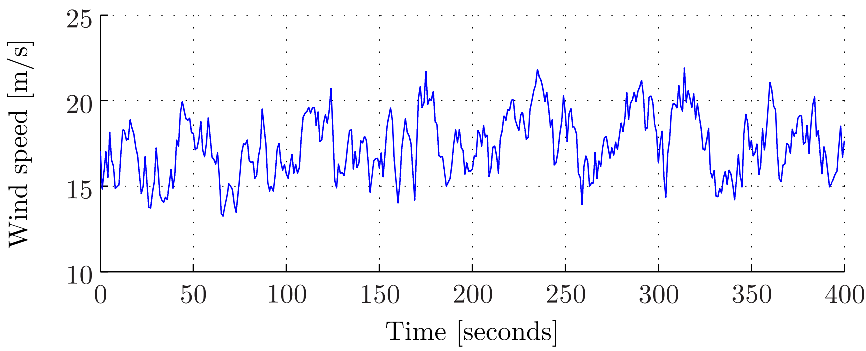


**Figure 12.4:** Wind speed

### 12.5.1 Stochastic wind

In this scenario, simulations are done with realistic hub height turbulent wind. The Kaimal model [iec05] is chosen as the turbulence model and TurbSim [Jon09] is used to generate the wind profile. Wind shear is included with 0.2 as the value for the power-law exponent. In order to stay in the full load region, a realization of turbulent wind speed is used from category $C$ of the turbulence categories of the IEC 61400-1 [iec05] with $18m/s$ as the mean wind speed. Table 12.1 compares simulation results for MPC IPC and PI IPC and the results are shown in figures 12.4-12.9. Damage equivalent loads (DELs) are calculated for out-of-plane blade roots and tower base in the fore-aft direction. As can be seen in the table in which short-term DELs at fixed mean are given, we get good regulation of rotational speed and generated power, while dynamic loads on the blade root and tower-base are less. Low generator reaction torque activity results in less dynamic loads on the drivetrain compared to the PI controller.

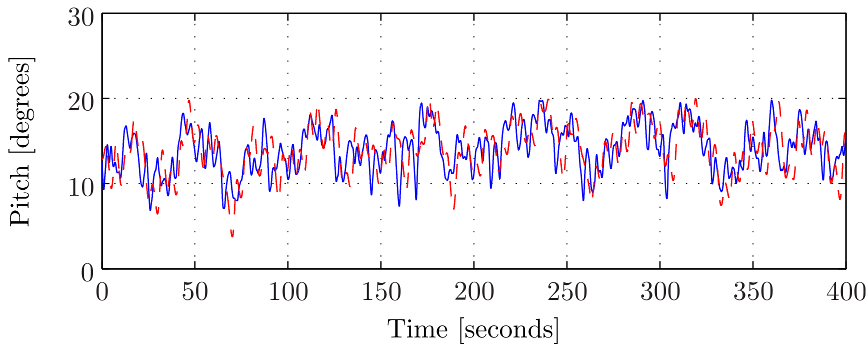


**Figure 12.5:** Blade-pitch reference, MPC IPC (blue-solid), PI IPC (red-dashed)

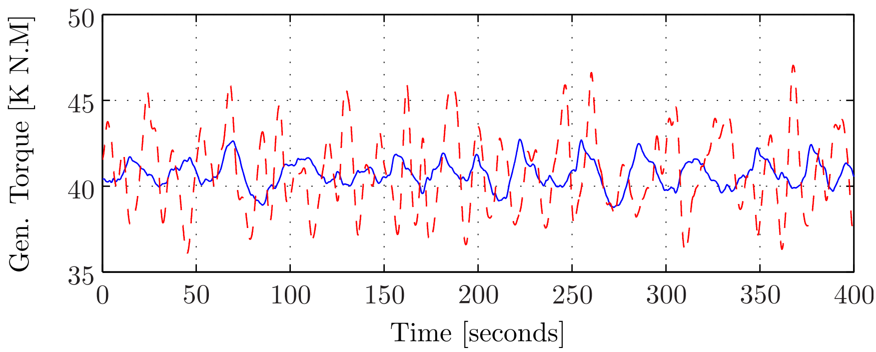


**Figure 12.6:** Generator-torque reference, MPC IPC (blue-solid), PI IPC (red-dashed)

### 12.5.2 Extreme wind shear

In this section simulation results for a vertical extreme wind shear (EWS) event are presented. A power law wind profile is used to demonstrate wind shear. In the vertical EWS event, the power law exponent ramps up from a normal value of 0.2 to an extreme value of 0.3 in 2 seconds and after 10 seconds ramps down to the normal situation. Controller performance for the MPC IPC and PI IPC are compared for this event. A comparison of blade pitch is given in 12.10, as it can be seen, the MPC IPC gives a smoother increase in blade pitch while PI IPC has an overshoot. Out-of-plane blade root bending moments of one of the blades are given in 12.11. Clearly the MPC IPC gives better performance in reducing both steady state and transient fluctuations. In order to simplify comparison of the signals, Coleman transformation [CF61] of the three out-of-plane blade root

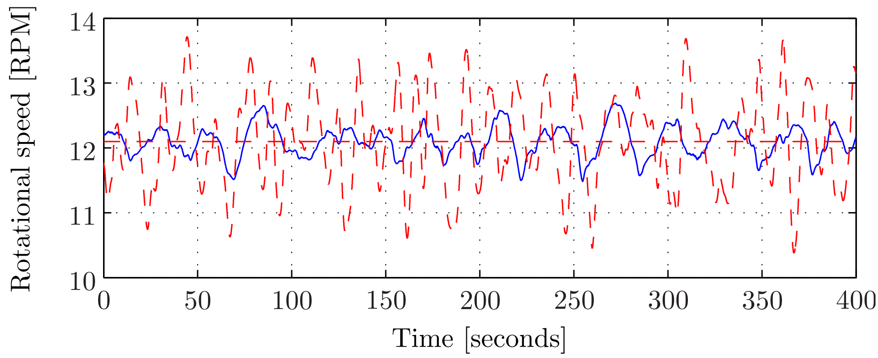


**Figure 12.7:** Rotor rotational speed ($\omega_r$), MPC IPC (blue-solid), PI IPC (red-dashed)

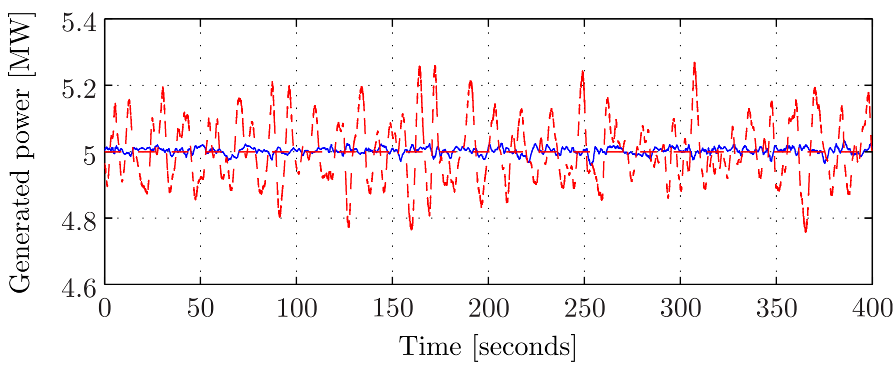


**Figure 12.8:** Electrical power, MPC IPC (blue-solid), PI IPC (red-dashed)

bending moments are calculated and the results, namely yaw and tilt signals, for both controllers are given in 12.12 and 12.13 respectively.

## 12.6 Conclusions

In this paper firstly we found a nonlinear model of a wind turbine, using blade element momentum theory (BEM) and first principle modeling of the flexible drive train and tower. Our control methodology is based on a family of linear models, therefore we have used Taylor series expansion to linearize the obtained nonlinear model around system operating points. Operating points are functions of wind speed, therefore wind speed is used as a scheduling variable. Model predictive control of LPV systems with known scheduling variable is used to

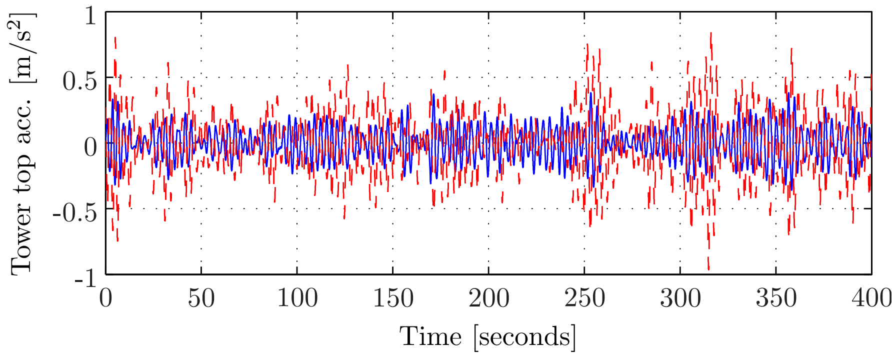


**Figure 12.9:** Tower top acceleration, MPC IPC (blue-solid), PI IPC (red-dashed)

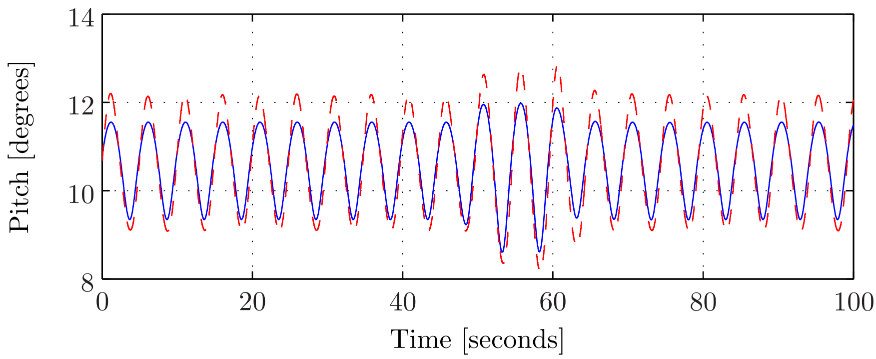


**Figure 12.10:** Pitch of one of the blades, (MPC IPC is solid-blue and PI IPC is red-dashed, degrees)

solve the control problem. The final controller was applied on a full complexity FAST [JJ05] model and was compared with a benchmark controller.

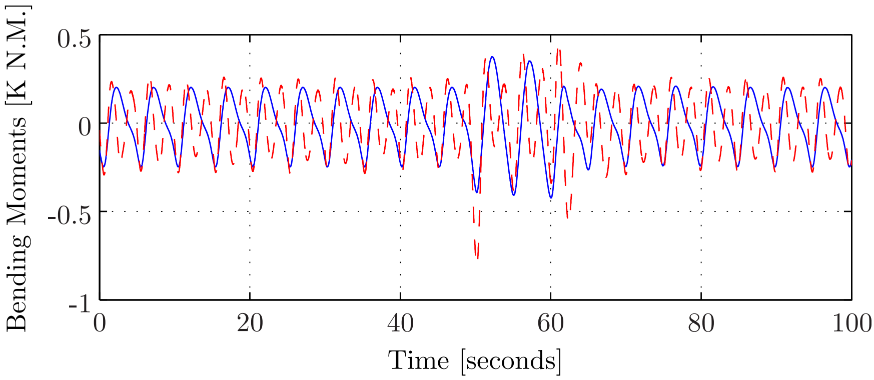


**Figure 12.11:** Out-of-plane blade root bending moment, (MPC IPC is solid-blue and PI IPC is red-dashed, Mega N.m)

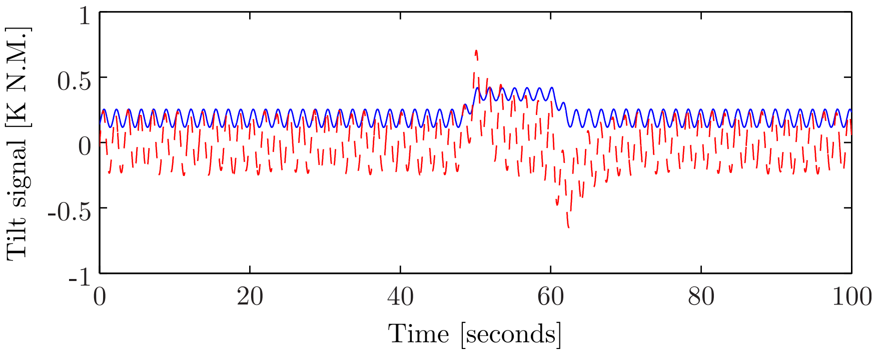


**Figure 12.12:** Tilt signal, (MPC IPC is solid-blue and PI IPC is red-dashed, Mega N.m)

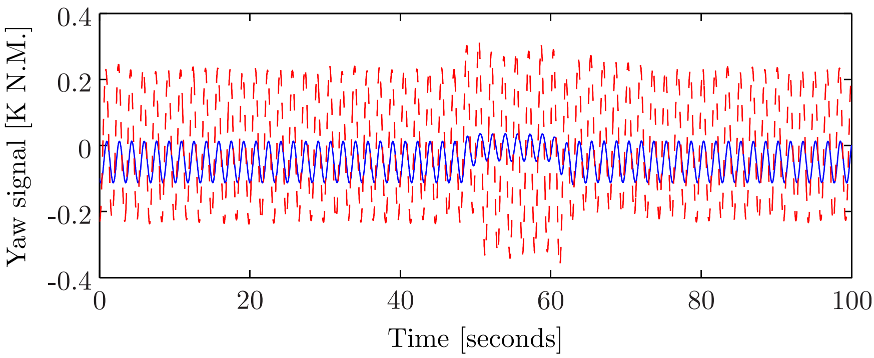


**Figure 12.13:** Yaw signal, (MPC IPC is solid-blue and PI IPC is red-dashed, Mega N.m)

## Paper H References


[AGB95] Pierre Apkarian, Pascal Gahinet, and Greg Becker. Self-scheduled $H_\infty$ control of linear parameter-varying systems: a design example. *Automatica*, 31(9):1251–1261, 1995.

[And10] Peter Bjørn Andersen. *Advanced Load Alleviation for Wind Turbines using Adaptive Trailing Edge Flaps: Sensoring and Control.* PhD thesis, Technical University of Denmark, Denmark, 2010.

[BBM06] Fernando D. Bianchi, Hernan De Battista, and Ricardo J. Mantz. *Wind Turbine Control Systems: Principles, Modelling and Gain Scheduling Design.* Springer, 2006.

[BM99] A Bemporad and M Morari. Robust model predictive control: A survey. *Lecture Notes in Control and Information Sciences*, 245:207–226, 1999.

[bMHHZ11] Edited by Morten Hartvig Hansen and Frederik Zahle. Aeroelastic optimization of mw wind turbines. Technical Report Risø-R-1803, Risø National Laboratory for Sustainable Energy, Technical University of Denmark, December 2011.

[Bos03] E. A. Bossanyi. Individual blade pitch control for load reduction. *Wind Energy*, 6(2):119–128, 2003.

[CF61] Robert P Coleman and Arnold M Feingold. Theory of self-excited mechanical oscillations of helicopter rotors with hinged blades. *CASI*, pages –, 1961.

[GC08] M. Geyler and P. Caselitz. Robust multivariable pitch control design for load reduction on large wind turbines. *Journal of solar energy engineering*, 130(3):–, 2008.

[Han08] Martin O. L. Hansen. *Aerodynamics of Wind Turbines*. Earthscan, 2008.

[Hen07] Lars Christian Henriksen. Model predictive control of a wind turbine. Master's thesis, Technical University of Denmark, Informatics and Mathematical Modelling, 2007.

[HHW06] M. Harris, M. Hand, and A. Wright. LIDAR for turbine control. Technical report, National Renewable Energy Laboratory, 2006.

[iec05] IEC 61400-1 wind turbines-part 1: Design requirements., August 2005.

[JBMS09] J. Jonkman, S. Butterfield, W. Musial, and G. Scott. Definition of a 5MW reference wind turbine for offshore system development. Technical report, National Renewable Energy Laboratory,, 1617 Cole Boulevard, Golden, Colorado 80401-3393 303-275-3000, 2009.

[JF08] Johnson and Fingersh. Adaptive pitch control of variable-speed wind turbines. *J. Sol. Energy Eng. (USA)*, 130(3):031012–1–7, 2008.

[JJ05] Jason M. Jonkman and Marshall L. Buhl Jr. Fast user's guide. Technical Report NREL/EL-500-38230, National Renewable Energy Laboratory, Golden, CO, August 2005.

[Jon09] B.J. Jonkman. Turbsim user's guide: Version 1.50. Technical report, National Renewable Energy Laboratory, 1617 Cole Boulevard, Golden, Colorado 80401-3393 303-275-3000, 2009.

[LC00] W.E. Leithead and Bill Connor. Control of variable speed wind turbines: Design task. *Int J Control*, 73(13):1189–1212, 2000.

[Lju99] L. Ljung. *System identification / Theory for the user.* Prentice Hall, Upper Saddle River, N.J., 1999.

[LPS+11] Jason Laks, Lucy Y. Pao, Eric Simley, Alan Wright, Neil Kelley, and Bonnie Jonkman. Model predictive control using preview measurements from lidar. In *49th AIAA Aerospace Sciences Meeting including the New Horizons Forum and Aerospace Exposition*, Orlando, Florida, January 2011.

[LPW09] J.H. Laks, L.Y. Pao, and A.D. Wright. Control of wind turbines: Past, present, and future. *Proceedings of the American Control Conference*, pages 2096–2103, 2009.

[MNP11] Mahmood Mirzaei, Hans Henrik Niemann, and Niels Kjølstad Poulsen. A $\mu$-synthesis approach to robust control of a wind turbine. In *the 50th IEEE Conference on Decision and Control and European Control Conference*, pages 645–650, Orlando, Florida, United States, 2011.

[Øst08] Kasper Zinck Østergaard. *Robust, Gain-Scheduled Control of Wind Turbines.* PhD thesis, Automation and Control Department of Electronic Systems, Aalborg University, 2008.

[QB96] S. Joe Qin and Thomas A. Badgwell. An overview of industrial model predictive control technology. pages –, 1996.

[SK08] D Schlipf and M. Kühn. Prospects of a collective pitch control by means of predictive disturbance compensation assisted by wind speed measurements. In *Proceedings of the German Wind Energy Conference, DEWEK*, 2008.

[SSG+10] D. Schlipf, S. Schuler, P. Grau, F. Allgöwer, and M. Kühn. Look-ahead cyclic pitch control using lidar. In *the Science of making Torque from Wind (TORQUE)*, 2010.

[Tho06] Sven Creutz Thomsen. Nonlinear control of a wind turbine. Master's thesis, Technical University of Denmark, Informatics and Mathematical Modelling, Lyngby, Denmark, 2006.

Paper I

# Model Predictive Control of Wind Turbines using Uncertain LIDAR Measurements

**Authors:**
M. Mirzaei, M. Soltani, N. K. Poulsen, H. H. Niemann

**Submitted to:** American Control Conference 2013

**Model Predictive Individual Pitch Control of Wind Turbines Using LIDAR Measurements**[1]

Mahmood Mirzaei[2], Mohsen Soltani [3], Niels K. Poulsen[2] and Hans H. Niemann[4]

**Abstract**

The problem of Model predictive control (MPC) of wind turbines using uncertain LIDAR measurements is considered. A nonlinear dynamical model of the wind turbine is obtained. We linearize the obtained nonlinear model for different operating points which are determined by the effective wind speed on the rotor disc. We take the wind speed as a scheduling variable. The wind speed is measurable ahead of the turbine using LIDARs, therefore the scheduling variable is known for the entire prediction horizon. By taking the advantage of having future values of the scheduling variable, we will simplify state prediction for the MPC. Consequently the control problem of the nonlinear system is simplified into a quadratic programming. We consider uncertainty in the wind propagation, which is the traveling time of wind from the LIDAR measurement point to the rotor. An algorithm based on wind speed estimation and measurements form the LIDAR is devised to find an estimate of the delay and compensate for it before it is used in the controller. Comparisons between the MPC with error compensation, without error compensation and an MPC with re-linearization at each sample point based on wind speed estimation are given. It is shown that with appropriate signal processing techniques, LIDAR measurements improve the performance of the wind turbine controller.

# 13.1 Introduction

In recent decades there has been increasing interest in green energies, of which wind energy is one of the most important. Horizontal axis wind turbines are the most common wind energy conversion systems (WECS) and are hoped to

[1]This work is supported by the CASED Project funded by grant DSF-09- 063197 of the Danish Council for Strategic Research.

[2]DTU Informatics, Technical University of Denmark, Asmussens Alle, building 305, DK-2800 Kgs. Lyngby, Denmark

[3]department of Energy Technology, Aalborg University, 6700 Esbjerg, Denmark

[4]Department of Electrical Engineering, Technical University of Denmark, Ørsteds Plads, Building 349, DK-2800 Kgs. Lyngby, Denmark

be able to compete with fossil fuel power plants on energy price in near future. However, this demands better technology to reduce the electricity production price. Control can play an essential part in this context. This is because, on the one hand improved control methods can decrease the cost of energy by keeping the turbine close to its maximum efficiency. On the other hand, they can reduce structural fatigue and increase the lifetime of the wind turbine. There are several methods of wind turbine control, ranging from classical control methods, which are the most commonly used methods in real applications [LC00], to advanced control methods, which have been the focus of research in the past few years [LPW09]. Gain scheduling [BBM06], adaptive control [JF08], MIMO methods [GC08], nonlinear control [Tho06], robust control [Øst08], model predictive control [Hen07], $\mu$-Synthesis design [MNP11] and robust MPC [MPN12b] are just to mention a few. Advanced model-based control methods are thought to be the future of wind turbine control, as they can conveniently employ new generations of sensors on wind turbines (e.g. LIDAR [HHW06]), new generation, of actuators (e.g. trailing edge flaps [And10]) and they also treat the turbine as a MIMO system. The last feature seems to have become more important than before, as wind turbines are becoming bigger and more flexible. This trend makes decoupling different modes, specifying different objectives and designing controllers based on paired input/output channels more difficult. Model predictive control (MPC) has proved to be an effective tool to deal with multivariable constrained control problems [Mac02]. As wind turbines are MIMO systems [GC08] with constraints on inputs and outputs, using MPC is reasonable. MPC has been an active area of research and has been successfully applied on different applications in the last decades [QB96]. In this work, we extend the idea of linear MPC to formulate a tractable predictive control of the nonlinear system of wind turbines. To do so, we use future values of the effective wind speed that acts as a scheduling variable in the model. LIDAR measurements are used to calculate the effective wind speed ahead of wind turbines [HHW06]. Several works have considered wind turbine control using LIDAR measurements [SWBB11], [LPS$^+$11] and [MPN12a]. However it is also important to take uncertainty in the measurements into account as small errors in the calculations of the wind propagation time can severely reduce performance of the controller. The paper is organized as follows. In section 13.2, modeling of the wind turbine is explained, the nonlinear model is derived and a linear model is given whose parameters vary as a function of effective wind speed. In section 13.3, our proposed method for solving model predictive control of the system is presented. Then, the control design is explained, and control objectives are discussed. In section 13.4, uncertainty in the LIDAR measurements are explained, and a method is proposed to reduce the most severe source of uncertainty. Finally, in section 13.5, simulation results are given.

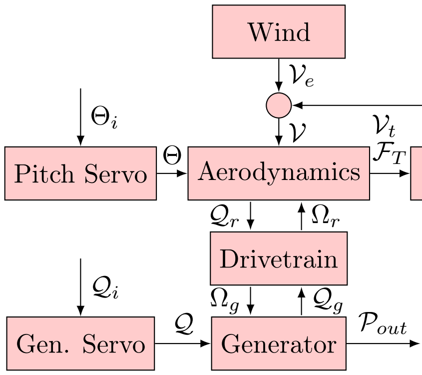


**Figure 13.1:** Wind turbine subsystems

## 13.2 Wind Turbine Modeling

In this section the nonlinear model and important degrees of freedom are explained. Afterwards the linearization procedure is described and the linear parameter varying model is given.

### 13.2.1 Nonlinear model

For modeling purposes, the wind turbine can be divided into 4 subsystems: Aerodynamics, mechanical, electrical and actuator subsystems. The aerodynamic subsystem converts wind forces into mechanical torque and thrust on the rotor. The mechanical subsystem consists of drivetrain, tower and blades. Drivetrain transfers rotor torque to electrical generator. Tower holds the nacelle and withstands the thrust force. And blades transform wind forces into toque and thrust. The generator subsystem converts mechanical energy to electrical energy and finally the blade-pitch and generator-torque are the actuators of the control system. To model the wind turbine, models of these subsystems are obtained and connected together. A wind model is obtained and augmented with the wind turbine model to be used for wind speed estimation. Figure 13.1 shows the basic subsystems and their interactions. The dominant dynamics of the wind turbine come from its flexible structure. Several degrees of freedom could be considered to model the flexible structure, but for control design a few important degrees of freedom are considered. In figure 13.2, basic degrees of freedom, which are normally being considered in the design model are shown. However, in this work we only consider three degrees of freedom, namely the

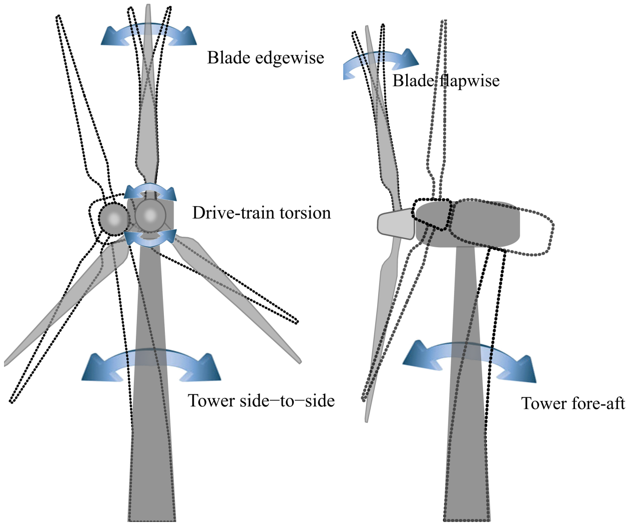


**Figure 13.2:** Basic degrees of freedom

rotational degree of freedom (DOF), the drivetrain torsion and the tower fore-aft displacement. Nonlinearity of the wind turbine model mostly comes from its aerodynamics. Blade element momentum (BEM) theory [Han08] is used to numerically calculate aerodynamic torque and thrust on the wind turbine. This theory explains how torque and thrust are related to wind speed, blade pitch angle and rotational speed of the rotor. In steady state, i.e. disregarding unsteady aerodynamics, the following formulas can be used to calculate aerodynamic torque and thrust.

$$\mathcal{Q}_r = \frac{1}{2}\frac{1}{\Omega_r}\rho\pi R^2 \mathcal{V}_e^3 C_p(\Theta, \Omega, \mathcal{V}_e) \tag{13.1}$$

$$\mathcal{Q}_t = \frac{1}{2}\rho\pi R^2 \mathcal{V}_e^2 C_t(\Theta, \Omega, \mathcal{V}_e) \tag{13.2}$$

In which $\mathcal{Q}_r$ and $\mathcal{Q}_t$ are aerodynamic torque and thrust, $\rho$ is the air density, $\Omega_r$ is the rotor rotational speed, $\Theta$ is the collective pitch of the blades, $\mathcal{V}_e$ is the effective wind speed, $C_p$ is the power coefficient and $C_t$ is the thrust coefficient. The absolute angular position of the rotor and generator is not needed in our work, therefore we use the drivetrain torsion $\psi$ instead. Having aerodynamic torque and modeling the drivetrain and the tower fore-aft degrees of freedom with simple mass-spring-damper, the whole system equation with 3 degrees of freedom becomes:

$$J_r\dot{\Omega}_r = \mathcal{Q}_r - C_d(\Omega_r - \frac{\Omega_g}{N_g}) - K_d\psi \tag{13.3}$$

$$(N_g J_g)\dot{\Omega}_g = C_d(\Omega_r - \frac{\Omega_g}{N_g}) + K_d\psi - N_g\mathcal{Q}_g \tag{13.4}$$

$$\dot{\psi} = \Omega_r - \frac{\Omega_g}{N_g} \tag{13.5}$$

$$M\ddot{x}_t = \mathcal{Q}_t - C_t\dot{x}_t - K_t x_t \tag{13.6}$$

$$\mathcal{P}_e = \mathcal{Q}_g\Omega_g \tag{13.7}$$

In which $J_r$ and $J_g$ are rotor and generator moments of inertia, $\psi$ is the drivetrain torsion, $\mathcal{Q}_g$ and $\Omega_g$ are the generator torque and rotational speed, $N_g$ is the gearbox ration, $C_d$ and $K_d$ are the drivetrain damping and stiffness factors, respectively, lumped in the low speed side of the shaft. The tower mass, damping and stiffness factors are represented by $M$, $C_t$ and $K_t$, respectively, and $\mathcal{P}_e$ and $x_t$ are the generated electrical power and tower displacement, respectively. Values of the parameters can be found in [JBMS09].

### 13.2.2 Linearized model

To get a linear model of the system we need to linearize the model (13.3-13.7) around its operating points, which are determined by wind speed averaged on the rotor area. Wind speed changes along the blades and with the azimuth angle (angular position) of the rotor. This is because of wind shear, tower shadow and stochastic spatial distribution of the wind field. Therefore a single wind speed does not exist to be used and measured in order to find the operating point. We bypass this problem by defining a fictitious variable called effective wind speed ($\mathcal{V}_e$), which shows the effect of wind on the rotor disc of the wind turbine. Using the linearized aerodynamic torque and thrust, state space matrices for the 3 DOFs linearized model become:

$$\dot{\omega}_r = \frac{\alpha_1(v_e) - c}{J_r}\omega_r + \frac{c}{J_r}\omega_g - \frac{k}{J_r}\psi \tag{13.8}$$

$$+ \beta_{11}(v_e)\theta + \beta_{12}(v_e)(v_e - v_t) \tag{13.9}$$

$$\dot{\omega}_g = \frac{c}{N_g J_g}\omega_r - \frac{c}{N_g^2 J_g}\omega_g + \frac{k}{N_g J_g}\psi - \frac{Q_g}{J_g} \tag{13.10}$$

$$\dot{\psi} = \omega_r - \frac{\omega_g}{N_g} \tag{13.11}$$

$$\dot{x}_t = v_t \tag{13.12}$$

$$\dot{v}_t = \frac{\alpha_2(v_e)}{M}\omega_r + \frac{\beta_{21}(v_e)}{M}\theta + \frac{\beta_{22}(v_e)}{M}(v_e - v_t) \tag{13.13}$$

$$- \frac{C_t}{M}v_t - \frac{K_t}{M}x_t \tag{13.14}$$

$$P_e = Q_{g0}\omega_g + \omega_{g0}Q_g \tag{13.15}$$

In which the lower-case variables are deviations away from steady state of the upper-case variables given in the equations (13.1-13.7). Consequently, the parameters of the linearized model are functions of wind speed, which in our approach acts as a scheduling variable. A detailed description of the model and linearization is given in [MNP11].

### 13.2.3 Linear parameter varying model

According to the model given in the equations (13.8-13.15), matrices of the state space model become:

$$A(\gamma) = \begin{pmatrix} \frac{\alpha_1(\gamma)-c}{J_r} & \frac{c}{J_r} & -\frac{k}{J_r} & 0 & -\frac{\beta_{12}(\gamma)}{J_r} \\ \frac{c}{N_g J_g} & -\frac{c}{N_g^2 J_g} & \frac{k}{N_g J_g} & 0 & 0 \\ 1 & -1 & 0 & 0 & 0 \\ 0 & 0 & 0 & 0 & 1 \\ \frac{\alpha_2(\gamma)}{M_t} & 0 & 0 & -\frac{K_t}{M_t} & -\frac{C_t+\beta_{22}(\gamma)}{M_t} \end{pmatrix} \tag{13.16}$$

$$C(\gamma) = \begin{pmatrix} 1 & 0 & 0 & 0 & 0 \\ 0 & Q_{g0} & 0 & 0 & 0 \\ \frac{\alpha_2(\gamma)}{M_t} & 0 & 0 & -\frac{K_t}{M_t} & -\frac{C_t+\beta_{22}(\gamma)}{M_t} \end{pmatrix} \tag{13.17}$$

$$B(\gamma) = \begin{pmatrix} \frac{\beta_{11}(\gamma)}{J_r} & 0 \\ 0 & -\frac{1}{J_g} \\ 0 & 0 \\ 0 & 0 \\ \frac{\beta_{21}(\gamma)}{M_t} & 0 \end{pmatrix} \quad D(\gamma) = \begin{pmatrix} 0 & 0 \\ 0 & \omega_{g0} \\ \frac{\beta_{21}(\gamma)}{M_t} & 0 \end{pmatrix} \tag{13.18}$$

in which $x = \begin{pmatrix}\omega_r & \omega_g & \psi & x_t & \dot{x}_t\end{pmatrix}^T$, $u = \begin{pmatrix}\theta & Q_g\end{pmatrix}^T$ and $y = \begin{pmatrix}\omega_r & P_e & \dot{v}_t\end{pmatrix}^T$ are states, inputs and outputs respectively.

# 13.3 Controller Design

Wind turbine control is a challenging problem as the dynamics of the system changes based on wind speed which has a stochastic nature. In this paper, we use the wind speed as the scheduling variable. With the advances in the LIDAR technology [HHW06] it is possible to measure wind speed ahead of the turbine and this enables us to have the scheduling variable of the plant for the entire prediction horizon. As it was mentioned in section 13.2, wind turbines are nonlinear dynamical systems and if we use the nonlinear model directly in the MPC formulation, the optimization problem associated with the MPC becomes non-convex. In general, non-convex optimization problems are very complicated to solve and there is no guarantee that we could achieve a global optimum. One way to avoid complex and non-convex optimization problems is to linearize the system around an equilibrium point and use the obtained linearized model as an approximation of the nonlinear model. However, for wind turbines, assumption of the approximate linear model does not hold for long prediction horizons. This is because the operating point of the system changes as a function of wind speed which, as mentioned, has a stochastic nature.

## 13.3.1 Linear MPC formulation

The problem of linear MPC could be formulated as:

$$\min_{u_k, u_{k+1}, \ldots, u_{k+N-1}} \|x_N\|_{Q_f} + \sum_{i=1}^{N-1} \|x_{k+i|k}\|_Q + \|u_{k+i|k}\|_R \tag{13.19}$$

$$\text{Subject to} \quad x_{k+1} = Ax_k + Bu_k \tag{13.20}$$

$$u_{k+i|k} \in \mathbb{U} \tag{13.21}$$

$$\hat{x}_{k+i|k} \in \mathbb{X} \tag{13.22}$$

Convexity of the optimization problem given above, makes the problem tractable and guarantees that the solution is the global optimum. The problem above is based on a single linear model of the plant around one operating point. However we formulate our problem using different linear models in which different models are obtained based on a scheduling variable and the scheduling variable is known for the entire prediction horizon. We linearize the nonlinear dynamics of the system for different operating points and since the operating points depend on a single parameter (in our case effective wind speed), we can write the linear model as a function of one scheduling variable $\gamma$ as follows:

$$x_{k+1} = A(\gamma_k)x_k + B(\gamma_k)u_k \tag{13.23}$$

which $A(\gamma_k)$ and $B(\gamma_k)$ are functions of the scheduling variable $\gamma_k$ at instant $k$. The variables $x_k \in \mathbb{R}^{n_x}, u_k \in \mathbb{R}^{n_u}$, and $\gamma_k \in \mathbb{R}^{n_\gamma}$ are the state, the control input and the scheduling variable respectively. This is the well known Linear Parameter Varying (LPV) system.

### 13.3.2 Problem formulation

The linear parameter varying (LPV) model of the nonlinear system is of the following form:

$$\tilde{x}_{k+1} = A(\gamma_k)\tilde{x}_k + B(\gamma_k)\tilde{u}_k \tag{13.24}$$

This model is formulated based on deviations from the operating point. However we need the model to be formulated in absolute values of inputs and states. Because in our problem the operating point changes as a function of the scheduling variable, we need to introduce a variable to capture its behavior. In order to rewrite the state space model in the absolute form we use:

$$\tilde{x}_k = x_k - x_k^* \tag{13.25}$$

$$\tilde{u}_k = u_k - u_k^* \tag{13.26}$$

where $x_k^*$ and $u_k^*$ are values of states and inputs at the operating point. Therefore, the LPV model becomes:

$$x_{k+1} = A(\gamma_k)(x_k - x_k^*) + B(\gamma_k)(u_k - u_k^*) + x_{k+1}^* \tag{13.27}$$

which could be written as:

$$x_{k+1} = A(\gamma_k)x_k + B(\gamma_k)u_k + \lambda_k \tag{13.28}$$

with

$$\lambda_k = x_{k+1}^* - A(\gamma_k)x_k^* - B(\gamma_k)u_k^* \tag{13.29}$$

Now having the LPV model of the system we proceed to compute state predictions. In linear MPC, predicted state at step $n$ is:

$$\begin{gathered} x_{k+n} = A^n x_k + \sum_{i=0}^{n-1} A^i B u_{k+(n-1)-i} \\ \text{for} \quad n = 1, 2, \ldots, N \end{gathered} \tag{13.30}$$

However in our method the predicted state is also a function of the scheduling variable $\Gamma_n = \left(\gamma_{k+1}, \gamma_{k+2}, \dots \gamma_{k+n}\right)^T$ for $n = 1, 2, \dots, N-1$ and we assume that the scheduling variable is known for the entire prediction. Therefore, the predicted state could be written as:

$$x_{k+1}(\gamma_k) = A(\gamma_k)x_k + B(\gamma_k)u_k + \lambda_k \tag{13.31}$$

and for $n \in \mathbb{Z}, n \geq 1$:

$$\begin{aligned} x_{k+n+1}(\Gamma_n) = &\left(\prod_{i=0}^{n} A^T(\gamma_{k+i})x_k\right)^T \\ &+ \sum_{j=0}^{n-1} \left(\prod_{i=1}^{n-j} A^T(\gamma_{k+i})\right)^T B(\gamma_{k+j})u_{k+j} \\ &+ \sum_{j=0}^{n-1} \left(\prod_{i=0}^{n-j} A^T(\gamma_{k+i})\right)^T \lambda_{k+(n-1)-j} \\ &+ B(\gamma_{k+n})u_{k+n} + \lambda_{k+n} \end{aligned} \tag{13.32}$$

Using the above equations we write down the stacked predicted state as:

$$X = \Phi(\Gamma)x_k + \mathcal{H}_u(\Gamma)U + \Phi_\lambda(\Gamma)\Lambda \tag{13.33}$$

with

$$X = \begin{pmatrix} x_{k+1} & x_{k+2} & \dots & x_{k+N} \end{pmatrix}^T \tag{13.34}$$

$$U = \begin{pmatrix} u_k & u_{k+1} & \dots & u_{k+N-1} \end{pmatrix}^T \tag{13.35}$$

$$\Gamma = \begin{pmatrix} \gamma_k & \gamma_{k+1} & \dots & \gamma_{k+N-1} \end{pmatrix}^T \tag{13.36}$$

$$\Lambda = \begin{pmatrix} \lambda_k & \lambda_{k+1} & \dots & \lambda_{k+N-1} \end{pmatrix}^T \tag{13.37}$$

In order to summarize formulas for matrices $\Phi, \Phi_\lambda$ and $\mathcal{H}_u$, we define a new function as:

$$\psi(m, n) = \left(\prod_{i=n}^{m} A^T(\gamma_{k+i})\right)^T \tag{13.38}$$

Therefore the matrices become:

$$\Phi(\Gamma) = \begin{pmatrix} \psi(1,1) \\ \psi(2,1) \\ \psi(3,1) \\ \vdots \\ \psi(N,1) \end{pmatrix}$$

$$\Phi_\lambda(\Gamma) = \begin{pmatrix} I & 0 & 0 & \dots & 0 \\ \psi(1,1) & I & 0 & \dots & 0 \\ \psi(2,1) & \psi(2,2) & I & \dots & 0 \\ \vdots & \vdots & \vdots & \ddots & \vdots \\ \psi(N-1,1) & \psi(N-1,2) & \psi(N-1,3) & \dots & I \end{pmatrix}$$

$$\mathcal{H}_u(\Gamma) = \begin{pmatrix} B(\gamma_k) & 0 & \dots & 0 \\ \psi(1,1)B(\gamma_k) & B(\gamma_{k+1}) & \dots & 0 \\ \psi(2,1)B(\gamma_k) & \psi(2,2)B(\gamma_{k+1}) & \dots & 0 \\ \vdots & \vdots & \ddots & \vdots \\ \psi(N-1,1)B(\gamma_k) & \psi(N-1,2)B(\gamma_{k+1}) & \dots & B(\gamma_{N-1}) \end{pmatrix}$$

$$\mathcal{H}_d(\Gamma) = \begin{pmatrix} B_d(\gamma_k) & 0 & \dots & 0 \\ \psi(1,1)B_d(\gamma_k) & B_d(\gamma_{k+1}) & \dots & 0 \\ \psi(2,1)B_d(\gamma_k) & \psi(2,2)B_d(\gamma_{k+1}) & \dots & 0 \\ \vdots & \vdots & \ddots & \vdots \\ \psi(N-1,1)B_d(\gamma_k) & \psi(N-1,2)B_d(\gamma_{k+1}) & \dots & B_d(\gamma_{N-1}) \end{pmatrix}$$

After computing the state predictions as functions of control inputs, we can write down the optimization problem similar to a linear MPC problem as a quadratic program.

### 13.3.3 Control objectives

The most basic control objective of a wind turbine is to maximize captured power during the life time of the wind turbine that is to to maximize captured power when wind speed is below its rated value. This is also called maximum power point tracking (MPPT). However when wind speed is above rated, control objective becomes regulation of the outputs around their rated values while trying to minimize dynamic loads on the structure. These objectives should be achieved against fluctuations in wind speed which acts as a disturbance to the system. In this work we have considered operation of the wind turbine in above rated (full load region). Therefore, we try to regulate rotational speed and generated power around their rated values and remove the effect of wind speed fluctuations.

### 13.3.4 Offset free control

Persistent disturbances and modeling error can cause an offset between measured outputs and desired outputs. To avoid this problem we have employed an offset free reference tracking approach see [MB02] and [PR03]. Our RMPC solves the regulation problem around the operating point. However we regulate around the operating point ($x_k^*$ and $u_k^*$) which results in offset from desired outputs. To avoid this problem in our control algorithm we shift origin in our regulation problem to $x_k^0$ and $u_k^0$ instead. In order to find new origins, we have augmented linear model of the plant with a disturbance model that adds fictitious disturbances to the system. The fictitious disturbances compensate the difference between measured outputs and desired outputs. State space model of the augmented system is:

$$\tilde{x}_{k+1} = \tilde{A}\tilde{x}_k + \tilde{B}u_k \tag{13.39}$$

$$y_k = \tilde{C}\tilde{x}_k + Du_k \tag{13.40}$$

in which the augmented state and matrices are:

$$\tilde{x}_k = \begin{pmatrix} \hat{x}_{k+1} \\ \hat{d}_{k+1} \\ \hat{p}_{k+1} \end{pmatrix} \qquad \tilde{A} = \begin{pmatrix} A & B_d & 0 \\ 0 & A_d & 0 \\ 0 & 0 & A_p \end{pmatrix} \tag{13.41}$$

$$\tilde{B} = \begin{pmatrix} B & 0 & 0 \end{pmatrix}^T \qquad \tilde{C} = \begin{pmatrix} C & 0 & C_p \end{pmatrix} \tag{13.42}$$

$\hat{x}_k, \hat{d}_k$ and $\hat{p}_k$ are system states, input/state and output disturbances respectively. $(A, B, C, D)$ are matrices of the linearized model, $B_d$ and $C_p$ show effect of disturbances on states and outputs respectively. $A_d$ and $A_p$ show dynamics of input/state and output disturbances. For more information and how to choose these matrices we refer to [MB02] and [PR03]. Since the disturbances are not measurable, an extended Kalman filter is designed to estimate them. The estimated disturbances are used to remove any offset between desired outputs and measured outputs. Based on this model and estimated disturbances, $x_k^0$ and $u_k^0$ which are offset free steady state input and states can be calculated:

$$\begin{pmatrix} A - I & B \\ C & D \end{pmatrix} \begin{pmatrix} x_k^0 \\ u_k^0 \end{pmatrix} = \begin{pmatrix} -B_d\hat{d}_k \\ -C_p\hat{p}_k \end{pmatrix} \tag{13.43}$$

After calculating these values, we simply replace $x_k^*$ and $u_k^*$ in (13.29) with $x_k^0$ and $u_k^0$ which results in:

$$\lambda_k = x_{k+1}^0 - A(\gamma_k)x_k^0 - B(\gamma_k)u_k^0 \tag{13.44}$$

## 13.4 Uncertain LIDAR measurements

LIDAR measurements are used to have a preview of the wind speed [HHW06], however these measurements are erroneous and uncertain. In this work, we have considered the uncertainties to be the measurement noise and uncertainty in the estimation of the wind propagation time. The propagation time is the time that the wind travels between the LIDAR measurement point to the rotor disc. The unknown delay is the most important uncertainty in the wind propagation time estimation. Lead or lag errors in the wind speed measurement, which is fed to the controller, severely reduce the performance of the controller. In order to bypass this problem, in this work, we have designed an Extended Kalman filter which estimates the effective wind speed on the rotor plane. Then this estimate is compared against the filtered information that comes from LIDAR measurements. Cross-covariance of the estimated wind speed and LIDAR measurements are used to get an estimate of the delay between the two signals. Subsequently, the estimated delay is compensated for in LIDAR measurements and the resulting wind speed information is fed to the controller.

### 13.4.1 Wind speed estimation

Wind speed estimation is essential in our control algorithm. A one DOF model of the wind turbine, including only rotor rotational degree of freedom is used for wind speed estimation. This model is augmented with a linear model of the effective wind speed. The effective wind speed can be modeled as a complicated nonlinear stochastic process. However, for practical control purposes, it could be approximated by a linear model [JLSM06]. In this model, the wind has two elements, mean value term ($v_m$) and turbulent term ($v_t$). The mean wind speed varies relatively slowly and could be considered constant during one simulation. The turbulent term could be modeled by the following transfer function:

$$v_t = \frac{k}{(p_1 s + 1)(p_2 s + 1)} e; \quad e \in N(0,1) \tag{13.45}$$

Which in the state space form could be written as:

$$\begin{pmatrix} \dot{v}_t \\ \ddot{v}_t \end{pmatrix} = \begin{pmatrix} 0 & 1 \\ -\frac{1}{p_1 p_2} & -\frac{p_1+p_2}{p_1 p_2} \end{pmatrix} \begin{pmatrix} v_t \\ \dot{v}_t \end{pmatrix} + \begin{pmatrix} 0 \\ \frac{k}{p_1 p_2} \end{pmatrix} e \tag{13.46}$$

The parameters $p_1, p_2$ and $k$ which depend on the mean wind speed $v_m$ could be found by second order approximation of the wind power spectrum [JLSM06]. This state space model is augmented with the following model to be used in the

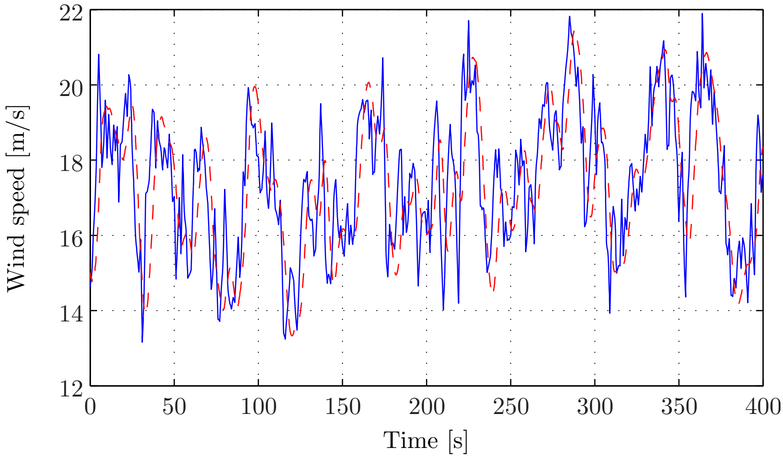


**Figure 13.3:** Wind speed estimation (red-dashed line is the estimated wind speed and solid-blue line is the effective wind speed)

extended Kalman filter:

$$\dot{\Omega} = \frac{1}{J_r}\mathcal{Q}_r(\Omega, \Theta, \mathcal{V}_e) - \frac{1}{J_r}\mathcal{Q}_g \tag{13.47}$$

$$y = \begin{pmatrix}\Omega & \mathcal{P}_e\end{pmatrix}^T \tag{13.48}$$

Figure 13.3 shows wind speed and its estimate.

### 13.4.2 LIDAR measurements

The high frequency content of the LIDAR measurement is filtered before it is used. Therefore, the cut-off frequency of the low-pass filter has to be determined. Assume that the turbulent content of the wind can be modeled by a first order low-pass filter whose time constant ($a(v_m)$) is a function of the mean wind speed. The aim is to obtain an approximation for this time constant.The approximation is achieved using the spectral models for turbulence. Turbulence with the length scale of less than $1000m$ is described by spectral models such as Kaimal, Von Karman, Harris and Højstrup [PD83]. All models have similar frequency decay of $f{-}5/3$, and they are all parameterized and normalized in similar way. In this work, we use the Kaimal spectrum that is widely used in wind energy sector. Kaimal spectrum is explained by

$$S_U(f) = \sigma_U^2 \frac{4\frac{L}{U_{10}}}{\left(1 + 6f\frac{L}{U_{10}}\right)^{\frac{5}{3}}}, \tag{13.49}$$

where $\sigma_U$ is the standard deviation, $U_{10}$ is the average wind speed (over 10 minutes), and $L$ is the turbulence length scale. As indicated in [KBS11], the time constant of the filter is determined by demanding similar peak frequencies for the filter and $fS_U(f)$ which is given by:

$$a(v_m) = \frac{\pi v_m}{2L}. \tag{13.50}$$

### 13.4.3 Lead-Lag error estimation and compensation

For lead-lag error estimation, cross covariance of the estimated wind speed and measurements from the LIDAR for a window of size $m$-seconds is found. The result is a sequence which has $2m-1$ elements. By finding the maximum of the cross covariance, an estimate of the lead-lag error can be found. The window size is important as it should be long enough to avoid erroneous results. The errors especially emerge when the window of effective wind speed signal has big autocorrelation values. By choosing a window with sufficiently large size this problem could be avoided. However, choosing a too big window size will result in slow delay detection which reduces performance of the controller. Cross covariance of the estimated wind speed and LIDAR measurements, can be found using the following formula:

$$\phi_{\hat{v}v}(t) = E\{(\hat{v}_{n+t} - \mu_{\hat{v}})(v_n - \mu_v)^T\} \tag{13.51}$$

in which $\hat{v}$ is the estimated wind speed and $v$ is the LIDAR measurements. Having the sequence of $\phi_{\hat{v}v}(t)$, one can calculate lead-lag error by the following formula:

$$t_e = \arg\max_t \phi_{\hat{v}v}(t) \tag{13.52}$$

in which $t_e = t_{\text{measurment}} - t_{\text{actual wind speed}}$. $t_e$ is then passed through a low pass filter to remove fluctuations due to numerical errors and possible autocorrelations. Then it is used to shift LIDAR measurements. Afterwards the shifted signal is used in the controller. Figure 13.4 shows a comparison of the effective wind speed and the wind speed measured by LIDAR. There is a 4 seconds lead error at time $100s$ (in which the measurement is lead) and then at time $300s$ the same amount of lag error. Figure 13.5 shows a comparison between the introduced delay in the measurements and its estimation. The lead-lag error estimation is delayed, however it follows the shape of the actual delay. In the worst cases, when the LIDAR measurements does not give a good correlation with the wind speed estimation on the turbine, the measurements could be discarded and the turbine can operate without LIDAR measurements.

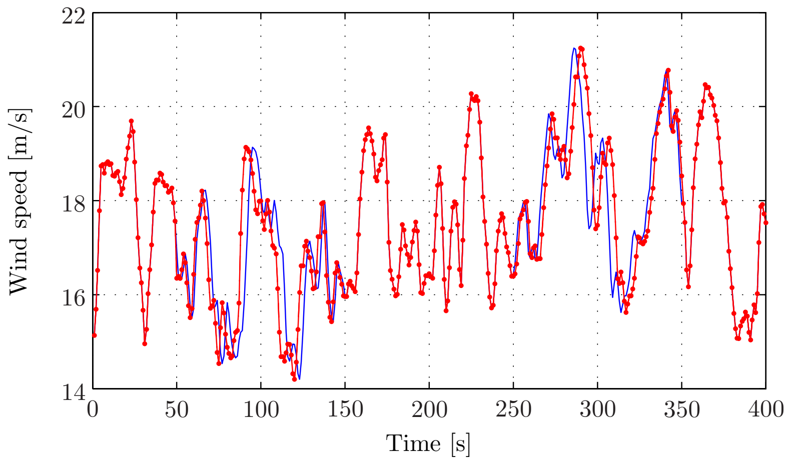


**Figure 13.4:** Effective wind speed and LIDAR measurement with lead-lag errors (solid-blue is the effective wind speed, dotted-red is the LIDAR measurement)

**Table 13.1:** Performance comparison (SD stands for standard deviation)

| Parameters | MPC+LIDAR+ Compensation | MPC+ LIDAR | Linear MPC |
|---|---|---|---|
| SD of $\omega_r$ (RPM) | 0.198 | 0.264 | 0.431 |
| SD of $P_e$ (M Watts) | 0.108 | 0.123 | 0.179 |
| Pitch travel (degrees) | 554.8 | 606.5 | 842.9 |
| SD of shaft moment (k N.M.) | 0.702 | 0.812 | 1.159 |
| SD of tower fore-aft acc.(m/$s^2$) | 0.233 | 0.240 | 0.311 |

## 13.5 Simulations

In this section, simulation results for the obtained controllers are presented. The controllers are implemented in MATLAB and tested on a high fidelity wind turbine simulation software FAST [JJ05] using the model of the reference wind turbine [JBMS09]. The results of the proposed approach with lead-lag error estimation are compared against two controllers with the same tunings. An MPC with the same LIDAR measurements but without error compensation and an MPC with re-linearization at each sample point based on estimated wind speed. Simulations are done using turbulent wind speed, with Kaimal model [iec05]. And TurbSim [Jon09] is used to generate the wind profile. In order to stay in the full load region, a realization of turbulent wind speed is used from category $C$ of the turbulence categories of the IEC 61400-1 [iec05]

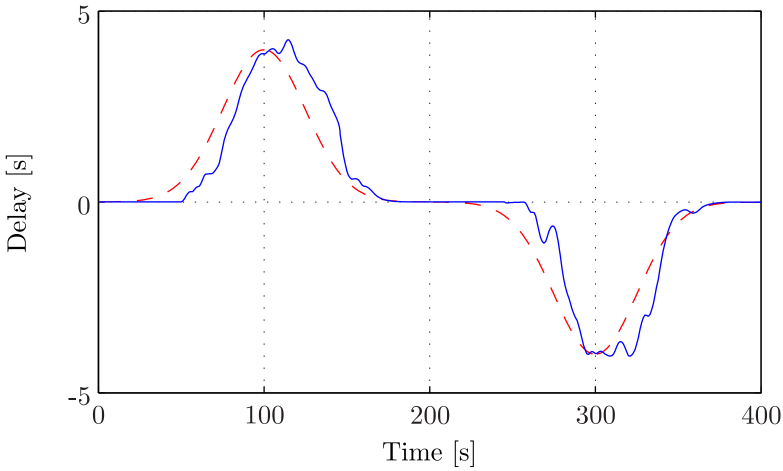


**Figure 13.5:** Comparison of introduced delay and its estimation (solid-blue is the estimated delay, dashed-red is the introduced delay)

with the mean wind speed of $18m/s$. Control inputs are collective pitch of the blades $\theta$ and generator reaction torque $Q_g$. System outputs are rotor rotational speed $\omega_r$, electrical power $P_e$ and tower fore-aft acceleration $\ddot{x}_t$ that are plotted in figures 13.7-13.15. Table 13.1 shows a comparison of the results between the proposed approach with lead-lag error estimation, the linear MPC based on estimated wind speed, the linear MPC with LIDAR measurements and without compensation. For comparisons, we have used pitch travel to take into account an approximation of the damage on the pitch actuator. Standard deviations (SD) of the rotational speed and generated power are also compared. As it in the table 13.1 and figures 13.7-13.15, the proposed approach gives better regulation on rotational speed and generated power (smaller standard deviations) while maintaining a smaller pitch activity and less deviations on tower fore-aft acceleration and drivetrain torsion.

## 13.6 Conclusions

LIDAR measurements are improve performance of wind turbines. However, errors in the calculation of the wind propagation time severely degrade the performance of the controller. In this work, we have shown that using appropriate signal processing techniques, these errors can be removed form the measurements and even in the worst cases, when LIDAR measurements are not reliable, the turbine can operate without using the data from the LIDAR.

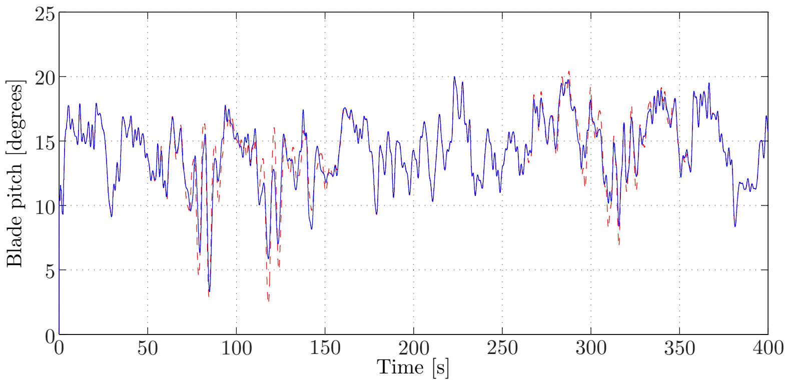


**Figure 13.6:** Blade-pitch (degrees, solid-blue line is MPC with LIDAR measurements and delay compensation and dashed-red line is MPC with LIDAR measurements without delay compensation)

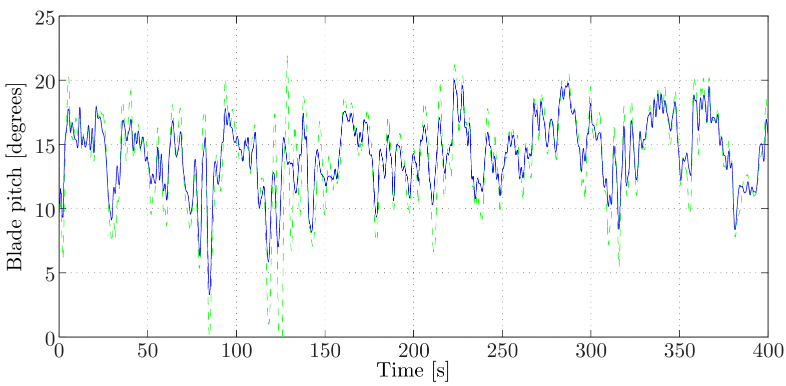


**Figure 13.7:** Blade-pitch (degrees, solid-blue line is MPC with LIDAR measurements and delay compensation and dashed-green line is MPC using estimated effective wind speed)

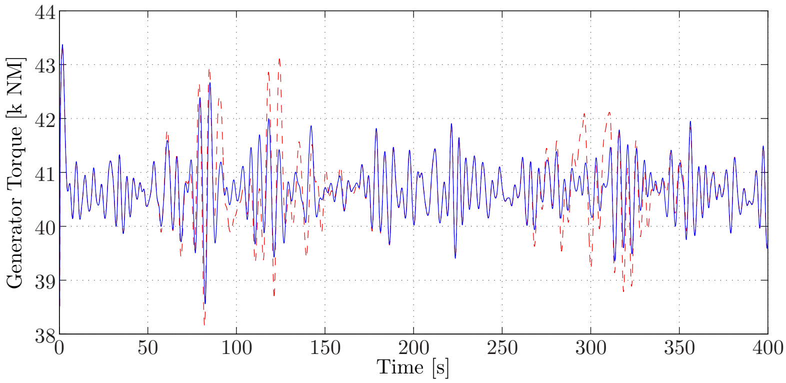


**Figure 13.8:** Generator-torque (k NM, solid-blue line is MPC with LIDAR measurements and delay compensation and dashed-red line is MPC with LIDAR measurements without delay compensation)

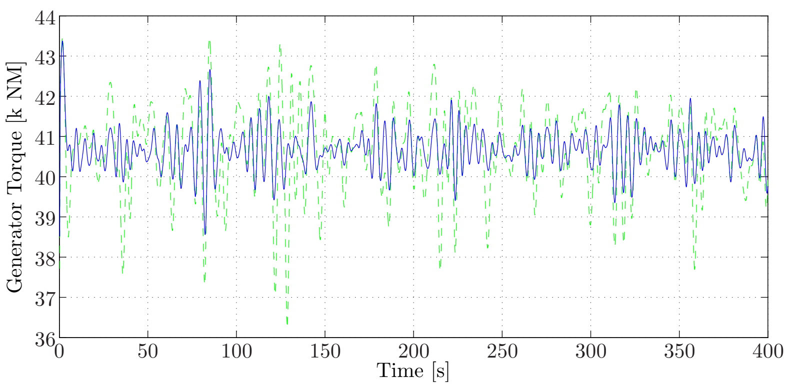


**Figure 13.9:** Generator-torque (k NM, solid-blue line is MPC with LIDAR measurements and delay compensation and dashed-green line is MPC using estimated effective wind speed)

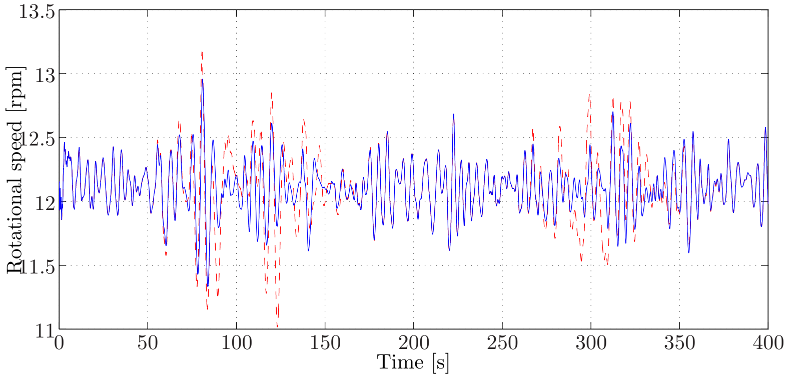


**Figure 13.10:** Rotor rotational speed (RPM, , solid-blue line is MPC with LIDAR measurements and delay compensation and dashed-red line is MPC with LIDAR measurements without delay compensation)

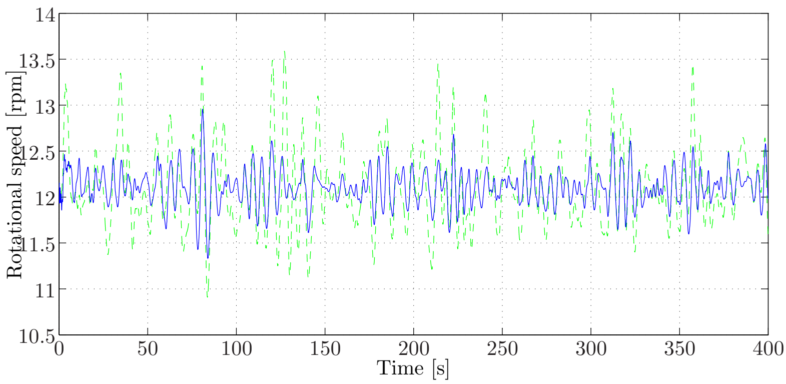


**Figure 13.11:** Rotor rotational speed (RPM, solid-blue line is MPC with LIDAR measurements and delay compensation and dashed-green line is MPC using estimated effective wind speed)

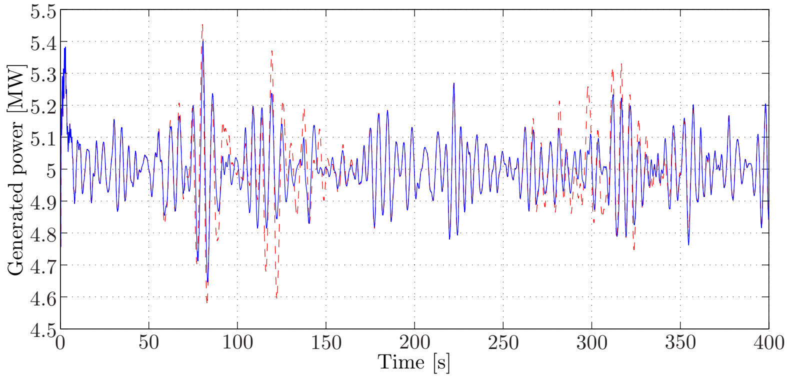


**Figure 13.12:** Electrical power (M Watts, solid-blue line is MPC with LIDAR measurements and delay compensation and dashed-red line is MPC with LIDAR measurements without delay compensation)

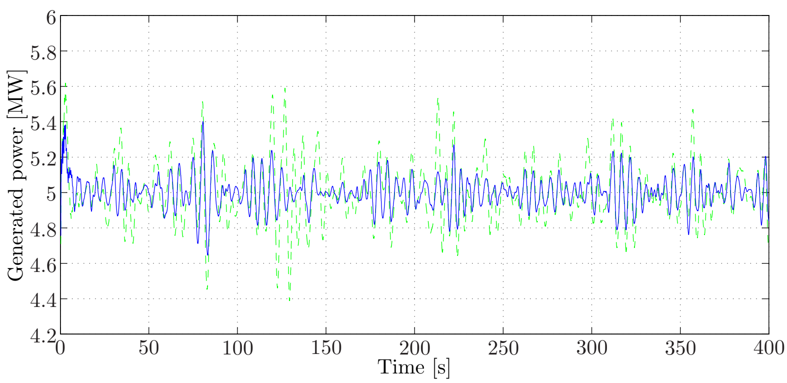


**Figure 13.13:** Electrical power (M Watts, solid-blue line is MPC with LIDAR measurements and delay compensation and dashed-green line is MPC using estimated effective wind speed)

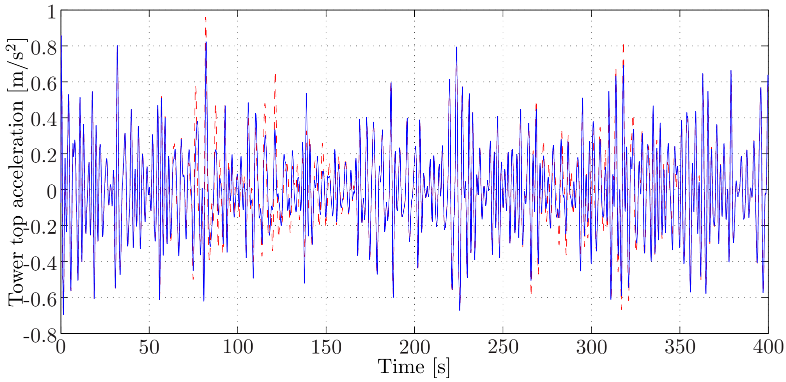


**Figure 13.14:** Tower top velocity ($m/s^2$, solid-blue line is MPC with LIDAR measurements and delay compensation and dashed-red line is MPC with LIDAR measurements without delay compensation)

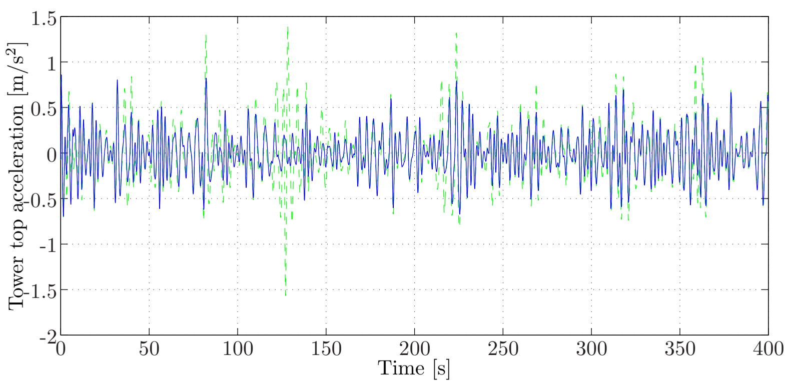


**Figure 13.15:** Tower top velocity ($m/s^2$, solid-blue line is MPC with LIDAR measurements and delay compensation and dashed-green line is MPC using estimated effective wind speed)

## Paper I References


[And10] Peter Bjørn Andersen. *Advanced Load Alleviation for Wind Turbines using Adaptive Trailing Edge Flaps: Sensoring and Control*. PhD thesis, Technical University of Denmark, Denmark, 2010.

[BBM06] Fernando D. Bianchi, Hernan De Battista, and Ricardo J. Mantz. *Wind Turbine Control Systems: Principles, Modelling and Gain Scheduling Design*. Springer, 2006.

[GC08] M. Geyler and P. Caselitz. Robust multivariable pitch control design for load reduction on large wind turbines. *Journal of solar energy engineering*, 130(3):–, 2008.

[Han08] Martin O. L. Hansen. *Aerodynamics of Wind Turbines*. Earthscan, 2008.

[Hen07] Lars Christian Henriksen. Model predictive control of a wind turbine. Master's thesis, Technical University of Denmark, Informatics and Mathematical Modelling, 2007.

[HHW06] M. Harris, M. Hand, and A. Wright. LIDAR for turbine control. Technical report, National Renewable Energy Laboratory, 2006.

[iec05] IEC 61400-1 wind turbines-part 1: Design requirements., August 2005.

[JBMS09] J. Jonkman, S. Butterfield, W. Musial, and G. Scott. Definition of a 5MW reference wind turbine for offshore system development. Technical report, National Renewable Energy Laboratory,, 1617 Cole Boulevard, Golden, Colorado 80401-3393 303-275-3000, 2009.

[JF08] Johnson and Fingersh. Adaptive pitch control of variable-speed wind turbines. *J. Sol. Energy Eng. (USA)*, 130(3):031012–1–7, 2008.

[JJ05] Jason M. Jonkman and Marshall L. Buhl Jr. Fast user's guide. Technical Report NREL/EL-500-38230, National Renewable Energy Laboratory, Golden, CO, August 2005.

[JLSM06] Allan Juul Larsen and Thomas Stampe Mogensen. Individuel pitchregulering af vindmølle. Master's thesis, Technical University of Denmark, Informatics and Mathematical Modelling, Lyngby, Denmark, 2006.

[Jon09] B.J. Jonkman. Turbsim user's guide: Version 1.50. Technical report, National Renewable Energy Laboratory, 1617 Cole Boulevard, Golden, Colorado 80401-3393 303-275-3000, 2009.

[KBS11] Torben Knudsen, Thomas Bak, and Mohsen Soltani. Prediction models for wind speed at turbine locations in a wind farm. *Wind Energ.*, 14(7):877–894, 2011.

[LC00] W.E. Leithead and Bill Connor. Control of variable speed wind turbines: Design task. *Int J Control*, 73(13):1189–1212, 2000.

[LPS$^+$11] Jason Laks, Lucy Y. Pao, Eric Simley, Alan Wright, Neil Kelley, and Bonnie Jonkman. Model predictive control using preview measurements from lidar. In *49th AIAA Aerospace Sciences Meeting including the New Horizons Forum and Aerospace Exposition*, Orlando, Florida, January 2011.

[LPW09] J.H. Laks, L.Y. Pao, and A.D. Wright. Control of wind turbines: Past, present, and future. *Proceedings of the American Control Conference*, pages 2096–2103, 2009.

[Mac02] J.M. Maciejowski. *Predictive control with constraints.* Pearson Education Lim., Essex, 2002.

[MB02] Kenneth R. Muske and Thomas A. Badgwell. Disturbance modeling for offset-free linear model predictive control. *Journal of Process Control*, 12(5):617–632, 2002.

[MNP11] Mahmood Mirzaei, Hans Henrik Niemann, and Niels Kjølstad Poulsen. A $\mu$-synthesis approach to robust control of a wind turbine. In *the 50th IEEE Conference on Decision and Control and European Control Conference*, pages 645–650, Orlando, Florida, United States, 2011.

[MPN12a] Mahmood Mirzaei, Niels Kjølstad Poulsen, and Hans Henrik Niemann. Individual pitch control using lidar measurements. In *IEEE Multiconference on Systems and Control*, Dubrovnik, Croatia, 2012.

[MPN12b] Mahmood Mirzaei, Niels Kjølstad Poulsen, and Hans Henrik Niemann. Robust model predictive control of a wind turbine. In *American Control Conference*, Montr, Canada, 2012.

[Øst08] Kasper Zinck Østergaard. *Robust, Gain-Scheduled Control of Wind Turbines.* PhD thesis, Automation and Control Department of Electronic Systems, Aalborg University, 2008.

[PD83] H. A. Panofsky and John A. Dutton. *Atmospheric Turbulence.* 1983.

[PR03] Gabriele Pannocchia and James B. Rawlings. Disturbance models for offset-free model-predictive control. *AIChE Journal*, 49(2):426–437, 2003.

[QB96] S. Joe Qin and Thomas A. Badgwell. An overview of industrial model predictive control technology. pages –, 1996.

[SWBB11] M. Soltani, R. Wisniewski, P. Brath, and S. Boyd. Load reduction of wind turbines using receding horizon control. *The proceedings of the IEEE Conference on Control Applications*, pages 852–857, 2011.

[Tho06] Sven Creutz Thomsen. Nonlinear control of a wind turbine. Master's thesis, Technical University of Denmark, Informatics and Mathematical Modelling, Lyngby, Denmark, 2006.